Delivery of mesenchymal stem cells in biomimetic engineered scaffolds promotes healing of diabetic ulcers

R Assi[1], TR Foster[1], H He[1], K Stamati[2], S Homer-Vanniasinkam[2], U Cheema[2], A Dardik[1]

[1] Yale University, New Haven, CT, USA. [2] University College London, London, UK.

INTRODUCTION: One of the most important complications of diabetes is the development of lower extremity ulcers. Approximately 2-3% of diabetics develop foot ulcers each year, affecting approximately 15-25% of diabetics during their lifetime. The etiology of delayed and poor wound healing in diabetic ulcers is complex and includes poor vascular perfusion, neurological injury, and trauma, as well as limited cellular angiogenic potential, a diminished population of mesenchymal stem cells and reduction in the deposition of appropriate extracellular matrix.

Mesenchymal stem cells (MSC) are a promising source of cells for multiple regenerative processes; MSC enhance angiogenesis via multiple cytokines that ameliorate ischemia, including vascular endothelial growth factor (VEGF). Culturing MSC in hypoxic conditions enhances their angiogenic potential, which is not surprising since MSC reside in the bone marrow niche in vivo.

We hypothesized that use of a biomimetic scaffold to deliver MSC will enhance their therapeutic potential. We previously showed that plastic compression of a collagen scaffold to a density approaching that of tissue also creates a hypoxic central core that would be of particular use as a biomimetic scaffold for MSC [1-3]. We used these compressed collagen scaffolds to deliver MSC into a mouse model of diabetic wounds to determine their therapeutic potential in this translationally relevant model [4].

METHODS: Rolled collagen scaffolds containing MSC were implanted or applied topically to diabetic C57BL/6 mice with excisional wounds.

RESULTS: Rolled scaffolds were hypoxic, inducing MSC synthesis and secretion of VEGF. Diabetic mice with wounds treated with rolled scaffolds containing MSC showed increased healing compared to controls (Fig. 1). Histologic examination showed increased cellular proliferation, increased VEGF expression and capillary density, and increased numbers of macrophages, fibroblasts, and smooth muscle cells. Addition of laminin to the collagen scaffold enhanced these effects. Topical delivery of unrolled scaffolds remained effective to heal wounds (Fig. 2).

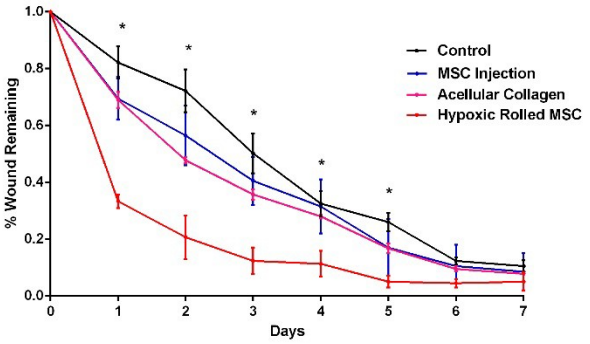

*Fig. 1: Delivery of MSC in a rolled collagen scaffold enhances wound healing in a diabetic mouse leg wound model. *, p < 0.0001 (ANOVA)*

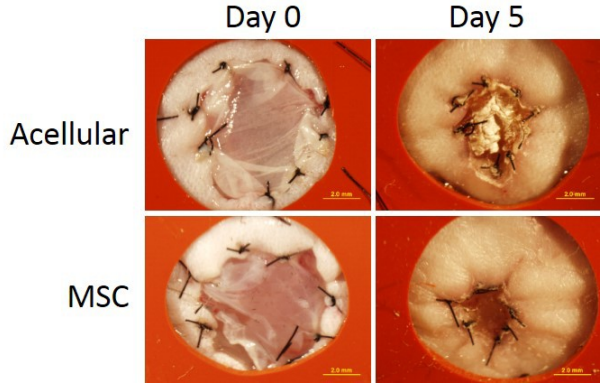

.Fig. 2: Topical application of collagen scaffolds containing MSC enhances wound healing in a diabetic mouse splinted back wound model.

DISCUSSION & CONCLUSIONS: Delivery of MSC in biomimetic scaffolds promotes wound healing in a translationally relevant diabetic mouse model. These results suggest that a tissue engineering approach is a viable approach to this difficult and complex clinical problem. These results also suggest that a biomimetic scaffold can mimic a stem cell niche environment, promoting stem cell survival and/or function in vivo, potentially increasing their therapeutic application.

Oxygen microbubbles for reducing tissue hypoxia

E Stride[1], J Owen[1], C McEwan[2], E Beguin[1], H Nesbitt[2], M Borden[2], A McHale[2], J Callan[2]

[1]Institute of Biomedical Engineering, University of Oxford, UK, [2]Biomedical Sciences Research Institute, Ulster University, Coleraine, Northern Ireland, [3]Department of Mechanical Engineering, University of Colorado, USA.

INTRODUCTION: Hypoxia, i.e. a reduction in dissolved oxygen concentration below physiologically normal levels, has been identified as playing a critical role in the progression of many types of disease[1] and as a key determinant of the success of cancer treatment[2]. It poses a particular challenge for treatments such as radiotherapy, photodynamic and sonodynamic therapy which rely on the production of reactive oxygen species. Strategies for treating hypoxia have included the development of hypoxia-selective drugs[3] as well as methods for directly increasing blood oxygenation, e.g. hyperbaric oxygen therapy, pure oxygen or carbogen breathing, ozone therapy, hydrogen peroxide injections and administration of suspensions of oxygen carrier liquids. To date, however, these approaches have delivered limited success either due to lack of proven efficacy and/or unwanted side effects[4]. Gas microbubbles, stabilised by a biocompatible shell have been used as ultrasound contrast agents for several decades and have also been widely investigated as a means of promoting drug delivery. The aim of this study was to determine whether microbubbles could be used to deliver both a sonodynamic therapy drug and oxygen simultaneously to a tumour to facilitate treatment.

METHODS: Phospholipid coated microbubbles containing either oxygen (O_2) or sulphur hexafluoride (SF_6) were produced by sonication and conjugated to a sonosensitiser (Rose Bengal) via an Avidin-Biotin linker. Tumours were induced in BALB/c SCID mice using the BxPc-3 human pancreatic cell line and exposed to ultrasound for 3.5 mins (3.5 Wcm^{-2} at 1MHz centre frequency, 100 Hz pulse repetition frequency and 30% duty cycle) following injection of either O_2 or SF6 microbubbles.

RESULTS: Five days after treatment a 45% reduction in tumour volume was seen in the mice receiving the O_2 bubbles, compared with a 35% increase in volume for those receiving the SF_6 microbubbles. As shown in Fig.1, the control groups (no ultrasound) showed an increase of 180% in tumour volume over the same period. Fibre optic oxygen probe measurements and subsequent analysis of the levels of hypoxia inducible factor (HIF1-α) confirmed an increase in the partial pressure of oxygen in the tumour.

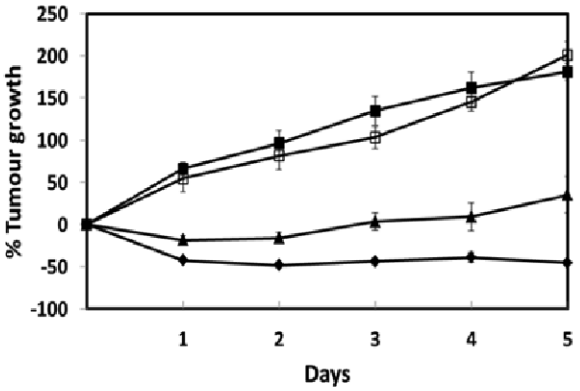

Fig.1: Plot of % tumour growth against time for mice bearing BxPc-3 tumours and treated with (i) O2-RB microbubbles and ultrasound (filled diamonds) (ii) O2-RB microbubbles only (open squares) (iii) SF6-RB microbubbles and ultrasound (filled triangles) (iv) SF6-RB microbubbles only (filled squares) (n = 3).

DISCUSSION & CONCLUSIONS: The results indicate that intravenously administered oxygen filled microbubbles can temporarily reduce tumour hypoxia and facilitate sonodynamic therapy. This potentially represents a new treatment option for recalcitrant tumours for which existing therapeutic options are extremely limited.

ACKNOWLEDGEMENTS: We thank the Engineering and Physical Sciences Research Council for supporting this work through EP/I021795/1. John Callan thanks Norbrook Laboratories Ltd. for an endowed chair.

Development of 3D printed silica-gelatin hybrid scaffolds for cartilage tissue engineering - effect of material geometry on cartilaginous matrix formation

S Li[1], M Nelson[1], MM Stevens[1], JR Jones[1]

[1] *Department of Materials, Imperial College London, London, United Kingdom*

INTRODUCTION: Cartilage regeneration has increasingly focused on the concept of "in situ" approach, based on the micro-fracture surgical procedure in combination with the use of scaffolds for cell ingrowth and guidance towards tissue formation. Our research group has previously reported the development of silica-gelatin sol-gel hybrid material, which has nano-scale co-networks of inorganic and organic components that allow tailorable degradation rate and mechanical properties [1]. The present study aims to utilise 3-D printing technology to produce silica-gelatin 3-D scaffolds with various structures and, investigate their effects on chondrogenic differentiation.

METHODS: The hybrid sol was synthesised using a TEOS based sol-gel process with GPTMS as a coupling agent between silica and gelatin. The rheology of gels was optimised for 3-D extrusion printing process direct from the sol. Scaffold structure and pore size was controlled by print file variables including strut spacing, print head speed, nozzle diameter and material deposition rate and, retained by freeze drying. The scaffolds were characterised by scanning electron microscopy, X-ray microtomography and mechanical tests prior to *in vitro* biocompatibility screening in accordance to ISO 10993 (Biological evaluation of medical devices). ATDC5 chondrogenic cells were seeded onto scaffolds with average pore sizes ranging from 250 to 1000 μm and cultured for up to 21 days. Cell-seeded constructs were analysed for cell attachment, proliferation, and cartilaginous matrix formation.

RESULTS: SEM and X-ray imaging confirmed the scaffolds contained open and interconnected pores (Fig 1). The Young's moduli of the wetted scaffolds improved significantly to a level comparable to the range of articular cartilage as the pore size reduced to 250 μm.

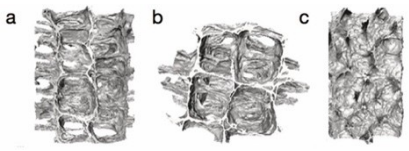

Fig. 1: Reconstructed images X-ray images of 3D printed silica-gelatin scaffolds. (a) YZ view, (b) XY view and (c) XZ view.

MTT metabolic activity assay performed in accordance to ISO 10993 confirmed the silica-gelatin material was biocompatible. Cytoskeletal constituents F-actin and Vimentin were evident in attached and spreading ATDC5 cells following 72 hours of cell culture. WST-1 cell proliferation assay demonstrated improved rate of cell growth in scaffolds with larger pores (500 and 1000 μm), however, the expression of fibrocartilage marker Collagen Type I was up-regulated. In comparison, scaffolds with smaller pores (250 μm) up-regulated the expression of hyaline cartilage specific marker Collagen Type II and the amount of sulphated glycosaminoglycan formation (Fig 2).

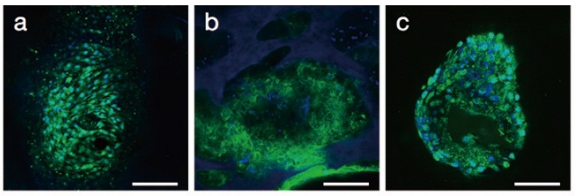

Fig. 2: Immunohistochemical staining of day-21 cell-seeded silica-gelatin scaffolds. (a) Sox9, (b) Type II Collagen and (c) Aggrecan.

DISCUSSION & CONCLUSIONS: The improved cartilaginous matrix formation was likely due in part to the improved mechanical properties of scaffolds with smaller pores. In addition, cells in larger pores likely experienced environments closer to monolayer culture and, gradually lose chondrocytic phenotype in a process known as dedifferentiation. Silica-gelatin sol-gel hybrid material and 3-D printing with tailorable pore size and mechanical properties represent promising approach for tissue engineering applications. The results from the present study also demonstrated that scaffold architecture plays an important role in cellular behaviour and matrix formation.

RAFT tissue equivalents: 3D biomimetic disease tissue model of keratoconus

AK Kureshi[1], C Putri[1], JB Phillips[2], JL Funderburgh[3], JT Daniels[1].

[1]Ocular Biology & Therapeutics, Institute of Ophthalmology, University College London, UK. [2]Biomaterials & Tissue Engineering, Eastman Dental Institute, University College London, UK. [3]Department of Ophthalmology, UPMC Eye Centre, University of Pittsburgh, Pittsburgh, Pennsylvania, USA.

INTRODUCTION: Keratoconus (KC) is a corneal disorder characterized by progressive structural thinning, resulting in a conical-shaped cornea causing loss of vision. Cell-extracellular matrix interactions are thought to control normal tissue organization and transparency and it is expected that these interactions may be perturbed in KC. The aim of this study was to develop a 3D RAFT tissue equivalent (TE) model of KC to compare the phenotypic and functional behavior of stromal cells.

METHODS: Stromal cells were characterised by phenotypic assessment using a variety of stromal cell markers and a contraction assay to compare their contractile capacity. RAFT TE were seeded with normal and KC stromal cells (n=3) and cultured for 3 weeks. Functional characterization of RAFT TE included assessment of material properties using an Electroforce Bose tensile testing device; assessment and quantification of MMP activity in stromal cells using gelatin zymography and ELISA respectively; measurement of collagen production using a Sircol collagen assay; and assessment of collagen fibril organization using scanning electron microscopy.

RESULTS: A 3D *in vitro* model of KC was achieved using RAFT TE. Normal and KC stromal cells both exhibited stromal cell markers in culture. KC stromal cells exhibited a significantly greater contractile capacity at 72 hours of culture with 75 ± 3% compared to normal cells at 29 ± 7% and acellular gels at 3 ± 1% (n=3) ($p<0.0001$). Statistically significant differences in RAFT TE material properties were observed. Mean break strength of KC and normal RAFT TE were 0.17 ± 0.02 MPa and 0.25 ± 0.03 MPa respectively (n=3) ($p<0.05$). A reduced stiffness of 0.01 ± 0.002 MPa in KC RAFT TE compared to 0.02 ± 0.002 MPa was observed. Increased activity of MMP-2 in normal RAFT TE was observed but no differences in pro-MMP-1 or collagen production. Collagen fibril ultrastructure in KC RAFT TE appeared markedly thinner and loosely packed compared to normal RAFT TE.

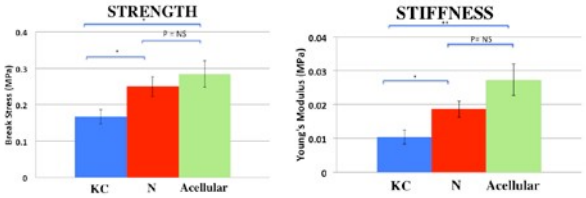

Fig. 1: Histograms illustrating (a) mean break strength and (b) mean stiffness of KC, normal and acellular RAFT TE.

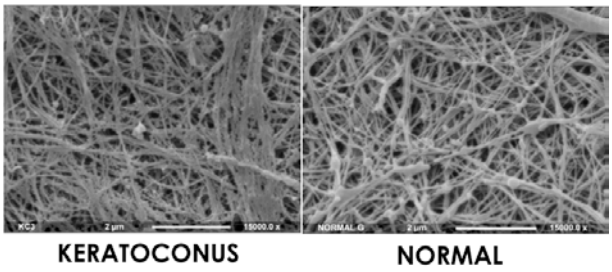

Fig 2: Scanning electron microscopy images of KC and normal RAFT TE following 3 weeks culture. Scale bar 2μm.

DISCUSSION & CONCLUSIONS: To our knowledge, this is the first 3D tissue equivalent model of KC. RAFT TE serves as an ideal biomimetic model to investigate normal and abnormal tissue organization in the corneal stroma. Significant differences in contractile capacity of KC cells and strength and stiffness of KC RAFT TE suggests the remodeling capacity of stromal cells is perturbed in KC, leading to ultrastructural changes of the corneal stroma.

ACKNOWLEDGEMENTS: This study was funded by Special Trustees of Moorfields Eye Hospital and in part by NIHR Moorfields Biomedical Research Centre.

Single cell encapsulation based bio-inks for inkjet bioprinting

R Ribeiro[1, 2], AM Ferreira[1], M Benning[1], D Pal[3], D Jamieson[3], KS Rankin[2, 3], K Dalgarno[1]

[1] School of Mechanical and Systems Engineering, Newcastle University, Newcastle Upon Tyne, UK. [2] Institute of Cellular Medicine, Newcastle University, Newcastle Upon Tyne, UK. [3] Northern Institute for Cancer Research, Newcastle University, Newcastle Upon Tyne, UK.

INTRODUCTION: Single cell encapsulation with a semi-permeable biodegradable shell is an attractive procedure for a range of biomedical applications, including cell printing. Nozzle clogging is the major limitation of inkjet bioprinting, which makes the process unreliable[1]. This work explored the use of poly-L-lysine (PLL), a polycation, on single cell coating for the development of reliable bio-inks for inkjet bioprinting, evaluating the effect of different PLL concentrations on the viability and morphology of the cells, as well as analyzing the effect of polycationic shells on the printing process.

METHODS: Single cells (osteosarcoma, Ewing's sarcoma, neo-natal dermal fibroblasts – U2OS, TC-71 and Neo-NHDF, respectively) were encapsulated into PLL shells using three concentrations: 100, 50 and 10 µg/ml. Cell viability was evaluated by MTT and Live-Dead assays, fluorescence-activated cell sorting (FACS) and image flow cytometry, with the latter two also used to assess the encapsulation efficiency. The mechanism of capsule release was studied using Transmission Electron Microscopy (TEM), and cell morphology by confocal microscopy. Coated and non-coated cells were printed using a modified inkjet bioprinter and its reliability assessed by printing droplets at 10-minute intervals over a one hour period, and subsequently counting cells.

RESULTS: Encapsulation efficiencies of over 99% were achieved. The best cell survival was obtained for the lowest polycation concentration (10 µg/ml). Encapsulated cells with this polymer concentration were able to recover and self-renew within three days post-encapsulation, achieving after one week more than 85% of viability, when compared to the control. Both cancer and non-cancer cells ingested the polymer using different endocytotic pathways, maintaining karyotype through the process. The mechanism of coating release was found to be through polymer internalization followed by metabolisation, with the coating degradation beginning almost immediately. The polycationic shell induced changes on basal cell surface charge. Reliable bio-inks were obtained with a consistent print yield, when compared to an uncoated cells bio-ink that blocked the inkjet nozzle (Fig. 1 - A). Printed cells were morphologically identical to unprinted cells and found to be viable (Fig.1 - B, C, D).

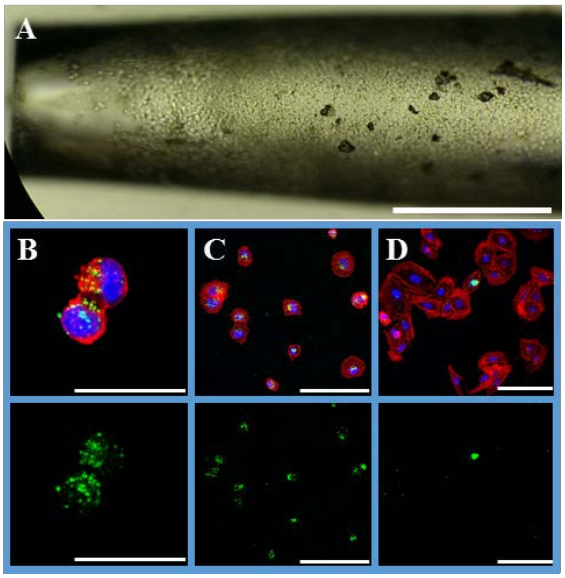

Fig. 1: Confocal microscopy images of printed 10 µg/mL U2OS cells. A) Blocked inkjet nozzle with uncoated cells; B) Cells fixed immediately after printing; C) Cells fixed after 4 h of incubation; D) Cells fixed after 24 h of incubation;

DISCUSSION & CONCLUSIONS: Shell formation was influenced by PLL concentration and is mainly through attachment to the cell membrane. The cell encapsulation process can be used as a harmless temporary mechanism to stabilise bio-inks in order to achieve consistent printing yields over extended time periods of up to an hour, avoiding cell agglomeration and nozzle clog.

ACKNOWLEDGEMENTS: The research reported in this paper has been partly funded through MeDe Innovation, the EPSRC Centre for Innovative Manufacture in Additive Manufacture, the Arthritis Research UK Tissue Engineering Centre, and a Newcastle University Doctoral Studentship.

Delivery of osteogenic liposomal bone morphogenetic protein-2 from poly(methyl methacrylate) bone cement

W Nishio Ayre[1], RJ Waddington[1], SL Evans[2], DJ Mason[3], B Evans[4], JC Birchall[5], R Morgan-Jones[6], SP Denyer[7], AJ Sloan[1]

[1] School of Dentistry, [2]School of Engineering, [3]School of Biosciences, [4]School of Medicine, [5]School of Pharmacy and Pharmaceutical Sciences, Cardiff University, Wales. [6]Cardiff & Vale University Health Board, Cardiff, Wales; [7]School of Pharmacy and Biomolecular Sciences, University of Brighton, England

INTRODUCTION: In England and Wales in 2013, approximately 181,648 knee and hip replacements were performed, 15,395 (8.5%) of which were revisions primarily caused by aseptic loosening [1]. Aseptic loosening is caused by a combination of wear particles, stress shielding and micromotion, all of which have been linked to poor early implant osseointegration [2]. Although implant coatings have reduced loosening rates, there is currently no effective technology to enhance osseointegration of cemented implants, a technique preferred for elderly patients. A previous research project has resulted in the development of a novel patented nano-vesicle delivery system capable of releasing large, prolonged doses of antibiotic from bone cement, whilst simultaneously toughening the material [3]. This study employs this system to deliver an osteogenic molecule, recombinant human bone morphogenetic protein 2 (rhBMP-2).

METHODS: rhBMP-2 was encapsulated into 100nm phosphatidylserine (PS) liposomes using passive loading methods. Encapsulation efficiency and release from Palacos R bone cement was determined using size exclusion (sephadex filtering) combined with a commercially available BMP-2 ELISA kit. The cytotoxicity of 1pg/mL, 10pg/mL, 100pg/mL, 1ng/mL, 10ng/mL and 100ng/mL rhBMP-2 and 10µg/mL, 100µg/mL and 1mg/mL liposome concentrations were determined against human bone marrow stem cells using an MTT assay and a TUNEL assay for DNA fragmentation (apoptosis). The effects on stem cell differentiation and osteoblast mineralisation was determined by monitoring alkaline phosphatase activity; collagen type I, RUNX2 and osteocalcin gene expression using qPCR; and by alizarin red staining at 3, 9 and 21 days.

RESULTS: The encapsulation efficiency of rhBMP-2 was approximately 10% when employing passive loading techniques at low concentrations. Low cytotoxicity was observed with lower concentrations of liposomes (10 and 100µg/mL) and all concentrations of rhBMP-2. The PS-liposomes increased the expression of osteogenic markers at day 9, whilst combining rhBMP-2 with the liposomes resulted in higher levels of mineralisation at day 21 (Fig 1). Physiologically relevant and therapeutic doses of rhBMP-2 were released from Palacos R bone cement over 72 hours.

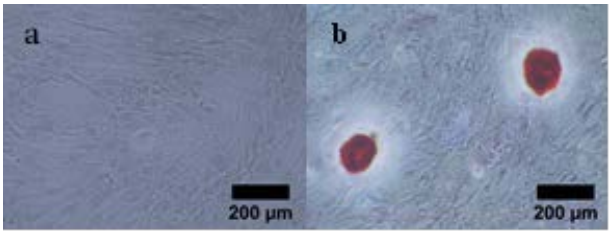

Fig. 1: Alizarin red staining of human bone marrow cells at day 21 for (a) osteogenic media and (b) liposomal BMP-2. Bright red staining indicates mineralisation.

DISCUSSION & CONCLUSIONS: Liposomal rhBMP-2 had a beneficial effect on the osteogenic differentiation of bone marrow stem cells and caused early mineralisation *in vitro*. Therapeutic levels of rhBMP-2 were successfully delivered from a commercial bone cement. Local release of rhBMP-2 from bone cement may encourage early bone repair and osseointegration of the implant, ultimately reducing the likelihood of long-term aseptic loosening.

ACKNOWLEDGEMENTS: This work was supported by the Life Science Research Network Wales, an initiative funded through the Welsh Government's Ser Cymru program.

The influence of a hyperglycemic environment on the osteogenic and adipogenic potential of mesenchymal stem cell populations

A Al-Qarakhli[1], AJ Sloan[1], R Moseley[1] and RJ Waddington[1]
[1]Oral and Biomedical Sciences, School of Dentistry, Cardiff University, UK

INTRODUCTION: High glucose (HG) concentrations can alter cellular signalling that has implications for tissue repair. Hyperglycemia causes a delay in the healing ability of tissues including bone[1], although the biological mechanisms are currently unknown. Mesenchymal stem cells (MSCs) are essential for tissue regeneration and known to represent a heterogeneous population containing sub-populations that vary in relation to their proliferative and differentiation capacities. We have previously isolated and characterized MSCs from compact bone containing both immature MSCs and more linage restricted cells. The latter cells are lost during culture expansion, while cells with greater proliferative capacities and multi-potentiality survive. Continued culture leads to the development of an aged senescent phenotype. This study aims to examine the effect of HG levels on the osteogenic and adipogenic potential of these different cell populations.

METHODS: MSCs were isolated from bone chips derived from the femurs of 28 day old male rats. Cells at specific population doubling levels (PDs) were cultured under physiologically normal (5.5mM) and high (25mM) glucose levels for 28 days in osteogenic and 21 days in adipogenic media. RNA samples were analysed at days 2-28 to investigate the gene expression of osteogenic markers, osterix (OSX), osteopontin (OPN) and osteocalcin (OCN) and adipogenic markers, adiponectin and PPARϒ, using qPCR. At day 28, mineral deposition was quantified by Alizarin Red staining and at day 21, adipogensis was visualised by Lipid TOX™ stain.

RESULTS: PD15 cells (previosuly characterised to represented a mixed population of immature and lineage restricted MSCs) demonstrated a higher potential for osteogenic differentiation and medium adipogenesis, as indicated by Alizarin Red and Lipid Tox staining (fig 1 and 2) and qPCR. HG increased this osteogenic potential. PD50 cells (more immature MSCs) had a delayed osteogenic potential and increase adipogenic potential. However, HG reduced adipogenic staining at day 21, but did not alter osteogenic potential at day 28. PD 100 (cells showing a more aged, scenescent phenotype demonstrated the highest osteogenic potential, which was reduced in HG. Adipogenic staining was reduced in HG media.

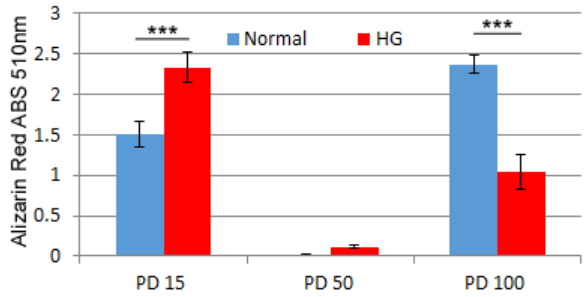

*Fig.1: Quantification of Alizarin Red staining, following culture of cell populations in osteogenic media with high and physiological glucose levels. *** p<0.001*

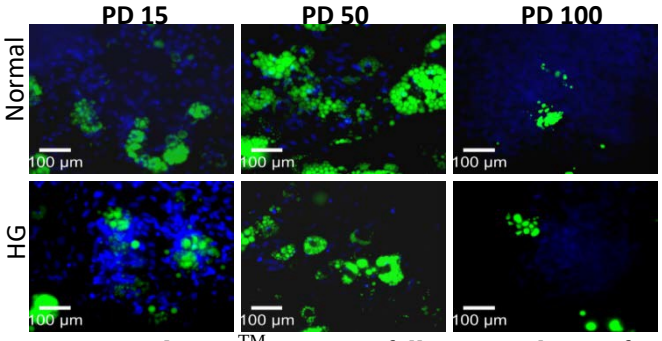

Fig.2: Lipid TOX™ staining following culture of cell populations in adipogenic media with high and physiological glucose levels.

DISCUSSION & CONCLUSIONS: Each cell population responded differently to supra-physiological glucose levels. In HG, young cells at PD15, with a high proportion of lineage restricted cells, demonstrated an increase in osteogenic potential. Conversely, more aged cells at PD100, demonstrated reduced osteogenic potential in HG. HG appeared to reduce adipogenesis in both cell populations, irrespective of the proportion of young immature or lineage restricted cells. These results contribute to our understanding of delayed bone repair observed with type 2 diabetes, which is an age-related condition and the impact of tissue engineering in these patients.

ACKNOWLEDGEMENTS: Iraqi Ministry of Higher Education and Scientific Research for their financial support.

Optical measurement of oxygen concentration in melanoma spheroid and skin engineered models

A Raza[1], HE Colley[2], E Baggaley[3] , N Green[1], S Botchway[4], JA Weinstein[3], S MacNeil[2], JW Haycock[1]

[1] Kroto Research Institute, Material Science and Engineering, [2] School of Clinical Dentistry, [3] Department of Chemistry, The University of Sheffield, UK. [4] STFC RAL, Oxford, UK.

INTRODUCTION: Non-invasive quantitative measurement of oxygen concentration within cells and tissues is essential for understanding of normal and pathological processes, in particular tumourigenesis. One of the most promising optical methods for measuring oxygen concentration is by 2-photon laser scanning phosphorescence lifetime imaging microscopy (2PE-PLIM). We have used a phosphorescent dye (PtL^{s}Cl) that is ubiquitously but heterogeneously distributed within a whole cell and quenches in the presence of oxygen [1, 2]. Phosphorescence lifetime imaging (PLIM) has many advantages over intensity measurement, for example it does not depend on fluorophore concentration and provides auto-fluorescence nullified imaging [3-5]. Furthermore, PLIM used with 2-photon laser excitation is useful as it allows deep imaging as the excitation light penetrates to greater depths than 1-photon excitation. The aim of this study was to investigate if a PtL^{s}Cl label could be combined with 2PE-PLIM for detection of a hypoxic microenvironment in a 3D *in vitro* melanoma spheroid model surrounded by a normal skin epithelium.

METHODS: Human melanoma cell lines (HBL, A375-SM and C8161) were cultured in 2D monolayer or in to a multicellular tumour spheroid. In addition, a novel tissue engineered model was developed – this was comprised of the melanoma spheroids contained within a native human de-epidermized dermis, plus cultured human keratinocytes and fibroblasts in order to mimic developing melanoma tumours. Using the resultant model we then established a PLIM imaging method to detect the tumours by way of the oxygen concentration therein.

RESULTS: Our results showed a steep increase in phosphorescence lifetime in cells under hypoxic conditions compared to normoxic conditions. Similarly, measurements through the depth of the melanoma spheroids showed that oxygen concentrations were highest at the outer region and gradually decreased towards the core (*Fig. 1*). Lifetime measurements on melanoma tissue engineered models showed short, normoxic lifetime values in normal stroma and longer, hypoxic values in melanoma spheroid areas (*Fig. 2*).

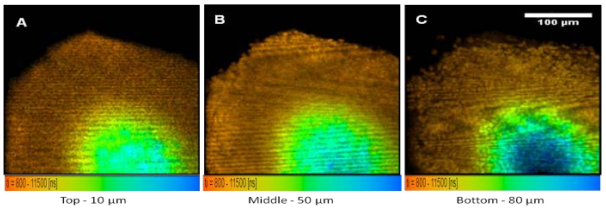

Fig. 1: Lifetime distribution of PtL^{s}Cl through a human melanoma spheroid using 1PE-PLIM.

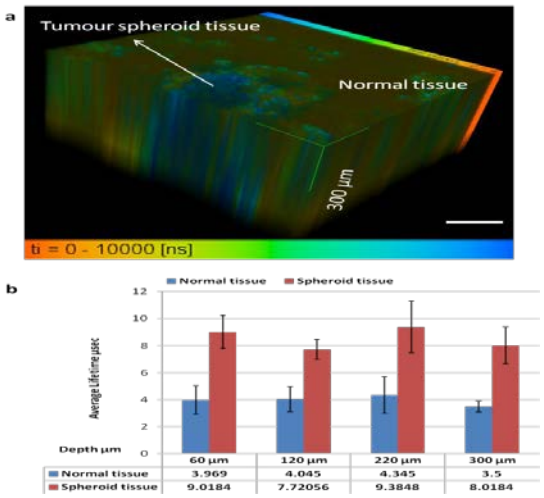

Fig. 2: Lifetime distribution of PtL^{s}Cl through a tissue engineered skin model containing melanoma spheroids using 2PE-PLIM.

DISCUSSION & CONCLUSIONS: The method provides a high-resolution, non-invasive, auto-fluorescence free measurement of oxygen concentration, which can be used to detect melanoma cells within a tissue engineered skin construct.

ACKNOWLEDGEMENTS: We thank the BBSRC for funding AR with a PhD studentship, EPSRC for post-doc funding and STFC for PLIM expertise.

Development of an acellular porcine peripheral nerve graft

L Zilic[1, 2], SP Wilshaw[2], JB Phillips[3] JW Haycock[1]

[1]Department of Materials Science & Engineering, University of Sheffield. [2]School of Biomedical Sciences, University of Leeds.[3]Department of Biomaterials and Tissue Engineering, UCL, London

INTRODUCTION: Peripheral nerve injuries affect 1 in 1000 of the population [1]. Injuries greater than 1-2cm are normally bridged using autografts, which direct regenerating axons, by topographic guidance [2]. Commercially available products such as nerve guide conduits are not particularly suitable as they lack architecture similar to that of the native ECM of the nerve. It is hypothesised that an acellular nerve would facilitate regeneration of axons at the cellular level, encouraging regeneration within a native microenvironment. The present aim was therefore to develop compatible non-immunogenic nerve grafts using low concentration SDS to decellularise porcine peripheral nerves. In addition, the acellular nerve may be used as a scaffold, additionally seeded with Schwann cells - as the delivery of such cell types is reported to improve nerve regeneration.

METHODS: Porcine peripheral nerves were decellularised using low concentration (0.1 %; w/v) sodium dodecyl sulphate and nuclease enzymes. The structure and ECM components of the acellular nerves were characterised using histological, immunohistochemical staining as well as biochemical assays and biomechanical testing. The acellular nerves were repopulated with primary rat Schwann cells and immunolabelled for Schwann cell markers. To assess regenerative capacity acellular and recellularised nerve grafts (n =6) were implanted in a 10 mm rat sciatic nerve injury model for four weeks.

RESULTS: Decellularisation of nerves resulted in a 95 % (w/w) DNA reduction with the preservation and retention of the native nerve architecture and important ECM components [3]. Biomechanical testing indicated that the decellularisation process had minimal effect on the mechanical properties. Characterisation of the repopulated nerve showed expression of the Schwann cell markers S100β, p75NGFR and GFAP proteins. *In vivo* data demonstrated axon regeneration in both acellular and recellularised nerve grafts.

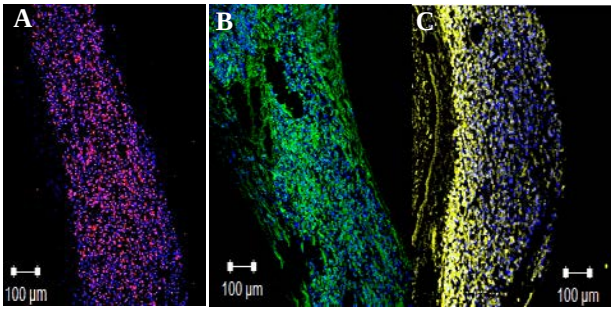

Figure 1: Recellularised nerves maintain Schwann cell phenotype. Primary rat Schwann cells immunolabelled for p75NGFR (A); S100β (B); GFAP (C). Scale bar = 100µm.

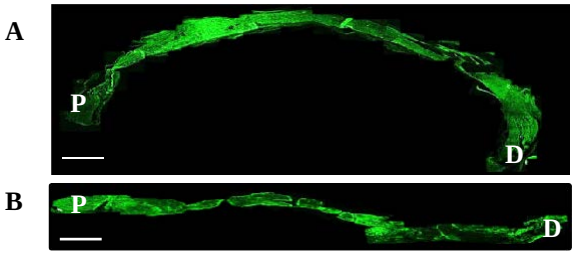

Figure 2: Axonal immunolabelling of nerve grafts. Images show the PGP 9.5 immunolabelling of regenerating nerves in autologous (A) and acellular (B) grafts. P = proximal & D = distal. Scale bar = 100µm.

DISCUSSION & CONCLUSIONS: An optimised decellularisation process for porcine nerves was developed to create acellular grafts, which preserve the native nerve histoarchitecture and ECM components. Seeded Schwann cells were shown to have retained normal cellular phenotype when cultured within acellular porcine nerve. *In vivo* studies established that acellular porcine nerves could promote axonal regeneration; however this was not comparable to autologous grafts in this model. In conclusion, acellular porcine nerves have the potential to promote nerve regeneration.

ACKNOWLEDGEMENTS: This work was funded by the EPSRC (U.K.)

'Dip and dry' micropattern capable bioactive surface coatings for modulating biomaterial associated inflammation

P.J. Taylor[1], N.H. Williams[1], J.W. Haycock[2]

[1]Department of Chemistry, University of Sheffield, S3 7HF, UK. [2] Department of Materials Science & Engineering, University of Sheffield, S1 3JD, UK.

INTRODUCTION:

As quality of life improves there is an increase in the use of implantable biomaterials as medical devices. Although biomaterials are designed to be inert they can trigger host inflammation at the interface, which left untreated can lead to device failure. α-Melanocyte stimulating hormone (α-MSH) is a pleiotropic peptide hormone recognised for its anti-inflammatory properties. Our initial work successfully immobilised a synthetic version of α-MSH [GKP(D)V] onto glass using calixarene surface chemistry which attenuated an inflammatory response *in vitro* [1]. Our latest work incorporates α-MSH onto aryl azide functionalised silanes offering micropatterning capabilities via photolithography based on an established method within the group [2]. The present aim of this work is to optimise the photochemistry of the aryl azide silanes by immobilising a variety of bioactive molecules to provide a direct method for the surface modification of biomaterials. As well as observing the effects of surface patterning we aim to create highly ordered coatings with multifunctional bioactive properties.

METHODS:

Glass coverslips were functionalised with calixarene-PEG-3-GKP(D)V and subjected to biological inflammatory testing (Fig.1). Thereafter, glass coverslips were coated with a photoactive aryl azide organosilane and the surface irradiated to immobilise a modified azido-PEG-6-GKP(D)V tether for micropatterning and subjected to inflammatory testing.

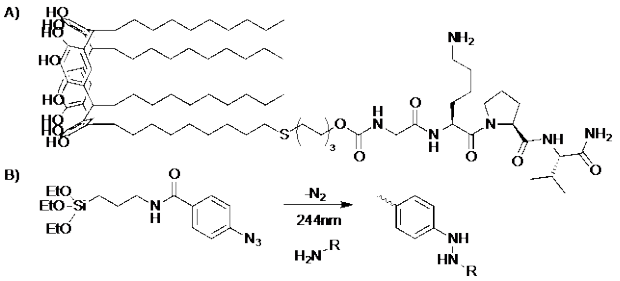

Fig. 1: (A) GKP(D)V peptide attached to a calixarene surface via PEG-3 tether. (B) Summary of aryl azide surface patterning via photolithography [2].

Surfaces were characterised by XPS, SIMS, ellipsometry, and contact angle goniometry. NIH-3T3 mouse fibroblasts and Human umbilical vein endothelial cells were seeded onto surface treated coverslips before stimulation with TNF-α (300 U/mL). To monitor inflammatory cell-signalling activity, the p65 subunit of NF-κB was immunolabeled and quantified by confocal microscopy based on a previous method [3].

RESULTS:

XPS and SIMS confirmed that GKPV(D) was immobilised onto calixarene and aryl azide coated surfaces. Calixarene-PEG-GKP(D)V surface coatings inhibited TNF-α stimulated NF-κB activity by 23% ± 4% (n=3, p=0.001). Inhibition was comparable to control untreated surfaces stimulated with TNF-α and 10^{-9}M GKP(D)V (39% ± 3%; n=3, p=0.003) indicating that coatings require relatively a low peptide load. Similarly, the aryl azide silanated surfaces with N3-HEG-GKP(D)V also reduced NF-κB activity by 28% ± 4% (n=3, p=0.01).

DISCUSSION & CONCLUSIONS:

Data demonstrates that both calixarene and silane immobilisation methods can inhibit NF-κB cell signalling activity involved in the inflammatory response. Current work is focussed on how surface patterning controls anti-inflammatory properties and extends through to carbon monoxide releasing molecules using inorganic carbonyl compounds as a therapeutic approach.

ACKNOWLEDGEMENTS:

We thank the BBSRC and EPSRC for funding this work.

X-ray phase contrast computed tomography as a new imaging modality for three-dimensional, non-destructive analyses of tissue engineering scaffolds

CK Hagen[1], P Maghsoudlou[2], G Totonelli[2], PC Diemoz[1], M Endrizzi[1], A Bravin[3], P De Coppi[2], A Olivo[1]

[1] *Department of Medical Physics and Biomedical Engineering, University College London, London, UK.* [2] *Institute of Child Health, University College London, London, UK.* [3] *European Synchrotron Radiation Facility, Grenoble, FR.*

INTRODUCTION: Scaffolds which allow and promote cell growth are a key instrument in tissue engineering. Imaging is crucial for the development of such scaffolds, initially to gain understanding of the internal structure, and then to monitor interactions with cells and other organs, including ideally post-implantation. Histology and electron microscopy are often the imaging methods of choice; however, they require slicing and/or staining of the sample and provide local information only (rather than across the full sample volume), leaving the field of tissue engineering without a practicable imaging alternative for volumetric analyses, longitudinal studies and post-implantation scaffold monitoring *in vivo*[1]. This talk will focus on the potential of x-ray phase contrast computed tomography (PCT), an emerging imaging modality providing volumetric images without need for destructive sample preparation, to fill this gap. PCT is based on variations of the x-ray wave velocity in materials, introducing phase shifts which can be exploited for contrast generation. For comparison, standard x-ray CT is based on x-ray attenuation differences, which for soft biological samples (e.g scaffolds) often leads to poor image quality. In those cases, phase contrast can be comparably stronger and provide substantially improved visualizations[3]. While PCT had initially been restricted to synchrotrons, at UCL Medical Physics we have developed a translational approach allowing the implementation with standard x-ray sources[4].

METHODS: Scaffolds were derived from a wide range of small rodent organs (e.g. esophagus, lung and liver) via a "gentle" decellularization procedure known as detergent enzymatic treatment (DET) and variations thereof[5,6]. Samples were scanned with PCT, first at beamline ID17 of the European Synchrotron Radiation Facility (ESRF), and then in the radiation laboratory at UCL Medical Physics.

RESULTS: Phase contrast tomograms showed a high image quality in all cases; notably, a comparable image contrast was obtained from the synchrotron and laboratory data. As an example, Fig. 1 shows phase contrast tomograms (axial cross-sections) of esophageal scaffolds (rabbit); in both images, contrast is sufficiently high to identify and assess the structural integrity of all native anatomical layers of the esophagus (mucosa, sub-mucosa, muscularis propria, adventitia, as indicated by arrows in the figure). The images allowed confirming previous histology and electron microscopy-based assessments of the used decellularization protocols, but without the need for slicing/staining of the sample.

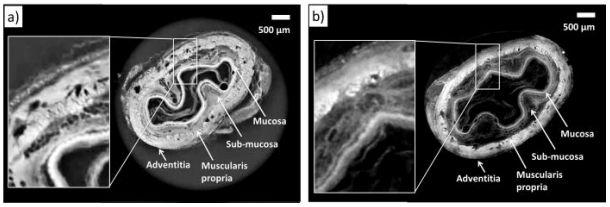

Fig. 1: Phase contrast tomograms of esophageal scaffolds (rabbit) acquired with x-ray phase contrast tomography (a) at a synchrotron and (b) in the radiation laboratory at UCL Medical Physics.

DISCUSSION & CONCLUSIONS: Our results show that PCT has indeed a strong potential to become a valuable imaging tool to the field of tissue engineering. PCT provides three-dimensional images of the full sample volume, is quantitative (i.e. the grey values in the tomograms are directly linked to physical properties of the sample material), and does not require destructive sample preparation. Most importantly, the fact that synchrotron-like image contrast can be obtained in with standard x-ray sources makes the method widely accessible. This implies that PCT could ultimately become a tool for routine inspections and quality control for clinical applications of tissue engineering.

Tendon repair techniques; stress analysis using CT imaging and FE modelling

SD Rawson[1], T Shearer[2], M O'Brien[1], T Lowe[3], JKF Wong[4], L Margetts[5], SH Cartmell[1]

[1] School of Materials, University of Manchester. [2] School of Mathematics, University of Manchester. [3]Manchester X-Ray Imaging Facility, School of Materials, University of Manchester. [4]Plastic Surgery Research, Stopford Building, University of Manchester. [5]School of Mechanical, Aerospace and Civil Engineering, University of Manchester.

INTRODUCTION: Over 50,000 people are treated for tendon injury in the UK per annum [1]. Flexor tendon injury occurs in 4.8 people per 100,000 and of these, 25% attain poor postoperative mobility and over 7% require further surgery [2]. *In silico* mathematical modelling can predict regions of high and low stress in a repair, which indicate acellular regions and poor collagen realignment respectively [3]. Our aim was to observe stresses in a barbed suture repair further to recent re-emerging interest in barbed devices for tendon. Using X-ray micro-CT (μCT), the exact tendon and suture geometry can inform a finite element (FE) model for stress analysis. We have developed a surface staining method that minimises change to tissue mechanical properties to allow scans of the same sample when relaxed and under tension to provide validation for FE results [4]. This method may be modified for *in silico* prototyping of tissue engineered products.

METHODS: Porcine *flexor digitorum profundus* tendons, 3cm in length, were stained in iodine potassium iodide solution (IKI; 0.1%I, 0.2%KI in solution in phosphate buffered saline (PBS)) for 24 hours. 10mm of IKI-stained Quill (Angiotech) suture was passed through the tendon centre from the cut end and samples were submerged in PBS at room temperature in custom tension apparatus.

Two μCT scans were obtained, one with the sample in the relaxed position and the other following a 0.5mm suture withdrawal using the custom bay Nikon Metris 225/320 kV system in the Manchester X-ray Imaging Facility (MXIF). Data was reconstructed using Nikon Metris CTPro (Metris XT 1.6, Version 2.1) and segmented using Avizo standard 7.0 (Visualisation Science Group).

A mesh of mixed hex and tet quadratic elements was produced using ScanIP (Simpleware) and exported to Abaqus (6.13, Simulia), in which a 0.5mm suture withdrawal was simulated. Tendon tissue behaviour was described as anisotropic linear elastic based on multi-scale modelling of tendon fibrils and their surrounding tissue and the suture was described as isotropic linear elastic. [3]

RESULTS: Figure 1 shows the reconstructed volume and FE results, detailing stress in the suture and tendon. The highest stress in both tendon and suture is observed towards the cut end of the tendon (black arrow).

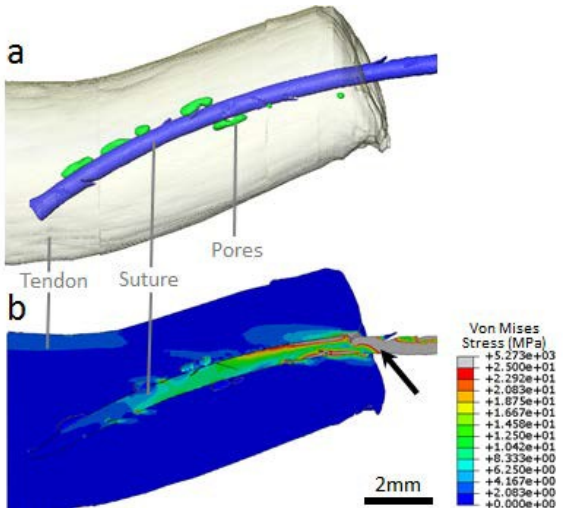

Fig. 1: (a) μCT reconstructed volume and (b) FE results showing stress in tendon and suture following 0.5mm suture withdrawal.

DISCUSSION & CONCLUSIONS: μCT scans reveal pores within the tissue around the suture, indicating tissue damage which impedes barb anchorage. Barbs fail by bending, peeling or tissue pull-out. FE results demonstrate high stress at the initial barbs (Fig 1. black arrow), which suggests uneven loading along the length of the barbed suture. The μCT results for 0.5mm suture pull agree with the deformation predicted by FE analysis, validating the method of analysis.

ACKNOWLEDGEMENTS: The authors would like to thank the MRC (grant code: MRC:G1000788/1) and the EPSRC (DTA studentship) for funding this work along with the MXIF at the University of Manchester for μCT equipment access and expertise.

Engineering the kidney: The effects of scaffold architecture

TP Burton[1], A Callanan[1]

[1] *Institute for Bioengineering, School of Engineering, University of Edinburgh, Scotland*

INTRODUCTION: Polymer based scaffolds, such as polycaprolactone (PCL), have been highlighted as a potential avenue for tissue engineered kidneys, but there is little investigation down this stream[1]. Electrospinning is a fabrication technique used in tissue engineering (TE) producing fiber diameters from 10's of nanometers to 10's of microns. This variation in morphology has been shown to effect the way cells behave and integrate with the scaffold. With larger fibers allowing greater cell integration, nanofibers representing the natural ECM and aligned fibers guiding cell growth[2]. The aim of this study is to examine the cellular response to scaffold architecture of novel electrospun scaffolds for kidney TE.

METHODS: Two sets of parameters were used for electrospinning PCL to yield 'large' and 'small' fibers. Large fibers were created using 19% w/v PCL in chloroform/methanol (5:1) and parameters: 4 ml/hr, +15kV, -4kV, 23 cm working distance and 0.8mm needle bore. Small fibers were made using 7% w/v PCL in HFIP and parameters: 0.8 ml/hr, +14kV, -4kV, 12cm working distance and a 0.4mm needle bore. Traditional random fibers were spun onto a mandrel rotating at 250 rpm, aligned at 1800 rpm with novel cryogenic fibers spun onto a mandrel loaded with dry ice rotating at 250 rpm. SEM was used to confirm fiber diameter and morphology.

RC-124 human kidney epithelial cells used to assess the scaffolds, validated by cell viability assay (CellTitre-Blue), DNA quantification assay (Pico Green), RT-qPCR (GAPDH, AQP-2, KRT-8, KRT-18, E-CAD) and two-photon excitation fluorescence (TPEF) along with coherent anti-stokes Rahman scattering (CARS).

RESULTS: Scaffolds had average fiber diameters of 1.1±0.16 µm and 4.49±0.47 µm. Cryogenic fibers has a significantly larger porosity and aligned considerably less. This resulted in a considerable difference in mechanical properties.

Cryogenic scaffolds presented with considerably less cell attachment compared with random and aligned. Large fibers showed greatest cell viability after 3 and 7 days, *fig. 1*.

TPEF and CARS images clearly show the effects of scaffold architecture and how the cells distribute between the fibres, *fig. 2*.

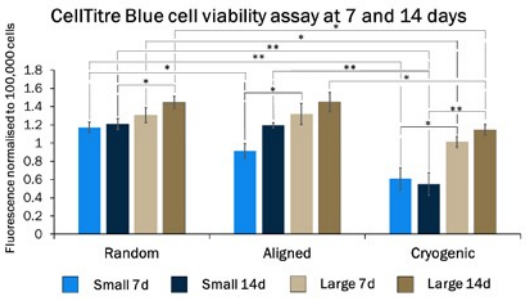

Fig. 1: Cell viability assay at 3, 7 and 14 days of large and small fibers.

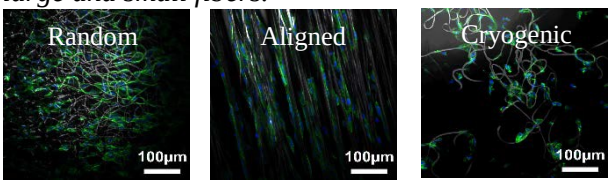

Fig. 2: TPEF and CARS images of RC-124 cells on scaffolds with a large fibre diameter at 7 days. Green highlights the actin filaments, blue shows the cell nucleus and white is the PCL scaffold; clearly showing the impact of the scaffold architecture on cells growth.

DISCUSSION & CONCLUSIONS: Architecture of the scaffold has a profound effect on kidney cells; whether that is effects of fibre diameter on the cell attachment and viability or the effect of fibre arrangement on the distribution of cells and their alignment with fibers. Results demonstrate that PCL scaffolds have the capability to maintain kidney cells life and should be investigated further as a potential scaffold in kidney tissue engineering.

Future strategies of greater clinical relevance in kidney TE will require the exploration of self-organising kidney stem cells in 3D environments, such as electrospun polymer scaffolds, to see if they are a viable conduit for creating embryonic stage kidneys.

ACKNOWLEDGEMENTS: This research is funded by an Engineering and Physical Sciences Research Council (EPSRC) Doctoral Training Partnership (DTP) Studentship.

A BioArtificial Liver machine to treat patients with acute liver failure: pivotal results in a pre-clinical trial

C Selden, J Bundy, E Erro, S Modi, S Chalmers, B Fuller, H Hodgson, D Kahn*, D Thomson, G Chinnery, M Miller*, N Mankahla*, A Isaacs* R Lucas*, I Botes*, G Dankers*, H Ilsley*, L Loo*, R Ginsburg, W Spearman*.

*UCL Institute for Liver and Digestive Health - The Liver Group, Royal Free Hospital Campus, UCL Medical School, London, UK. * University of Cape Town, Groote Schuur Hospital, Cape Town, South Africa*

INTRODUCTION: Acute liver failure (ALF) has a very poor outcome unless patients receive a transplant, however, donor organs are scarce and many patients die on the waiting list. As the liver has capacity to repair and regenerate given time, there is an opportunity to temporarily support the failing liver. We developed a bioartificial liver machine with human-derived encapsulated 3-D spheroids[1], to provide a range of liver function to support a failing liver. Here we tested it at clinical scale in porcine ischaemic acute liver failure, where pigs had livers equivalent to human size.

METHODS: Anaesthetised 30-35kg pigs, n=10 (livers 1.2-1.7kg) were subjected to permanent surgical liver ischaemia. After ~2.5h ischaemia severe ALF was established. Biomass containing ~$7x10^{10}$ cells (BAL) was produced in UK, shipped at ambient temp. to South Africa, and connected to the pig via a plasma-exchange machine in an extracorporeal circuit, for up to 8h. Blood samples were analysed for chemical pathology, blood gases and haematology. A control group was treated with the same circuit containing alginate beads without cells. Brain probes estimated Intracranial Pressure and brain oxygenation. Haemodynamic parameters were estimated with Picco technology, via intra-arterial and jugular venous probes.

RESULTS: All measured parameters of liver failure worsened with time in the control group as expected. The BAL treated group demonstrated improved acidosis, eg pH, lactate, base excess, and improved blood clotting as estimated by Thromboelastography, Prothrombin time and INR. Intracranial pressure rose more slowly in the BAL treated than in the control group, and brain oxygenation was improved in the BAL treated group. The haemodynamic status of the pigs in the control group required high doses vasopressor throughout without effect at the later times, whereas on addition of the BAL treatment requirements for vasopressors (noradrenaline) were stabilised and reduced (Fig 1). Biomass viability was maintained throughout. The treatment occurred at a site far removed from biomass production and demonstrated this approach would be deliverable worldwide.

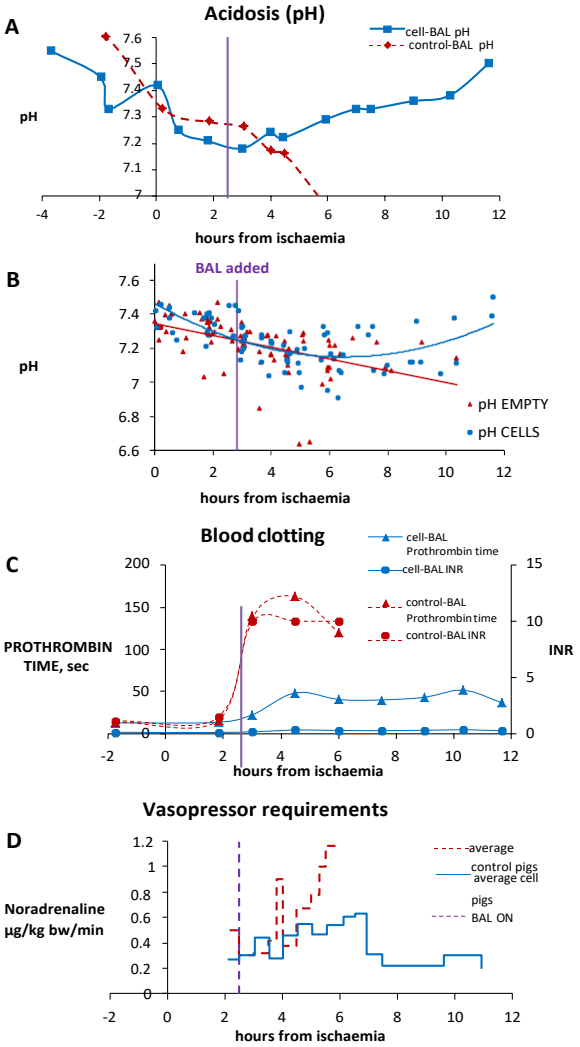

Fig. 1. ***CONTROL-treated pigs (red) vs. a CELL-BAL (blue) treated pigs.*** *BAL started 2.5h.*

DISCUSSION & CONCLUSIONS: The BAL was efficacious at human scale porcine model of ALF. Significant changes in blood clotting implied synthesis of clotting factors, confirmed by human proteins identified in pig plasma.

ACKNOWLEDGEMENTS: Template modified with kind permission from eCM Journal. We thank the Wellcome Trust for funding. (096861/Z/11/Z). We also thank Prof. P. Zilla for use of his large animal operating theatre and lab facility.

Safety of Real Architecture for 3D tissues - Tissue Equivalent in the live cornea

L Morgan[1], A Peters[1], AJ Shortt[2], S Tuft[3], and JT Daniels [1]

[1] Department of Ocular Biology and Therapeutics, UCL Institute of Ophthalmology, London, EC1V 9EL, UK. [2] UCL Institute of Immunity and Transplantation, Royal Free Campus, Rowland Hill Street, London, NW3 2PF, UK. [3]Cornea & External Eye Disease, Moorfields Eye Hospital NHS Foundation Trust, 162 City Road, London EC1V 2PD, UK.

INTRODUCTION: Real Architecture for 3D Tissues - Tissue Equivalent (RAFT-TE) is a plastic compressed collagen type-1 membrane comprising collagen alone, or containing live cells. RAFT-TE was developed as a potential treatment for persistent corneal deficit[1]. The present study evaluated host response to RAFT-TE in the live cornea.

METHODS: RAFT-TE (with, or without live human keratocyte cells) was set into a recess cut into the center of the anterior cornea of 12 rabbits.

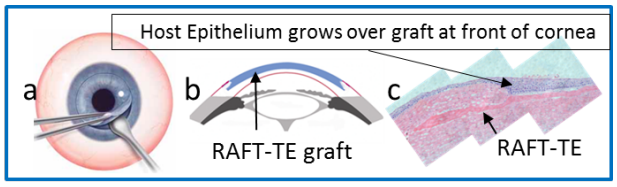

Fig. 1: Superficial anterior lamellar keratectomy (SALK) is used to remove a small circle of the anterior corneal stroma and epithelium (a), graft was applied with fibrin glue (b), graft edges were tucked into a pocket cut into the stroma (c, H&E stain)

Two ophthalmic surgeons independently analysed identity-masked eye surface images, they rated neovascularization (limbal vascular plexus vessels growing into the cornea), scarring, epithelial integrity, inflammation, and looked for RAFT-TE changes.

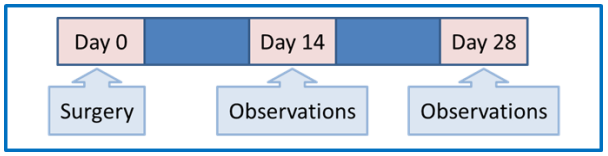

Fig. 2: RAFT-TE is observed for 28 days

Host response to the graft was analysed following termination on day 28 by immunohistochemistry, immunofluorescence, lectin histochemistry and H&E stain of tissue sections.

RESULTS: Analysis of *in vivo* images showed that epithelium cover of RAFT-TE was near complete and RAFT-TEs were all more transparent by day 14, no neovascularisation was seen by day 28. *Ex vivo* analysis of tissue sections indicated that RAFT-TE was still in place after 28 days. Small gaps in the RAFT-TE indicated that some remodelling of RAFT-TE collagen had occurred. Epithelial growth over RAFT-TE appeared normal and only a very few macrophage-like cells were detected, all near the site of the SALK cut. There was a small increase in cell density under the RAFT-TE in places but no sign of inflammation in response to RAFT-TE.

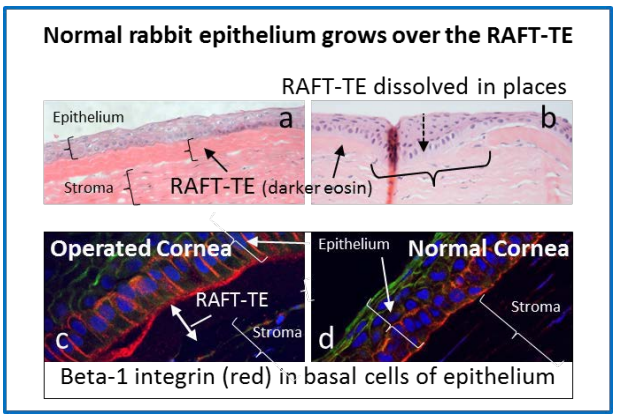

Fig. 3: After 4 weeks in vivo RAFT-TE remains in place on the stromal surface and is now covered by host epithelium (a). In places the RAFT-TE has disappeared (b). The newly synthesised epithelium covering the graft shows normal beta-1 integrin distribution (c); compare to control cornea (d).

DISCUSSION & CONCLUSIONS: RAFT-TE was successfully incorporated between newly synthesised host corneal epithelium and the anterior stroma. RAFT-TE did not stimulate inflammation, corneal scar formation or neovascularisation indicating that the RAFT-TE is well tolerated *in vivo* and that no safety issues have been revealed.

ACKNOWLEDGEMENTS: Medical Research Council MRC, Cells for Sight, NHS National Institute for health research, Moorfields Eye Hospital NHS Foundation Trust, Dept. Surgical Research, Northwick Park Institute for Medical Research.

Mapping the viscoelastic mechanical properties of spinal cord tissue: implications for regenerative medicine and tissue engineering in the CNS

RD Bartlett[1,2], D Choi[2], JB Phillips[1]

[1] *Biomaterials & Tissue Engineering, UCL Eastman Dental Institute, UCL, England.* [2] *Brain Repair & Rehabilitation, Institute of Neurology, UCL, England*

INTRODUCTION: It is widely regarded that the mechanical properties of a tissue have the potential to profoundly affect cell behaviour [1]. As such, to optimise the cell response in tissue engineered constructs, it is important to consider the mechanical properties of the host tissue. Given that the spinal cord is viscoelastic, accurate mechanical characterisation has so far been difficult. Thus, we aimed to develop a reliable testing protocol to probe the mechanical properties of spinal cord tissue, and one which could ultimately be used to screen candidate biomaterials for tissue engineered constructs of the future.

METHODS: Wistar rats (male) weighing between 340 - 400 g were culled and spinal cords displaced using a fluid-filled syringe. These were then placed immediately into iced tissue-preservation media. Cord was cut into ~5 mm sections, and height measurements for each sample were taken using a goniometer. Mean height was then calculated, and this used to compute a 0.5 % dynamic strain specific for each sample.

Samples were then placed in a Dynamic Mechanical Analysis (DMA) system (Bose ElectroForce 3200), where they underwent an ascending frequency sweep of 1 – 100 Hz. A 1 Hz validation frequency was repeated to test for signs of mechanical destruction. Pre- and post-DMA geometric measurements were also taken as a means of validation. Testing occurred at room temperature, and 100 % humidity was maintained throughout. All samples underwent a 1 Hz pre-conditioning cycle before being tested.

RESULTS: Testing revealed that rat spinal cord had a compound modulus of 10 – 22 kPa over a 1 – 100 Hz frequency range. This was strain-rate dependent, and stiffness increased non-linearly towards higher frequencies. Tan delta also increased with frequency, indicating that the viscous phase (E”) of mechanical behaviour became increasingly dominant at higher strain-rates. Validation revealed that testing was minimally destructive to tissue, and comparison of modulus in the cervical, thoracic, and lumbar regions revealed no significant differences in tissue stiffness by local anatomical location.

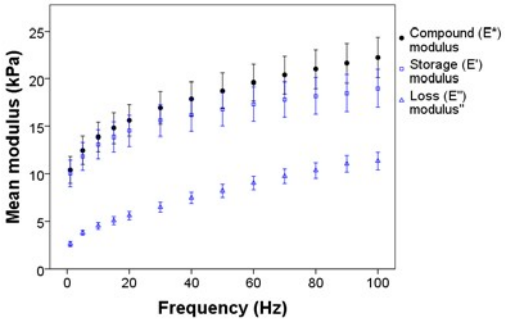

Fig. 1: Compound (E*), storage (E’) and loss (E”) moduli for fresh rat spinal cord over an ascending frequency sweep. Error bars depict ± SEM (n = 6).

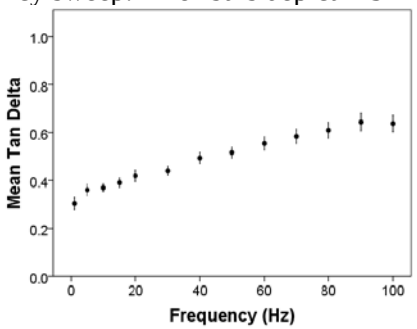

Fig. 2: Scatter graph of tan delta, displaying how the viscous component of spinal cord tissue became more dominant as frequency increased. Error bars depict ± SEM (n = 6).

DISCUSSION & CONCLUSIONS: Values obtained for rat spinal cord modulus were in accordance with previously published literature [2]. However, in contrast to other mechanical characterisation techniques available, and concordant with viscoelastic behaviour, our protocol elucidated a range of modulus values for spinal cord tissue. We believe it offers a useful method to directly compare the mechanical properties of spinal cord tissue to candidate biomaterials, and overall represents a useful new addition to the CNS tissue engineering toolbox.

UCL-BAL: Development of three-dimensional mammalian cell culture at clinical scale

E Erro, J Bundy, S Modi, S Chalmers, B Fuller, H Hodgson, C Selden.
UCL Institute for Liver and Digestive Health (ILDH) - The Liver Group, Royal Free Hospital Campus, University College Medical School, Upper Third floor, Rowland Hill St, London, NW3 2PF.

INTRODUCTION: Acute liver failure is a rising problem in healthcare with a high likelihood of mortality. Current treatment in most cases requires a liver transplant, however there is a shortage of donor organs - many patients succumb to the acute injury before one can be procured, or before spontaneous hepatic regeneration can occur. The UCL-BAL (bioartificial liver) system could provide support, 'buying time' for a positive outcome.

A human hepatoblastoma-derived cell line (HepG2) was encapsulated in an alginate matrix and cultured in a perfused fluidised-bed bioreactor (FBB). Both the semipermeable alginate hydrogel and the FBB microgravity environment maximise mass transfer of metabolites to and from the perfusate, and promote the formation of 3D multicellular spheroids[1], a better approximation of liver tissue architecture than achieved with monolayer culture[2] or other BAL types (e.g. hollow-fibre cartridge-based BALs).

Encapsulated-HepG2 biomass was cultured for 11-13 days to reach 'performance competence'. The methodology used was developed from re-usable stainless steel[3] to single-use technology for translation to a future GMP setting and first-in-man trial.

METHODS: HepG2 cells were first rederived as a GMP Master- and Working-Cell Bank, then cultured as monolayers in T-flasks (500cm^2, triple-layers) using modified alphaMEM media, until seeding into Thermo Fisher Cell Factories (6320cm^2, 10-layers) for 6 days. Harvested cells were encapsulated into a sterile 1% alginate solution using the GeniaLab Jetcutter system (8 nozzle jets, ~20mL/min), producing >2-3L spherical 'beads' of ~500µm diameter.

Beads were transferred to a chamber and perfused with media in a batch fed process from a 100L Single-Use Bioprocess Container (SUB, Thermo Fisher); fresh media was replaced in the reservoir regularly. An Applikon ezControl system provided temperature, pH and Dissolved Oxygen (DO) control in the reservoir, and additional oxygenation directly to the biomass chamber at higher levels of oxygen consumption.

Beads were seeded at ~2x10^6 cells/mL (measured using Chemometec NC-100 Nucleocounter). Cell viability was assessed using Fluorescein Diacetate (FDA) and Propidium Iodide (PI) staining of beads. Synthetic capacity of spheroids was assessed via production of α-fetoprotein (AFP), a protein produced by the biomass but not normally found in normal human plasma. A fluidised bed was established at a flow rate of ~380mL/min.

RESULTS: Cell Factories yielded 1.57x10^{10} ± 2.45x10^9 cells from monolayer (n=19, ±SD). Encapsulated-HepG2s in the FBB proliferated to 3.05x10^7 ± 5.9x10^6 cells/mL biomass; 7.52x10^{10} ± 1.7x10^{10} total viable cell biomass (n=15; ±SD) in ~2.5L alginate beads, with cell viability >98%. AFP production was 7864 ± 2557 ng/million-cells/day (n=12, ±SD). Lactate concentration in FBB media did not increase >12mM; glucose did not drop below 15mM. Sterility was assured by regular sampling and testing in Bactec tubes, Royal Free Hospital Microbiology. Average bead diameter did not change significantly during FBB proliferation phase.

DISCUSSION & CONCLUSIONS: Whilst the exact number of cells in a human liver is disputed (~1-2x10^{11}), we can deliver 30-70% of this in our viable biomass, sufficient to treat a patient. We have successfully developed a closable, GMP-like methodology to be translated at each stage to a clinical setting with single-use/sterile technology. Encapsulated cell spheroids can be effectively cryopreserved, and may also have a range of other applications.

ACKNOWLEDGEMENTS: This template was modified with kind permission from eCM Journal.

A postoperative treatment for Barrett's oesophagus using injectable, self assembling peptides.

D Kumar[1], V L Workman[2], Krish Ragunath[3], A Saiani[2], FRAJ Rose[4] and J E Gough[1].

[1] *School of Materials, Materials Science Centre, University of Manchester, UK.* [2] *Polymer and Peptides Group, Manchester Institute of Biotechnology, University of Manchester, UK.* [3] Nottingham Digestive Diseases Centre, Queens Medical Centre Campus, *Nottingham University Hospital NHS, UK.* [4] *School of Pharmacy, Centre for Biomolecular Sciences, University of Nottingham, UK.*

INTRODUCTION: Barrett's oesophagus is a precancerous condition whereby a change in the epithelium is observed caused by gastro-oesophageal reflux disease[1] (GORD). Current surgical treatments elicit rapid inflammatory responses resulting in subsequent strictures. Though this can be suppressed by direct injection of steroids, an intervention is required to improve treatment outcome. In this study, we propose the use of synthetic peptide hydrogels, which are injectable, mimic nano-architectural structure of extracellular matrix, to provide a protective barrier following thermal ablation, and encourage rapid re-epithelialisation to suppress the inflammatory response.

METHODS: A variety of synthetic peptides (containing a sequence of 8-9 amino acids; www.peptigeldesign.com) were dissolved at 30mg/mL in HPLC grade water and neutralized to allow hydrogel formation. Following buffering in culture media overnight, primary rat oesophageal stromal fibroblasts (rOSFs) were incorporated into the peptide hydrogels, whereas mouse oesophageal epithelial cells (mOECs) were seeded on top mimicking the *in vivo* arrangement of these cell types. Cell-gel constructs were validated for cell viability, proliferation and migration of epithelial cells across the hydrogel surface. The composite model was assessed using histology, which included the characterization of key epithelial markers. Mechanical and degradation properties of hydrogels were investigated in acellular conditions when cultured under standard media or simulated gastric fluid (SGF) conditions, mimicking the *in vivo* GORD environment.

RESULTS: The inherent mechanical properties and peptide sequence of the hydrogels influenced cell viability (mOECs and rOSFs) and behavior. mOECs proliferated well and formed a sheet on top of the hydrogels, whilst retaining morphology, cell-cell tight junctions and the expression of expected cytokeratins (Fig 1A). rOSFs were homogenously incorporated into hydrogels and demonstrated good cell viability and typical morphology after 7 and 14 days of culture (Fig 1B). No significant differences were determined in the stiffness of gels when immersed in cell culture media and SGF culture conditions over 14 days. However, each peptide hydrogel displayed a unique stiffness profile over 14 days.

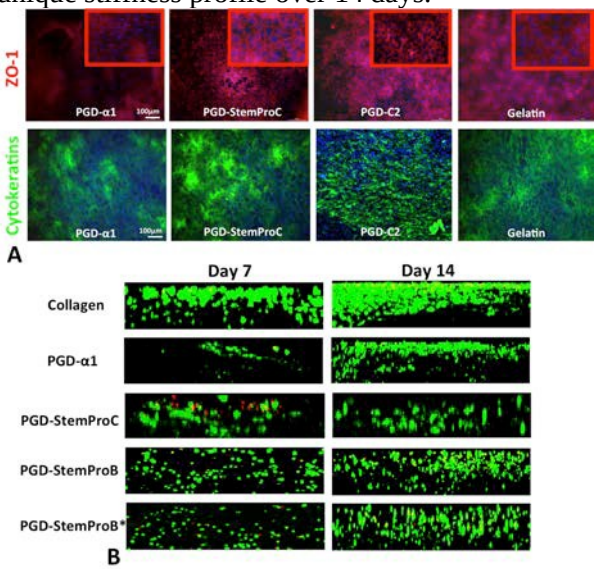

Fig. 1: (A) Expression of ZO-1 and cytokeratins in mOECs cultured on top of peptide hydrogels for 3 days. (B) Demonstrating cell viability and distribution of rOSFs when incorporated into the peptide hydrogels and cultured up to 14 days.

DISCUSSION & CONCLUSIONS: Assessment of these peptides provides a platform to further develop a composite hydrogel system with incorporated anti-inflammatory properties, which will be tested further under simulated gastric conditions.

ACKNOWLEDGEMENTS: Medical Research Council, the Engineering and Physical Sciences Research Council and the Biotechnology and Biological Sciences Research Council UK Regenerative Medicine Platform Hub "Acellular Approaches for Therapeutic Delivery" (MR/K026682/1)

Changes in human mesenchymal stem cells behaviours in low-voltage direct current electrical field

S Mobini[1], K Srirussamee[1], R Xue[1], Ü Talts[1], R Balint[1], NJ Cassidy[2], SH Cartmell[1]

[1] *School of Materials, The University of Manchester, Manchester, UK*

[2] *School of Physical and Geographical Sciences, Keele University, Stoke-on-Trent, UK*

INTRODUCTION: Electrical stimulation (ES) has been utilized as clinical solution to reduce pain and inflammation and to promote healing and regeneration. Mesenchymal stem cells (MSCs) are known as key player in regeneration and healing procedures. While the mechanism is still poorly understood, *in vitro* studies showed that ES alters several MSCs' behaviours such as, morphology, orientation, proliferation, migration and differentiation [1, 2]. In this study we investigate the effect of low-voltage direct current ES on morphology, proliferation and osteogenic differentiation of human bone marrow derived MSCs.

METHODS: 100mV/mm DC electrical field was applied to the cells in 2D culture, for 1hr per day by means of a custom-made electro-bioreactor. The device is basically the L-shaped pure platinum electrodes secured to the top lid of 6-well cell culture plates and connected to a DC electrical power generator [3]. The electrical field distribution in the culture area was modelled using Finite Element Method (FEM) by COMSOL-Multiphysics software. Electrically stimulated (ES) were compared with not stimulated (Control) cell groups, cultured both in osteogenic induced medium (OM) and growth medium (GM), at different time points (7, 14 and 21 days). To observe cell orientation, cytoskeleton and actin filament distribution changes, Phalloidin and DAPI staining were applied to both groups and images were analysed using CellProfiler and visualized by custom-made software. Proliferation was assessed by Alamar Blue assay and DNA concentration measurement. Calcium accumulation, as an indicator for osteogenic differentiation, were evaluated by AlizarinRed staining. AlizarinRed stain was quantified by reading absorbance with spectrophotometer. Calcium amount in cell lysate was measured by colorimetric calcium assay. Total RNA was isolated in each time point from cell lysate and expressions of osteogenic genes (Runx2, Osteopontin, Col1A2, BMP2, ALP) were assessed by RT-qPCR technique.

RESULTS: Computational model of the electrobioreactor showed that electrical field in the culture area between the electrodes is almost homogeneous. Semi-quantitative analysis of cell orientation and actin fibers alignment in relation to the electrical field indicated that low voltage electrical filed influence the cell and cytoskeleton alignment in the vicinity of the cathode. Proliferation capacity of the ES groups was sustained slightly higher than control specifically in OM medium. Calcium contents are significantly higher in ES groups at day 7, however this amount become similar for both ES and control groups at day 14 and the trend was reversed at day 21.

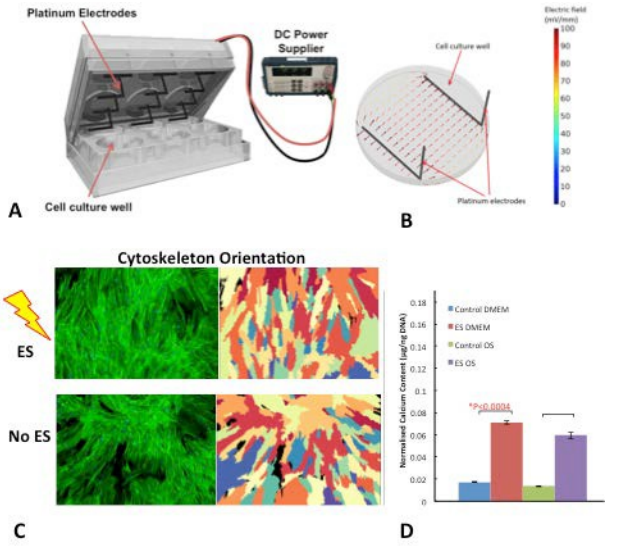

Fig. 1: A) Custom-made electro-bioreactor, compatible with 6-well plates. B) Computational modelling shows homogenous electrical field C) Cell alignment near the cathode D) Calcium concentration in ES vs. controles

DISCUSSION & CONCLUSIONS: This study shows low voltage electrical stimulation evidently influences hMSCs' orientation, cytoskeleton alignment, proliferation and differentiation within the first week. These reactions are dissimilar in different culture conditions.

ACKNOWLEDGEMENTS: This work is financially supported by BBSRC BB/M013545/grant.

Novel PGSm nerve guidance conduits for peripheral nerve repair *in vivo*

DS Singh[1], E Albadawi[2], A Harding[2], F Boissonade[2], JW Haycock[1], F Claeyssens[1]
Department of Materials Science & Engineering, University of Sheffield, U.K.[1]
School of Clinical Dentistry, University of Sheffield, U.K.[2]

INTRODUCTION: There are three clinical approaches to aid peripheral nerve regeneration: i) suturing; ii) autograft surgery or iii) the use of nerve guide conduits (NGCs)[1]. NGCs are an attractive alternative to autografts, mainly because autografts lead to loss of function, pain and potential morbidity in the donor site. Both synthetic and natural material-based NGCs are commercially available. These products are often simple designs with material properties far stiffer than the native tissue. This leads to current NCGs being relatively ineffective for anything other than very short nerve gaps. To address this we have developed a novel methacrylated version of polyglycerol sebacate (PGSm). PGSm is a soft material, which has mechanical properties (i.e. Young's modulus) similar to that of nerve. It is also is biocompatible, biodegradable and can be structured by 3D printing (micro-stereolithography). This allows for more complex designs of NGCs to be produced via CAD, maintaining the beneficial material properties of PGS, whilst avoiding some of the limitations (e.g. time for thermal curing, and the instability of the reagents in the similarly acrylated versions of the polymer[2].)

METHODS: PGS was synthesised through polycondensation reactions of glycerol and sebacic acid. Methacrylate moieties were added to create, with the addition of a photoinitiator, a photocurable material. The material was characterized by GPC, FTIR, NMR, DSC, rheology, nanoindentation, tensile mechanical analysis, water contact angle measurements and suture tests. Several forms of PGSm were produced with a tuneable extent of methacrylation, to control material properties. Long term degradation studies and *in vitro* enzymatic degradation studies were performed on PGSm NGCs. Samples were evaluated *in vitro* using NG108-15 neuronal and primary Schwann cells. PGSm was then structured by stereolithography into NGCs (5mm long / 1.3mm internal diameter) and used to bridge a Thy-1-YFP-H mouse 3mm common fibular nerve injury, with nerve graft as control.

RESULTS: Neuronal cell live dead analysis showed PGSm samples had a live cell percentage of 92% compared to glass controls (84%), confirming that PGSm samples were a good substrate for neuronal cell adhesion and had no neuronal toxicity. Through neurite analysis it was found that PGSm was able to support neuronal cell differentiation, and primary Schwann cell adhesion and growth. Overall, *in vitro* analyses indicated that PGSm was permissive for use as a novel NGC material. *In vivo* studies using a mouse Thy-1-YFP-H common fibular nerve 3mm gap injury showed regeneration over a 3 week period, from proximal to distal stump [Fig.1]. Fluorescent axons are currently being analysed and quantified.

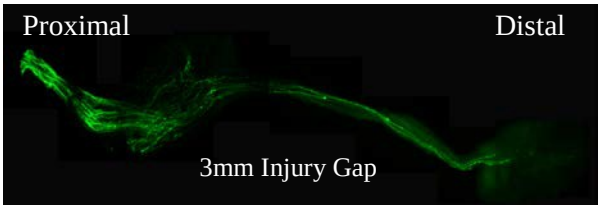

Fig. 1: A composite confocal micrograph showing common fibular nerve regeneration of fluorescent axons through a PGSm NGC across a 3mm injury gap (3 weeks - Thy-1-YFP-H mouse model).

DISCUSSION & CONCLUSIONS: PGSm has tuneable material properties such as Young's modulus and degradation rate. It is a permissive substrate for neuronal and Schwann cell growth and is easily structured using UV light-based stereolithography. This makes PGSm a good candidate biomaterial for peripheral nerve regeneration using NGCs. Initial *in vivo* studies indicate nerve regeneration through 5mm NGCs to the distal stump of the nerve (using a 3mm injury gap). Initial histology of regenerating fluorescent nerves confirms that axons regenerate from the proximal stump, through the NGC and into the distal stump [Fig.1]. We are currently conducting detailed quantification of axon regeneration for comparison with that achieved using 'gold standard' nerve graft repair.

In vitro experiments to inform cell seeding strategies and parameterize a mathematical model for peripheral nerve repair

G Kennedy[1,2], RH Coy[3], C Kayal[2], C O'Rourke[4], PJ Kingham[5], RJ Shipley[2], JB Phillips[4]

[1] Department of Mathematics, University College London, UK. [2] UCL Mechanical Engineering, University College London, UK. [3] CoMPLEX, University College London, UK. [4] Biomaterials & Tissue Engineering, UCL Eastman Dental Institute, University College London, UK. [5] Department of Integrative Medical Biology, Umea University, Sweden.

INTRODUCTION: Cellular collagen constructs have been used to support peripheral nerve regeneration using stem cells that have been differentiated to a Schwann cell-like phenotype [1]. These cells are also likely to release vascular endothelial growth factor (VEGF) in response to local hypoxia, thus promoting vascularisation of the construct. However, prolonged hypoxia caused by overly dense cell seeding and insufficient vascularisation could cause cell death. To inform the cell seeding strategies of the constructs to optimise cell survival and VEGF release**,** and parameterize a mathematical model of the construct in vivo, the effect of low oxygen concentration on the cells at a range of seeding densities was investigated in a 3D collagen environment similar to that used in engineered neural tissue [1].

METHODS: Differentiated adipose-derived stem cells (dADSCs) were seeded at a range of densities in 2mg/ml type I rat tail collagen hydrogels in a 96-well plate, and stabilized using RAFT^{TM} (TAP Biosystems, UK). The gels were maintained at one of five selected oxygen concentrations for 24h.
Viable cell density was calculated using CellTiter-Glo 3D Reagent (Promega) to measure metabolic activity and relate this to a number of viable cells, and the concentration of VEGF released into the media was measured using ELISA.

RESULTS: The analyses revealed a comprehensive pattern of cell responses to both seeding density and oxygen environment, examples of which are shown in Figures 1 and 2. There was a greater increase in viable cells at 24h with an initial cell density of 1 x 10^6 cells/ml than with the higher initial densities (Fig 1). Lower oxygen environments resulted in increased VEGF release compared to higher oxygen environments (Fig 2).

DISCUSSION & CONCLUSIONS: The results suggest a strong link between seeding density, oxygen environment and resulting viability and

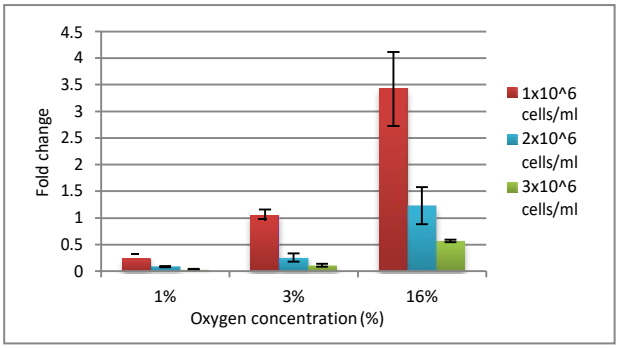

Fig. 1: Fold change in number of viable cells at 24h for initial seeding densities of 1, 2, 3 million cells/ml of gel before stabilisation.

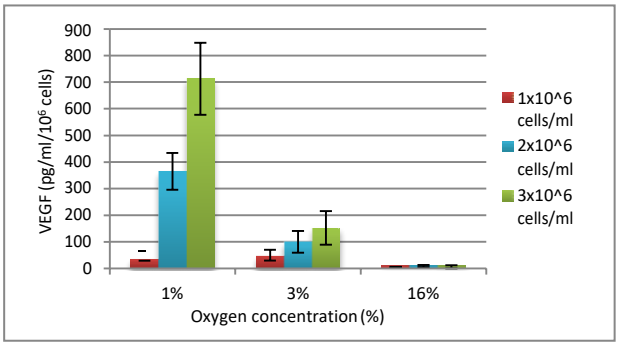

Fig. 2: VEGF present at 24h (pg/ml/10^6 cells).

VEGF release. The viability data show a strong indication that lower initial densities should be favoured for the survival of therapeutic cells, particularly for repairs in poorly vascularised tissue environments. These results further motivate the need for a more sophisticated way of optimising cell-seeding strategies in nerve repair and other regenerative medicine scenarios. Future research will use these and other data to parameterize a mathematical model to enable optimisation of cellular constructs.

ACKNOWLEDGEMENTS: This work was supported by EPSRC, and a doctoral training grant SP/08/004 from the British Heart Foundation (BHF) to RC.

Bioprinting using mechanically robust core-shell cell-laden hydrogel fibres

P Mistry[1], A Aied[1], M Alexander[1], K Shakesheff[1], A Bennett[2], J Yang[1]

[1]*Division of Drug Delivery and Tissue Engineering, School of Pharmacy, University of Nottingham, UK*

[2]*FRAME Laboratory, School of Life Sciences, University of Nottingham, UK*

INTRODUCTION: Core-shell cell-laden fibres represent an innovative approach to the formation of 3D tissues in the field of regenerative medicine [1]. They resemble many native tissues such as tendons, nerves, muscles and blood vessels. Fabricated fibres must: 1) provide an extracellular matrix-like environment to support cell growth, 2) be mechanically robust to withstand forces during *in vitro* manipulation and after implantation, and, 3) be spatially manipulatable to produce desired 3D tissue-like structures. In this study, we demonstrate a method to 3D print core-shell cell-laden fibres which are both mechanically robust and supportive for cell survival and function.

METHODS: The fibres were printed into 3D structures using a commercial 3D printer modified with a custom-built co-axial needle for core-shell fibre extrusion. We have used a hybrid shell material consisting of alginate and poly(ethylene glycol) diacrylate (PEGDA). ECM-like materials were used to form the core. Tensile testing was performed to characterise the mechanical properties of the shell material. Cell viability and function within the fibres were characterised. Furthermore, the release profiles of proteins and peptides from these fibres were examined.

RESULTS: Addition of PEGDA to alginate synergistically improved the mechanical properties of the hybrid hydrogel in a composition-dependent manner (Figure 1). We have also demonstrated the printability of the fibres into complex 3D structures with different core materials (Figure 2). Both cell lines and primary cells were encapsulated within the core of the fibres and demonstrated sustained cell viability for two weeks (Figure 3). The cells were also able to proliferate, indicating core stability and sufficient nutrient diffusion through the shell material.

DISCUSSION & CONCLUSIONS: We have 3D printed complex structures from core-shell fibres and shown compatibility with cells. Furthermore, we have demonstrated improved elasticity and strength of the hybrid shell material.

REFERENCES: [1]Onoe *et al.* Meter-long cell-laden microfibres exhibit tissue morphologies and functions. *Nature Materials*, 2013.

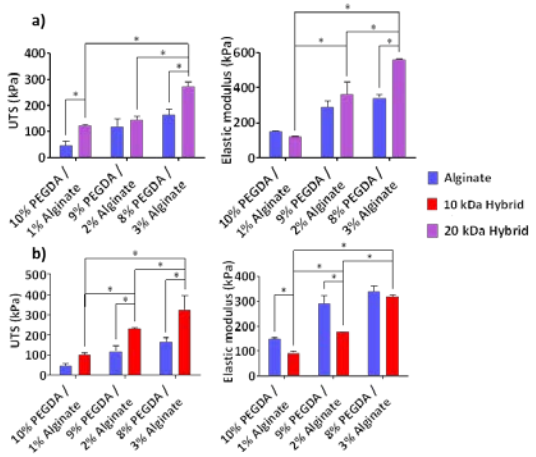

Figure 1: Mechanical properties of hybrid hydrogels versus pure alginate hydrogels, showing tensile strengths (UTS) and elastic moduli. The molecular weight of PEGDA was also varied. A) 20 kDa PEGDA. B) 10 kDa PEGDA.

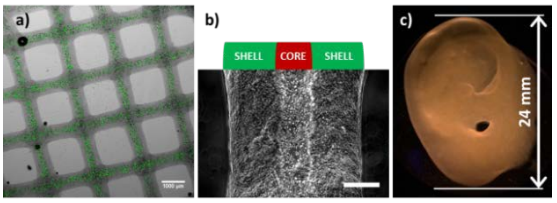

Figure 2: Core-shell fibres were printed into various 3D structures. A) A lattice with a core of 3T3 fibroblasts. Scale = 1 mm. B) A single printed fibre. Scale = 200 µm. C) An ear shape.

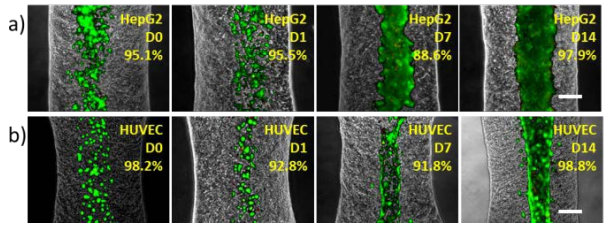

Figure 3: Cell viability and morphology in the core of printed fibres. Cells were stained with calcein-AM (live) and ethidium homodimer-1 (dead). A) HepG2 hepatoma cells in collagen. B) Human umbilical vein endothelial cells in Matrigel. Scale = 200 µm.

ACKNOWLEDGEMENTS: We would like to acknowledge the EPSRC & MRC Centre for Doctoral Training in Regenerative Medicine and the EU CASCADE fellowship scheme for supporting this research.

PDGF is a potent osteogenic factor that can be modulated by TNF-alpha and IL-1 in a bioengineered model of skeletal muscle

OG Davies[1,2], LM Grover[2], MP Lewis[1], Y Liu[3]

[1] School of Sport, Exercise and Health Sciences, Loughborough University, UK. [2] School of Chemical Engineering, University of Birmingham, UK. [3] Wolfson School of Mechanical and Manufacturing Engineering, Loughborough University, UK.

INTRODUCTION: Heterotopic ossification (HO) is a highly complex condition defined by the formation of bone in soft tissues. What makes HO fascinating is firstly the rate at which bone is deposited, and secondly the fact that the tissue formed is structurally and compositionally similar to healthy adult bone. Its rapid formation is thought to be primarily associated with the body's hyper-inflammatory response to trauma[1]. Consequently, NSAIDs are frequently prescribed for HO prophylaxis. The present study utilised an *in vitro* model of skeletal muscle to better define the relationship between post-trauma inflammation and HO. Our findings have considerable implications for HO diagnosis and treatment, and could even potentially be exploited to develop new methods for bone regeneration.

METHODS: A skeletal muscle model was developed by seeding C2C12 muscle precursor cells within a type-I collagen gel[2]. Uniaxial tension was produced by anchoring the gel at opposing ends of a well plate. The model was cultured with high glucose DMEM and 20% FBS for 4 days, after which the FBS was replaced with 2% horse serum to facilitate myoblast fusion along the axis of tension. After myotube formation the model was exposed to combinations of cytokines identified in serum/effluent following trauma[3]. Myotubes and unfused cells were released from the model by digestion with 0.1% collagenase. Phenotypic cell profiling was performed using flow cytometry for Sca-1, CD73, CD90 and CD105. Unfused cells were plated at $10x10^4$ per cm^2 and cultured in osteogenic medium. Differentiation was analysed using alizarin red staining and qRT-PCR for osteogenic genes. The interactive effect of cytokines on osteogenesis was examined using principal component analysis.

RESULTS: Following culture in a 3D environment, with and without the addition of inflammatory cytokines, unfused "reserve" cells were released by enzymatic digestion. This population could not be subsequently induced to fuse under standard myogenic conditions. Cells released from gels exposed to PDGF demonstrated spontaneous ossification (Fig.1a). Exposure to PDGF promoted significantly ($P<0.05$) more mineral deposition and expression of osteogenic genes (Runx2, Osterix and Patched 1) than BMP-2, the current gold-standard osteogenic factor. The presence of PDGF or BMP-2 caused phenotypic reversion to a novel $Sca\text{-}1^+/CD73^+$ osteogenic progenitor (Fig.1b). However, spontaneous ossification was prevented in the presence of pro-inflammatory cytokines, TNFα and IL-1.

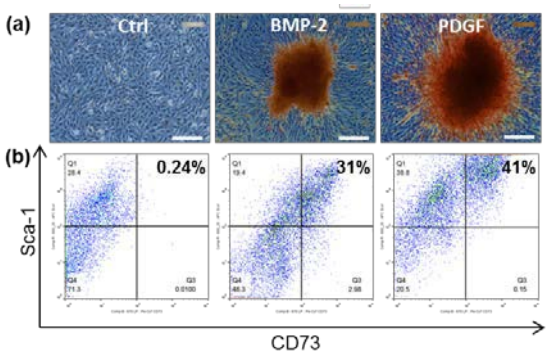

Fig. 1: (a) Alizarin red staining of unfused cells released from 3D constructs after exposure to BMP-2 or PDGF. (b) Corresponding flow cytometry profiling of unfused cells for Sca-1 and CD73.

DISCUSSION & CONCLUSIONS: Our study identified the presence of a novel non-myogenic population of unfused "reserve" cells that showed spontaneous ossification following exposure to PDGF. We further identified that a local pro-inflammatory environment may act to modulate ossification in the presence of this potent osteogenic inducer. These findings have considerable implications when one considers the current use of NSAIDS for HO prophylaxis, identifying a possible explanation for the limited clinical efficacy of these drugs.

Engineering the extracellular matrix for a three-dimensional liver organoid

R Grant[1], D Hay[2], A Callanan[1]

[1]*Institute for Bioengineering, School of Engineering, The University of Edinburgh, Scotland.*
[2]*Scottish Centre for Regenerative Medicine, The University of Edinburgh, Scotland.*

INTRODUCTION: As a result of insufficient treatment options for patients with liver disease[1], a solution is sought in the form of liver 'organoids'; lab grown devices which can support the survival and function of hepatocytes. While scientists can maintain liver organoids in the lab, decades worth of scientific research has failed to translate this into a fully functional organ[2]. This in part is due to the complexities of recapitulating a vital part of the *in vivo* environment; the extracellular matrix [ECM]. Tissue engineering novel scaffolds provides a strategy to tackle the problem of mimicking the ECM[3,4]. This study demonstrates that manipulating cell derived ECM via chemical means improves scaffolds for liver tissue engineering.

METHODS: Polycaprolactone [PCL] scaffolds were created by electrospinning and seeded with epithelial cells. The cells were subjected to drug treatment using histone deacetylase inhibitors to encourage protein production and subsequently stripped from the scaffolds to leave behind their ECM. The resulting hybrid ECM-PCL scaffolds were re-seeded with HepG2s, and cultured for 3/5 days before scanning electron microscopy [SEM], mechanical and biochemical quantification, histology, and gene expression analysis were performed.

RESULTS: SEM demonstrated markedly different scaffold topography [Fig1]. Gene expression was altered between conditions [Fig2] due to biochemical differences in the scaffolds as opposed to mechanical differences [Fig3].

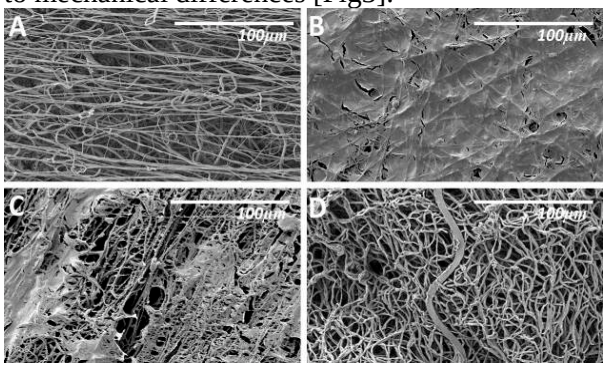

Fig. 1 ECM-PCL scaffold SEM images, 500x magnification. [A] Scaffold only, [B] Scaffold & untreated cells, [C] Scaffold & drug 1 treated cells and [D] Scaffold & drug 2 treated cells.

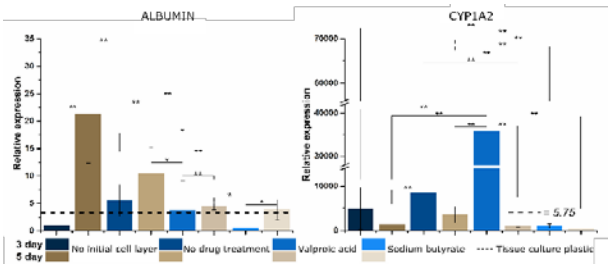

*Fig 2. HepG2 gene expression of liver associated genes. Normalised to GAPDH, relative to culture plastic HepG2s. N = 4, error bars represent SD. *p<0.05, **p<0.01; one way ANOVA with Tukey post hoc analysis.*

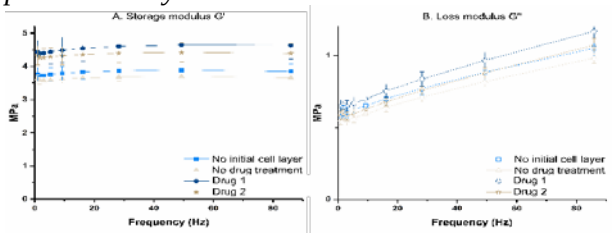

Fig 3. [A] Storage and [B] Loss modulus of ECM-PCL decellularized scaffolds, established by nanoindentation. N = 3

DISCUSSION & CONCLUSIONS: The production of extracellular matrix is significantly altered by drug treatment. Cytochrome P450 [CYP] genes are significantly upregulated, as is albumin. Exposure to the drug induced decellularized ECM influences the gene expression profile of the HepG2s [data not shown; Collagens I & IV, Fibronectin, CYP 1A1 & 3A4]. These results demonstrate the value of these drugs for the production of bespoke ECMs; and their potential for liver tissue engineering.

ACKNOWLEDGEMENTS: This work is funded by an Engineering & Physical Sciences Research Council [EPSRC] doctoral training partnership studentship and UK Regenerative Medicine Platform II [RMPII] grant MR/L022974/1.

Development of a biomimetic tissue-engineered colorectal cancer model investigating invasion patterns and angiogenesis

J Pape[1], M Emberton[2], U Cheema[1]

[1]*Division of Surgery and Interventional Science, UCL, London, UK.*

[2]*Faculty of Medical Sciences, UCL, London, UK.*

INTRODUCTION: One of the main challenges of investigating disease progress is the development of physiologically relevant disease models. Although the traditional set up of studying 2D monolayers of cells has proven as a base line for further work, it is now relevant to develop more biomimetic models that recapitulate all aspects of the tumour microenvironment[1]. The aim of this study is to develop a 3D biomimetic model, which reproduces the solid tumour microenvironment including matrix composition, cell spatial configuration and a primitive vascular network in order to compare invasion and angiogenesis.

METHODS: HT29 and HCT116 immortalised colorectal cancer cell lines were used to generate an artificial cancer mass (ACM) utilising monomeric rat-tail type 1 collagen (FirstLink, UK) and plastic compression with RAFT™ absorbers (Lonza, Switzerland). This ACM was then nested into a stromal co-culture containing HDF and HUVEC cell lines and mouse laminin (Corning, UK) at a 50 µg/mL concentration. The second step of the biomimetic tumour microenvironment development involved using three different patient-specific primary cancer associated fibroblast (CAF) tissue samples in the stromal component instead of the HDFs used previously. The resulting tumouroids were then plastic compressed and grown for 21 days, with samples (n=3) being formalin fixed at day 1, 7, 14 and 21 as well as being extracted for protein and RNA at day 21 (n=3). Invasion patterns and endothelial structures were measured utilising ImageJ software.

RESULTS: The invasion of cancer cells into the stromal compartment was significantly different between the two colorectal cancer cell lines and also differed when using a CAF stromal component as compared to non-cancer associated HDF cells. There was a significantly increased average distance (76.2%, $p<0.0001$) and average surface area (72.5%, $p<0.0001$) of invasion seen by day 21 in tumouroids containing HCT116 ACMs although the number of invasive bodies decreased with the fusion of invasive bodies over time. The endothelial structures observed in the stromal component of the tumouroids had greater complexity when grown containing HT29 ACMs and endothelial structures were observed to grow angled <0° away from the ACM for both cell lines progressively by day 21. The presence of CAFs in the stroma when compared to HDFs increased distance and surface area of invasion from the ACM on days 7, 14 and 21 by ≥10% for each patient-specific tissue sample but decreased or diminished the development of endothelial structure and network formation.

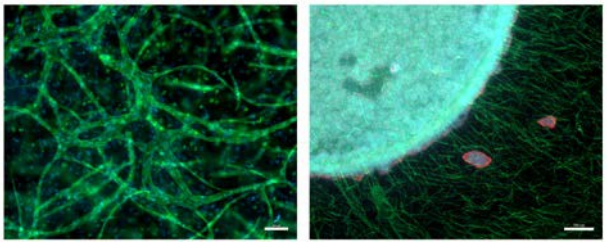

Fig. 1: Left image showing endothelial networks formed by HUVEC cells in stromal component of tumouroid (x10). Right image demonstrates metastatic bodies that budded from ACM into stromal component (x2.5). Both images were taken 21 days after HT29 ACM implantation into a stroma containing HDFs. (Scale bar represents 100 µm for left and 500 µm for right image.) green=CD31, red=CK20 and blue=DAPI

DISCUSSION & CONCLUSIONS: These results indicate that this 3D tissue-engineered colorectal cancer model can be used to study cancer invasion patterns and angiogenesis. Making the model more biomimetic by adding more physiologically relevant components such as patient-specific CAFs to the tumour microenvironment, allows studying the exact molecular pathways involved and deriving a methodology applicable to personalised healthcare.

ACKNOWLEDGEMENTS: The EPSRC as the funding body for this project. CAF tissue samples were kindly provided by Dr. Agata Nyga and Dr. Katerina Stamati at the Royal Free Hospital, UCL, London, UK.

Improved Schwann cell isolation and culture after extracorporeal shockwave treatment

C.M.A.P. Schuh[1,2], D. Hercher[1,2], M. Stainer[1,2], R. Hopf[1,2], A. Teuschl[2,3], R. Schmidhammer[1,2], H. Redl[1,2]

[1] Ludwig Boltzmann Institute for Experimental and Clinical Traumatology, Vienna AT; [2]Austrian Cluster for Tissue Regeneration, Vienna AT; [3] University of Applied Sciences Technikum Wien, Department for Biochemical Engineering, Vienna AT

INTRODUCTION: Peripheral nerve lesions occur with an incidence of approximately 300.000 cases annually in Europe, representing a frequent cause of hospitalization and displaying a major burden to patients and social health-care[1]. Recently, Hausner et al.[2] showed a novel approach of accelerating regeneration after peripheral nerve injury, bridged with an autologous nerve graft. After dissecting and bridging the sciatic nerve in the rat, extracorporeal shockwave treatment (ESWT) was performed at the site of injury. Six weeks after surgery animals of the ESWT group exhibited a significantly improved functional recovery relative to the controls. The mechanisms underlying this positive effect, however, remain widely unknown. Based on the *in vivo* findings of this study we investigated *in vitro* Schwann cell behavior after ESWT treatment, focussing on their regenerative capacity.

METHODS: Sciatic nerves from adult male Sprague Dawley rats were dissected and treated with ESWT. Subsequently, Schwann cells were isolated and cultured for up to 15 passages. ATP release in combination with LDH release was assessed directly after ESWT. Schwann cells were evaluated concerning morphology as well as expression of Schwann cell specific marker S100b and markers indicating regenerative phenotype ($P75^+$,c-Jun^+, $GFAP^+$, $P0^-$).

RESULTS: Single treatment of the whole nerve *ex vivo* led to significantly increased extracellular ATP release (but not LDH) as an immediate consequence, and subsequently a number of effects on the culture were observed, starting with a significantly increased Schwann cell yield after isolation. In the ESWT the group quality of culture, reflected in consistently higher purity, proliferation rate (BrdU, population doublings per passage) and expression of regenerative phenotype-associated markers (P75, GFAP, c-Jun), was significantly improved. In contrast, the control group exhibited progressively senescent behaviour, reflected in a decrease of proliferation, loss of specific markers and increase in $P16^{INK4A}$ expression.

DISCUSSION & CONCLUSIONS: We observed a higher proliferative activity without phenotype commitment, increased purity of the culture as well as reduced expression of senescence associated marker even after long cultivation periods. These positive effects of ESWT on Schwann cell isolation and cultivation may partly be explained by the stimulative effects of extracellular ATP. However, in order to gain a deeper understanding of the effects of ESWT on Schwann cells and their natural habitat, the nerve, further studies *in vitro* as well as *in vivo* focusing on purinergic signalling, mechanotransduction and epigenetic processes have to be performed.

ACKNOWLEDGEMENTS: The financial support by the City of Vienna Project (MA23#14-06) is gratefully acknowledged.

Development of a peripheral nerve bio-substrate for neural regeneration

Glen A[1*], Castanon A[1], Evans C[2], Zilic L[1], Claeyssens F[1], Haycock JW[1].

[1]*Department of Materials Science and Engineering and* [2]*Department of Chemical and Biological Engineering, The University of Sheffield, UK.*

**a.glen@sheffield.ac.uk*

INTRODUCTION:

Nerve guide conduits, consisting of tubular structures manufactured from synthetic and biological materials, are emerging as comparable alternatives to autologous nerve grafts for the treatment of peripheral nervous system injury[1]. Decellularised tissue from peripheral nerves offers an organ specific source of biomaterial suitable for nerve regeneration[2]. Hybrid devices comprising both natural and synthetic materials may overcome the respective limitations in physical and biological properties of monodevices. We therefore hypothesised that the derivation of extracellular matrix proteins from a neural specific tissue source would support enhanced maturation of neuronal tissue *in vitro.*

METHODS:

Porcine sciatic nerve was decellularised as previously described[2], manually homogenised, freeze dried[3] and digested overnight in pepsin[4] prior to acid neutralisation and coating of well plates (Fig 3B) until all solvent had evaporated. NG108 neuronal cells were seeded on either tissue culture plastic (TCP), matrigel^{TM} or decellularised nerve extracellular matrix (dnECM) at 1 x 10^4/cm^2 in DMEM supplemented with 10% FCS. To initiate differentiation the culture medium was switched to serum free medium after 12 hours for 24, 48 and 72 hours. Matrigel^{TM} was prepared according to manufacturer's instructions. Samples were subsequently stained with anti-beta III tubulin antibodies or stained using SYTO9/propidium iodide and analysed for neurite length/viability utilising ImageJ. One-way ANOVA was performed using GraphPad Prism. For proteomic analysis, dnECM, pre and post pepsin digestion and Matrigel^{TM} was electrophoretically separated on 12% polyacrylamide gels (PAGE), Coomassie stained, bands excised, tryptically digested, subjected to mass spectrometry and peptide sequence analysis against non-human species in the Mascot database.

RESULTS:

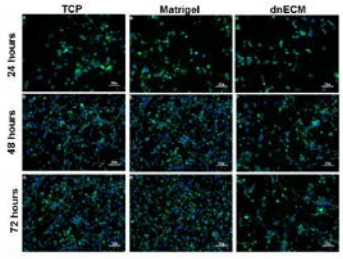

Fig 1: Representative time course images of NG108 cells grown on tissue culture plastic (TCP), Matrigel^{TM} and dnECM fixed at 24, 48 and 72 hours and stained with anti-beta III tubulin antibodies (green) and DAPI (blue).

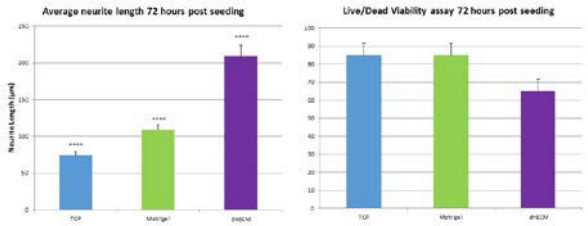

*Fig. 2: Neurite length analysis (A) and live/dead viability analysis 72 hours post seeding (B) of NG108 cells as shown in figure 1. ****p<0.0001.*

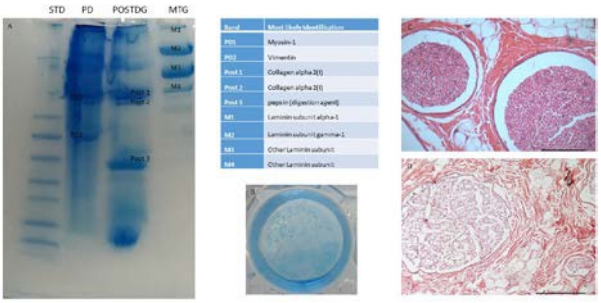

Fig 3: 1 dimensional PAGE proteomic (A, STD = standard, PD = pre-digestion, POSTDG = post digestion, MTG = matrigel) and basic histological characterisation (H&E) of dnECM (D) and non-decelluarised porcine sciatic nerve (C), most likely protein identification via mass spectrometry (table) with representative protein coating visualised via Coomassie staining a dnECM coated six well plate (B). Scale bar = 200µm.

DISCUSSION & CONCLUSIONS: A novel extracellular matrix derived from decellularised porcine peripheral nerve has been found to promote neurite elongation in a neuronal cell line in comparison to matrigel and tissue culture plastic. No significant differences in cell viability between coatings was observed. 1D PAGE data indicates differences in protein composition between matrigel and dnECM with the former predominantly comprising laminin and the latter predominantly different collagen isoforms. Future work will focus on assessing regenerative effects in more physiologically relevant biological samples coupled with incorporation of this material into nerve guide conduits/as an ink for bioprinting.

ACKNOWLEDGEMENTS: *Dr M Frydrych and Dr B Chen for assistance and access, respectively, to a Labconco FreeZone Triad freeze-dryer.*

Mathematical Modelling of a Liver Hollow Fibre Bioreactor

SD Webb[1], I Sorrell[2], RJ Shipley[3], S Regan[4], I Gardner[5], MP Storm[6], M Ellis[6], K Luetchford[6], J Ward[7], P Sharma[8], J Firman[8], D Williams[4]

[1] Applied Mathematics, Liverpool John Moores University, UK. [2] Unilever, UK. [3] Department of Mechanical Engineering, University College London, UK. [4] AstraZeneca, UK. [5] CERTARA, UK. [6] Chemical Engineering, University of Bath, UK. [7] Mathematics, University of Loughborough, UK. [8] Molecular and Clinical Pharmacology, University of Liverpool, UK.

INTRODUCTION: Current 2D in vitro test systems are poorly predictive of the toxicity of chemicals entering the systemic circulation [1]. There is therefore an urgent need for models of systemic toxicity with improved predictivity across the pharmaceutical and chemical industry. We are currently developing a hollow fibre bioreactor (HFB) system for hepatotoxicity testing. Previously HFBs have shown promise for use as bioartificial livers and their use in hepatotoxicity testing is a natural extension to this work [2,3,4]. To assist with the development of the HFB, the design has been mathematically modelled to inform its operating set up, interpret data from HFB outputs and aid in optimizing design to mimic certain hepatic physiological conditions.

METHODS: Based on in vitro data, a cell-scale in silico cellular metabolism model was derived to describe the kinetics of cellular drug uptake, phase 1/2 metabolism and excretion of resulting metabolites. Most reactions took the form of Michaelis-Menten functions in systems of ordinary differential equations. The cell-scale model was then incorporated into a model for a functional liver sinusoid - represented as a cylindrical channel lined with individual hepatocytes which each cell having its own set of parameters to capture zonated variations of enzyme and transporter expressions. Sinusoid fluid flow was then incorporated as advection-diffusion rate equations. Whole body predictions were obtained by representing the liver as a collection of in silico sinusoids and incorporating this into a physiologically based pharmacokinetic (PBPK) framework.

RESULTS: The analysis of this model has produced novel analytical results that allow the operating set up to be calculated and predictions of compound clearance generated efficiently and in a highly accessible form. The mathematical model predicts the inlet oxygen concentration and volumetric flow rate that gives a physiological oxygen gradient in the HFB to mimic a liver sinusoid. It has also been used to predict the concentration gradients and clearance of a test drug and paradigm hepatotoxin, paracetamol (APAP). The effect of altering the HFB dimensions and fibre properties on paracetamol clearance under the condition of a physiological oxygen gradient is analysed.

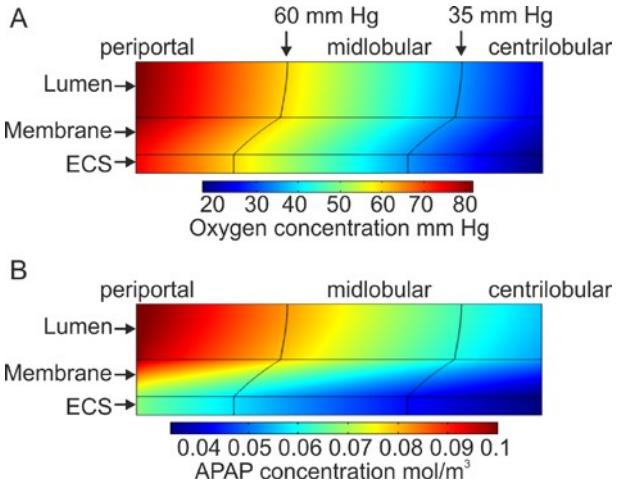

Fig. 1: Computer simulation of concentration gradients of (A) oxygen and (B) APAP within a hollow fibre bioreactor seeded with primary rat hepatocytes with zonal regions indicated.

DISCUSSION & CONCLUSIONS: Our predictions indicate that APAP clearance for a fixed inlet dose is likely to be significantly sensitive to the density of cells, membrane permeability and width. These theoretical predictions can be used to design the most appropriate experimental set up and data analysis to quantitatively compare the functionality of cell types that are cultured within the HFB to those in other systems.

ACKNOWLEDGEMENTS: This work was funded through the NC3Rs CRACK-IT: challenge 5 IVIVE Award.

The development of decellularised cartilage scaffolds as a novel biomimetic implant for the treatment of non-union bone defects

WJ Vas[1] M Shah[1], TS Blacker[2], MR Duchen[2], P Sibbons[3], SJ Roberts[1]

[1] *Department of Materials and Tissue, Institute of Orthopaedics and Musculoskeletal Science,*
[2] *Department of Cell and Developmental Biology, University College London, London UK.*
[3]*Northwick Park Institute for Medical Research, Northwick Park Hospital, London, UK*

INTRODUCTION: Failure of bone healing, resulting in fracture non-union, is estimated to occur in approximately 5-10% of the 850,000 fractures seen in the UK on a yearly basis[1]. The current gold standard for treatment of non-unions using autologous bone grafts is associated with multiple complications[2]. Due to this, the tissue engineering field has attempted to produce implants that mimic mature bone tissue as graft replacement. However, these tissues are intrinsically unresponsive to the cues observed during bone fracture. This study aims to develop an implant that mimics the initial reparative stages of the body's response to fracture, the cartilaginous callus, through the development of decellularised xenogeneic hyaline cartilage in combination with skeletal stem cells.

METHODS: Two distinct decellularisation methodologies, based on osmotic shock and detergents, were optimised for hyaline cartilage. The resultant scaffolds were histologically assessed for efficient cellular removal. Analysis of DNA and GAG content was also assessed along with collagen denaturation temperatures using Differential Scanning Calorimetry (DSC) and Fluorescence Lifetime Imaging Microscopy (FLIM) to define matrix integrity. Human chondrocyte attachment and scaffold associated cytotoxicity were assessed. The functional biological capacity of the scaffolds to induce chondrogenic differentiation of human periosteal stem cells (hPDSC's) was also analysed by qPCR.

RESULTS: Histological analysis revealed both decellularisation approaches yielded vastly reduced cellular content. Both decellularisation methodologies lead to DNA content falling below the recommended 50ng/mg threshold for xenogeneic transplantation, with a 91% (n=3; p <0.01) reduction with the osmotic shock and 88% (n=3 p <0.01) reduction with the detergent-based methodology. Both methodologies were further optimised with reference to tissue size, which resulted in enhanced GAG content retention with the osmotic shock protocol (reduction of 16.5% (n=3; p<0.001) compared to controls). Thermal analysis indicated that osmotic shock methodology had minimal effects on collagen denaturation temperature with a reduction of 7.5% (n=3; p<0.001). Interestingly, the assessment of collagen fluorescence lifetimes yielded no significant differences, further illustrating that the decellularisation process had no detrimental effects on the scaffold architecture. The application of primary human chondrocytes revealed robust attachment and migration into empty lacunae. Furthermore, the scaffolds promoted hPDSC *SOX9* (n=3; p<0.05) and *SOX5* (n=3; p<0.01), marker gene expression under basal conditions, highlighting their chondrogenic potential. This was further amplified through the addition of TGF-β, with significant upregulation of *ACAN* (n=3; p<0.01), along with hypertrophic markers such as COLLX (n=3; p<0.05) and *VEGF* (n=3; p<0.0001).

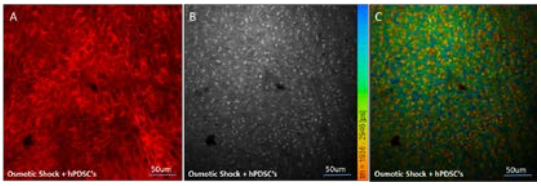

Fig. 1: Second harmonic generation (SHG) (A), Auto fluorescence (B) and FLIM (C) images of osmotic shock decellularised scaffolds seeded with human periosteal stem cells (hPDSC's).

DISCUSSION & CONCLUSIONS: Histological and biochemical assessment indicates that the scaffolds produced were not only extensively decellularised but also retained a sufficient amount of the biological cues, for cell attachment, migration and differentiation. These data demonstrate the potential of creating clinically viable biomimetic cartilage scaffolds and highlight their potential use in combination with specific cell types for bone tissue regeneration.

ACKNOWLEDGEMENTS: We thank ORUK for funding this research and all members of the Institute of Orthopaedics and Musculoskeletal Science, UCL for their assistance.

Perfluorocarbons – potential for successful expansion of bone marrow-derived human mesenchymal stem cells in a liquid/liquid two phase system

M.P.Hanga[1], K. Coopman[1], A.W. Nienow[1,2], C.J. Hewitt[1,3]

[1]Centre for Biological Engineering, Chemical Engineering Department, Loughborough University, Loughborough; [2]School of Chemical Engineering, University of Birmingham, Birmingham; [3]School of Health and Life Sciences, Aston University, Birmingham.

INTRODUCTION: The traditional *in vitro* culture systems of adherent cells typically make use of solid surfaces. However, that approach generates monolayers that require the use of harsh enzymatic treatments for cell harvest which could result in the long term damage of cell adhesion proteins[1]. Our solution is using a non-toxic, biocompatible and cost effective liquid/liquid system as an alternative to the complicated, polymer-based systems currently available on the market. A „flexible surface" provided by the interfacial area of two immiscible liquids: a perfluorocarbon liquid (hydrophobic; Fluorinert FC40) and cell culture medium (hydrophilic) is to be used as a cell culture platform. The benefits of using perfluorocarbon liquids to cell culture systems include: easy sterilisation, recoverable and recyclable and scalability[2].

METHODS: Bone marrow derived hMSC were seeded at 5,000 cells/cm^2 on the interfacial area formed between the two immiscible liquids. The cells were kept in culture for up to 10 days, then harvested by aspirating the interface and replated on TCPS. Cell morphology was assessed by phase contrast and by Live/Dead staining. Cell counts were done with the Nucleocounter NC-3000. Spent medium samples were collected at different time points in culture to assess the metabolic activity of the cells in different conditions and analyzed on the Cedex Bio HT analyser. Cell identity and multipotency were assessed post-harvest by flow cytometry and differentiation studies.

RESULTS: hMSCs attached and proliferated on the flexible liquid/liquid interfacial area provided, while exhibiting the typical spindle-like morphology, similarly to traditional TCPS (*Fig. 1a*). Moreover, cells remained viable during culture in the liquid/liquid system (*Fig. 1b*). The cells were expanded at the interface with the option of harvesting as intact cell sheets without the use of proteolytic enzymes by simply aspirating the interface. After 10 days in culture on the flexible interface, harvested hMSCs were successfully sub-cultured on TCPS. In addition, the harvested cells maintained their identity as demonstrated by flow cytometry and multipotency by differentiation and CFU-F efficiency.

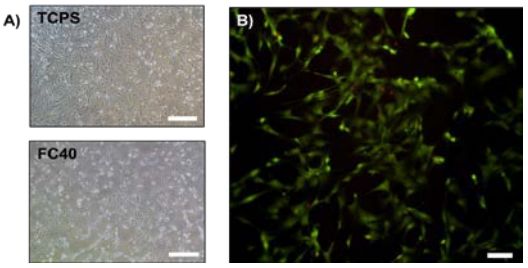

Fig. 1: A) Phase contrast images of hMSC morphology on TCPS and FC40. B) Live/Dead staining of hMSCs at the interfacial area. Scale bar 500 µm.

Table 1. hMSC growth rate on TCPS compared to the FC40/DMEM system

	TCPS	FC40/DMEM
Specific growth rate / h^{-1}	0.0117	0.0061

DISCUSSION & CONCLUSIONS: Despite the lower growth rates of hMSCs on the flexible interface of the liquid/liquid system compared to TCPS (*Table 1*), the cells remained viable during and post-expansion. Moreover, the cells remained undifferentiated as shown by their expression of CD90, CD73 and CD105 cell surface markers (>95%) and lack of expression of CD34 and HLA-DR markers (<2%). Also, the cells maintained their differentiation potential and ability to form colonies.

ACKNOWLEDGEMENTS: BRIC, BBSRC.

Extended culture and passage of primary human corneal stromal stem cells (hCSSCs) on 3D thermo-responsive co-electrospun scaffolds

Afnan Aladdad[1], Laura Sidney[2], Andrew Hopkinson[2], Cameron Alexander[1], Felicity R. A. J. Rose [1]
[1] *Division of Drug Delivery and Tissue Engineering*, Centre for Biomolecular Sciences, School of Pharmacy, University of Nottingham, UK
[2]*Academic Ophthalmology*, Division of Clinical Neuroscience, University of Nottingham, UK

INTRODUCTION: *In vivo*, corneal stromal stem cells known as keratocytes exhibit a quiescent, dendritic cell phenotype, responsible for maintaining the extracellular matrix. During 2D *in vitro* culture, keratocytes differentiate into an undesirable fibroblastic repair phenotype which in the eye would lead to scarring and blindness. Our previous work [1] has shown that 3D environments can promote the reversion of activated corneal stromal cells to a quiescent keratocyte phenotype. However, difficulties in using enzymatic digestion to extract cells from 3D culture has led to the development of thermo-responsive 3D scaffolds for longer-term culture and passaging.

METHODS: Primary human corneal stromal stem cells (hCSC) were extracted from the limbus of the cornea, and then seeded on 3D thermo-responsive electrospun fibres or on 2D culture flasks. Six thermal and enzymatic passages on scaffolds and flasks respectively were performed. The effect of extended passaging and 3D culture on hCSC was assessed by RT-qPCR, immunocytochemistry. Additionally, cell viability assay (Almar Blue) was performed to measure the difference in cell populations while changing the culture temperature.

RESULTS: hCSCs were not affected by the thermo-responsive polymer as cells were viable and proliferated in a similar manner to those cultured on the control. From RT-qPCR studies in Fig.1, culture on 3D scaffolds promoted the quiescent keratocyte phenotype with increased expression of the keratocyte markers CD34 and ALDH and decreased expression of the myofibroblast marker ACTA2 compared to 2D-culture flasks. Immunocytochemistry studies in Fig. 2, showed that CD34 expression was seen in all cells at all passages when cultured on the thermo-responsive 3D scaffolds, while this expression was lost after passage 3 when cells were cultured on 2D TCPS. The myofibroblast marker, α-SMA, is visible in individual cells cultured on TCPS at all passages, but not on the 3D electrospun scaffolds.

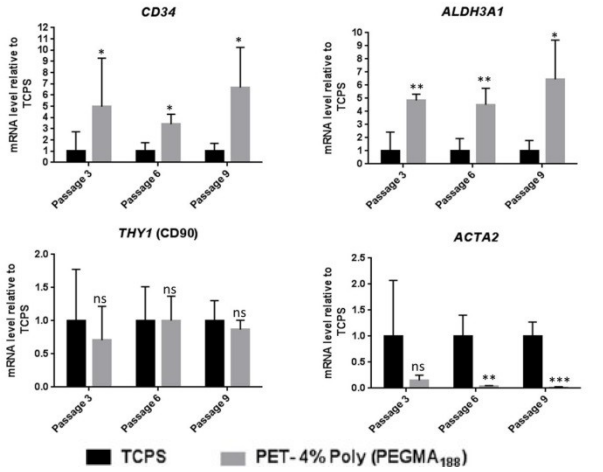

Fig. 1: Comparative effects of culture environment TCPS and PET- Poly ($PEGMA_{188}$) scaffolds on gene expression of hCSSCs at different thermal (3D scaffold) and enzymatic (2D TCPS) passages of 3, 6 and 9.

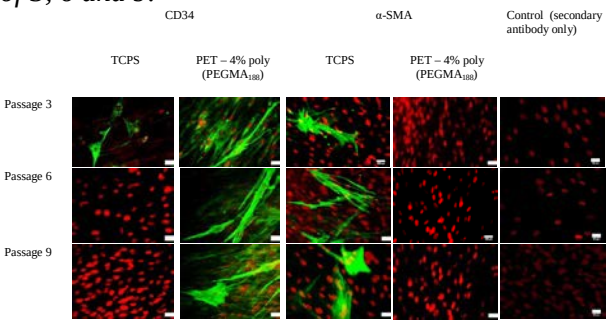

Fig. 2: *The effects of culture environment on keratocyte and myofibroblast markers of hCSSCs.*

DISCUSSION & CONCLUSIONS: Thermo-responsive 3D scaffolds supported the culture and detachment of hCSC without enzymes, and promoted a quiescent keratocyte phenotype over multiple passages. This culture system has the potential to provide high numbers of a desirable cell phenotype for regeneration of the ocular surface in cases of disease or trauma.

Bone-on-chip to study osteocyte mechano-transduction and ECM formation

E Budyn[1,3], M Bensidhoum[2], S. Sanders[1], E. Schmidt[3], P Tauc[4], E. Deprez[4], H. Petite[2]

[1] LMT Lab, Ecole Normale Supérieure de Cachan, France. [2] B2OA Lab, University Paris 7, France. . [3] RRC Center, UIC, USA. [4] LBPA Lab, Ecole Normale Supérieure de Cachan, France.

INTRODUCTION: With increasing life expectancy, pathologies related to massive bone loss carry $10 billion financial burden on the U.S. healthcare system. Successful techniques to repair massive tissue regeneration can be however difficult and require the addition of functional materials. Human bone displays a complex microstructure resulting from continuous remodeling of microdamage that are mechanical stimuli initiating tissue resorption by osteoclasts before tubular osteons are formed by osteoblasts. Trapped osteoblasts differentiate into osteocytes that are mechano-sensitive and orchestrate healthy remodeling process. It is essential to quantify the relationship between *in situ* mechanical stimulation and the cell biological response to design successful engineered tissues.

METHODS: Dual experiment and 3D modeling investigate bone-on-chip composed of progenitor and mature osteocytes reseeded on donor human fresh bone. These systems showed osteocyte *in vitro* biological response subjected to *in situ* mechanical loads in the vicinity of controlled sub-microscopic damage. The energy balance at the experimental global and numerical local scales identified the multiscale local constitutive damage to fracture mechanisms to measure the 3D *in situ* stress field near the live cells. A multi-scale image-based FEM model was subjected to the experimental boundary conditions and included the material properties from μCT and nano-indentation measurements while fluorescent microscopy measured the released chemicals by the cells under mechanical load.

RESULTS: The live systems mechanically behaved as fresh human bone at the macro scale and the FEM model measured the local stress field. The cells reorganized *in vitro* as they would *in vivo* at the different stage of differentiation. The fluorescent observations revealed the calcium membrane transport adaptation of the cells to the *in situ* mechanical cyclic loading at successive stages of differentiation [1]. The systems were functional and allowed osteoconduction, osteoinduction and osteogenicity monitoring.

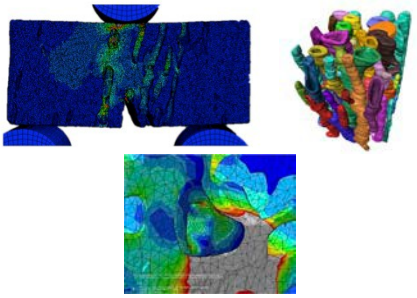

Fig. 1: A- FEM model of a bone-on-chip where subjected to mechanical load is monitored, B- 3D explicit Finite Element Model of the osteons inside the bone-on-chip, C- Visualization of the in situ *local mechanical stress field inside an osteon and the interstitial bone.*

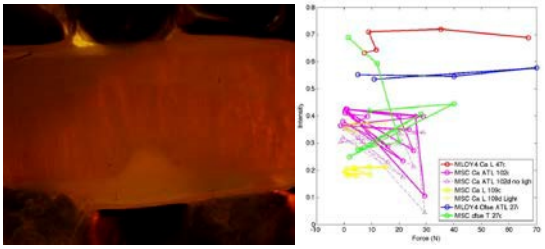

Fig. 2: A- Flurescent microscopy of the calcium response of progenitor and maturing osteocytes in the bone-on-chip, B- Calcium response of progenitor and mature osteocytes at 27 to 109 days.

DISCUSSION & CONCLUSIONS: The Bone-on-Chip produced after 109 days an ECM of which the strength is nearly a quarter of native bone. The cytoplasmic Calcium concentrations were higher in mature osteocytes than in progenitor cells and were maintained constant under mechanical loading.

ACKNOWLEDGEMENTS: With the support from NSF CMMI BMMB 1214816, the Farman Institute, the Fulbright Foundation.

The molecular response of fibrin tissue engineered skeletal muscle constructs to electrical pulse stimulation (EPS).

MC Turner[1 2], NRW Martin[1 2], DJ Player[1 2], MP Lewis[1 2]

[1]School of Sport, Exercise and Health Sciences, Loughborough University, Loughborough, UK. [2] National Centre for Sport and Exercise Medicine, Loughborough University, Loughborough, UK,

INTRODUCTION: Stimulation of skeletal muscle by physical exercise is paramount for physiological adaptation [1]. The activation of the metabolic sensing protein, AMP activated protein kinase (AMPK) by exercise regulates glucose disposal in skeletal muscle independent of insulin [2]. In addition, metabolic genes such as hexokinase II (HKII), glucose transporter 4 (GLUT4), and peroxisome proliferator-activated receptor-α (PPARα) coactivator 1α (PGC-1α) are activated by exercise. Three dimensional tissue engineered skeletal muscle has the potential to provide an *in vitro* model with which to elucidate the mechanisms of exercise physiology and metabolism [3] through the exposure to acute electrical pulse stimulation (EPS).

METHODS: *Construct formation*: C2C12 skeletal muscle myoblast cells were seeded at $1x10^5$ cells in fibrin constructs as previously described [4] for a total of 14 days in culture. Constructs were grown in growth medium supplemented with aminocaproic acid (AA) (DMEM, 20% FBS, 1% P/S). Upon confluence, media was changed to differentiation media (DMEM, 2% HS, 1% P/S, AA), for two days. Constructs remained in maintenance media for the duration of the experiment (DMEM, 7% FBS, 1% P/S, AA).

Electrical Pulse Stimulation: Constructs were serum starved for 2 hours before being subjected to EPS (*Figure 1*) for 0, 1, 2 and 4 hours using the parameters outlined in table 1. Parallel constructs were stimulated with 2mM ACIAR, an agonist for AMPK phosphorylation, for the same duration of time. After simulation, constructs were blot dried and snap frozen in liquid nitrogen.

Analysis: Constructs were analysed for protein expression of phosphorylated (pAMPK Thr^{172}) and total AMPK by immunoblot. qPCR analysis for mRNA expression of PGC-1α, GLUT4 and HKII. The culture media was analysed for glucose, lactate and the concentrations of Interlukin-6 (IL-6) in the media was analysed by ELISA.

RESULTS: Exposure of skeletal muscle constructs to 2mM AICAR increased pAMPK Thr^{172} at all times points compared to 0 hours. pAMPK Thr^{172} did not increase in response to EPS. Both EPS and AICAR stimulation increased the mRNA expression of HKII and PGC-1α respectively. However, neither EPS nor AICAR had an effect upon GLUT4 mRNA expression.

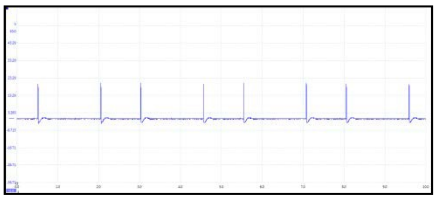

Fig. 1: Electrical Pulse stimulation output on fibrin tissue engineered skeletal muscle constructs.

Table 1. Electrical pulse stimulation (EPS) parameters used on fibrin based skeletal muscle tissue engineered constructs.

Freq. (Hz)	Amp (V)	Pulses	Phase	Duty Cycle (5)	Delay Time (Sec)
1	20	1	180	0.2	0.5

DISCUSSION & CONCLUSIONS: The findings from these experiments show that this EPS regime did not increase phosphorylation of the metabolic sensing protein, AMPK with only a small increase in HKII mRNA expression. AICAR stimulation activated AMPK and PGC-1α, which are activated by are exercise in skeletal muscle. Further investigation is required to determine an EPS protocol that will induce the molecular responses of fibrin tissue engineered skeletal muscle constructs.

Linking bioreactor technology with optical coherence tomography to monitor mechanical properties of tissue engineered constructs

Yvonne Reinwald[1], Pierre O. Bagnaninchi[2], Wesam Gamal[2], Ying Yang[1], Yanny M. Baba Ismail[1], Alicia J. El Haj[1]

[1]Institute of Science and Technology in Medicine, Keele University, Medical School, Guy Hilton Research Centre, UHNM, Stoke-on-Trent, ST4 7QB, United Kingdom. [2]MRC Centre for Regenerative Medicine, the University of Edinburgh, EH16 4UU, United Kingdom.

INTRODUCTION: The maturation of cell-seeded scaffolds to repair tissue damage is promoted through the utilisation of bioreactors mimicking the physical *in vivo* growth environment. Monitoring the maturation of tissue constructs during culture and their performance prior to implantation into the patient is important for defining their quality, manufacturing criteria and clinical translation. Key properties include scaffold mechanical and structural properties. Hence, non-invasive three-dimensional (3D) imaging modalities are required providing rapid results and translational solutions. Elastography allows the mapping of mechanical properties by measuring the deformation in correlation to external mechanical loading. However, it is limited in resolution and sensitivity. To overcome these drawbacks elastography has been coupled with optical coherence tomography known as optical coherence elastography (OCE) and a hydrostatic pressure bioreactor into a new image modality, HP-OCE.

METHODS: Hydrogels were prepared by dissolving agarose in distilled water to final concentrations of 0.5%, 1.0% and 1.5%. hMSC ($1x10^5$) were incorporated before gelation to prepare cellular gels. Scaffolds were imaged utilizing OCT during mechanical stimulation at 1, 5, 10, 15 and 25 kPa at 1Hz frequency in the hydrostatic force bioreactor. Displacements maps were generated using elastography algorithms[1].

RESULTS: Phase-resolved OCE allows the detection of small displacements in heterogeneous tissue phantoms caused by either differences in gel concentration or the presence of cells. Clear differences in displacement were detected for hybrid hydrogels prepared from 0.5% and 1.5% agarose compared to 1.0% and 1.0% hydrogels (Figure 1) and between cellular and acellular gels. Interfaces between stiffer and softer gels can be identified.

DISCUSSION & CONCLUSIONS: A novel dynamic OCE technique, HP-OCE, with cyclic compression as the external excitation generated by hydrostatic pressure was established. Phase-resolved OCE algorithms were applied to determine the scaffolds displacement in OCT phase-based images of various tissue phantoms. Our results indicate that HP-OCE allows real-time non-invasive monitoring of the displacement and strains of tissue phantoms. It enables the investigation of scaffold degradation, material interfaces and heterogeneity as well as changes in scaffold porosity. It further allows the investigation of the effect of mechanical forces on cellular activities during dynamic culture. Future experiments will investigate the maturation of tissue engineered constructs during dynamic culture.

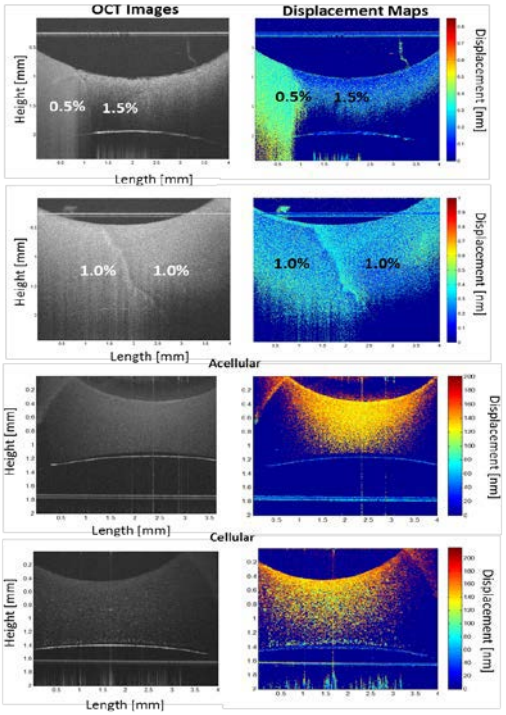

Fig. 1: Monitoring hydrogels during mechanical stimulation in the hydrostatic force bioreactor. Relative displacement maps were generated by elastography algorithms. Colour represents displacement.

ACKNOWLEDGEMENTS: The authors would like to acknowledge the EPSRC Centre for Innovative Manufacturing in Regenerative Medicine and the UKRMP Hub for funding.

Engineered Neural Tissue with Human Dental Pulp Stem Cells: Potential for Peripheral Nerve Repair?

K Sanen[1], W Martens[2], T Vangansewinkel[2], M Georgiou[3], M Ameloot[1], I Lambrichts[2], J Phillips[4]
[1] Biophysics group, BIOMED, Hasselt University, Diepenbeek, Belgium
[2] Morphology group, BIOMED, Hasselt University, Diepenbeek, Belgium
[3] Advanced Centre for Biochemical Engineering, University College London, London, UK
[4] Biomaterials & Tissue Engineering, UCL Eastman Dental Institute, London, UK

INTRODUCTION: Despite the spontaneous regenerative capacity of the peripheral nervous system, large gap peripheral nerve injuries (PNI) require bridging strategies. The limitations and suboptimal results obtained with autografts or hollow nerve conduits in the clinic indicate the need for alternative treatments. Recently, we have described promising neuroregenerative capacities *in vitro* of Schwann cells derived from differentiated human dental pulp stem cells (d-hDPSCs). They not only increased neuron survival and neurite outgrowth, but were also able to self-align within collagen type I hydrogels, thereby forming engineered neural tissue (EngNT) to guide outgrowing neurites, and myelinate neurites *in vitro* (Fig. 1A). Here, we evaluated the use of d-hDPSCs in EngNT as a regenerative strategy for PNI.

METHODS: First, the pro-angiogenic effects of d-hDPSCs were evaluated. To this end, various *in vitro* assays were performed to assess endothelial cell proliferation, migration and differentiation. Next, EngNT seeded with d-hDPSCs, allograft nerves or empty nerve conduits were used to reconstruct a 15 mm nerve gap in a rat model of PNI. Eight weeks after transplantation, constructs were analyzed by immunohistochemistry and transmission electron microscopy.

RESULTS: Although secretion of vascular endothelial growth factor (VEGF) was significantly higher in d-hDPSCs compared to undifferentiated hDPSCs, their effects on endothelial cell proliferation, migration and tube formation were comparable. *In vivo* data showed that the number of ingrowing neurites and blood vessels in EngNT-transplants was similar to that of allograft treated animals (Fig. 1B), whereas the number of myelinated neurites was comparable to the empty conduit treated animals.

DISCUSSION & CONCLUSIONS: hDPSCs are able to retain their pronounced angiogenic properties following differentiation into Schwann-like cells *in vitro* and provide revascularization of EngNT nerve grafts to a similar extent as the gold standard treatment. The suboptimal growth of neurites throughout the scaffold could be attributed to the delivery of EngNT as tightly packed rods, the relatively short recovery time frame after transplantation or the use of immunosuppressants to limit host-versus-graft responses. Although further research is required to optimize the transplantation of this engineered neural tissue, our findings suggest that d-hDPSCs are able to exert a positive effect in the regeneration of peripheral nerve tissue *in vivo*.

A

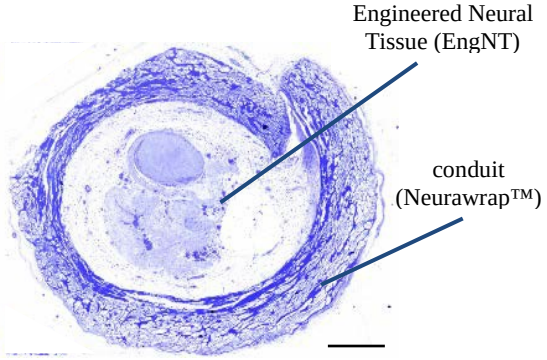

B

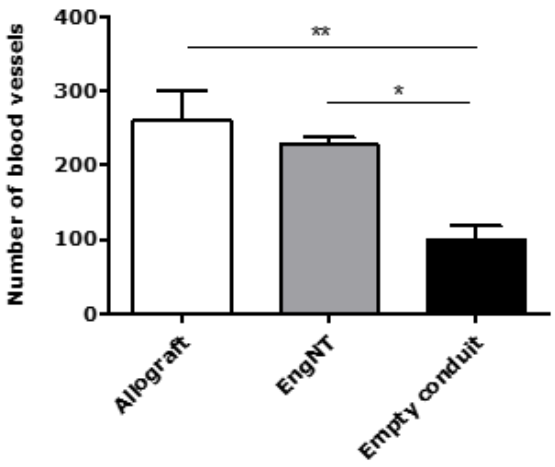

Fig. 1: Improved blood vessel formation by Engineered Neural Tissue after a large gap nerve

A mathematical model informed by in vitro experiments to advance engineered nerve repair construct design

RH Coy[1], G Kennedy[2], C Kayal[3], C O'Rourke[4], PJ Kingham[5], JB Phillips[4], RJ Shipley[3]

[1]CoMPLEX, University College London, UK. [2]UCL Engineering, University College London, UK. [3]UCL Mechanical Engineering, University College London, UK. [4]Biomaterials & Tissue Engineering, UCL Eastman Dental Institute, University College London, UK. [5]Dept. of Integrative Medical Biology, Umeå University, Sweden.

INTRODUCTION: Mathematical modelling has unexploited potential as a highly cost effective and quick way of analysing and comparing the efficacy of different nerve repair construct designs prior to *in vitro* and *in vivo* experiments. Within a mathematical framework, in this case describing a cell culture well containing media and seeded collagen gel, parameter values are required to describe important attributes such as cell proliferation and VEGF release rates. In this study, data fitting against the results of corresponding *in vitro* experiments allows us to identify parameter values that were uncertain based upon the current literature. These parameters can now be used within a mathematical model describing a collagen-based engineered tissue, in order to study interactions between crucial species such as oxygen and cells, and eventually aid the design of future nerve repair constructs.

METHODS:

Differentiated adipose-derived stem cells (dASCs) were seeded in plastic compressed collagen gels at varying densities and maintained with different external oxygen levels. After 24h, viability and VEGF release was measured using CellTiter-Glo (Promega) and ELISA respectively.

A set of coupled partial differential equations was developed to describe the interactions within the *in vitro* gel between the three species of interest: cell density, oxygen concentration and VEGF concentration. The equations incorporate processes such as diffusion and cell death, alongside known parameter values from the literature [1-3]. Initial conditions representing the prescribed oxygen chamber partial pressures and initial seeded cell densities are applied. The equations were solved over a geometry representative of a cell culture well using the Multiphysics software COMSOL, and fitted to the experimental data to derive new values for uncertain parameters.

RESULTS: The approximate values of previously unknown parameters have been calculated via data fitting. Subsequent simulation results suggest that the distributions of the three species over time are, to varying degrees, sensitive to key parameters within the model.

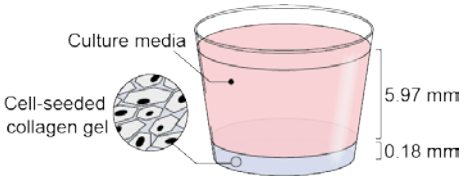

Fig. 1: In vitro experimental setup.

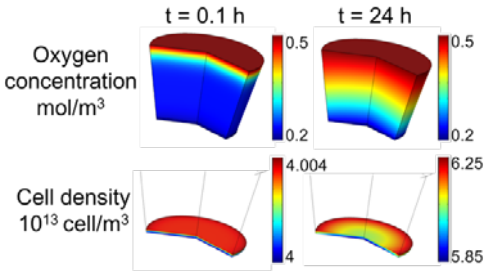

Fig. 2: Simulated oxygen concentration and cell density distributions across cell culture well, at times t = 0.1h and t = 24h.

DISCUSSION & CONCLUSIONS: The *in vitro* simulation results highlight the need to properly consider properties such as seeded cell density when designing engineered tissue, due to the impact that changing distributions of species can have upon processes that are key to clinical efficacy, such as angiogenesis and neuronal growth in this context. Values of the parameters obtained using data fitting can now be used to complete simulations of species within different *in vivo* nerve repair construct designs.

ACKNOWLEDGEMENTS: This work was supported by EPSRC and a doctoral training grant SP/08/004 from the British Heart Foundation (BHF) to RC. RC is also supported through the UCL CoMPLEX doctoral training programme.

Investigation into the importance of maintaining CD34 expression in the therapeutic potential of corneal stroma-derived stem cells

LE Sidney, A Hopkinson

Academic Ophthalmology, Division of Clinical Neuroscience, University of Nottingham, UK

INTRODUCTION: Keratocytes are specialised mesenchymal fibroblasts populating the corneal stroma, which can be characterised by expression of the progenitor marker CD34. We have previously demonstrated that $CD34^+$ limbal keratocytes become multipotent progenitor cells *in vitro*, known as corneal stroma-derived stem cells (CSSC). CSSC potentially play a regenerative role *in vivo*, and therefore have considerable potential as a stem cell therapy for ocular surface regeneration. However, expansion in conventional foetal bovine serum (FBS)-containing medium leads to loss of CD34 and associated progenitor activity. We investigated methods of optimising *in vitro* culture for maintenance of CD34, with subsequent assessment of the importance of CD34 expression in CSSC.

METHODS: CSSC were extracted from human corneoscleral rims and phenotype assessed at early (P1) and late (P4) passage, when cultured in either: M199 with 20% FBS; DMEM-F12 with 20% KSR, 4 ng/mL bFGF and 5 ng/mL LIF (SCM); endothelial growth medium (EGM); or MethoCult™ (MC). Gene expression of isolated $CD34^+$ CSSC and effect of CD34 siRNA knockdown were then evaluated by RT-qPCR.

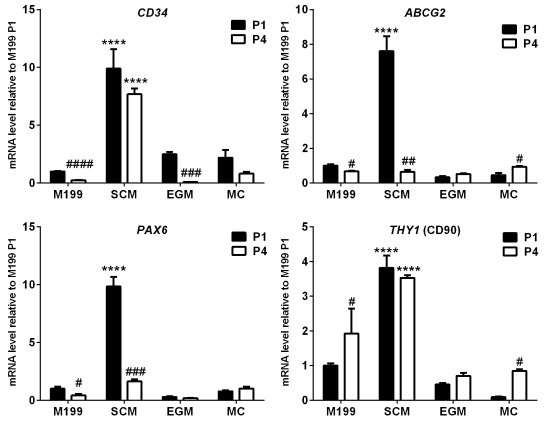

*Fig. 1: Comparative effect of media on gene expression of CSSC. Relative levels of mRNA were determined by RT-qPCR for the following genes CD34, ABCG2, PAX6, THY1 (CD90). *Statistical significance vs. M199 P1. # Statistical significance of P1 vs. P4, same media.*

RESULTS: SCM was the only medium to maintain *CD34* gene expression from P1 to P4 (fig. 1), and exhibited upregulation of progenitor cell markers *ABCG2*, *PAX6* and *THY1*. Immunocytochemistry demonstrated increased expression of CD34, CD90, ABCG2 and SSEA4 in SCM compared to other media (fig. 2). $CD34^+$ CSSC had significantly increased expression of pluripotency markers compared to $CD34^-$ cells. Knockdown of CD34 had significant effects on the regulation of pluripotency genes.

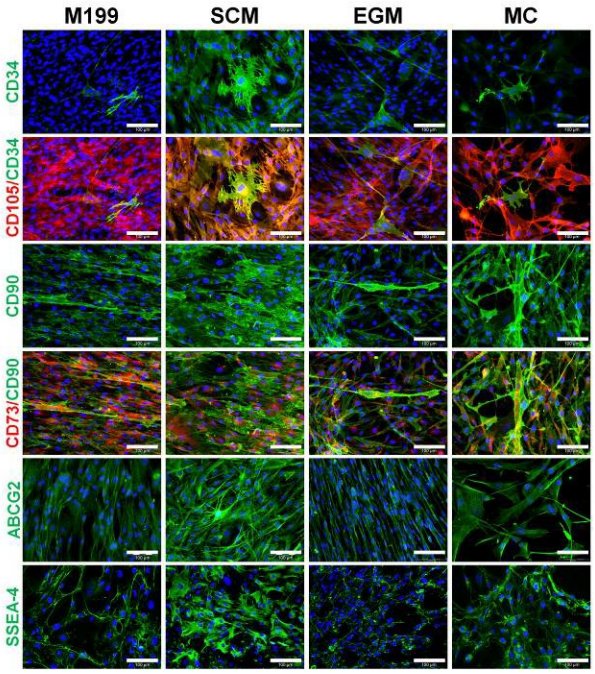

Fig. 2: Comparative effect of media on protein expression of CSSC at P1. Immunocytochemistry was performed at P1. All images shown with DAPI counterstain (blue), scale bar=100 μm.

DISCUSSION & CONCLUSIONS: Results demonstrate that maintenance of an optimal progenitor phenotype is medium-dependent, and CD34 expression is linked to CSSC stem cell properties. Once standardised and bankable, a CSSC therapy could lead to the next generation of ocular regeneration strategies.

ACKNOWLEDGEMENTS: Funding provided by Royal College of Surgeons of Edinburgh and Fight for Sight.

Using holographic optical tweezers as a tool to investigate cellular interactions

Thomas Upton[1], Emily Britchford[1], Glen Kirkham[1], James Ware[1], Graham Gibson[2], Alice Carstairs[3], Paul Genever[3], Yannick Devaud[4], Martin Ehrbar[4], Lee DK Buttery[1], Miles Padgett[2], Stephanie Allen[1], Kevin M Shakesheff[1]

[1]*University of Nottingham, Nottingham, NG7 2RD, United Kingdom*
[2]*School of Physics and Astronomy, University of Glasgow, G12 8QQ, United Kingdom*
[3]*Department of Biology, University of York, York, YO10 5DD, United Kingdom*
[4]*Department of Obstetrics, University Hospital Zurich, 8091 Zurich, Switzerland*

INTRODUCTION: Biological, chemical and physical cues all play major roles in the differentiation of stem cells into terminally differentiated cells. The investigation of cellular microenvironments is currently limited by the technologies available to manipulate cells in 3D at a high enough resolution. Here we demonstrate the application of holographic optical tweezers to precisely control and manipulate cells and microparticles in 3D on a microscopic scale. The holographic optical tweezers provide a high resolution tool for investigating cellular interactions with other cells and their environment. Using this technology we aim to improve our knowledge of fundamental stem cell biology to help guide future tissue engineering research on a larger scale.

METHODS: Holographic optical tweezers were constructed similar to a previous system[1].

Mouse embryonic stem cells, wnt3a reporter cells and wnt3a releasing were seeded onto gelatin coated glass bottomed coverslips and manipulated into desired structures. These 3D micro architectures were stabilized using a PEG based hydrogel[2], a biotin-avidin based method[3]. The growth factor gradient work was done using wnt3a spheroids and wnt3a loaded microparticles in a u-bottomed 96 well plate.

RESULTS:

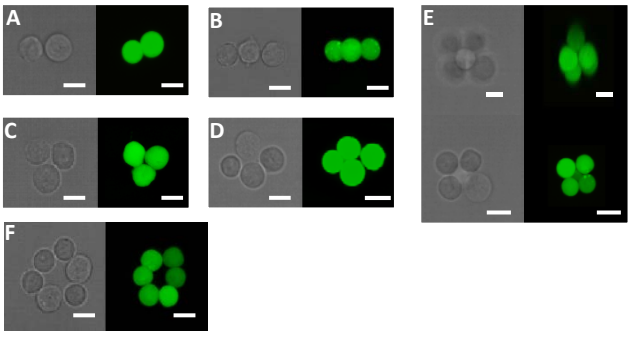

Fig 1. Bright field and confocal images of cells patterned into small scale structures using holographic optical tweezers and stabilized using biotin-avidin. Sale bar = 10 μm.

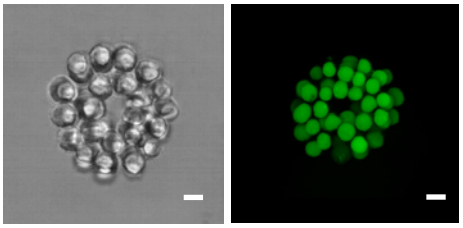

Fig 2. Bright field and confocal images of cells patterned into a larger 66 cell structure using holographic optical tweezers and stabilized using a PEG based hydrogel. Sale bar = 10 μm.

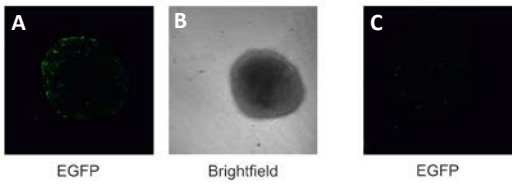

Fig 3. Brightfield image of a spheroid formed from wnt3a reporter cells and a single wnt3a loaded microparticle (B). (A) is a fluorescence microscopy image of the same spheroid in (B), cells that are exposed to wnt3a fluoresce green. (C) is a fluorescence microscopy image of a spheroid in the absence of wnt3a loaded microparticles.

DISCUSSION & CONCLUSIONS: We are able to precisely position cells and microparticles in 3D on a microscopic scale using holographic optical tweezers. We have also demonstrated that we are able to vary the architectures of these patterns (fig 1 and 2), expose them to different growth factors (fig 3) and different physical environments (fig 1 and 2). This could enable investigation of fundamental stem cell biology, development and potentially even allow us to artificially generate stem cells niches.

ACKNOWLEDGEMENTS: My PhD was funded by the BBSRC and the equipment was bought with funds from the ERC.

3D Bioprinting of mechanically strong chondrocyte-laden constructs for major nose reconstruction

L. A. Ruiz Cantu[1], A. Gleadall [2], C. Faris [3], J. Segal [2], K. Shakesheff [1], J. Yang [1]

[1]Tissue Engineering Group, School of Pharmacy, University of Nottingham, United kingdom. [2]Department of Mechanical, Materials and Manufacturing Engineering, School of Engineering, University of Nottingham, United Kingdom. [3]Department of Otolaryngology and Facial Plastic Reconstructive Surgery, Poole Hospital, United Kingdom.

INTRODUCTION: Current gold standard for nasal reconstruction after rhinectomy or severe trauma includes transposition of autologous cartilage grafts in conjunction with coverage using an autologous skin flap. Harvest of autologous cartilage requires a major additional procedure which creates donor site morbidity. Major nasal reconstruction also requires sculpting autologous cartilages to form a cartilage framework, which is complex and time-consuming. The reconstructed nose has a risk of deformity due to the force exerted from scar tissue formation in the first 6 months after surgery and the lack of structural integrity of the reconstructed nose. [1]. To address these clinical challenges, we aim to fabricate a mechanically robust cartilaginous constructs by using bioprinting of a polymer scaffold for structural support and a chondrocyte-laden hydrogel for cartilage regeneration.

METHODS:

Design of a personalised 3D nose model: The 3D nose model was obtained with the MIMICS software using the CT scan from the patient.

3D printing of thermoplastic nose scaffolds: The scaffolds were printed using a bioprinter (RegenHU, Switzerland). Polycaprolactone (PCL) was melted at 74˚C and then extruded thought at 23G needle at a deposition speed of 16mm/s. Poly (lactic-co-glycolic) acid (PLGA) was melted at 120 ˚C and deposited at the same speed than PCL.

3D Bioprinting: Chondrocytes were encapsulated in three different gelatin methacrylate (GelMA) concentrations and bioprinted using a 27G needle at a deposition speed of 10mm/s. Scaffolds were UV cross-linked for 20 sec. Samples were cultured in complete medium supplemented with TGF-β1for 45 days.

Co-printing: PCL and chondrocytes encapsulated in 20% GelMA were co-printed 1 mm apart in an offset arrangement so pores remained in the overall structure.

RESULTS: Personalised nose scaffolds were printed using two different thermoplastic polymers, PCL and PLGA (Fig. 1A and 1B).

A porous scaffold was obtained after the co-printing of PCL and GelMA (Fig. 1C). Cells remained viable after the deposition process.

The encapsulated bioprinted chondrocytes proliferated and secreted a cartilage-relevant matrix during 45 days in culture (Fig 1D and 1E).

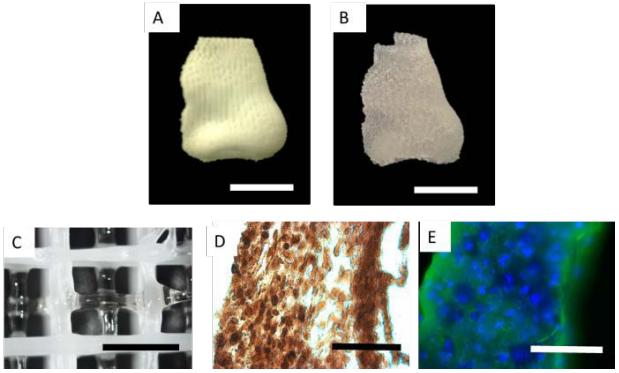

Fig. 1: A,B) printed PCL and PLGA nose-shaped scaffolds, Scale bars 1.5cm. C) co-printing of PCL (white material) and GelMA scale bars 2mm. D) Safranin O staining and E) Collagen II expression in green. Scale bars 100µm.

CONCLUSIONS: We have demonstrated the feasibility of 3D printing personalised nasal scaffolds using PCL and PLGA. Further to this, we have demonstrated that co-printing facilitates the formation of scaffolds with a mechanically supportive component and a biological component (chondrocyte-laden GelMA). Formation of a cartilage-relevant matrix in GelMA has been observed during long-term culturing.

ACKNOWLEDGEMENTS: Financial support was received from EPSRC and CONACYT Mexico.

Angiogenic potential of adipose derived stem cells compared to the stromal vascular fraction

S Roman[1], N Mangir[1], V Hearnden[1]

[1] *Kroto Research Institute, Department of Materials Science and Engineering, University of Sheffield, UK*

INTRODUCTION: The success of tissue engineered grafts relies on a functional blood supply developing following implantation. Adipose tissue is a rich source of adipose derived stem cells (ADSC) which can be collected from patients easily and safely. Adipose tissue also contains the stromal vascular fraction (SVF), a heterogeneous mix of cells including blood cells, endothelial cells, stromal cells and ADSC. Both ADSC and SVF have been shown to improve angiogenesis however very few studies have directly compared these two cell populations. Our aim is to determine the pro-angiogenic properties of ADSC and SVF for use in tissue engineered grafts.

METHODS: SVF and ADSC were isolated from subcutaneous fat (ethics approval 15/YH/0177) using mechanical and enzymatic digestion. ADSC were purified from the SVF by adherence to plastic and both ADSC and SVF were characterised using flow cytometry markers (eBioscience). 5 x10^5 SVF cells or ADSC were cultured in 0.77mg/ml Collagen I (rat tail) gels and viability was measured by resazurin assay. Conditioned media from the gels was collected and a cytokine array was performed to quantify the release of proteins involved in angiogenesis.

RESULTS: ADSC and SVF were successfully isolated from adipose tissue. ADSC from 3 different patients were CD31-, CD34-, CD45-, CD73+, CD90+, CD105+ and CD146- while the SVF contained a heterogeneous cell population in line with previous findings (1). SVF and ADSC cultured in collagen gels remained viable for 7 day in culture. Gels containing ADSC contracted by 40% compared to control gels without cells; however contraction was not observed for gels containing SVF. After 24 hours in culture, conditioned media from gels containing ADSC and SVF showed release of pro-inflammatory cytokines including GRO, IL6, IL8, PDGF and VEGF-D (Fig 1). Gels containing SVF cells also released EGF, PLGF and VEGF-A. A similar pattern of expression was observed after 4 days in culture (Fig 2).

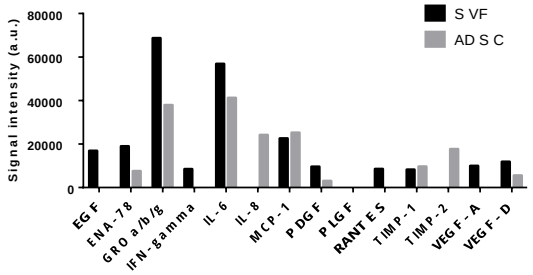

Fig. 1: Cytokine release from collagen gels containing SVF and ADSC after 24 hours in culture.

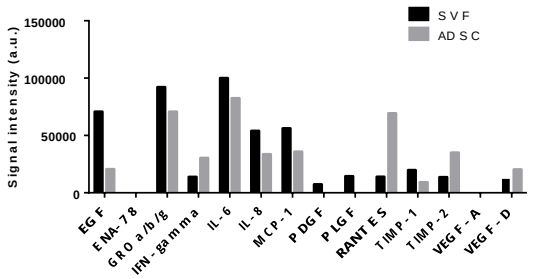

Fig 2: Cytokine release from collagen gels containing SVF and ADSC after 4 days in culture.

DISCUSSION & CONCLUSIONS: Collagen gels containing SVF cells released higher or equal levels of pro-angiogenic cytokines when compared to gels containing ADSC, with the exception of TIMP2 and RANTES. The levels of TIMP2 and RANTES may, in part, explain the increased contraction observed in these gels. In conclusion we have demonstrated SVF cells, which can be harvested with less manipulation compared to ADSC, may be an attractive alternative to ADSC for tissue engineered grafts and that both cell types are capable of sustained cytokine release.

ACKNOWLEDGEMENTS: This work was funded by the Engineering and Physical Sciences Research Council. Thanks to Prof Sheila MacNeil for her support and to the Plastic Surgeons at Sheffield Teaching Hospitals for tissue collection.

Development of an *in vitro* model of reactive gliosis using stabilized collagen gels with defined and monitored stiffness environments.

C O'Rourke, T Eriksson, J B Phillips

Biomaterials & Tissue Engineering, UCL Eastman Dental Institute, University College London, UK.

INTRODUCTION: Following injury or insult, failure of the injured CNS to repair is in part attributed to the inhibitory environment of the lesion site, most notably the formation of the glial scar. This consists predominantly of astrocytes, which exhibit a reactive hypertrophic phenotype exemplified by upregulation of various markers, including GFAP[1]. *In vitro* models have been employed to explore the cellular mechanisms occurring during reactive gliosis but there is little understanding of the relationship between astrocytes and their mechanical environment[2]. Astrocytes within soft 3D hydrogel cultures have been shown to adopt a less reactive phenotype than in stiff 2D cultures and the progression of reactivity can be monitored[3], however there are difficulties in maintaining and monitoring soft gels that may discourage wider adoption. The aim of this study therefore was to investigate whether stiffer stabilised collagen gels containing astrocytes could be used as a high throughput tool for the study of reactive gliosis, and also to develop methods for measuring gel stiffness to enable the mechanical environment to be controlled and monitored.

METHODS: Primary astrocyte cultures were prepared from P2 GFP+ rat cortices. Astrocytes were dissociated and expanded for 2 weeks before seeding in 3D collagen gels[3] and some gels were treated with 10ng/ml TGFβ1. Gels were stabilised using RAFT™ absorbers (TAP Biosystems, UK). GFAP gene expression was assessed using quantitative real-time PCR analysis. The mechanical properties of the collagen environment were measured using dynamic mechanical analysis (DMA; BOSE Electroforce 3200).

RESULTS: Compressive DMA enabled the mechanical properties of the astrocyte-seeded hydrogels to be characterised (Fig 1). Astrocyte-seeded hydrogel stiffness increased between 0 and 5 days in culture (Fig 1). Addition of TGFβ1, a cytokine considered to be a likely trigger of reactive gliosis *in vivo*, led to an increase in GFAP expression at day 10 and day 15 (Fig 2).

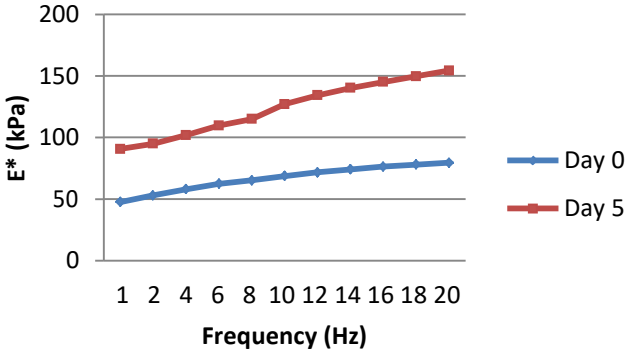

Fig1. DMA on stabilised astrocyte gels at 0 and 5 days. Frequency sweep (1-20Hz) revealed change in compound compressive modulus.

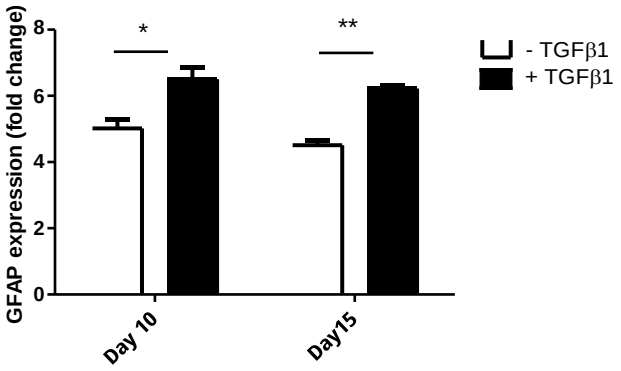

Fig2. Gels with and without TGFβ1 treatment were analysed using qRT-PCR. Mean ± SEM.

DISCUSSION & CONCLUSIONS: The TGFβ1-mediated upregulation of GFAP in astrocytes within stabilised gels mirrors their response during astrogliosis in vivo, indicating the utility of this approach as a research model. The stabilized gel system is more robust than previous softer hydrogel approaches and is amenable to widespread adoption. DMA permitted detailed analysis of the mechanical properties of stabilised collagen gels and provides a way to investigate the role of biomechanics in reactive gliosis.

Directing T cell phenotype with multi-functional biomaterials

D. Delcassian[1, 2], O. Qutachi[1], K. Shakesheff[1]

[1] *Tissue Engineering, University of Nottingham, Nottingham, UK.*

[2] *Koch Institute of Integrative Cancer Research, MIT, Cambridge, USA.*

INTRODUCTION: Immune cells are implicated in many of the world's leading diseases including auto-immune disorders, cancer, and infection. Using immune-engineering, we can create material substrates that allow us to probe a range of factors known to be important to immune cells. Immune cell activation is controlled through a range of chemical and physical cues, including cytokine gradients, cell-surface ligand engagement and topographical cues. Current materials have broadly focused on delivering these cues statically and *ex vivo* to relevant immune cell populations. *In vivo*, immune cell responses are co-ordinated dynamically, hinting that new biomaterials with control over dynamic delivery of these factors may allow greater control of immune cell activation. We have designed biomaterials capable of delivering localised soluble and physical cues to targeted immune cells *in vivo*, which offer promise as next-generation aAPCs for immunotherapy design. These new materials allow an exploration of a range of chemical and physical cues thought to be important to signalling, and help us explore their dynamic interaction with the host immune system. These aAPCs include materials capable of the selective delivery of soluble factors to immune cells through biodegradable and controlled release systems for long term control of T cell behaviour.

METHODS: Primary human blood mononuclear cells were provided by the NHS and used in a Human Tissue Authority licenced premises. Cells were extracted from leukocyte cones using density centrifugation, and negatively depleted to isolate CD4+ cells. Human cells were incubated with immunomodulatory materials, and the response to directed activation measured by flow cytometry analysis of surface markers and ELISA analysis of cytokine secretion. Immunomodulatory materials were also tested in ethically approved protocols to explore the *in vivo* capabilities of these systems to activate T cells in the immune system in a localised fashion with controlled dynamics.

RESULTS: Advanced aAPCs were fabricated with a range of morphologies and release kinetics (Figure 1). In the example highlighted, PLGA materials were conjugated with organ specific ligands to enable selective and localised delivery of immunotherapeutics, and encapsulated inside a hydrogel matrix. We have used these materials to deliver immunomodulatory therapeutics to specific locations, enabling temporal control of the behaviour of T cells *ex vivo* and *in vivo.*

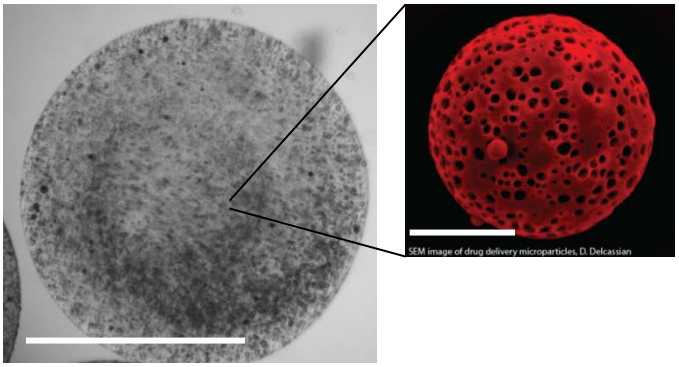

Fig. 1:Biodegradeable microparticles allow spatial and temporal control of solute release. These materials can also be encapsulated within hydrogel matrices. Scale bar left- 1mm, right, 20µm.

CONCLUSIONS: These materials allow for precise localisation, immune-isolation and controlled kinetic release of desired soluble factors. Cellular responses to these materials indicate they may offer an attractive solution for the localised long–term control and directed differentiation of specific immune cell function.

ACKNOWLEDGEMENTS: This research was supported by an EPSRC E-TERM Landscape Fellowship and funding from the UKRMP Acellular Hub.

Mathematical models for tissue engineering

SL Waters

Mathematical Institute, Radcliffe Observatory Quarter, Woodstock Road, Oxford, OX2 6GG

INTRODUCTION: Successful strategies for tissue engineering and regenerative medicine utilise advances from the fields of biology, biochemistry and biomechanics, biomaterials, bioengineering and biotechnology: mathematics is a powerful language to integrate data from these complementary fields. Tissue regeneration requires the interplay between a myriad of biophysical and biochemical effects which regulate an enormous variety of processes, from intracellular transduction pathways to tissue-level mechanics. We demonstrate how mathematical modelling, analysis and computation, in combination with experimental studies, can provide insight into how the many different underlying biological processes interact. Furthermore, such modelling approaches can be utilised to determine how these interactions may be optimised (via experimentally controllable parameters) to achieve the end goal of producing functional tissues for implantation.

METHODS: We discuss the insights gained via a mathematical modelling approach for two bioreactor systems: the High-Aspect Rotating Vessel (HARV)[3] and hollow-fibre membrane systems[2]. In both systems, a porous biomaterial scaffold, seeded with cells, is cultured in a nutrient-rich fluid. Fluid flow is exploited to improve mass transfer of nutrient and growth factors to, and removal of waste products from, the cells. Additionally, the fluid flow influences the cells' mechanical environment, the consequences of which will be specific to the cell population in question. We develop multiphase models, accounting for the fact that biological tissue is composed of a wide variety of interacting components, coupled with flow and transport equations for the nutrient-rich culture medium surrounding the bioactive scaffold.

RESULTS: The resulting mathematical models may be validated against measurable experimental data, such as inlet flow rate and outlet nutrient concentration, and then exploited to provide important local spatial information regarding the concentration and stress fields experienced by the mechanosensitive cells within the bioactive porous scaffold. Such insights are not straightforward (or even possible) to obtain experimentally.

DISCUSSION & CONCLUSIONS: Mathematical modelling, performed in combination with experiments, has an essential role to play in tissue engineering. Validated theoretical models limit the need for numerous and expensive bioreactor experiments (saving time and money) as they can be exploited to predict the outcome of a particular experimental scenario. Furthermore, such models can be employed to optimise bioreactor operating conditions.

Laser fabrication of 3D limbal epithelial crypts: a first step towards cornea regeneration

E Prina[1], J Yang[1], R Wildman[2], FRAJ Rose[1]

[1] *Division of Drug Delivery and Tissue Engineering, Centre for Biomolecular Sciences, School of Pharmacy, University of Nottingham, UK.* [2] *Faculty of Engineering, University of Nottingham*

INTRODUCTION:

Limbal epithelial crypts (LECs) are stem cell niches in the human limbus. The regeneration of the cornea occurs when stem cells migrate from these crypt-like niches within the limbus, towards the center of the cornea. Limbal stem cell deficiency is a cause of vision loss. The purpose of this study was to develop a 3D biocompatible gelatin methacrylate (GelMa)-based scaffold, mimicking the size and shape of native LECs by using a Two-Photon Polymerization system (2PP).

METHODS:

GelMa (degree of methacrylation = 74%) was prepared, and mixed with a cyclic benzylidene ketone-based photoinitiator[1] (PI, P2CK). 2PP technique (emission laser: 780 nm) was used to photopolymerize GelMa into a LEC model generated using CAD software and dimensions taken from histology sections[2]. The hydrogel was prepared with 15% w/v of GelMa and 0.3% w/v of P2CK. Polyethylene glycol diacrylate (PEGda, 5% v/v) was added to the optimized scaffold (GelMa-PEGda), and volumetric degradation rate and water uptake were studied by a combination of time lapse and confocal microscope techniques. Human corneal epithelial cells (hCECs) were seeded onto the scaffolds and LIVE™ assay was used to monitor the cells viability over 7 days.

RESULTS:

The addition of 5% v/v of PEGda to GelMa limits the degradation rate to 27.3% after 5 days, following the addition of collagenase type I.

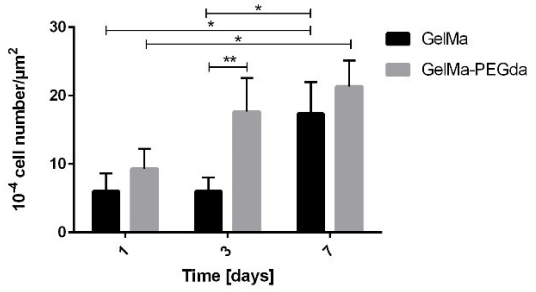

*Fig.1: proliferation curve of hCECs seeded onto flat scaffolds (n=3,*p≤0.05 **p≤0.01).*

The water content was 86.29% ± 3.17 and 72.46% ± 3.13 for GelMa and GelMa-PEGda scaffolds, respectively and was found to be comparable to native cornea tissue[3]. hCECs adhered and proliferated on flat scaffolds for both gels (Fig.1) and were viable on 3D scaffolds (Fig.2a-d).

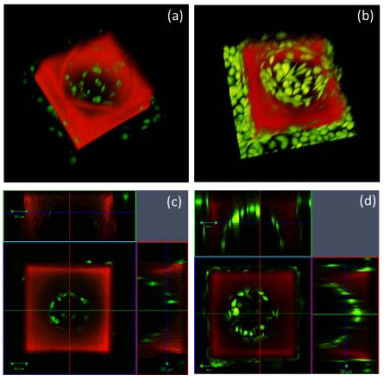

Fig.2: Confocal images of hCEC cells stained with live staining (green) after 1 day (a,c), and 7 days (b,d), surrounded by the printed scaffold (red, 15GelMa-PEGda) in 3D view (a,b) and orthogonal view (c,d). Scale bar 50µm.

DISCUSSION & CONCLUSIONS:

The addition of PEGda reduced the degradation rate without affecting cell adhesion. Cells adhered to and proliferated on the scaffold. These results suggest that the development of a biocompatible architecture that mimics native LECs is feasible. This is a first step towards understanding the relationship between geometry and cell differentiation within the limbus, leading to the design of biomaterials for limbal reconstruction and cornea regeneration.

ACKNOWLEDGEMENTS: The study has been supported by EPSRC (UK).

Controlled release of get peptides and enhanced intracellular delivery of therapeutics

H M Abu Awwad[1], K M Shakesheff[1], J E Dixon[1]

[1] School of Pharmacy, Wolfson Centre for Stem Cells, Tissue Engineering, and Modelling, Centre of Biomolecular Sciences, University of Nottingham, Nottingham, NG7 2RD, United Kingdom

INTRODUCTION: Cell penetrating peptides (CPPs) are an attractive and non-genetic means of delivering therapeutic molecules into cells for treatment of many different conditions. Complexes of CPPs and their cargoes are macromolecular in nature, which makes them challenging systems to formulate and deliver in a controlled manner. There is a need for intracellular protein delivery systems that can provide active therapeutic doses and restrict their administration to specific locations.

We have developed novel fusion proteins that couple a membrane-docking peptide which binds heparan sulfate glycosaminoglycans (GAGs) with a CPP[1]. This GET (GAG-binding enhanced transduction) system can be utilised to enhance delivery of different cargos, including proteins (i.e. transcription factors and enzymes), nucleic acids, nanoparticles and drugs.

Here, we aimed to develop a controlled delivery system, based on poly (lactide-co-glycolide) (PLGA) microparticles, which would provide a localised release of the encapsulated GET-fused therapeutic molecules at the treatment site.

METHODS:.

Microparticles were formed from poly (DL-lactide-co-glycolide, 50:50, 52kDa), using solid in oil in water (S/O/W) solvent evaporation method.

The generated microparticles were characterised for average size, morphology, encapsulation efficiency and protein release profile.

The encapsulated and released GET - protein molecule transduction activity was tested using mammalian cells (NIH 3T3). Protein was delivered into cells by addition to culture media. Cells were imaged using fluorescence microscope, then harvested and analysed for fluorescence intensity by flow cytometry. Protein transduction activity was compared to the experiment control.

RESULTS: The manufactured microparticles were in size of 40 – 60µm, with spherical shape. The encapsulation efficiency was in range of 60 – 80%, the total protein loading was fixed to be 0.5% (w/w).The released protein showed gradual loss of activity over time; however, the released protein activity was enhanced by the addition of a proton scavenger, L-Histidine, which was co-encapsulated with the GET – protein molecule during the microparticles manufacturing process.

The results suggested possible GET peptides interaction with carboxylic acid groups resulted from PLGA degradation over time. However, use of the proton scavenger, L-Histidine, showed enhanced protein activity even in presence of carboxylic acid group.

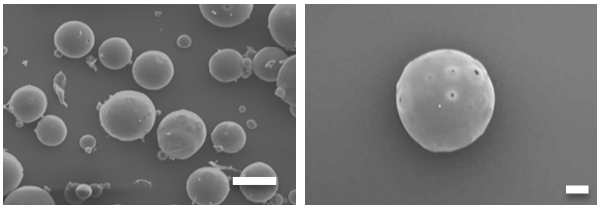

Fig. 1: Representative SEM images of PLGA 50:50 microparticles prepared using S/O/W method (15% (w/v) PLGA), loaded with P21mR8R (0.5% (w/w)), mixed with 0.1 % (w/w) PBS, 25% (w/w) L-Histidine (scale bars represent 50µm on left images, and 10µm on right images).

CONCLUSION: We presented here an extensive study of the possible factors affecting GET peptide biological activity, during the encapsulation and release from PLGA microparticles.

A robust method of fabricating protein-loaded microparticles was optimised, using S/O/W emulsion technique. L-Histidine was used as a stabiliser to maintain the protein activity during release from microparticles.

The advantage of this delivery system is to provide localised release of GET-tagged therapeutic molecules with minimised risk of systemic dosing that may lead to non-targeted activity. This delivery technology has potential to be valuable in the controlled delivery of various potent therapeutic molecules, coupled with GET peptides, which can be used for drug delivery and regenerative medicine applications.

3D Biofabrication of soft tissue: Material challenges

A Aied[1], A Sigen[2], K Shakesheff[1], W Wang[2], J Yang[1]

[1] *Centre for Biomolecular Sciences, School of Pharmacy, University of Nottingham, UK*

[2] The Charles Institute of Dermatology, University College of Dublin, Ireland

INTRODUCTION: Three dimensional bioprinting is being applied to tissue engineering and regenerative medicine as a manufacturing tool to produce 3D tissues and organs suitable for transplantation. Difficulties with printing cell-laden natural materials such as collagen as well as concerns over immunogenic responses to these materials are well documented. In our present work we synthesised easily printable, stimuli responsive polymers specifically tailored for housing cells to serve as wound dressings for wound healing.

METHODS: The copolymer was synthesized by the copolymerizing of PEGMEMA, MEO_2MA and PEGDA via an *in situ* deactivation-enhanced atom transfer radical polymerization (DE-ATRP) approach as previously described [1]. ^{1}H NMR was carried out on a 300 MHz Bruker NMR with Mnova processing software. To make the polymer more semi-solid than viscous, 5% porcine gelatin (sigma, UK) was added to the polymer solution and stored at 4°C for 20 minutes until a clear gel of polymer was formed. Specialised pressure syringes were filled with this polymer combination and printed using the RegenHu 3DDiscovery printer at constant pressure, strand diameter and print-head speed. The PMP is crosslinked after printing using UV light (350nm) for 2 minutes.

RESULTS: The polymer (termed PMP) molecular weight and polydispersity index were determined using Gel permeation chromatography (M_w=10,800 Da, PDI=1.32).

Investigation into the effect of UV light on cell viability found that 2 minutes was ideal to maintain around 90% of cells viable without affecting the crosslinking efficiency of the polymer. This crosslinking efficiency created a strong rubbery like hydrogel that supports cell growth and proliferation.

In situ DE-ATRP is a well-controlled method of synthesis to produce polymers with unique and multiple properties. In this case, a polymer with photocurable property and cell entrapment capability is synthesised. The polymer can be easily printed when mixed with 5% gelatine and cells at 4°C. Preliminary data show high cell viability post printing too (results not shown here).

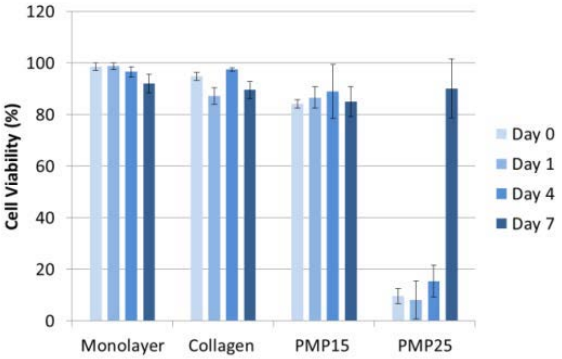

Fig. 1: Cell viability of 3T3 Fibroblasts in the PMP hydrogel before printing. (15% polymer:PMP15, 25% polymer: PMP25)

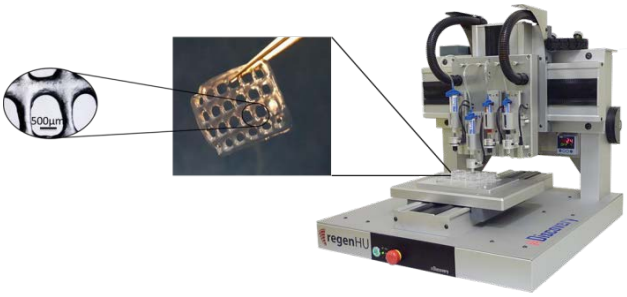

Fig. 2: 3D printed PMP hydrogel after photocuring and removing gelatine showing precise and accurate printing of 5 layers of the polymer.

DISCUSSION & CONCLUSIONS: With the aid of 3D printing technology, the photocurable property of the synthesised polymer means that strong and flexible hydrogels, faithful to the precise shape of the injury, can be made to replicate many of the tissues including human skin. Moreover, cells can survive and proliferate within the gel (results not shown here) for more than seven days a testimony for the future application of such polymers in tissue engineering.

ACKNOWLEDGEMENTS: The research leading to these results has received funding from the People Programme (Marie Curie Actions) of the European Union's Seventh Framework Programme (FP7/2007-2013) under REA grant agreement No PCOFUND-GA-2012-600181.

Decoding matrisome changes during development and ageing: on the path to IVD regeneration

J Caldeira[1,2,3], M Molinos[1,3,4], H Osório[2,3], C Santa[5], B Manadas[5], R Gonçalves[1,3], R Seruca[2,3,6], M Barbosa[1,3,4]

[1] Instituto de Engenharia Biomédica (INEB), University of Porto, Portugal. [2] Institute of Molecular Pathology and Immunology of the University of Porto (IPATIMUP), Portugal. [3] Instituto de Inovação em Saúde, University of Porto, Portugal. [4] Instituto de Ciências Biomédicas Abel Salazar (ICBAS), Porto, Portugal. [5] Center for Neuroscience and Cell Biology, University of Coimbra, Biocant - Parque Tecnológico de Cantanhede, Portugal. [6] Faculdade de Medicina da Universidade do Porto (FMUP), Portugal

INTRODUCTION: Intervertebral disc (IVD) is often the cause of low back pain. Degeneration occurs with age and is accompanied by extracellular matrix (ECM) depletion, culminating in nucleus pulpous (NP) extrusion and IVD destruction. [1, 2]

Current surgical treatments reduce pain but do not restore function and do not provide a long-term clinical solution. [2, 3] In contrast, IVD regenerative therapy holds great promise but is still at a very immature state, and many limitations persist. [4]

We propose a totally new strategy: to expand and differentiate the autologous NP cells in vivo, by ECM modulation. We intend to recreate a microenvironment similar to that of early developmental stages.

METHODS: We have compared the NP ECM proteomic profile of bovine IVDs from foetus, young and old animals by quantitative iTRAQ LC-MS/MS. Protein expression levels have been confirmed by Western Blot analysis.

RESULTS: We identified 170 bovine proteins, of which 77 were commonly expressed by the three distinct age groups. From the 26 matrix proteins detected and quantified, 5 were further validated by Western Blot analyses, being expressed in different proportions in fetus, young and old animals.

DISCUSSION & CONCLUSIONS: Herein, we demonstrate novel and previously described differences in ECM protein expression levels that occur in the bovine IVD with development and ageing. Such molecular cues can be used to try to modulate intervertebral disc regeneration, either alone or in combination with cell therapy to improve its efficacy.

Synthesis and characterisation of novel bio-scaffolds using layered double hydroxide-carbonate and lactone monomers

T Zhou[1], ED McCarthy[1], C Soutis[1], SH Cartmell[1]

[1] *School of Materials, The University of Manchester, UK*

INTRODUCTION: The physical and chemical properties of a scaffold greatly influence a cell's bio-activity. By chemically synthesising the materials of a scaffold, one can better simulate the natural extracellular environment to provide optimum conditions for cell adhesion and differentiation. Herein, we employ in-situ polymerisation to produce various 3D polylactone acid ionomer cell-scaffold structures using Mg/Al layered-double-hydroxide (CO_3^{2-}) as the initiator using the method first published by McCarthy et al[1]. The key product of this reaction is a polymer-based ionomer complex that is insoluble in methylene chloride and has a pore-morphology that enables its use as a biodegradable scaffold for osteoblasts.

METHODS: The initial hybrid product is prepared by the reaction of 95% lactone monomer by mass and 5% LDH by mass heating at 150 °C for 24 h. The ring structure of the L,D-lactide, ε-caprolactone and γ-valerolactone are opened by the carbonate-intercalated LDH initiator to form a copolymer-based ionomer complex. Then, methylene chloride (CH_2Cl_2) is used to extract soluble phase from the polymer product by centrifugation at 8000 rpm for 10 min leaving the insoluble scaffold phase. Finally, the insoluble component is dried in air for 12 h to fully remove the solvent. This technique is based on a previous polymerisation of pure L,D-lactide with stearate-intercalated LDH[1].

RESULTS: Various SEM images (Fig. 1) were taken to examine the microstructure and morphology of the insoluble powder material, which remained after extraction from the hybrid polymerization products. A porous structure is visible in all images, indicating that polymerization of various lactone monomers using carbonate-intercalated layered double hydroxide (hydrotalcite) as an initiator can result in porous structures. By inspection, these structures are quite heterogeneous in terms of having networks with wide pore size distributions. The pore walls of the networks show thickness ranging from 50-130 nm due to the composition differences, which might have an effect on scaffold mechanical properties. Further characterisation of polymer conversion and composition was also performed for these potential bio-scaffold materials (not shown here).

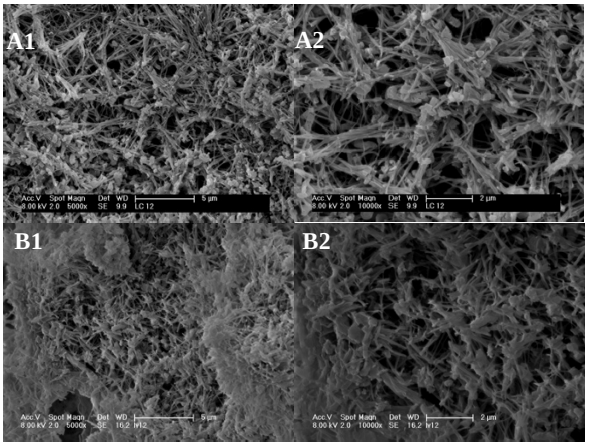

Fig. 1: SEM micrographs of ionomer scaffolds synthesised from (A) L,D-lactide and caprolactone or (B) L,D-lactide and valerolactone (monomer mass ratio 1:2) with 5% mass LDH (CO_3^{2-}) concentration at the magnifications of (1) ×5K (2) ×10K.

DISCUSSION & CONCLUSIONS: This study has confirmed the formation of different porous structures suitable for use as potential cell-growth scaffolds. These were chemically identified as variations of a polymer/magnesium lactate complex (c.f. Xray spectrum in [2]) using XRD. There is a possibility that Al-salts may also exist in these complexes, which remains to be confirmed. Nanoindentation will be used to determine the mechanical properties of the scaffold. Based on the material morphology, it is expected that osteoblast (bone cells) can be successfully seeded in-vitro. Then, PicoGreen and Alamar Blue Assays will be used to test the biocompatibility of the material by indicating the distribution of any live cells across its pores. Once the biocompatibility of the materials is confirmed, fabrication of these materials by 3D printing methods will be explored.

The potential of using human periodontal ligament cells and silk scaffolds for *in vitro* periodontal tissue regeneration

F Al-Dabbagh[1, 2], D Musson[3], S Sapru[4], V Clerehugh[1], M Kellett[1], J Cornish[3], A Ghosh[4], SC Kundu[4], and XB Yang[1]

[1]Leeds Dental School, University of Leeds, UK. [2]College of Dentistry, University of Mosul, Iraq. [3] Department of Medicine, University of Auckland, NZ, [4]Indian Institute of Technology Kharagpur, India.

INTRODUCTION: Periodontal disease is a significant oral condition that affects about 50% of population. This condition would negatively impact both dental health and aesthetics. Classical treatment approaches help in arresting the pathological process; however, more advance techniques are required to restore the multi-tissues constructing the periodontal structure. This study aims to investigate the potential of regenerating this 3D complex using human periodontal ligament cells (HPDLCs) and different types of silk scaffold.

METHODS:

- HPDLCS isolation and characterisation:

Human periodontal ligament cells were isolated from healthy extracted third molar teeth. Colony forming unit-fibroblast (CFU-F) was used to determine the presence of progenitor cells within isolated cell population. Further characterisation was conducted using flow cytometry to assess the levels of mesenchymal stem cells markers (CD73, CD90, CD166) expression as well as other hematopoietic markers (CD34, CD45).

- Immunogenicity assay of silk scaffold:

Commercial Bombyx mori fibroin (cBMF) silk fibres and 2% BMF silk foam were examined for their immunogenicity. Using RT-PCR, relative expression levels of THP-1 cells' inflammatory cytokines were measured in response to those two materials, with rat tail collagen type I scaffold used as control.

- Growth of HPDLCs on silk scaffolds:

HPDLCs were seeded on 2% BMF and cBMF scaffolds (10 x 10^4 cell/scaffold). Cells viability was evaluated by labelling cells with CMFDA/EthD-1 to identify live and dead cells respectively at different time points. At day 28, the scaffolds were processed for histological and immunohistochemical examination. Cellular growth and distribution pattern were also evaluated with SEM.

RESULTS:

- Characteristics of isolated HPDLCs:

Isolated HPDLCs demonstrated fibroblast-like spindle shape with prominent cell body and long processes. After 10 days of culture, 14.2% of cultured cells were attached and proliferated to form colonies (> 50 cells / each). Furthermore, the isolated cells expressed higher levels of mesenchymal stem cells markers (CD73, CD90 and CD166), with lower levels of CD34 and CD45 hematopoietic markers.

- Immunogenicity and cytocompatibility of silk scaffolds:

In 2% BMF foam group, THP-1 cells expressed higher levels of IL-1β and TNF-α after 24hr compared to cBMF fibres and collagen type I control groups. This was similar between cBMF fibres and collagen type I groups. After 7 days, all groups showed increased levels compared to that at 24 hrs with 2% BMF inducing the highest effect. However, both types of silk scaffold can support HPDLCs attachment and growth (in situ images and SEM). Live/Dead fluorescent images showed that the majority of cells on the scaffolds were viable with only a few dead cells after 21 day of culture. Van Gieson and HE stain demonstrated cellular ingrowth into 2%BMF silk with collagen matrix formation. For cBMF fibres, HPDLCs aligned along and parallel to the fibres, with evidence of bridging the gap between them. Moreover, IHC results confirmed that the extra cellular matrix was positive to human collagen type 1 antibody. In the 2%BMF scaffolds group, von Kossa stained sections showed presence of extracellular mineral deposits.

CONCLUSIONS: This study demonstrated that silk scaffolds could be used to support HPDLCs attachment and growth, which indicated the potential of using this combination of silk scaffolds and HPDLCs for periodontal tissue engineering.

ACKNOWLEDGEMENTS: F Al-Dabbagh is funded by the higher committee of education development in Iraq (HCED). This project is partially funded the British Council - UKIERI and the EUFP7 under the agreement number 318553-SkelGEN.

Bone-forming potential of calvarial-derived progenitor cells

GS Mandair[1], Steenhuis P[1], MD Morris[2]

[1] *School of Dentistry, University of Michigan, Michigan, Ann Arbor, USA.* [2] *Department of Chemistry, University of Michigan, Ann Arbor, USA*

INTRODUCTION: Cell source plays a critical role in achieving successful repair of craniofacial bone defects. Studies show that the calvaria can provide a source of progenitor cells that can be isolated, expanded, and transplanted *in vitro* to form mineralized bone [1]. However, the quality of mineral formed in culture has yet to be assessed. This kinetic study aims to follow bone collagen maturation and bone mineral forming potential of calvarial-derived progenitor cells in culture using Raman microscopy. The quality of bone collagen and mineral formed in culture will be compared against immature and mature bone tissues.

METHODS: Bone-forming progenitor cells (Sca-1$^-$ cell fractions) were isolated from fetal-day 18.5 (FD18.5) old mouse calvaria [1] and plated on to fused-silica slides. Confluent cells were cultured in standard osteogenic media for 35 days [1]. At specific times, slides were removed and analysed by Raman microscopy. Three bone compositional parameters were calculated: Crystallinity (inverse of the phosphate 957 cm^{-1} band width at FWHM); mineralization (959/853 cm^{-1} ratio); and collagen quality (1663/1640 cm^{-1} ratio) [2-3]. Estimates were also obtained from FD18.5 immature calvaria tissue (CT) and mature 6-month old mouse tibia (MT). After Raman microscopy, select slides were stained *via* the von Kossa method to visualize mineralized bone tissues in culture.

RESULTS: As shown in Fig.1A, mineralized bone first appeared at day 8. Raman microscopy showed that this deposit was mineralized (Fig.1B). Crystallinity, which represents perfection of mineral crystalline domains and crystal size, was also increased at days 8 and 11 (Fig.1B-C). Mineralization and crystallinity decreased at days 11 and 14, but increased at days 25 and 35. At day 35, bone formed in culture was over-mineralized compared to immature and mature bone, while crystallinity was lower than that of immature bone. As shown in Fig.1D, the quality of bone collagen formed in culture increased with culture time, owing to the translation of less ordered collagen secondary structure (high 1663/1640 cm^{-1} ratios) to a more ordered collagen helical structure (low 1663/1640 cm^{-1} ratios) [3]. Collagen quality of bone formed at day 35 was similar to that of immature bone, but less than that of mature bone.

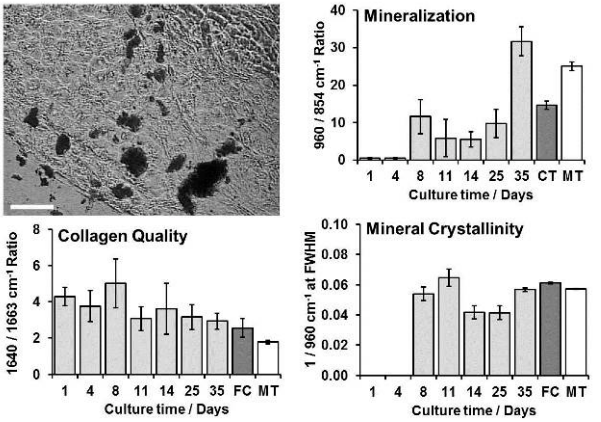

Fig.1: Image of von Kossa stained mineral at day 8 (A). Bone compositional values for cell cultures (days 1-35), immature calvarial tissue (CT), and mature mouse tibia (MT) (B-D). Bar: 200 μm.

DISCUSSION & CONCLUSIONS: We show that bone mineral formed in culture by calvarial-derived progenitor cells is aperiodic with periods of fast and slow mineral deposition. The decrease in mineral deposition after day 8 and increase at day 25 is unclear. However, aperiodic mineral deposition have been reported in calvaria organ culture studies in which periodic bursts in mineral deposition was followed by periods of little or no mineral deposition [4]. In summary, the quality of bone collagen formed in culture by calvarial-derived progenitor cells are similar to that of immature bone, while bone mineral formed in culture can become over-mineralized with prolonged culture time and is less crystalline compared to immature bone.

ACKNOWLEDGEMENTS: Supported by NIH Grant, R01 AR047969.

Attachment of bacteria involved in peri-implantitis to titanium and cobalt chromium.

C Haury[1], A Wescott[2], D Beeby[2], B Austin[2], SQ Jones[1], WN Ayre[1], R Waddington[1], AJ Sloan[1]

[1]Mineralised Tissue Group, School of Dentistry, Cardiff University, Wales, UK. [2]Renishaw plc, Gloucester, England, UK.

INTRODUCTION: Peri-implantitis is an infectious disease associated with inflammatory destruction of bone tissues leading to implant failure and removal[1]. Common pathogens implicated in the majority of peri-implantitis cases are Gram negative bacillo-cocci such as *Porphyromonas gingivalis*, *Prevotella spp*, and *Fusobacterium spp*[2]. It is historically considered that implants are sequentially colonised. A conditioning film composed of salivary proteins is formed, allowing commensal early colonisers to bind to the tooth surface. Early colonisers are then bound by late colonisers, including the studied pathogens[3].

The aim of this study is to investigate the attachment of pathogenic Gram negative bacteria involved in peri-implantitis to titanium and cobalt chromium abutments.

METHODS: Titanium alloy (titanium 6-aluminium 4-vanadium) and cobalt chromium laser sintered discs were supplied by Renishaw plc – Medical and Dental Products Division, and milled titanium discs were purchased from GoodFellow. The surfaces of the discs were imaged by Scanning Electron Microscopy, characterised by Fourier Transform InfraRed spectroscopy and X-Ray Diffraction and their roughness and hydrophobicity compared. Bacteria were sub-cultured in Fastidious Anaerobe Broth for 12 h under anaerobic conditions, and diluted at starting concentrations corresponding to 1 x 10^6, 1 x 10^7 and 1 x 10^8 cells/mL, for *F. nucleatum*, *P. gingivalis* and *P. intermedia*, respectively. Growth was monitored by optical density measurements and bacterial counts every 4 h. Bacterial attachment to titanium and cobalt chromium discs was studied for each species and mixed species using live dead staining combined with confocal microscopy. Images were analysed using ImageJ to determine the percentage of coverage by fluorescence. All experiments were performed in triplicate.

RESULTS: Titanium and cobalt chromium surfaces, laser sintered then polished, were very smooth (0.129 µm +/- 0.067, mechanical R_a +/- sd), whilst the milled discs were significantly rougher (0.809 µm +/- 0.034, mechanical R_a +/- sd). These results were visually confirmed by SEM imaging. Contact angle measurements demonstrated no differences between all samples, independent of the roughness.

A difference in growth rate was observed between the species, whereby *F. nucleatum* grew more rapidly than the other bacteria.

The attachment studies (Fig.1) showed that *P. gingivalis*, *P. intermedia*, and *F. nucleatum* are able to attach to titanium and cobalt chromium discs without the need for protein surface conditioning or the attachment of early colonisers. Similar results were found for polished and milled discs. Roughness was therefore not found to affect bacterial adhesion.

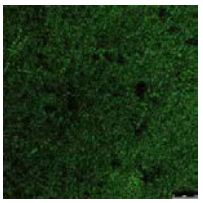

Fig. 1: Confocal imaging of bacterial species on milled Ti disc.

DISCUSSION & CONCLUSIONS:

Attachment of pathogenic Gram negative bacteria on discs without the help of salivary proteins and early colonisers indicates that late colonisers may be able to directly attach to dental implants and abutments immediately after implant placement. This fact is clinically important as the produced virulence factors induce inflammatory destruction of mucosal and osseous tissues surrounding the implant. The ability of Gram negative pathogenic bacteria to bind to abutments directly may promote migration towards the gum and therefore increase the probability of chronic inflammation leading to peri-implantitis and tissue destruction.

ACKNOWLEDGEMENTS: This project is supported through a research collaboration funded by Renishaw plc and Cardiff University.

Cell culture and cell analysis using the Real Architecture For 3D Tissue (RAFT™) Culture System

S Schaepermeier[1], S Buesch[1], J Langer[2], K Atze[1], T D'Souza[2], L Hussain[2], V Vogel[1], J Schroeder[1]
[1]*Lonza Cologne GmbH, Cologne, Germany;* [2]*Lonza Walkersville Inc., Walkersville, MD, USA*

INTRODUCTION: Conventional *in vitro* assays are based on cells grown on two-dimensional (2D) substrates, which are not representative of the true *in vivo* cell environment. In tissue environments, cells interact with neighboring cells and with the extracellular matrix (ECM). Three-dimensional (3D) cell culture methods, in contrast, allow cells to grow in structures resembling more the *in vivo* environment. Cells can develop cell-cell and cell-ECM interactions in 3D.

METHODS: The RAFT™ 3D Cell Culture System uses a collagen matrix that more closely resembles physiologically relevant concentrations. Cells and neutralized collagen are mixed and dispensed into wells of standard cell culture plates, and subsequently incubated at 37°C to allow the formation of a cell-seeded hydrogel. Specialized RAFT™ Absorbers are placed on top of the hydrogels. The RAFT™ Absorbers gently remove the abundant medium, thus condensing the cell/collagen hydrogel to a layer approximately 120 µm thick, which is robust and easy to handle for downstream assays. These cultures are then ready to use, but additional epithelial or endothelial cells may be added as overlays on top to study co-cultures or more complex cultures.

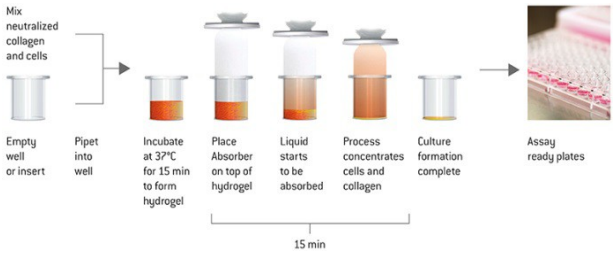

Fig. 1: The RAFT™ Process. RAFT™ Cultures are formed within less than one hour.

RESULTS: This presentation explains how the RAFT™ 3D Culture System can be analysed using standard cell biology methods like immuno-cytochemistry. Fluorescence-based imaging of cells is possible with subcellular resolution.

It will be shown that the Lonza Vialight™ Plus Bioassay can be applied with a slightly modified protocol to determine cell viability in RAFT™ 3D Cell Cultures. A broad linear range as well as a similar assay performance as in standard 2D cultures were observed with the HCT 116 cell line.

In addition, the RAFT™ 3D Culture System is compatible with transient transfection approaches using the Lonza Nucleofector™ Technology. Dependent on the cell type, transfection efficiencies of up to 95% could be obtained.

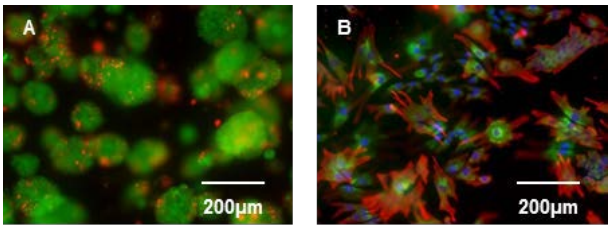

Fig. 2: A) HCT 116 cells in 6-day-old RAFT™ 3D Cultures (Calcein AM (green), Propidium Iodide (red)). B) Adult normal dermal human fibroblasts in 7 day old RAFT™ 3D Cultures (Vimentin (red), P4HB (green), Hoechst 33342 (blue)).

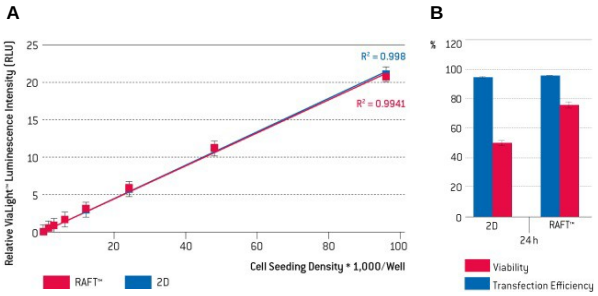

Fig. 3: A) Performance of the Vialight™ Plus BioAssay for HCT 116 cells in 2D or 96-well RAFT™ 3D cultures. B) HCT 116 cells were transfected with the 4D-Nucleofector™ System X-Unit. 24 hours after seeding into 2D or RAFT™ 3D Cultures transfection efficiency (pmaxGFP™ Vector) and cell viability was determined.

DISCUSSION & CONCLUSIONS: While 3D cultures more closely represent the *in vivo* environment than standard 2D cultures, they can be more difficult to analyze.

This presentation shows how standard analysis techniques, like fluorescence microscopy and viability assays, can be applied to RAFT™ 3D Cell Cultures. In addition, it will be shown how the RAFT™ Technology can be combined with transient transfection approaches using the Lonza 4D Nucleofector™ System.

Mechanical properties of tissue engineered bone-like tumour models

T Eriksson[1], S Fedele[2], R M Day[3], V Salih[4]

[1] Biomaterials and Tissue Engineering, [2] Oral Medicine, both UCL Eastman Dental Institute, 256 Gray's Inn Rd, London WC1X 8LD [3] Applied Biomedical Engineering, UCL, [4] PUPSMD, University of Plymouth

INTRODUCTION: Since the development of plastic compressed constructs[1], collagen scaffolds have been tailored for many applications, including tumour models[2]. Organotypic models should mimic the mechanical properties of the tissue they strive to model. This study examined the mechanical properties of collagen constructs with and without the decellularised bone substrate Bio-Oss, to ensure that the bone-invading tumour ameloblastoma was modelled in a bone-like environment. To date, little data exists on scaffolds similar to those used for these models.

METHODS: Collagen type I (First Link, UK) gels were neutralised with 1M and 5M NaOH and half were cellularised with human osteoblast cells. Bio-Oss (Geistlich Biomaterials, UK) was added to half the gels. Constructs were then plastic compressed[1] to a thickness of approximately 400µm. Constructs were kept either in DMEM, PBS, osteogenic media (DMEM with 1mM dexamethasone, 0.1M ascorbate-2-phosphate and 1M β-glycerophosphate and 10% FBS and 1% pen/strep) or keratinocyte serum-free media (KSFM) with 1% pen/strep. Construct mechanical properties were tested using a Bose Electroforce 3100 dynamic mechanical analysis (DMA) tester with associated WinTest 7 software. A dynamic amplitude of 12µm and a frequency range of 0.1-1.0 Hz were used.

RESULTS: Statistically significant differences were found between constructs with and without added Bio-Oss (fig 1; $p \leq 0.001$, one-way ANOVA). Different types of culture media were found not to result in a change in construct stiffness, although the constructs had previously been shown to mineralise faster using osteogenic media[3].

Interestingly, the osteoblast cells in the collagen-only constructs appeared to reduce the stiffness compared to the acellular collagen-only constructs (fig. 1; ($p \leq 0.001$). This was not expected, as previous data showed increased mineralisation in constructs even without Bio-Oss[3].

DISCUSSION & CONCLUSIONS: Neither the addition of proteins (FBS) in the media, nor an increase in culture time appeared to affect the constructs' mechanical properties.

However, as bone is also an anisotropic material, and the Bio-Oss granules were oriented randomly within the collagen scaffolds, this may have had an effect on the compressive strength of the scaffolds.

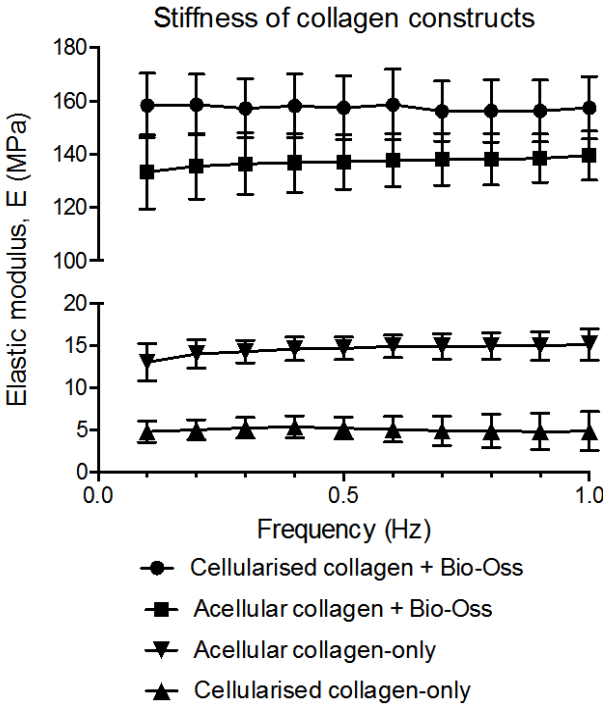

Fig. 1: Stiffness of the collagen-only and collagen + Bio-Oss constructs in MPa as measured using DMA. Error bars = standard deviation, n = 4.

Currently, very little reliable DMA data exists on the mechanical properties of Bio-Oss scaffolds and there is no consensus on testing, even though Bio-Oss is used clinically for bone augmentation. The decellularised and sterilisation processes are thought to affect the mechanical properties of Bio-Oss, as native bone stiffness is reported[4] as 23GPa, much higher than the bone-like model analysed here. Future studies should include more mechanical testing of organotypic models.

ACKNOWLEDGEMENTS: Thanks to Dr Celia Murray-Dunning and Dr James Phillips (both UCL BTE) for their assistance with the DMA. Thank you also to Prof Jonathan C Knowles for helpful insight into mechanical testing. The UCL Development Office and the Biss-Davies charitable trust provided sponsorship.

Developing a co-culture model to investigate fibroblast involvement in vascular inflammation

[1, 2]K Wright, [2]S Francis, [1]JW Haycock

[1]*Kroto Research Institute, Materials Science and Engineering,*
[2]*Department of Infection, Immunity & Cardiovascular Disease, University of Sheffield*

INTRODUCTION:

Although improvements in current treatments have seen a continuing decline in mortality for cardiovascular disease, without the design of preventative therapies, morbidity will continue to increase [1]. To discover novel targets for such therapies, *in vitro* EC/SMC co-culture models are often used to mimic the *in vivo* vascular environment. However, this is only representative of the immediate surroundings close to the vascular lumen. Other cells like fibroblasts are positioned within the *tunica adventitia* and potentially gain SMC-like properties to migrate towards the lumen [2]. Therefore, the aim herein is to incorporate and understand how the fibroblast is involved in a co-culture model to provide a more accurate understanding of the early stages of atherosclerosis.

METHODS:

Human umbilical vein endothelial cells (HUVEC) and normal human dermal fibroblasts (NHDF) were cultured as standard protocol. Cells were seeded at 20-30,000 cells/mL and grown until ~60-70% confluency. The cells were then incubated for 6-24 hrs in a TNF-α (0-400 U/mL) containing growth medium, before fixing. ICAM-1 was labelled using 1:100 mouse anti-human ICAM-1 at 4 °C overnight, followed by 1:1000 goat anti-mouse Alexa Fluor 633 for 2 hrs at RT. Samples were then stained with DAPI for 10 min to identify nuclei immediately prior to confocal microscopy. For co-culture studies, HDFs were incubated for 30 mins in green CMFDA dye cell tracker prior to seeding. Light microscopy images were obtained of paraffin-embedded coronary arteries; the right coronary artery (RCA) and left anterior descending (LAD). The number of adventitial cells (AC) and endothelial cells (EC) were counted in sections to estimate AC:EC ratios.

RESULTS:

The introduction of TNF-α caused a significant increase in the proportion of both NHDF and HUVEC cells expressing ICAM-1 *(Fig. 1)*.

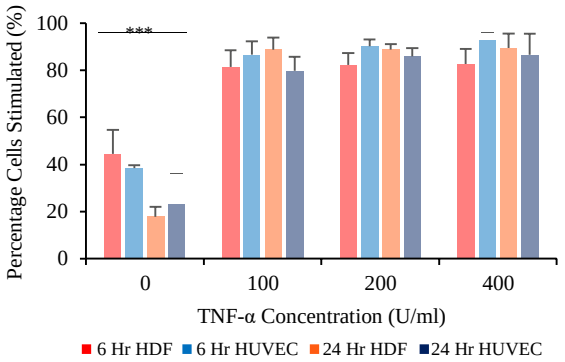

Fig. 1 ICAM-1 upregulation in HUVEC and HDF cells. Error bars represent σ and significant intragroup differences not displayed.

Expression continued to increase over a 24 hr period for NHDFs, whilst decline in expression was observed in HUVEC after 6 hr.

A comparison of the RCA and LAD determined AC number increases at various rates throughout the coronary tree (max 3.5:1 RCA vs 1.5:1 LAD). However, both vessels' minimum ratio was approximately 1:1, appearing in areas of complete *tunica intima*.

DISCUSSION & CONCLUSIONS:

Although both HUVEC and NHDF constitutively express ICAM-1 at low levels, NHDFs have been shown to have a much lower expression during the log phase of growth in comparison to the quiescent phase [3]. This may cause an increased number of cells to become stimulated at earlier time-points and explain the differing trends after 6 hrs.

NHDFs are highly stimulated by physiological levels of TNF-α. Future work will ascertain whether low shear stress can also induce ICAM-1 expression relevant to an *in vitro* vascular model and sites of atherosclerosis.

Comprehensive evaluation of the impact of injectable delivery on mesenchymal stem cells: Finding the winning combination

MH Amer[1], FR Rose[1], LJ White[1], KM Shakesheff[1]

[1] *Wolfson Centre for Stem Cells, Tissue Engineering and Modelling (STEM), School of Pharmacy, University of Nottingham, Nottingham, NG7 2RD, UK*

INTRODUCTION: Optimal delivery strategies for injectable cell-based therapeutics are required to enhance the efficacy and reproducibility of cellular therapy. The mode of delivery of fragile cells can compromise treatment efficacy, which is dependent on cell viability and functionality post-injection. Following on our previous work[1], where a comprehensive toolset was employed for the assessment of injectable cell delivery, the effects of ejection rate on trilineage differentiation potential was quantified. Biomaterial-assisted cell delivery was also investigated as a possible solution to the low cell numbers being delivered at low ejection rates.

METHODS: Primary human mesenchymal stem cell (hMSC) suspensions were drawn up into 100 µL Hamilton syringes with 30 and 34 gauge needles, before being ejected at rates ranging from 10-300 µL/min. Effects of ejection rate were comprehensively evaluated, using various standard and multiplex assays, in terms of percentage of cell dose being delivered as viable cells, phenotype, trilineage differentiation potential, and other parameters of cell health. Moreover, various injectable cell carriers were investigated to determine improvement of cell recovery and possible influence on hMSCs differentiation potential.

RESULTS: Ejections at slower flow rates resulted in a significantly lower percentage of dose being delivered as viable cells. Normalised caspase-3/7 activity measurements ejected at 10 µL/min were also significantly higher than control. Quantification of the differentiation of ejected hMSCs revealed that both ejection rate and cell carrier employed can exert an effect on hMSCs differentiation capacity, as exemplified by osteogenic differentiation in Fig. 1. The use of biomaterials as cell carriers significantly improved cell recovery, with gelatin resulting in 87.5±14% of the cell dose being delivered as viable cells, in comparison with 32.2±19% of the dose in phosphate buffered saline (PBS) (Fig. 2).

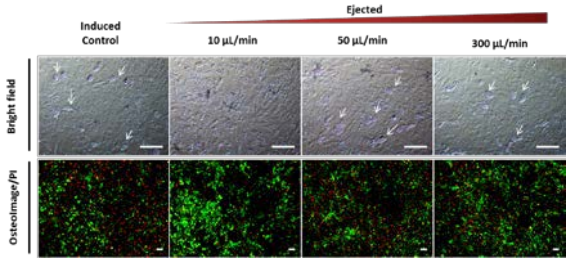

Fig. 1: Representative bright-field and fluorescence microscopy images showing the effect of ejection rate on osteogenic differentiation potential of hMSCs (Scale bar: 100µm)

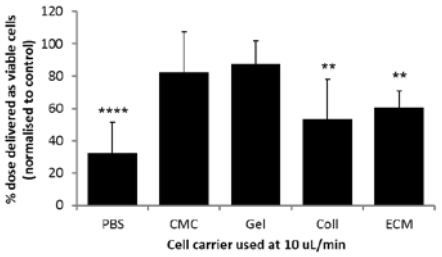

*Fig. 2: Percentage of hMSC cells delivered within phosphate buffered saline (PBS) and other carriers after ejection through a 30G needle at 10 µL/min, normalised to directly plated control (mean ± SD%, n = 5). Asterisks show statistically significant difference in number of ejected cells relative to control (** p < 0.01; **** p<0.0001)*

DISCUSSION & CONCLUSIONS: This study shows that ejection rate, needle size and cell carrier have a significant impact on the percentage of cell dose delivered, cell health and differentiation potential post-ejection. The combination of these factors, among others, may affect the fate of hMSCs injected, thereby influencing the success of cell-based therapies.

ACKNOWLEDGEMENTS: This study was supported by MRC, EPSRC and BBSRC UK Regenerative Medicine Platform Hub "Acellular Approaches for Therapeutic Delivery", University of Nottingham International Office, Schlumberger Foundation and Misr ElKheir Foundation.

Effect of transforming growth factor-β on up/down regulation of integrin-β1 in primary chondrocyte culture

SA Khaghani[1], F Sefat[1], M Youseffi[1], R Rehman[1], CF Soon[2], G Akbarova[3]

[1] *Medical and Healthcare Technology, School of Engineering, University of Bradford, UK.*

[2] *Biosensor and Bioengineering Laboratory, MiNT-SRC Research Centre, Universiti Tun Hussein Onn Malaysia, Malaysia.* [3]*Genetics Department of Baku State University, Baku City, Azerbaijan.*

INTRODUCTION: Regeneration of a damaged or non-functioning tissue requires adhesion of cells to their extracellular matrix (ECM). Thus the investigation of the level of synthesised cell adhesion molecules (CAMs) in cell culture systems play major roles in cell and tissue engineering. Adhesion of chondrocyte to a collagen type-II rich matrix, is dependent on cell adhesion molecules (CAMs) and integrins and cells adhere to ECM through integrins.

METHODS: Monolayer-expanded primary chondrocyte cells derived from forth passage were used in this work. The cells were isolated from knee joint of neonate Sprague-Dawley rat, and the protocol has been described in detail elsewhere [1]. Eight 22 mm² glass coverslips were sterilised with eight petri dishes labelled as Control, TGF-β1, TGF-β2, TGF-β3, TGF-β(1+2), TGF-β(1+3), TGF-β(2+3), and TGF-β(1+2+3).

Chondrocyte cells were cultured, expanded in monolayer culture system and $8x10^6$ cells were resuspended in 40 ml DMEM media supplemented with 10% FCS. Five ml of cell suspensions were subjected to seeding on each coverslip. Five ml of cell suspension was also seeded on coverslips labelled as control. Remaining cell suspensions were aliquoted in 5 millilitres and supplemented with TGF-β1, TGF-β2, TGF-β3, TGF-β(1+2), TGF-β(1+3), TGF-β(2+3), and TGF-β(1+2+3). All cell cultures were incubated at 37°C for 24 hours. After 24 hours, cells were fixed by 1% formaldehyde and immunocytochemically stained for integrin β1 (CD29).

RESULTS: The isolation and purification of cartilage cell (chondrocyte) and cultivation of this cell in planar culture system showed that cells with low density produced fibroblast like morphology and synthesised collagen type-I instead of collage type-II. Monolayer culture of the chondrocyte resulted in dedifferentiation of cells and production of stress fibres. This characteristic was prevented by high density and 3D multilayer chondrocyte culture. TGF-β2, TGF-β3, and manipulated TGF-β(2+3) exhibited similar synthesis of integrin-β1 (CD29) to control (Figure 1A-B), but TGF-β1, TGF-β(1+2), TGF-β(1+3), and TGF-β(1+2+3) decreased the expression of integrin-β (Figure 1C-D). This is likely due to gene expression level of TGF-β and the chondrogenic transcription factors Sox-9, c-fos, or c-jun seen to be necessary for chondrogenesis (remains unchanged), and on the other hand, to high expression of β1 integrin, which plays major roles in cell–matrix interactions in chondrocytes.

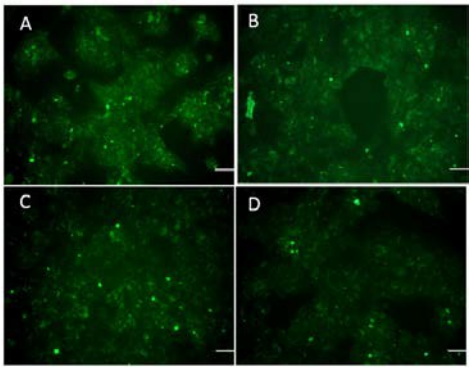

Fig. 1: Immunofluorescence micrographs of chondrocytes stained for integrin-β1 subunit: A) control; B) TGF-β3; C) TGF-β1 and D) TGF-β(1+2); (Scale bar = 50μm).

DISCUSSION & CONCLUSIONS: The weak presence of integrin β1 revealed that additions of such transforming growth factor-β and their manipulated forms down-regulated integrin β1 leading possibly to the down regulation of cartilage formation.

Results also suggested that TGF-β(1+2) (Figure 1D) could be utilized in fabrication of biodegradable scaffolds for 3D chondrocyte culture, due to its ability to induce cell proliferation.

Development and optimisation of a 3-D *in vitro* model of osteosarcoma

M. Pavlou, T. W. R. Briggs, P. Gikas, S. J. Roberts*, U. Cheema*

Institute of Orthopaedics and Musculoskeletal Science, University College London, UK

INTRODUCTION: Osteosarcoma is the most prevalent type of primary bone cancer, stemming predominantly from the intramedullary cavity at the metaphysis of long bones1. Overall 5-year survival lies at 68%, with poor responders to standard care dying of recurring disease within 5 years of diagnosis2. Failure to improve survival outcomes for poor responders persists, as evidenced by the results of EURAMOS-13. Heterogeneity, rarity and the lack of a flexible clinically relevant disease model, pose key limitations. As such, there is a requirement for a personalised medicine modality to assign postoperative osteosarcoma treatments. It is hypothesised herein that a modular tissue engineering approach to build a 3-D *in vitro* model of invasive osteosarcoma, which mimics the *in vivo* tumour microenvironment, could deliver a platform for assessing therapeutic agents.

METHODS: Osteosarcoma microenvironment cues were dissected into semi-autonomous modules i.e. the cellular Artificial Cancer Mass (ACM) nested inside an acellular Bone-Marrow-like Stroma (BMS); overall termed 'tumoroid'. Complexity in the form of cell-cell/cell-matrix interactions, spatiotemporal matrix composition and stiffness, were increased gradually so that the role of each of these elements in osteosarcoma invasion and drug-response may be determined. The tumoroid was created using the non-metastatic MG-63 and metastatic 143B osteosarcoma cell lines. ACMs were produced by combining osteosarcoma cells with Rat-tail Collagen type I (Col1A), which was left to crosslink before plastic compression as per the RAFT^{TM} 3D Cell Culture Kit Protocol (Lonza Group AG, Basel, Switzerland). Compressed ACMs were then nested inside BMS composed of Col1A, Laminin [25-50μg/ml] and/or Fibronectin [25-50μg/ml], which was subsequently left to crosslink and then plastic compressed as a whole. 3-D tumoroids were incubated at 37°C, 5% CO_2 for 14 days. Tumoroid invasion at the ACM/BMS boundary was assessed on Day 14 via Fluorescence Microscopy and ApoTome Optical Sectioning (Carl Zeiss Ltd, Cambridge, UK) for DAPI/Phalloidin detection.

RESULTS: Following the generation of metastatic and non-metastatic tumoroids, which were produced via ACM nesting inside BMS containing Collagen type I and Laminin [50μg/ml], it was observed that the mode of invasion for metastatic tumoroids was mainly sheet-like. Conversely, non-metastatic tumoroids invaded predominantly through spheroid-like cell masses. Moreover, metastatic tumoroids achieved a 45% ($p<0.01$) greater surface area (μm^2) of invasion compared to non-metastatic. To further mimic the bone intramedullary environment Fibronectin [25-50μg/ml] was added to the BMS of metastatic and non-metastatic tumoroids. This resulted in a 30% ($p<0.001$) increase of sheet-like invasion in metastatic tumoroids, but no significant changes with non-metastatic cells.

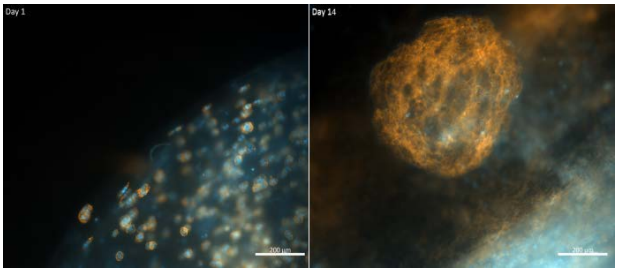

Fig. 1: Representative Images from 3 independent experiments: 143B osteosarcoma tumoroid invasion from ACM margin – Day 1 single cell morphology Vs Day 14 invasive spheroid mass.

DISCUSSION & CONCLUSIONS: Increasing the complexity and biomimicry of the matrix composition resulted in a significant increase of metastatic tumoroid invasiveness, compared to non-metastatic. These observations are in line with the known *in vivo* characteristics of the cells used to generate 3-D tumoroids, proving the capacity of this model to recapitulate native cell behaviour *in vitro.*

ACKNOWLEDGEMENTS: We are grateful to the project sponsors SCAT and BCRT for their generous support.

**these authors share senior authorship*

Development of a 3D neuronal-culture model for peripheral nerve studies

M Behbehani[1], A Glen[1], C Taylor[1], A Schuhmacher[2], JW Haycock[1]
[1] *Department of Materials Science and Engineering, Kroto Research Institute, Sheffield, UK*
[2] *Department of Applied Chemistry, Reutlingen University, Germany*

INTRODUCTION: More than 2.5% of trauma patients suffer injury to at least one peripheral nerve. The current gold standard treatment, of autografting, is often associated with side effects, such as donor site morbidity. This has lead to the fabrication of bioengineered nerve guidance conduits (NGC). To concurrently test candidate biomaterials and geometries potentially suitable for supporting nerve regeneration a more complex and physiological relevant 3D environment is appropriate. Therefore, the aim of the study was to develop a 3D *in vitro* system as a platform to investigate intraluminal materials and structures postulated to enhance neuronal regeneration.

METHODS: 5mm long polyethylene glycol (PEG) conduits and hemi tubes were fabricated by microstereolitography[1]. Electrospinning was used to spin aligned, micron sized polycaprolactone (PCL) fibres[2]. Neuronal cell maturation was examined using a combination of NG108-15 neuronal culture and rat dorsal root ganglion culture enabling concurrent examination of Schwann cell and neurite outgrowth. Guidance assessment was conducted by confocal microscopy via βIII-tubulin and S100β immunolabelling. Neuronal viability in culture was measured by an MTT assay and Syto-9/propidium iodide staining gave a live/dead cell overview.

RESULTS: A new kind of NGC with an internal fibre filling was fabricated (Fig. 1). Neurite guidance along the micrometre fibres was evident in the tested NGCs. Additionally the fibres supported aligned Schwann cell and neurite outgrowth from rat dorsal root ganglion. A cell migration distance of 2.20 mm was observed on 5 µm diameter fibres after 21 days (Fig. 2).

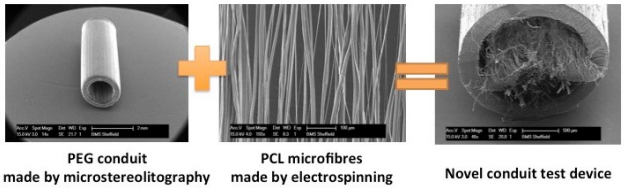

Fig. 1: Combination product of PEG NGC, fabricated by microstereolitography and 5 µm PCL fibres produced by electrospinning

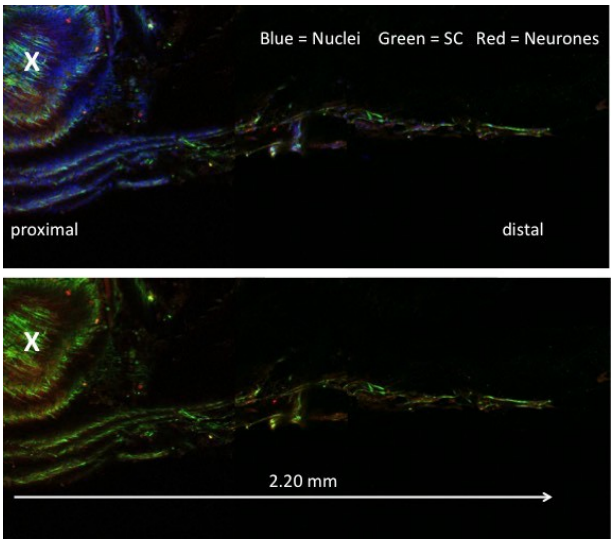

Fig. 2: *Confocal microscopy z-projection of a rat DRG cultured in vitro for 21 days on 5 µm PCL fibres in a 5 mm long PEG NGC. Cell migration distance of 2.20 mm from the proximal DRG (X) position into the NGC with incorporated microfibres (distal). Nuclei were labelled by DAPI (blue), neurites (red) by βIII-tubulin and Schwann cells (green) by S100β immunolabelling.*

DISCUSSION & CONCLUSIONS: The study shows on the one hand the potential of the developed system to test filling materials directly in NGCs in a 3D environment *in vitro* and on the other hand highlights the potential of PCL fibres as a filling material for NGCs. The study provides a platform to test different NGC and internal biomaterials and mimics a more physiologically relevant environment than *in vitro* material tests using flat surfaces.

ACKNOWLEDGEMENTS: This project was funded by the Erasmus programme.

Towards the development of robust and meaningful potency assays for MSCs

FS Abukar[1], IB Wall[1]

[1] *University College London (UCL), Department of Biochemical Engineering, Torrington Place, London, WC1E 7JE*

In the UK alone, there are 146,000 people that have a Myocardial Infarction (MI) every year. Multiple clinical trials have explored MSCs for therapeutic application for ischemic cardiac injury. Currently there are no potency assays in the clinical setting that give a reliable measurement of MSCs mode of action, other than simple surface marker expression, which does not predict function. For this reason, there is a need to develop *in vitro* assays that will be predictive of functional activity of the MSC product. To be predictive, the assays need to be performed using parameters that more closely mimic the environment in the body, because measuring cell attributes in ambient conditions does not inform on how the cells will behave *in vivo*. Vascular assays can be used as platforms to study the hypothesis that MSCs functionally support blood vessels as a key mode of action in ischemic injured tissues. Vascular assays have traditionally lacked robustness and reproducibility, particularly since biological materials are highly variable. Our work focuses on developing robust assays with increased reproducibility. To achieve this, one aim of the project is to use Design of Experiments (DOE) to systematically optimize key parameters that affect the tubule-formation capacity of human endothelial cells, with an aim of making the assays more standardized and lowering assay costs in the process. In the current work, we found that tubule network formation could be controlled using lower quantities of an optimized matrix hence increasing the number of assays achievable from a single batch of substrate. Previous literature has indicated that efficiency of tubule forming capacity decreases drastically after endothelial cells reach passage 10. Therefore further work was conducted to investigate the impact of passage number on tubule formation capacity on the optimized matrix. Automated cell counting methods were used and were validated using manual counts. Here we show that higher passages than the ones presented in the literature, are still able to form networks when using optimized matrices, therefore increasing the possibility for higher throughput release assay development. Ultimately the optimized methods will enable MSCs to become a real therapy and replace more costly and less reliable tests currently in the market.

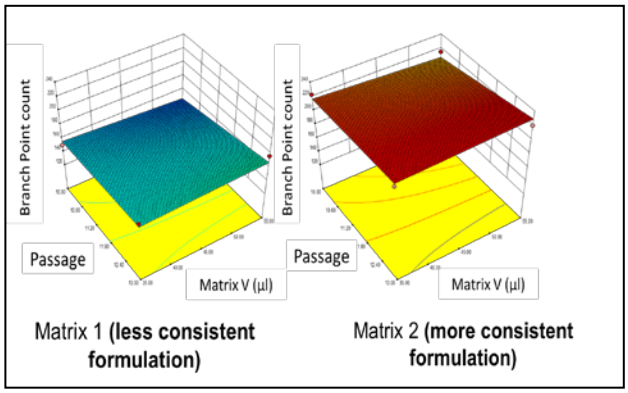

Fig. 1: 3D response graphs comparing branch point counts for two different types of matrix, passage number and matrix volume.

Antimicrobial hydrogels for the control of pulpal infection to facilitate regenerative endodontics

EP Everett[1, 2], R Waddington[1], A Paul[2], AJ Sloan[1]

[1] *Mineralised Tissue Group, Department of Oral and Biomedical Sciences, School of Dentistry, Cardiff University, Heath Park, Cardiff, CF14 4XY.* [2] *Soft Matter Research Group, School of Chemistry, Cardiff University, Main Building, Park Place, Cardiff, CF10 3AT.*

INTRODUCTION: The placement of dental restorations (fillings) aims to eliminate infection and inflammation of the tooth's pulp and allow for the production of regenerative dentine. A significant proportion of these restorations, however, will fail due to secondary bacterial infection, which hampers the regenerative process and leads to irreversible pulpal necrosis. It is therefore essential to prevent and control bacterial infection in order to allow for tissue repair and regeneration to occur.

Current dental restoration materials have no bioactive mechanism to prevent infection and systemic antibiotics are ineffective in these cases. It would therefore be advantageous to develop new filling materials that are antimicrobial, so that they can be used in restorative treatments and prevent secondary infection. Hydrogels have potential as a restoration material due to their tuneable physical properties and the ability to carry therapeutic agents in the aqueous component of the gel.

This study investigates the rheological and antimicrobial properties of antimicrobial nanovesicles incorporated into a methylcellulose hydrogel and considers its suitability for use in endodontic treatment.

METHODS: Nanovesicles containing the hydrophobic antimicrobial triclosan were produced and incorporated into a 10 % w/w methylcellulose solution. The rheological properties of the material were investigated, including viscosity, and amplitude and temperature dependant viscoelasticity. The effect of nanoparticle formulation and concentration was also measured.

The antimicrobial capability of the hydrogels was measured; both in broth suspension and on agar plates. This efficacy was compared to that of antimicrobial nanoparticles and free antimicrobial solutions alone.

RESULTS: Methylcellulose could be prepared under mild conditions, without the need for non-aqueous solvents, high temperature or harsh pH conditions. Solutions were viscous liquids at ambient temperature and formed a gel at higher temperatures. Viscoelastic characteristics indicated that the gelation temperature was around physiological temperature. Rheological properties were unaffected by the addition of nanoparticles, irrespective of nanoparticle formulation or concentration.

Antimicrobial assays showed inhibited growth of *Streptococcus anginosus* and *Enterococcus faecalis* in broth when cultured with antimicrobial nanoparticles; both in solution and in the methylcellulose gel. Zones of inhibition were observed when these bacteria were grown on agar plates inoculated with the antimicrobial nanoparticles; both in solution and in methylcellulose gel.

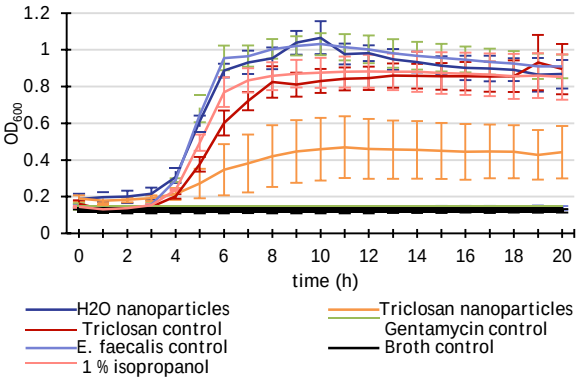

Fig. 1: Graph shows inhibited growth of E. faecalis *when incubated for 20 h with triclosan nanoparticles in 10 % methylcellulose gel (n=3)*

DISCUSSION & CONCLUSIONS: A potential hydrogel has been identified that can be prepared under mild conditions, has favourable rheological properties and has an antimicrobial effect against common oral pathogens when combined with antimicrobial nanoparticles.

Further work aims to measure the drug release profile of the gels in order to assess the potential for prolonged drug delivery. Additionally, the physical properties and antimicrobial efficacy will be assessed in an *ex vivo* tooth model of pulpal infection.

ACKNOWLEDGEMENTS: This PhD project is funded by a Health and Care Research Wales studentship.

Compressed collagen for the delivery of autologous keratinocytes on microcarriers to severe burn wounds

YH Martin[1], S Cutler[1], RA Brown[2], AD Metcalfe[1]

[1] *Blond McIndoe Research Foundation, East Grinstead, United Kingdom* [2] *UCL Tissue Repair and Engineering Centre, University College London, United Kingdom*

INTRODUCTION: The application of autologous keratinocytes to augment wound healing is well established in the clinical treatment of severe burns. Currently, cells are applied by spraying onto the wound bed, which leads to significant cell damage and cell loss. We address these issues by using microcarriers to transplant the cells, which we previously showed leads to reduction in wound contraction *in vivo* in the porcine model[1]. Here we show a method of incorporating human keratinocytes on microcarriers in compressed collagen for improved cell delivery.

METHODS: Keratinocytes were isolated from discarded human skin (REC: 06/Q1907/81) and cultured until sub-confluent. Subsequently, 5 x 10^6 cells were seeded on 0.1g Cultisphere-G gelatin microcarriers in stirring flasks and cultured for 4 days. Microcarriers were incorporated into compressed collagen gels[2] and inverted onto an acellular collagen sheet to model application to the wound bed *in vitro*.

RESULTS: Keratinocytes on microcarriers were viable after compression and continued to proliferate. When applied *in vitro*, keratinocytes readily proliferated and migrated from the microcarriers (Fig 1, top panel). H&E staining showed that keratinocytes populate the surface of the collagen sheets and interstitial space (Fig 1).

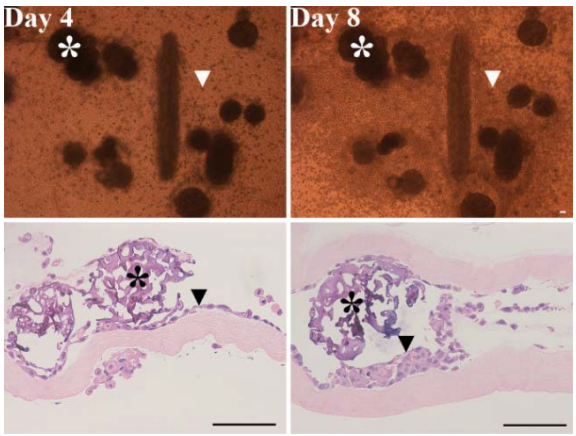

Fig. 1: Human keratinocytes on microcarriers in compressed collagen after 4 and 8 days. Top panel shows cells en face, bottom panel shows H&E of matching samples, scale bars = 100µm.
** microcarrier ▼keratinocytes*

Within 8 days, single as well as multiple layers of cells were observed. Immunocytochemistry and qRT-PCR further showed that keratinocytes retain their K14 and Collagen VII expression after 8 days.

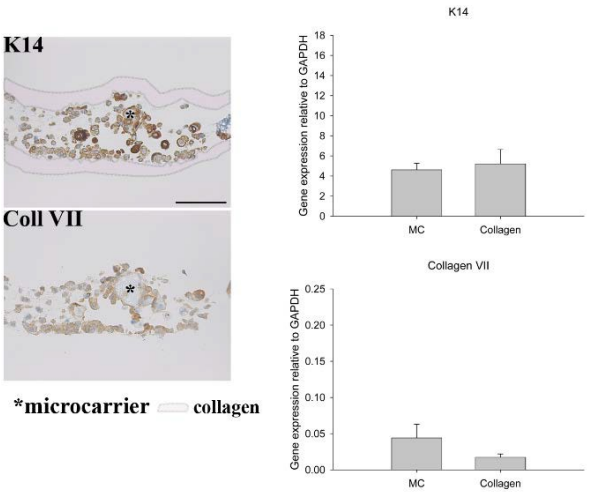

Fig. 2: Human keratinocytes retain their phenotype. Immunocytochemistry shows K14 and collagen VII expression, scale bar = 100µm. Quantitative RT-PCR shows no difference in expression between cells on microcarriers (MC) and those incorporated into collagen, n=3, error bars=SD.

DISCUSSION & CONCLUSIONS: Severe burns are treated with autologous keratinocytes within 10 – 20 days of hospital admission. The novel approach of using compressed collagen gels for transplantation of cells on microcarriers could significantly reduce cell loss and ensures retention of a highly proliferative cellular phenotype, suitable for clinical application.

ACKNOWLEDGEMENTS: This work was funded by The Charles Wolfson Charitable Trust.

Influence of solvent concentration on morphology, topography and mechanical properties of gelatin electrospun nanofibers: Analysis of induced cell behaviour

Elisa Roldán[1,*], Neil D. Reeves[2], Glen Cooper[3], Kirstie Andrews[1]

[1] *School of Engineering, Manchester Metropolitan University, UK.* [2] *School of Healthcare Science, Manchester Metropolitan University, UK.* [3] *School of Mechanical, Aerospace & Civil Engineering, University of Manchester, UK*

INTRODUCTION: Gelatin is a natural polymer derived from the hydrolysis of collagen, the most abundant protein of the extracellular matrix (ECM). Thanks to its low cost, high biocompatibility, biodegradability and bioactivity, gelatin is an attractive polymer to create tissue engineered implants through electrospinning technique; however, the gelation process is very sensitive to temperature and the concentration of solvent used, potentially adversely affecting its use within electrospinning solutions. An appropriate selection of the solvent and its concentration is crucial to produce nanofibers free of defects and with morphology, topography and mechanical properties ideal for application-specific cell viability and proliferation. The novelty of this work lies in understanding how changes in the solvent concentration affect the mechanical and morphological properties of the gelatin scaffolds and so induce associated cell behaviour. Acetic acid (HAc) enables optimizing the electrospinning process avoiding gelation and obtaining cell viability higher than 90% [1]. Dimethyl sulfoxide (DMSO) favours the creation of smoother fibres free of defects[2] promoting cell migration. This study aims to analyse the induced cell behaviour associated with mechanical and structural properties of gelatin electrospun scaffolds based on different solvent concentrations manufactured to mimic ECM for connective tissue implants.

METHODS: Nine variants of electrospun scaffolds were manufactured with 25% w/v of gelatin dissolved in concentrations of HAc and distillate water (dH_2O) of 3:1, 1:1 and 1:3, adding 0%, 5% and 10% of DMSO. All scaffolds were fabricated under the same parameters, at room temperature (25ºC), 26 kV of applied voltage, a flow rate of 2 ml/h, 15 G needle, 11 cm between the tip of the needle and the collector, 15 cm diameter rotating collector, 1300 rpm and 3 hours spin time. Fibre diameter, interfibre separation and orientation of the fibres were determined though scanning electron microscopy images and ImageJ software, measuring 40 fibres per scaffold. Average roughness was measured using 8 white light interferometry images per scaffold. 3 samples per scaffold were removed with a dog-bone cutting die (25 x 4 mm, test length x width) and tensile tested with a 100 N load cell and 1 mm/min test speed in order to determine the mechanical properties (Young's modulus, tensile strength and strain at break). Human fibroblast cells were seeded on the scaffolds with $5x10^4$ cell/cm^2 cell seeding density, cultured for 2 weeks and stained with Hoechst 33342 and oregon-green phalloidin in order to evaluate cell behaviour through confocal microscopy. Mean and standard error of the mean (SEM) were calculated for each structural and mechanical property.

RESULTS: Scaffolds with 3:1 HAc/ dH_2O and 10% DMSO exhibited the largest fibre diameter (1±0.04 μm) and average roughness (1.92±0.05 μm) which allowed greater initial adhesion; they also showed the greatest interfibre separation (4.42±0.45 μm), the most aligned fibres and an appropriate Young's modulus (136±30 MPa) for tissue engineered implants.

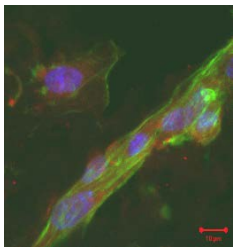

Fig. 1: Confocal image of human fibroblasts on an example scaffold at 2 weeks culture.

DISCUSSION & CONCLUSIONS: Promising cell results revealed that by optimising solvent concentration, scaffolds could be manufactured with morphologies, topographies and mechanical properties suitable for tissue engineered implants, wound dressings or artificial skin.

ACKNOWLEDGEMENTS: This research was funded by the Faculty of Science & Engineering, Manchester Metropolitan University.

Cells sense the nanoscale geometry and mechanical properties of their matrix

Dexu Kong[1], Stefania di Cio[1], Khai Nguyen[1] and Julien E. Gautrot[1]

[1] *Institute of Bioengineering and School of Engineering, Queen Mary University London, UK.*
j.gautrot@qmul.ac.uk, http://biointerfaces.qmul.ac.uk/

The extra-cellular matrix (ECM) provides important cues to direct cell phenotype and stem cell fate. In particular, cell adhesion plays an important role in such sensing of the micro-environment and is modulated by physical properties of matrix, such as stiffness, topography and geometry. Our laboratory focuses on the study of such interactions and the design of bio-materials allowing the control of physical properties of the ECM. Our studies highlight that cells respond differently to nanoscale physical properties than they do to bulk properties and that the two can be designed independently.

In order to control the geometry of materials at the nanoscale, we have developed patterning protocols to generate nano-patches and nano-fibres with controlled dimension and promoting cell adhesion. These platforms rely on the extreme protein resistance of some polymer brushes and the ease with which these coatings can be structure to control the geometry of protein pat-terns at multiple scales, from 100 nm to the millimeter scale(1-3). We find that stem cell fate is controlled by such geometry and that this behavior is mediated by changes in cell adhesion and spreading. At the nanoscale, protein recruitment dynamics (studied via live fluorescence mi-croscopy and fluorescence recovery after photobleaching) controls adhesion formation and nanoscale sensing(4).

Our recent studies also highlighted that cells may not feel bulk mechanical properties, at the single cell level, but rather directly sense nanoscale mechanics of the matrix(5). In some situa-tions, the two may match, but this is not necessarily the case. We use self-assembly processes to control the nanoscale mechanical properties of adhesive protein layers independently of the bulk mechanical properties of the matrix. We study such properties via scanning probe micros-copy and rheology and find that cell adhesion correlates with nanoscale properties rather than the bulk. This in turn controls fate decision in stem cells.

Hence our work highlights important rultes for biomaterials design: the bulk and interfacial physical properties can be controlled independently to modulate cell adhesion and phenotype. “Hard cell phenotypes” can be induced on soft matrices and “soft cell phenotypes” can be in-duced on very rigid materials.

ACKNOWLEDGEMENTS: Funding from the EPSRC and BBSRC is gratefully acknowledged.

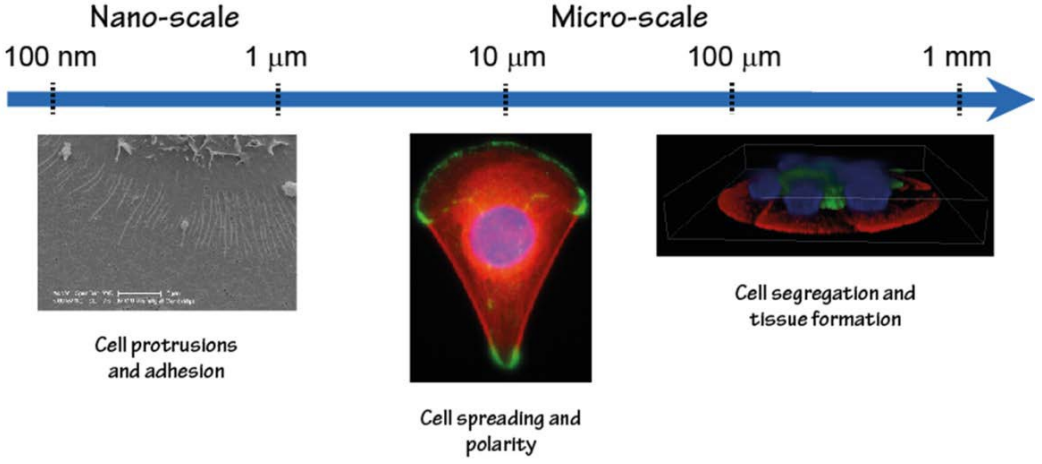

Bronchopulmonary dysplasia: an in vitro model

J Bratt[1], A El Haj[1], N Forsyth[1], P Wu[1]

[1] Institute for Science & Technology in Medicine, Keele University, Stoke-on-Trent, UK

INTRODUCTION: Bronchopulmonary dysplasia (BPD) is a neonatal disease affecting the lungs of premature infants. The disease develops due to abnormal development of the alveoli and pulmonary vasculature[1]. The pathogenesis of BPD remains poorly understood and currently relies on animal models for investigation. We aim to develop an *in vitro* model of the lung alveoli using cell seeded collagen-elastin hydrogels using a previously described protocol[2]. Collagen and elastin are key mediators in the lung biomechanics, however irregular deposition of collagen and elastin is a hallmark of BPD[3]. The hydrogels provide a 3D environment representative of the lung ECM. The constructs can be exposed to hydrostatic stimulation to represent the ventilation which BPD patients are exposed to. The initial stages of this study focuses on the potential co-culture of lung fibroblasts and endothelial cells in collagen gels to represent the lung alveoli.

METHODS: Hydrogel constructs were made using type I rat-tail collagen (BD Bioscience) using a previously described protocol[4]. Gels contained a collagen concentration of 3.5mg/ml or 1.5mg/ml. The hydrogels were seeded with lung fibroblasts 35FL at a cell density of $1.0x10^4$, $1.0x10^5$ or $2.5x10^5$ cells/gel prior to gelation. The constructs were incubated for 20 days at 37ºC, 5% CO_2. The contractibility of the cells and the mechanical stability of the hydrogels were tested by measuring the gel size and depth using a ruler and optical coherence tomography (OCT) system respectively. Endothelial cell line A549 were seeded at a density of $2.0x10^5$ on the surface of set 3.5mg/ml collagen gels. The gels were then exposed to hydrostatic stimulation at a pressure of 1.5KPa at 1Hz for 1 hour. These values represent the clinical ventilation of BPD infants. Cell viability was assessed using the LIVE/DEAD cell viability assay (Life Technologies) and imaged using a confocal microscopy.

RESULTS: Gel contraction was observed in the 1.5mg/ml collagen gels over 20 days. The rate of contraction correlates to cell number until the gels eventually disintegrated. The effect of cell contraction was hindered in the 3.5mg/ml collagen gels with only the 250,000 cells/gels causing a reduction in gel diameter. Cell imaging revealed good cell viability of the hydrostatic stimulated A549 cells.

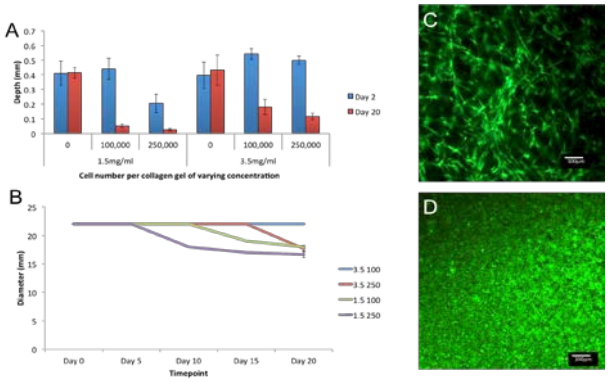

Fig. 1: 35FL cells were seeded at different seeding concentrations within 1.5mg/ml and 3.5mg/ml collagen gels. Gel diameter (A) and depth (B) were measured over 20 days. Error bars represent standard deviation, n=3. Cells were imaged using the LIVE/DEAD imaging on day 20 (C). A549 cell line were seeded as a monolayer on the surface of 3.5mg/ml collagen gels and exposed to hydrostatic stimulation. Cells were stained with the LIVE/DEAD cell viability assay (D).

DISCUSSION & CONCLUSIONS: After 20 days of observation, gel contraction is limited when cells are seeded within a 3.5mg/ml. This gel concentration would provide a stable construct for epithelial cells to be seeded as a monolayer on the gel surface. We also examined the possibility of seeding A549 cells as a monolayer on the collagen gel surface. Using LIVE/DEAD cell viability imaging, the cells were shown not to migrate through the gel but formed a confluent cell monolayer on the gel surface. The cell health was not hampered by hydrostatic stimulation. This study has revealed the possibility to produce a co-culture collagen gel construct to represent the lung alveoli *in vitro*.

ACKNOWLEDGEMENTS: The authors would like to thank the ESPRC & MRC for funding this work as part of the CDT Centre in Regenerative Medicine.

Smart scaffolds: Utilizing a microfluidic hydrogel platform to synthesize gelatin-based microchannel dermal scaffolds to enhance vascularisation

X Lim, J Dye, H Ye, Z Cui

CRMI Technology Centre, Institute of Biomedical Engineering, University of Oxford, UK.

INTRODUCTION: Vascularization of scaffolds remains one of the biggest challenges in the field of tissue engineering. [1] The conventional method of engineering vascularized tissues depend on self-organization of endothelial cells into tubules when seeded in 3D gel cultures or formation of pre-vascularized constructs prior to grafting. [2] However, this method is difficult to reproduce and requires a long time before graft perfusion is achieved. [1, 2] One method of circumnavigating this problem is to embed microchannels within scaffolds prior to grafting. This could promote migration of endothelial cells to establish tissue perfusion and thus, viability of the scaffold. In this project, we aim to utilize the microfluidic platform and soft photolithography to create microchannels within a biocompatible hydrogel to enhance endothelial cell migration.

METHODS: Patterned microchannels were designed using AutoCAD and printed on a polyester film photomask. SU8 was then spin-coated onto a silicone wafer, exposed to UV light with the photomask superimposed, baked, developed and silanized to fabricate a hydrogel casting template. 20% gelatin Type A was then carefully poured onto the template and crosslinked using 1-Ethyl-3-(3-dimethylaminopropyl)-carbodiimide and N-Hydroxysuccinimide (EDC-NHS) at 4 degrees overnight. The patterned hydrogels were then hydrated by soaking in deionized water for 1 hour, followed by EGM-2 media overnight. Microchannel patency was tested by injecting a red dye into the inlet ports. Human umbilical vein endothelial cells (HUVECs) were seeded within the scaffold and allowed to incubate for up to 14 days. Confocal microscopy was then used for 3D imaging of the scaffold to monitor behaviour and morphology of the endothelial cells, presence or angiogenesis as well as vasculogenesis.

RESULTS: An optimal molar ratio of 5:2 EDC:NHS was found to be ideal for synthesizing scaffolds that were rigid enough to be handled whilst being flexible enough as a dermal scaffold. HUVECs adhered to the walls of the micropatterned hydrogel and demonstrated budding/sprouting from the edges of the microchannels. Cross-section of the scaffold demonstrated patent endothelialized lumens when stained with Live/Dead assays.

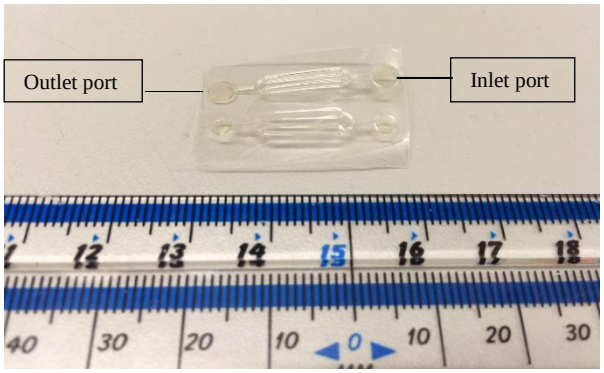

Figure 1: Micropatterned gelatin-based hydrogel before hydration.

DISCUSSION & CONCLUSIONS: We demonstrate successful endothelialisation of a novel microchannel dermal scaffold using HUVECs. Future works include co-culture with human dermal fibroblasts, mechanical testing of the scaffolds, studying effect of perfusion rates on vasculogenesis and quantifying rate of degradation of the material. This study could potentially pave the way for an intermediate scaffold design whereby the process of inosculation of synthetic microchannel grafts is used to enhance the vascularization process, as a bridge towards pre-vascularized dermal scaffolds.

ACKNOWLEDGEMENTS: X Lim is sponsored by the A*STAR Graduate Academy of Singapore to conduct her PhD study at Oxford University.

The effect of xeno-free media on human MSC viability and differentiation for bone tissue engineering

D A Qassim[1], H Colley[2], G.C. Reilly[1]

[1] *Department of Material Science and Engineering, INSIGNEO Institute for in Silico Medicine, and*
[2] *Integrated Bioscience group Unit of Oral and Maxillofacial Pathology,*

School of Clinical Dentistry, University of Sheffield, UK

INTRODUCTION: The most common culture cell media used in vitro cell expansion is a basal media, typically DMEM supplemented with animal serum.

The most common animal serum used is foetal bovine serum (FBS). However, there are problems with the use of bovine serum such as ill-defined composition, variability and difficulty of clinical use due to potential for disease transmission. Many biochemical media have been recently developed and a media type widely utilized in mammalian cell culture is xeno-free media[1] and in many cases cultures can be cultured and proliferated in serum-free media[2] to overcome the limitations of animal serum. Human mesenchymal stem cells derived from bone marrow are utilized for a range of tissue engineering applications. They have the ability to self-renewal and differentiate into different cells under specific culture media supplements[3].

METHODS: hBMSCs were seeded in 24 well plates at a density 10x103 cell/cm2 in different commercially available media which included10% FBS (as a control), 'Stem X VivoTM Xeno-Free Human MSC Expansion Media' (R&D; USA), (XF1) and 'Human Mesenchymal-XF Expansion Medium' (MILLIPORE; UK) (XF2). The osteogenic media were supplemented with dexamethasone 10 nM, ascorbic acid-2-phosphate 50 µM, and beta-glycerophosphate 10 mM. The amount of DNA was determined using 'Quant-iTTM picoGreen®® dsDNA Assay (PG) Kit, High Sensitivity, 1000 assay' (Invitrogen, life technologies, USA). The resazurin reduction assay was used to investigate the cell`s metabolic activity 24 hours, 4 and 9 days after seeding. The alkaline phosphatase activity was used to investigate the potential of the hBMSCs to differentiate along the osteoblast lineage.

RESULTS: The metabolic activity of hBMSCs increases over time in all conditions. Of the xeno-free media, XF2 was significantly supported faster cell growth and higher metabolic activity which was approximately 17% higher by day 9, compared to XF1 and 10% FBS containing media. Higher cell numbers in XF2 were confirmed by DNA assay. Interestingly, when osteogenic supplements were added, ALP activity was much higher (approximately two-fold) in XF2 compared with all other conditions.

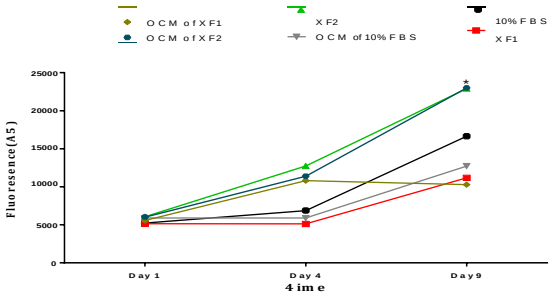

*Fig. 1: Mean of resazurin fluorescence, indicating metabolic activity of hBMSCs cultured in different media. * indicates significantly higher than 10% FBS P<0.05.*

DISCUSSION & CONCLUSIONS: XF2 appeared to upregulate the metabolic activity of hBMSCs compared to 10% FBS, especially without any dexamethasone or other supplements at later time-points of culture period (4th and 9th day). The reason for this may be that the XF2 which included serum extracted from human origin provides better nourishment for the MSCs than bovine serum because contains elements that support the biological activity of human cells and tissues. Our findings indicate that XF2 medium, a human-serum based composition, is an efficient pre-clinic medium for isolation, expansion, proliferation, and differentiation of mesenchymal stem cells and may enable faster bone differentiation for tissue engineering.

ACKNOWLEDGEMENTS: Funding for this project was providing by Republic of Iraq, Ministry of Higher Education and Scientific Research, Iraqi Culture Attaché-London. University of Mosul/ College of Dentistry.

Experimental measurement of energy dissipation in healthy and degenerate intervertebral discs

GM Dougill[1], P Nadipi-Reddy[1], K Andrews[1], ND Reeves[1], C LeMaitre[2], G Cooper[3]

[1] Manchester Metropolitan University, Manchester, UK. [2] Sheffield Hallam University, Sheffield, UK. [3] University of Manchester, Manchester, UK.

INTRODUCTION: Diseased Intervertebral Discs (IVDs) have been observed to contain elevated levels of Heat Shock Proteins (HSPs), with increased levels of HSP72 observed particularly in cellular clusters within herniated tissues and during degeneration with ageing [1].

Heat shock proteins are known to be upregulated in cells in response to a range of stresses including heat, load, hypoxia and catabolic enzymes [2]. Determining whether these stresses are prevalent within the IVD may help to identify activities or conditions which are potential causes of degeneration.

Direct heating of IVDs has been observed to upregulate HSP72 [3] however to date no studies have investigated whether increased heat could occur within the IVD during activities of daily living (ADLs).

This study aimed to determine if there is a significant generation of heat within the IVD due to energy dissipated when subjected to cyclic loading at levels and frequencies relevant to ADLs and whether this is effected by disc health.

METHODS: Bovine coccygeal discs were removed whole from tail sections and half of the discs were injected with a 2 mg/ml collagenase solution and incubated at 37°C for 2 hours to simulate moderate degeneration. Discs were then subjected to sinusoidal loading at 2Hz at force levels equivalent to those in the human spine during locomotion.

Mechanical data was analysed with MATLAB software to determine the energy dissipated by the discs for each cycle of loading. An idealised thermal model was generated to predict temperature change within the disc assuming that all dissipated energy was converted to heat. Temperature at time, t, was modelled such that:

$$T(t) = T(t\text{-}1) + (q_t + m)/c \qquad (1)$$

Where T is disc temperature at a given time, q the internal heat energy generated, m the disc mass and c the disc specific heat capacity.

RESULTS: Under axial loading equivalent to that in the lumbar spine during walking degenerate discs showed greater average compression than healthy discs (0.112 mm and 0.028 mm respectively) and therefore substantially lower average stiffness (714 N/mm and 3149 N/mm) and elastic modulus (12.9 MPa and 24.3 MPa). Average energy dissipation in degenerate IVDs (0.78 mW) was lower than that in healthy discs (4.13 mW). An idealised 3-Dimensional model of heat loss from the disc estimated small increases in disc temperature ($\Delta T < 0.5$°C) significantly lower than those previously shown to upregulate HSPs.

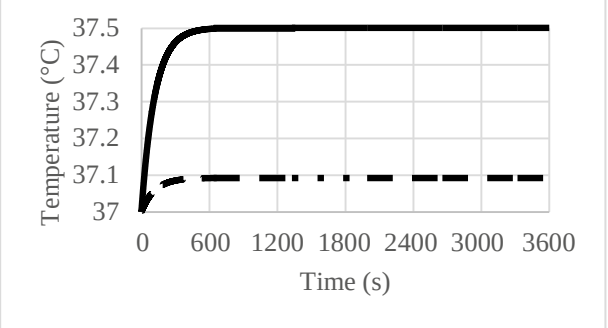

Fig. 1: Predicted temperature over one hour's continuous loading of healthy (solid) and degenerate (dashed) discs.

DISCUSSION & CONCLUSIONS: Healthy and degenerate bovine coccygeal Intervertebral Discs cyclically loaded at levels approximating those in the human lumbar spine during walking dissipated energy at rates of 4.13 and 0.78 mW respectively. An idealised 3-Dimensional model of heat loss from the discs suggests that this rate of energy dissipation by the disc is not sufficient to result in meaningful temperature increase within the disc. These results provide the first evidence that HSP upregulation in the IVD is not linked with loading related temperature changes in the disc.

Evaluation of Electrospun Scaffolds as Biocompatible Epidermal Carrier Delivery System

X Lim, J Dye, H Ye, Z Cui

CRMI Technology Centre, Institute of Biomedical Engineering, University of Oxford, UK.

INTRODUCTION: Epidermal skin scaffolds play an important role as coverage in the setting of acute large surface area partial thickness burns. Although cultured epidermal autografts are available, they have poor mechanical properties and may cause blistering. [1] Electrospun scaffolds have been extensively assessed as dermal substitutes, however limited studies have been done to evaluate the suitability of electrospun scaffolds as an integrated epidermal carrier delivery system. [2] In this study, we have characterized several pure and hybrid electrospun membranes such as polycaprolactone (PCL), poly-L-lactide (PLLA) and poly- poly(lactic-co-glycolic acid) (PLGA) 75:25, PCL/gelatin, PLLA/gelatin and PLGA/gelatin as potential scaffolds for epidermal replacement.

METHODS: 8% PCL, PLLA, PLGA, PCL/gelatin, PLLA/gelatin and PLGA/gelatin in HFIP were electrospun at 11.5kV with collector plate distance of 13.5cm at 1ml/h. Fibre morphology and diameter were determined by scanning electron microscopy. Membrane mechanical properties were tested using the Instron universal testing machine. Water retention of the membranes was monitored over 2 weeks. Membrane degradation by mass and contraction were observed over a period of 4 weeks by soaking the electrospun membranes in phosphate buffered saline. Viability and proliferation of keratinocytes seeded on electrospun membranes were determined using Live/Dead assay and MTT colorimetric assay.

RESULTS: Smooth fibres measuring approximately 1-2 microns in diameter were obtained for all pure and hybrid electrospun membranes apart from PLGA which was beaded. Addition of gelatin caused an increase in stress at break for PCL and PLGA, but not PLLA. PCL was the weakest membrane with tensile strength of 2.56 ± 0.53 MPa while tensile strength was highest for PLLA at 8.08 ± 1.04 MPa. Water retention of PLLA/gel and PLGA/gel were significantly better than the rest of the membranes. Degradation by mass of all electrospun membrane was negligible while membrane contraction was most for PLGA and PLGA/gel (80%, $p<0.05$), followed by PLLA/gel, PLLA, PCL/gel then PCL. Cell proliferation and viability was highest for PLLA/gel, PLGA/gel while cell proliferation and viability was lowest for PCL.

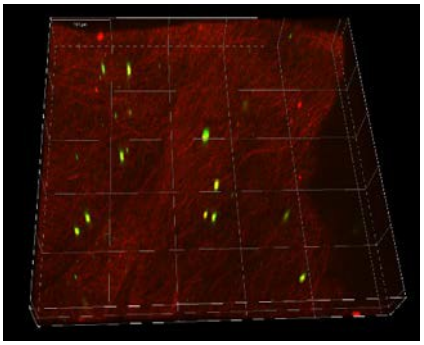

Figure 1: 3D confocal microscopy image of keratinocytes stained with Live/Dead Assay on electrospun PCL/gelatin membrane.

DISCUSSION & CONCLUSIONS: We conclude that electrospun PLLA/gel membrane is the most suitable material as an epidermal carrier dressing as its tensile strength, water retention capability, degree of contraction and biocompatibility as a whole was the best compared to other membranes. In general, hybrid gelatin blend membranes performed better in terms of biocompatibility and water absorbance. We plan to investigate the effect of enzymatic membrane degradation of the electrospun membranes and include in vivo implantation experiments in the future as well.

ACKNOWLEDGEMENTS: X Lim is sponsored by the A*STAR Graduate Academy of Singapore to conduct her PhD study at Oxford University.

Nanocarrier delivery of antimicrobial and bioactive matrices for dental tissue repair

GE Melling[1], SJ Avery[1], SL Evans[2], RJ Waddington[1], AJ Sloan[1]

[1]Mineralised Tissue Group, School of Dentistry, [2] Mechanical and Structural Performance Group, School of Engineering, Cardiff University, Wales.

INTRODUCTION: Recent data suggests that 50% of dental restorations fail within 10 years [1], resulting in recurrent endodontic infections and tooth loss. Demineralised dentine matrix (DDM) contains a myriad of growth factors and matrix proteoglycans, the bioactivity of which can utilised in dental restorations and bone augmentations [2]. Using a novel nanocarrier delivery system, this study aimed to develop an antimicrobial, bioactive dental cement which was able to prevent infection and promote reparative dentinogenesis, improving the longevity of current dental restorations.

METHODS: Nanocarriers containing DDM (extracted from non-carious dentine [3]; 1 - 100 μg/mL), and triclosan (300 μg/mL) were made. Human dental pulp stem cells (hDPSCs) were treated with DDM nanocarriers (10 ng/mL - 100 μg/mL) for 3, 9, 21 and 35 days. Cell proliferation and viability were assessed by cell counts, Caspase-Glo 3/7 (Promega) and MTT assays. qRT-PCR was used to examine the expression of osteogenic markers RUNX2 and osteocalcin at days 3, 9 and 21. Mineralisation of the cultures was assessed after 21 and 35 days by Alizarin red S staining. A transwell chemotaxis/ migration assay was used to assess the ability of DDM nanocarriers to recruit hDPSC progenitors.
Triclosan nanocarriers were tested using growth curves and zones of inhibitions for *Streptococcus Anginosus* and *Enterococcus Faecalis*. SEM and biomechanical tests were carried out on Vitremer (Henry Schein) dental cements containing loaded and empty nanocarriers.

RESULTS: DDM nanocarriers had no effect on proliferation or cell survival. DDM nanocarriers were able to significantly recruit hDPSCs and induce the expression of osteogenic markers in hDPSCs after 9 days. Increased mineralisation of hDPSCs treated with DDM was seen after 21 and 35 days.
Triclosan nanocarriers were able to inhibit the growth of *S. Anginosus* and *E. Faecalis.* Nanocarriers had limited effects on the biomechanical integrity of Vitremer cements.

DISCUSSION & CONCLUSIONS: Nanocarriers were used to successfully deliver DDM to hDPSC, promoting *in vitro* recruitment and differentiation, and triclosan to endodontic bacteria inhibiting their growth. The nanocarriers were incorporated into cements with minimal physical artefacts, therefore an antimicrobial, bioactive dental cement was produced, which could be a useful tool for dental tissue engineering and hard tissue repair.

ACKNOWLEDGEMENTS: This work was funded by the MRC/ UK Regenerative Medicine Platform.

Paracrine factors immobilised on collagen enhances endothelial cell function

C Hamilton[1], A Callanan[1]

[1] *Institute for Bioengineering, School of Engineering, The University of Edinburgh, Edinburgh,*

INTRODUCTION: In this *in vitro* study, we use the principle of paracrine cell secretion from endothelial cells and incorporate these media contained factors into porous collagen scaffolds either by direct absorption, or by initial surface cross-linking. This technique offers a further advantage of using a serum free environment to generate paracrine conditioned media and hence these biofactors produced are intrinsic, cell controlled and has been previously shown to elicit an enhanced response from host cells [1]. These scaffold properties have the potential to be used in treatment methods for cardiovascular disease [2].

METHODS: Human umbilical vein endothelial cells (HUVECs) were obtained cryopreserved (500,000 cells) at passage 1 (PromoCell® GmbH) and cultured and expanded to passage 5 using a previous endothelial cell culture protocol [2]. For basal media (BM) all supplements were used with the omission of 2% FBS and compared to paracrine cell conditioned adjusted BM (ABM), where ABM was incubated for 48 h in standard culture conditions then removed and filtered.

Ultrafoam™ (Davol Inc.) collagen scaffolds were prepared as 10 mm discs, 2 mm thick. Scaffolds were soaked overnight in PBS; BM; or ABM. Additionally prior to absorption, some scaffolds were cross-linked by soaking in a solution of 1-(3-Dimethylaminopropyl)-3-ethylcarbodiimide—EDC/N-hydroxysulfosuccinimide—sulfo-NHS (Sigma). Scaffolds were incubated with mild agitation for 24 h at 37 °C and then cell seeded with 5 x 10^5 serum-free autologous HUVECs. After 24 h and 48 h, scaffold functionality was evaluated by cell attachment, DNA quantification, fluorescent imaging of live/dead cells and endothelial regulatory and angiogenic gene expression. Scaffold integrity was evaluated by gene expression of collagen degradation on seeded scaffolds and the comparison of conditioned scaffolds by SEM.

RESULTS: Cellular attachment to scaffolds was found to be greatest at 48 h across all scaffold types but particularly the ABM E/N scaffolds [Fig 1A.]. This trend is comparable to the levels of angiopoietin 1 (*Ang1*) gene expression at 48 h from these scaffolds [Fig 1B.].

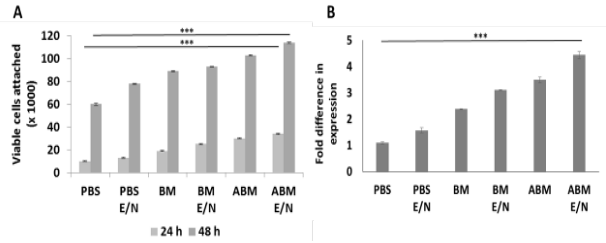

*Fig 1: Cellular attachment (A); RT-PCR of Ang1 gene expression (B). *** p-value < 0.01.*

SEM analysis revealed that mechanical integrity was not altered due to shaking or cross-linking. [Fig 2.].

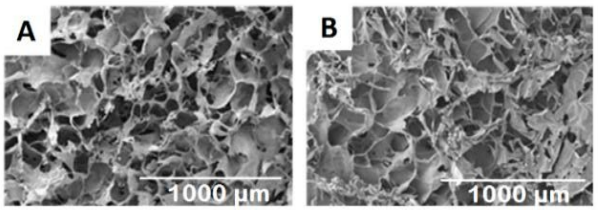

Fig 2: SEM of PBS scaffold cross-linked unshaken (A) and PBS scaffold cross-linked shaken (B).

DISCUSSION & CONCLUSIONS: Results have shown that paracrine conditioned scaffolds enhance functionality[1]. This method has potential to extend to other cell types, tissue environments, scaffold materials and demonstrates translatable serum-free, cellular-free paracrine conditioning. Future work focuses on the long retention of bioactivity in these scaffold to illustrate the potential as an off the shelf treatment strategy.

ACKNOWLEDGEMENTS: This research is funded by an Engineering and Physical Sciences Research Council (EPSRC) Doctoral Training Partnership (DTP) Studentship. SEM courtesy of Institute of Molecular Plant Sciences, imaging facility, University of Edinburgh.

Bubble-cell interactions in collagen hydrogels

C. Walsh[1,2,3], N. Ovenden[3], E. Stride[4], U. Cheema[2],
[1]CoMPLEX, UCL, London UK. [2] UCL Institute of Orthopaedics and Musculoskeletal Science, London, UK. [3] Department of Mathematics, UCL, London, UK. [4]Institute of Biomedical Engineering, University of Oxford, Oxford UK

INTRODUCTION: Understanding the interaction of bubbles and cells is of importance in preventing and treating decompression sickness DCS[1]. Cells may influence bubble formation and growth by providing bubble nucleation sites or altering the local dissolved gas concentration through oxygen metabolism. Bubbles may also interfere with normal cellular function though mechanical contact and adsorption of proteins on the air tissue interface[1]. Collagen hydrogels provide a controllable system in which dissolved gas concentrations, cellular and bubble dynamics can be measured, providing much needed data e.g. for improving dive algorithms and identifying therapeutic targets.

METHODS: Monomeric or blended monomeric-polymeric[2] collagen hydrogels were fabricated with the addition of Human keratinocyte (HaCaT), human adipose cells or varying concentrations of Human dermal fibroblasts (HDFs). Gels were placed in a microscope compatible pressure chamber, and time-lapse imaging was used to capture bubble dynamics following a pressure exposure. Cell viability was assessed prior to and post pressure exposure using live dead staining (Invitrogen). Oxygen concentrations of gels containing HDFs were measured via fluorescence quenching (OxylitePro, Oxford Optronix).

RESULTS: A significant reduction in cell viability was found following the pressure exposure, Fig 1. No significant differences were found between sham and pre-exposure or with gel orientation despite an anisotropic bubble distribution within the gel.

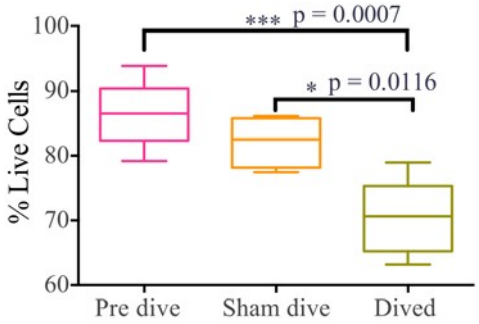

Fig. 1: The change in percentage of live cells following 30mins at 80psi with 13psi/s ascent (N=6).

Introduction of 500,000/ml HaCaT cells and 45,000/ml adipose cells to pure monomeric gels did not alter the bubble nucleation rate. HDF cells within blended gels significantly reduced nucleation for cell concentrations of 5000 (low), 50,000 (medium) and 500,000 (high) cells/ml as compared to the control and nucleation decreased with cell density. Oxygen tension was significantly lower for high cell density gels but low and medium cell densities did not differ significantly from each other or atmospheric tension (142mmHg).

DISCUSSION & CONCLUSIONS: Contrary to the currently accepted hypothesis,[1,3] that bubble nucleation occurs from cell surfaces or fat droplets, this work found either no change or a decrease in nucleation for three cell types. The lower oxygen tension measured within the high cell density gels suggests that reduced nucleation is a result of the reduced total gas supersaturation. Quantification of cell death due to both bubble proximity and increased oxygen partial pressure has not been reported previously[1,3]. The cell death found here as a result of pressure exposure is a novel indication of how extravascular bubbles may contribute to pathologies associated with DCS. The uniformity of cell death throughout the gels also indicates that direct bubble contact may not be the mechanism responsible.

ACKNOWLEDGEMENTS: This research was funded through UCL CoMPLEX by the BBSRC. Thanks also to Nick Bushell at Avon Underwater Systems.

Functionalised graphene layer-by-layer constructs as support for NIH-3T3 fibroblasts and implications in wound-healing applications.

P Shellard[1], D Kumar[2], F Fei[1], C Blanford[1], J Gough[2]

[1]*Manchester Institute of Biotechnology, University of Manchester, 131 Princess Street, Manchester, M1 7DN, UK* [2]*The Mill, University of Manchester, Manchester, M1 3AL, UK.*

INTRODUCTION:

We present a novel synthesis of graphene sulfonate (G-SO_3) and its incorporation in a layer-by-layer (LbL) construct, for thin, water-permeable films for use in dressing of superficial wounds. LbL construct biocompatibility was assessed using NIH-3T3 cells where viability, metabolic activity and proliferation were monitored. Furthermore, the adsorption of typical extracellular matrix proteins (fibronectin and bovine serum albumin) onto graphene oxide (GO) and G-SO_3 was profiled.

METHODS:

GO was produced by a modified Hummers' method.[1] G-SO_3 and GO-SO_3 were produced via electrophilic aromatic substitution of graphene and GO, respectively.

LbL constructs were made on 3-(Trihydroxysilyl)propane-1-sulfonic acid - coated 13 mm glass coverslips, with poly(ethylenimine) (PEI) as positive polymer and poly(styrene sulfonate) (PSS) as positive polymer. The compositions of the constructs are tabulated below.

Table. 1: LbL construct compositions

Surface	Components	# layers	Terminal layer
Glass	N/A	N/A	N/A
PEI/PSS (+)	PEI, PSS	7	PEI
PEI/PSS (-)	PEI, PSS	6	PSS
PEI/GO	PEI, GO	6	GO
PEI/GO-SO_3	PEI, GO-SO_3	6	GO-SO_3
PEI/G-SO_3	PEI/ G-SO_3	6	G-SO_3

Characterisation of GO, GO-SO_3 and G-SO_3 and LbL constructs was achieved using XPS, Raman mapping, FTIR, UV-vis, Zeta potential, CHNS and bright field imaging.

NIH-3T3 cells were cultured in DMEM supplemented with 10% FBS. Cells were seeded onto LbL constructs at 10^4 cells cm^{-3} under standard incubation conditions (37°C, 5% CO_2) up to day 6.

Cell viability was assessed via LIVE/DEAD® Viability Assay, DNA quantification performed using Quant-iT™ PicoGreen® dsDNA Assay and metabolic activity assessed using the AlamarBlue® assay. Protein adsorption quantification was performed using a NanoOrange® Protein Quantitation assay.

RESULTS:

Successful NIH-3T3 proliferation was observed on PEI/GO, PEI/G-SO_3 and PEI/GO-SO_3 over the three time points, for all assays. Figure 1 shows LIVE/DEAD® images of NIH-3T3s on LbL constructs.

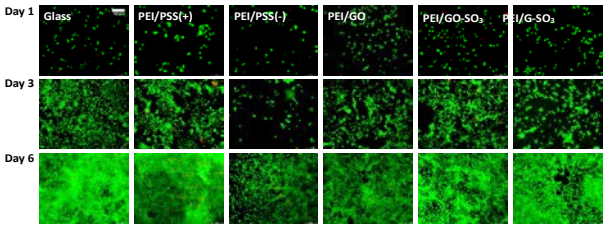

Fig. 1: Live/dead staining of NIH-3T3 cells cultured on LbL constructs, at day 1, 3 and 6. Scale bar represents 100 µm.
L-R: Glass, PEI/PSS(-), PEI/PSS(+), PEI/GO, PEI/GO-SO_3, PEI/G-SO_3.

Metabolic activity and proliferation of NIH-3T3 cells was lower on PEI/G-SO_3 than on PEI/GO-SO_3 PEI/GO constructs.

Fibronectin adsorption was also significantly lower on PEI/G-SO_3 than on PEI/GO-SO_3 or PEI/GO. No significant differences in BSA adsorption were observed between the graphene-containing LbL constructs.

DISCUSSION & CONCLUSIONS:

Good biocompatibility for all the graphene-containing LbL constructs has been demonstrated, making them suitable candidates for wound-healing applications.

Increased cell activity on PEI/GO-SO_3 and PEI/GO compared to PEI/G-SO_3, suggests that the oxygen-containing functionality in PEI/GO-SO_3 and PEI/GO has a positive influence on NIH-3T3 cell activity. Protein adsorption and conformation appear to be influenced by the charge and composition of grapheme, causing subsequent affects on cell behaviour.

ACKNOWLEDGEMENTS: BBSRC

Development of a small scale fluidised bed bioreactor for encapsulated cell systems to be tested simultaneously, thereby speeding up the R&D process.

JM Silva[1], E Erro[1], J Bundy[1], S Chalmers[1], T Mukhopadhyay[2], B Fuller[3], C Selden[1]

[1] UCL Institute for Liver and Digestive Health, Royal Free Campus, University College Medical School, UCL, UK , [2] Dept. Biochemical Engineering, UCL, UK, [3]Dept. Surgery, Royal Free Campus, University College Medical School ,UCL, UK

INTRODUCTION: Limitations of currently used 2D culture systems in mimicking the *in vivo* environment have motivated the development of several 3D constructs for cell culture. Using encapsulated cells in hydrogels allows them to form a tissue-like structure (cell-organoids)[1]. Providing the correct macro-environment to stimulate both cell proliferation and functionality is crucial. Static cultures do not promote a homogenous milieu, and the most common dynamic systems (e.g. stirred tank bioreactor) produce high shear stress which damages cells. In a fluidised bed bioreactor (FBB) upward fluid movement matched by downward force of gravity, enables encapsulated cells to fluidise, inducing homogenous mixing, maximising mass transfer between cells and environment and minimising shear stress.

Our aim was to develop a small scale FBB able to enhance proliferation and functionality of encapsulated cell spheroids in alginate to establish *in vitro* tissue-like structures which can be used for cost-effective tissue models as a test bed for several different protocols.

METHODS: The small scale fluidised bed bioreactor (sFBB) comprised a 140 mL glass column equipped with inlet and outlet ports connected to a reservoir with recirculation of the fluid from the reservoir to the column by a peristaltic pump. This system was assembled inside an incubator for controlled temperature and CO_2 parameters.

To evaluate the system ability to act as a device for 3D cell culture, hepatoblastoma-derived cells (HepG2) were cultured in monolayer to ~70% confluence, harvested and encapsulated in a sterile 1% alginate solution to form spherical beads, as described previously[2]. Encapsulated cell beads were transferred into the sFBB for culture in normal medium supplemented with 10% foetal calf serum and antibiotics over 12 days in a 1:32 ratio. As a control, cell beads were simultaneously cultured in static conditions in T-25cm^2 flasks.

Throughout culture period, cell viability, proliferation and synthetic ability were assessed by fluorescein diacetate and propidium iodide staining, cell counts, and analysis of albumin (Alb), α-glycoprotein (AGP) and α-1-antitrypsin production (A1AT) by enzyme-linked immunosorbent assay (ELISA), respectively.

RESULTS: The sFBB sustained a consistent and stable fluidisation of 2-fold the initial cell bead height in the column. Encapsulated HepG2 cells remained viable (>97%) and proliferative throughout, forming cellular spheroids (liver organoids). After the initial 4 days, culture of cell beads in dynamic conditions increased proliferation 1.5-fold in relation to static culture ($4.86x10^6 \pm 9.24x10^5$ vs. $3.23x10^6 \pm 3.72x10^5$ cells/mL beads, respectively) (n=3,SD). Moreover, specific activities of Alb, AGP and A1AT were significantly higher for cells in the sFBB compared to those in T-25 cm^2 flasks. Any shear stress induced by the fluidisation did not impact on bead shape or integrity. Sphericity and size were maintained throughout the 12 day culture period.

DISCUSSION & CONCLUSIONS: The small scale FBB demonstrated fluidisation was stably maintained, encapsulated HepG2 cells remained viable and proliferative, and their synthetic function (per cell performance) was markedly upregulated, validating their hepatic phenotype. In conclusion, this system enhanced the formation of functional cellular spheroids, constituting tissue-like structures *in vitro* that could be used as models for organs or diseases. Investigating other cell lines will corroborate the wide application of this system. Using this small scale model also enables multiple observations simultaneously, and condition comparisons, thereby speeding up the R&D process.

ACKNOWLEDGEMENTS: This template was modified with kind permission from eCM Journal. We thank the Liver Group Charity and UCL IBME for PhD Studentship support.

Extracellular fluid viscosity enhances cell-substrate interaction and impacts on cell size and morphology

J Gonzalez-Molina[1], Barry Fuller[2], C Selden[1],

[1] UCL Institute for Liver and Digestive Health, Royal Free Campus, University College Medical School, UCL, London, UK; [2] Division of Surgery and Interventional Science, Royal Free Campus, University College Medical School, UCL, London, UK.

INTRODUCTION: The cell microenvironment physical properties have a great impact on cell behaviour. Conventional tissue culture methods employ rigid polystyrene plastic and low viscosity cell culture media, which poorly mimics in vivo conditions. Cell substrate stiffness has been demonstrated to affect the cell phenotype. Also, increasing viscosity appears to be detrimental to receptor-ligand binding generally [1]. Here we explored the role of medium viscosity on cell-substrate adherence and its influence on cell morphology.

METHODS: Substrate stiffness-responsive NIH3T3 fibroblasts [2] and HepG2 hepatoblastoma cells [3] were used. HepG2 cells were seeded on fibronectin- and matrigel-coated glass. Non-spread (round) but adhered cells were treated with culture media containing 1% Na-alginate or 10% dextran, and the proportion of spread assessed over time. Cell area and "shape factor" (0 indicates a flattened object and 1 a perfect circle) was measured 24h post treatment. Also, matrigel was used as a soft substrate for HepG2 cells. NIH3T3 fibroblasts were seeded on plastic plates, and spreading time was calculated in addition to 1 and 4-day effect on cell morphology.

RESULTS: High viscosity reduced cell spreading time in cells adhered to fibronectin- and matrigel-coated glass and charged polystyrene plastic, suggesting that viscosity impacts on cell-substrate bond formation. Similar to substrate stiffness, viscosity had a positive effect on cell area with a 39.92% and 45.59% increase for 1% Na-alginate and 10% dextran-treated cells respectively (Fig. 1), and reduced cell shape factor (elongation) in HepG2 cells seeded on low fibronectin-coated rigid glass and soft matrigel. High fibronectin- and matrigel-coated rigid glass in low viscosity alone caused an increased cell area and elongation compared to polystyrene or low protein-containing glass, and it was further enhanced by increasing extracellular macroviscosity.

Opposite effects were observed on the morphological changes of NIH3T3 fibroblasts, with reduced area and higher shape factor than control cells. However, cell spreading was also facilitated by increased media viscosity.

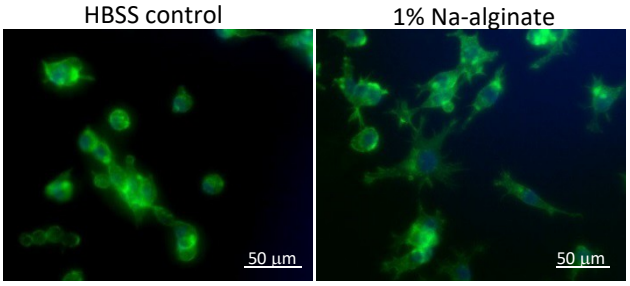

Fig. 1: Viscosity increases cell area and affects morphology. HepG2 cells treated for 24h with 1% Na-alginate (133 cP) and stained for F-actin and nuclei.

DISCUSSION & CONCLUSIONS: Extracellular fluid viscosity is a physical factor that has a major impact on cell-substrate interaction leading to changes in size and morphology and consequently could affect cell function and behaviour. Matching the cell culture media viscosity to that of the natural environment of a cell may influence the result of cell and tissue biology studies, especially when highly mechano-responsive cells including stem and cancer cells are used.

ACKNOWLEDGEMENTS: This work was funded by The Liver Charity and the Welcome Trust.

Investigation of the effect of growth factors and inhibitors on fibroblasts in a glaucoma conjunctival model

R Gater[1], T Ipek[1], S Bhunia[1], D Nguyen[1,2], AJ El Haj[1], Y Yang[1]

[1] *Institute for Science and Technology in Medicine, School of Medicine, Keele University, UK.*

[2] *Mid Cheshire Hospitals NHS Foundation Trust, Crewe, UK*

INTRODUCTION: Glaucoma is one of the leading causes of blindness worldwide, characterised by optic nerve damage and retinal ganglion cell death caused by increased intraocular pressure (IOP) inside the eye [1]. Glaucoma surgery (trabeculectomy) involves making an incision in the conjunctiva and sclera so that fluid can egress into the sub-conjunctiva of the eye, reducing IOP. However, excessive wound healing and fibrosis can significantly reduce the success rate of surgery to just 55% [2]. Therefore, more efficient anti-inflammatory agents are required to reduce fibrosis and scar tissue formation after surgery. We aim to utilise a glaucoma conjunctival model to investigate the effect of growth factors and inhibitors on conjunctival fibroblast proliferation, with the purpose of finding new therapies to reduce fibrosis after glaucoma surgery.

METHODS: Conjunctival tissue was obtained from porcine eyes via dissection, cut into smaller pieces and transferred into T25 flasks. Tissue explants were then cultured in high glucose media for approximately 1-2 weeks, until conjunctival fibroblasts outgrew from the tissues and became confluent in the flasks. Cells from each passage (P0- P5) were then seeded into wells of a 96 well plate at a density of 12,000cells/cm^2 and left for a further 2 days of culture. At day 2, growth factor TGF-β1 and inhibitor Activin-Like Kinase were administered to cells in high and low concentrations via addition to the culture media. Growth factor VEGF was also investigated by administration at different doses. Cell proliferation and morphology was then recorded for a further 3 days via MTT assay and actin staining.

RESULTS: As shown in figure 1, conjunctival fibroblast proliferation increased significantly with increasing doses (10ng/ml and 100ng/ml) of TGF-β1, in comparison to the control. In contrast, conjunctival fibroblast proliferation decreased significantly with increasing doses (20μM and 40μM) of inhibitor, in comparison to the control. Further data has also found growth factor VEGF to increase conjunctival fibroblast proliferation, with increasing dose.

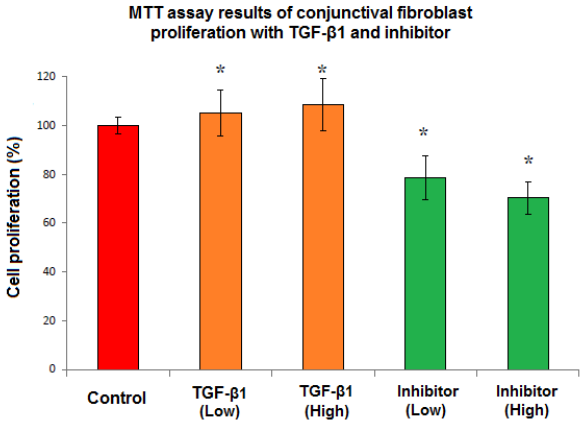

Fig. 1: MTT assay results of conjunctival fibroblast (P3) cell proliferation, following administration with high and low concentrations of growth factor TGF-β1 and inhibitor.

DISCUSSION & CONCLUSIONS: Results confirm that growth factors TGF-β1 and VEGF both increase conjunctival fibroblast proliferation with increasing dose. In comparison, the inhibitor Activin-Like Kinase was found to decrease conjunctival fibroblast proliferation with increasing dose. Therefore with further investigation, this inhibitor, along with other inhibitors of TGF-β1 and VEGF, could be considered as potential anti-inflammatory agents to reduce fibrosis and scar tissue formation after glaucoma surgery. In future work, we plan to investigate the effect of proteoglycan on the fibroblast proliferation at different dose.

ACKNOWLEDGEMENTS: North Staffordshire Medical Institute pump priming funding.

The presence of charge and arginine in self assembling peptide hydrogels affects initial cells morphology

I. Nawi[1,2], V.L. Workman[1,2], A.F. Miller[2,3], S.H. Cartmell[1], A. Saiani[1,2]

[1] School of Materials, The University of Manchester, M13 9PL [2] Manchester Institute of Biotechnology, The University of Manchester, M1 7DN [3] School of Chemical Engineering and Analytical Sciences, The University of Manchester, UK

INTRODUCTION: Self-assembly peptides (SAP) are seen to have high potential in tissue engineering applications, as the properties of peptide fibrils (e.g. functionality and geometry) can be controlled by changing peptide sequences, concentration and pH. We have shown that these peptide hydrogels have different storage modulus depending on the concentrations and the pH of hydrogels. This paper also discusses the effects of charged peptide hydrogels on the cells viability, cells proliferation and production of GAGs.

METHODS: Peptide solutions were prepared by suspending the solid phase peptide in distilled water. FEFKFEFKK (F9), FKFEFKFK (FK) and FEFKFRFK (FR) were prepared at 20mg/ml. Using 0.5M NaOH, the peptide solutions were neutralized to pH 5-6.

Bovine chondrocytes were physically mixed in prepared hydrogel, giving final cell density of 4 million cells per ml. Then, 350µl cell-hydrogel mixture was pipetted into each 12-well insert using positive displacement pipette. Samples were stained overnight with Oregon Green 488 phalloidin and Prolong Gold Antifade Reagent with DAPI.

RESULTS: To compare the effect of different peptide sequences on chondrogenic behavior of chondrocytes, all hydrogels were prepared with a G′ of 10kPa[1].

Figure 1 shows representative images of cells in F9, FK and FR after culturing for 3 days, which show that the morphology of the cells was affected by the peptide hydrogel. Chondrocytes seeded in F9 (+1 charge) display spherical morphology, while +2 charge FK supports spherical and stretched cells. In addition, cells seeded in FR have stretched and elongated morphology after 3 days of culturing. In FR, cells even migrated to the surface of the scaffold. Reports state that chondrocytes tend to change morphology when cultured without any biochemical or physical stimulation[2-4], however, not as early as day 3. Higher charge and presence of arginine in FR, may explain this modified morphology.

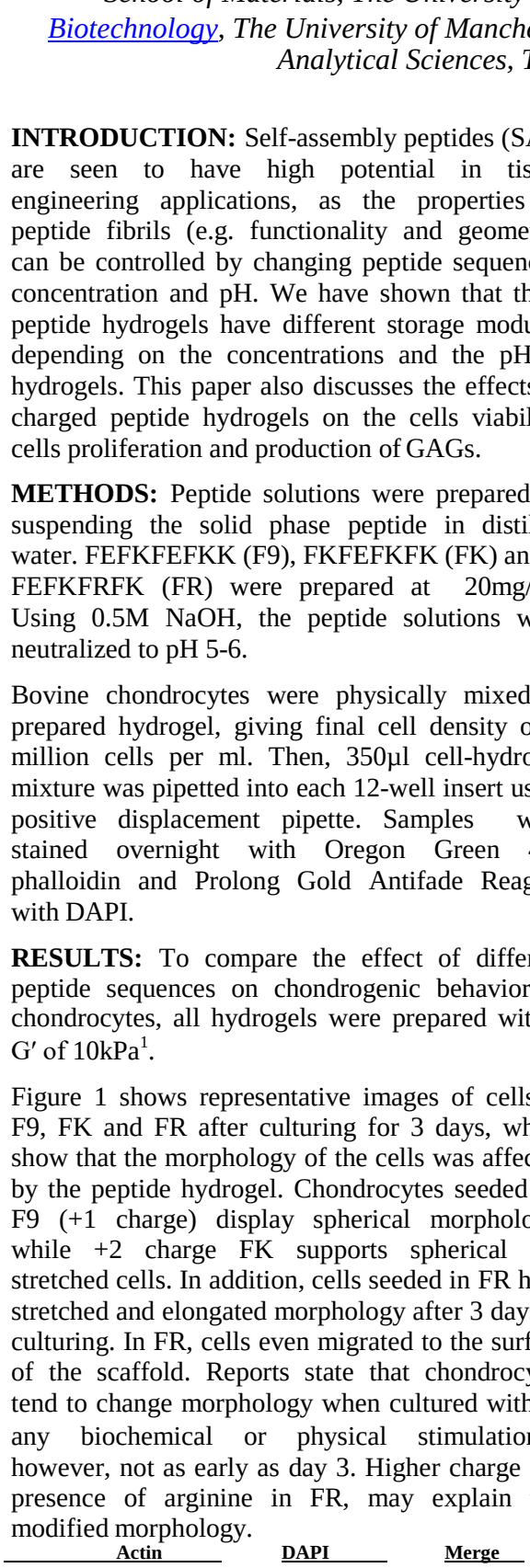

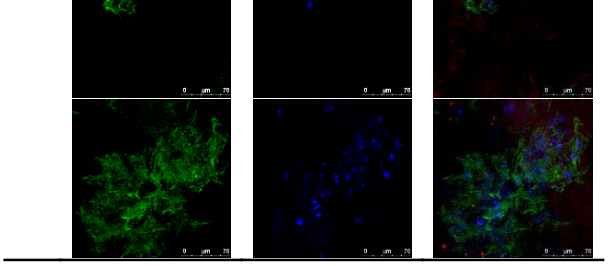

Figure 1 Images comparing different cells morphology when seeded in different types ofpeptide hydrogels, obtained from chondrocytes being cultured for 3 days. Specific staining for the cytoskeletal actin (green), aggrecan (red) and nuclei (blue). Scale bar=75μm.

DISCUSSION & CONCLUSIONS:

Higher charged SAP was observed to affect cell morphology. This may be described by the electrostatic interaction between the scaffold and F-actin.

Also, arginine was seen to affect cells' migration, morphology and protein production. Cell migration may be explained by the presence of arginine which induces migration via MAPK pathway. Stretched and networked morphology of cells have also been reported when another SAP, RAD16-I (containing arginine), was applied[2-4]. These hypotheses however need to be confirmed through further studies.

ACKNOWLEDGEMENTS: The authors acknowledge an EPSRC Fellowship (EP/K016210/1) and Government of Malaysia for providing financial support to this project.

Investigating the interaction between olfactory fibroblasts and olfactory ensheathing cells in co-culture

Rachael Wood, Dr. Melanie Georgiou, Joana dos Reis, Dr. Ivan Wall

Department of Biochemical Engineering, University College London, Gower Street, London WC1E 6BT, United Kingdom

i.wall@ucl.ac.uk

INTRODUCTION: Spinal cord injury is a serious injury that impacts 755 people per million (Wyndaele and Wyndaele, 2006). Olfactory ensheathing cells (OECs) are a candidate treatment for spinal cord injury as they can support neuronal survival and facilitate regeneration of severed axons (Lakatos et al., 2003). Despite their unique properties, OECs are very challenging to sustain in culture for prolonged periods as survival and proliferation are poor. The overall goal for the project is to identify methods to enhance the survival of OECs.

METHODS: It has been observed that pure populations of OECs have reduced regenerative function compared to those in co-culture with fibroblasts (Ramón-Cueto et al., 2000, Keyvan-Fouladi et al., 2003). Therefore, we investigated whether fibroblasts could have utility as a feeder layer to support OECs via cell-cell contact. Cells were also grown at different oxygen tensions to determine the impact on OEC survival and proliferation. An algorithm was generated using ImageJ to ascribe a mathematical value to the morphology of the cells to determine whether a correlation of morphology to expression of markers could be made.

RESULTS & DISCUSSION: A conditionally immortalised human mucosal fibroblast cell line was used as an immobilised feeder layer. Rat OECs were cultured for 14 days on the feeder layer or control substrate (laminin-coated dishes). After 14 days, cells cultured on feeders adopted a more spindle-like appearance compared with cells cultured on laminin, which adopted an enlarged morphology. The algorithm was used to analyse the circularity of positively stained cells. It was found that cells cultured on feeders had a lower circularity, and therefore more elongated shaped cells verses those cultured on laminin ($p=0.037$). Additionally, a significant increase in $p75^{NTR}$ expression (OEC marker) was observed ($p=0.01$) on feeders.

Finally, oxygen tension was examined to determine the effect of physiological (2-8%) versus ambient (21%) oxygen on cell circularity. When cells are cultured in ambient oxygen, a shifted normal distribution favoured elongated shaped cells.

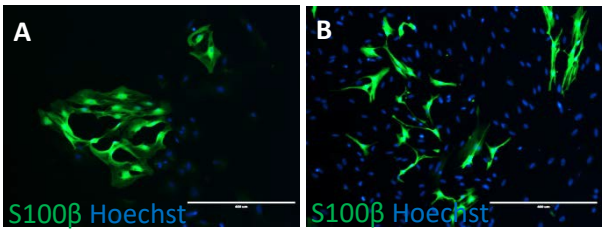

Fig. 1- Flourescent micrographs of a cell population derived from rat olfactory mucosa cultured on laminin (A) and a human feeder layer (B). The scale bar represents 400um.

CONCLUSIONS: From this work, we found that culturing olfactory ensheathing cells on a feeder layer resulted in a change of morphology and significantly more $p75^{NTR}$ cells. In addition, culturing OECs in normal oxygen conditions resulted in more elongated cells. This is promising because elongated cells are anticipated to be more supportive of regeneration. Work is currently ongoing to determine the functional significance of these findings.

Anterior cruciate ligamentocyte response to electrospun scaffolds decorated with fibrillin.

DR Marques[1], D Kumar[1], G Crichton[1], YA Kharaz[2], E Comerford[2], JE Gough[1]

[1] *School of Materials*, University of Manchester, UK

[2] *School of Veterinary Science*, University of Liverpool, UK

INTRODUCTION: Anterior cruciate ligament (ACL) graft ruptures subsequently occur due to the failure of their integration at the bone tunnel site. This occurs due to the mismatch in compliance between the two structures at the integration site, as well the slow rate of bone formation and healing at the injury site. Electrospun fibrous scaffolds are an ideal biomaterial, which are able to recapitulate the native extracellular matrix (ECM) architecture at the nano-level whilst providing adequate mechanical properties. However, these scaffolds lack biological recognition sites. To further improve cell response and to mimic ACL ECM at the enthesis site more accurately, this project explored the effects of coating electrospun scaffolds with fibrillin, identified as a key peptide fragment, which is critical in encouraging the secretion of important ECM proteins in ACL matrix.

METHODS: Medical grade Polycaprolactone (PCL - Durect Lactel) was used to produce random and aligned fibers. Electrospinning was proceeded for PCL 15%w/v applying 18 ±1KV and collection at 200rpm and 1400rpm rotational speed. Fibrous membranes were mounted into glass cover slips and the obtained scaffolds were characterized by scanning electron microscopy in order to analyze fibres orientation and diameter. Fibroblasts isolated from canine cranial ligament (CCL) were seeded onto scaffolds and metabolic activity was characterised using Alamar blue assay at day 7 and 14. ECM formation was characterized by histologically staining (Picrosirius red) for collagen present in the neomatrix tissue produced after day 7 and 14. Aligned fibres were coated with fibrillin and submitted to fibroblast cell culture. Live/Dead assay was performed in order to evaluate cell viability and proliferation, with observation points at 4h, 24h and 72h. All *in vitro* evaluations were carried with posterior observation of tissue under microsocope (Nikon Eclipse 50i) of incident and fluorescent light, conducting cell culture over TCP as control group.

RESULTS: Random and aligned fibres were attained successfully, presenting diameters of 3.42μm and 5.15μm, respectively. There was no significant difference between groups (p=0.025). Metabolic activity of ligamentocytes was witnessed to be higher on both PCL scaffolds compared to the control group. Histological staining showed evidence of collagen secretion, where on aligned scaffolds, collagen matrix followed the direction of the fibres. Better attachment and cell spreading was observed on scaffolds and TCP coated with fibrillin compared to non-coated substrates.

DISCUSSION & CONCLUSIONS: For a tissue to regenerate without producing scar tissue it requires cells capable of proliferation and for the underlying stromal framework to be intact, therefore tissue engineering using a biomimetic fibrous scaffold decorated with specific peptide fragments provides a logical solution to the current treatment of ACL repair [1]. All electrospun PCL scaffolds demonstrated the ability to support CCL attachment, proliferation and collagen matrix secretion. Matrix secretion also appears to be influenced by topographical cues, posing beneficial to increasing the mechanical properties of the graft [2]. Moreover, the presence of fibrilin over aligned fibres represents a relevant factor for tissue differentiation over those fibres [3]. Considering the ACL as a well organized tissue, the application of aligned fibres that successfully mimic these natural structures and expose the cells to a biological factor may be consider a promising alternative for ligament tissue engineering.

ACKNOWLEDGEMENTS: The authors would like to thank CNPq-Brazil for the financial support and the University of Liverpool for the cell line used in this study.

The Use of Modified Amino-Silane Coatings for use in Peripheral Nerve Tissue Engineering

Caroline S. Taylor[1], Rui Chen[2], John A. Hunt[2], Jude Curran[2], and John W. Haycock[1].

[1]*Department of Materials Science & Engineering, Kroto Research Institute, Broad Lane, Sheffield, S3 7HQ, UK.*

[2]*Centre for Materials and Structures, and Institute of Ageing and Chronic Diseases, University of Liverpool, Liverpool, U.K..*

INTRODUCTION: Peripheral nerve injuries affect 2.8% of all trauma patients. Current treatments involve direct end to end suturing or using an autograft, the current 'gold standard' treatment to bridge larger gaps. However, there is limited donor nerve available and limited nerve function is restored. Synthetic and natural nerve guide conduits are available but each has its limitations, such as high degradation rates. Coatings have been used to improve the biocompatibility of synthetic nerve guide conduits, as well as providing surface chemistry guidance for the regenerating axon. Natural coatings, such as collagen, can cause an immune response, depending on where they are derived. However, synthetic coatings, such as aminosilanes, avoid this issue and are much cheaper to produce and have the ability to control chemical group deposition at the sub-micron scale and associated topographical profiles.

METHODS: 13mm glass coverslips were immersed in 3% aminosilanes (*Short Chain*: 3-aminopropyl triethoxysilane; *Long Chain*: 11-aminoundecyltriethoxysilane) isopropanol solution for 2 hours, washed, and dried overnight. Surfaces were characterised using Water Contact Angle (WCA) and AFM. 40,000 NG108-15 neuronal cells were seeded onto short and long chain amino silane coated glass coverslips, as well as a plain glass coverslip control for 6 days. Serum was removed on day 2 to promote neurite growth. 60,000 rat primary Schwann cells were cultured for 6 days onto the coverslips in Schwann cell medium. Live / dead analysis was used to confirm the biocompatibility of the glass coverslips and immunolabelling for β-tubulin III, NG108-15 neuronal cell differentiation and neurite marker, and for S100β, a Schwann cell marker, was performed.

RESULTS: The highest numbers of live NG108-15 neuronal cells and primary Schwann cells were on the long chain functionalised coverslips. NG108-15 neuronal cells cultured on long chain amino-silane coated glass coverslips had a higher average number of neurites per neuron, a higher average neurite length and the highest maximum neurite length.

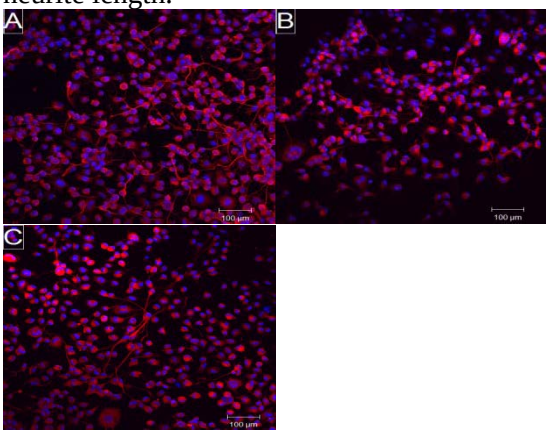

Figure 1. Confocal Images of NG108-16 neuronal cells grown on A) plain glass control, B) short chain aminosilane modified coverslips and C) long chain aminosilane modified coverslips.

DISCUSSION & CONCLUSIONS: This study confirmed that long chain amino siloxane coatings were the most efficient for NG108-15 neuronal cell neurite outgrowth and supported primary Schwann cell proliferation. Future work will involve applying this treatment to synthetic nerve guide conduits for investigations in vitro and in vivo.

ACKNOWLEDGEMENTS: This work was funded by the Universities of Sheffield and Liverpool, UK.

Osteoblast chemotaxis: differential responses to PDGF-BB and TGF-B1 at defined stages of differentiation

Mathew Hollingworth[1], James Ware[1], Lee Buttery[1]

[1]*Centre for Biomolecular Sciences, School of Pharmacy, University of Nottingham*

INTRODUCTION: During bone remodelling the migration of bone cells and their progenitors is regulated in part by numerous growth factors, allowing temporal recruitment of specific cell types throughout the process of bone turnover [1]. Previous studies have revealed PDGF-BB as a potent chemoattractant for osteoblasts [2], whilst TGF-β influences migration of osteoblast progenitors. This study describes the chemotactic responses to growth factors of osteoblasts at varying stages of differentiation, helping to characterise the migration of bone cells throughout their development.

METHODS: Chemotaxis of mouse primary calvarial cells (MPCs) was assessed by 2D chemotaxis slides (Ibidi), and Boyden chamber assay, in response to varying concentrations of PDGF-BB and TGF-β1 (R&D).

RESULTS:

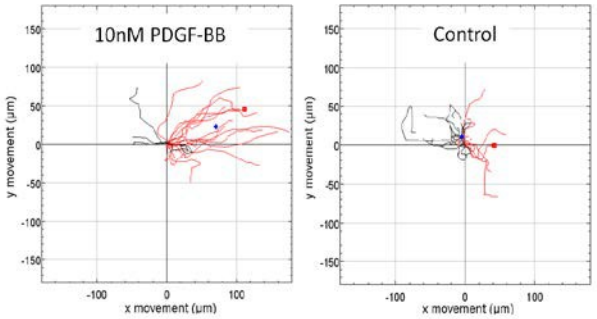

Figure 1. Migration of MPCs in response to PDGF-BB (24 hours). Red cell paths show net movement towards stimulus, black show movement away from stimulus. + shows final centre of mass.

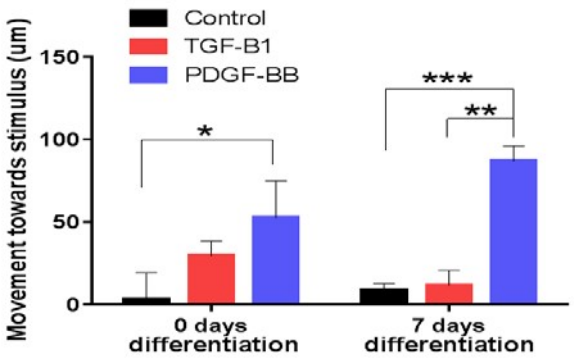

*Figure 2. Movement of MPC cells towards PDGF-BB and TGF-β1. n=10 * = p<0.02; ** = p<0.002; *** = p<0.0001*

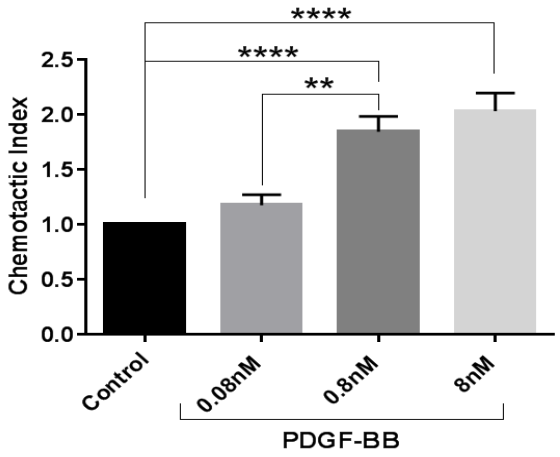

*Figure 3. Chemotactic response of MPCs to PDGF-BB, assessed using Boyden chamber assay. ** = p < 0.0012 ; **** = p < 0.0001*

DISCUSSION & CONCLUSIONS: Tracking of MPC migration **(figure 1)** revealed chemotaxis towards PDGF-BB, whilst controls showed no directional movement. Net cell movement **(figure 2)** showed migration towards PDGF-BB increased after culture in osteogenic medium for 7 days, whilst migration towards TGF-B1 decreased. MPCs also showed a dose-dependent chemotactic response to PDGF-BB **(figure 3)**. Immunocytochemical staining of MPCs at 0 & 7 days revealed alteration in key osteogenic markers (bone sialoprotein and osteocalcin) suggesting different states of differentiation.

Chemotactic responses to PDGF-BB and TGF-β1 were significantly altered following exposure to osteogenic media, suggesting a temporal response to these factors throughout osteoblast differentiation. These results contribute to a better understanding of cell recruitment during bone turnover and repair, and have implications on the use of bone cells during cell therapies, which rely upon effective cell recruitment upon delivery.

The power of bespoke biocompatible and biodegradable hydrogels with tailored properties and functionalities

A Mujeeb, G Saint-Pierre

PeptiGelDesign Technologies Ltd., The BioHub, Alderley Park, Alderley Edge, SK10 4TG, UK

INTRODUCTION: PeptiGelDesign Technologies Ltd. has developed a family of self-assembling peptide-based hydrogel systems that mimic the cell microenvironment and provide a natural physiological environment for 3-dimensional (3D) cell culture. In addition to its standard formulation, PeptiGelDesign Technologies Ltd. also offers a design service, which allows it to deliver hydrogels with tailored properties. These systems have tunable mechanical strength to suit a range of different cell types and can be functionalised with biological epitopes or formulated with small or large molecules such as growth factors. These products have great potential for applications in the regenerative medicine and tissue engineering fields, as they are animal free, biocompatible, and biodegradable. They can therefore potentially be used as primary packaging for the in vivo delivery of drugs, cells, and other biological factors. Our hydrogels are designed to be injectable, sprayable and naturally mucoadhesive systems.

METHODS: The hydrogels are prepared and fabricated by PeptiGelDesign Technologies Ltd. (Alderley Park, UK). The product catalogue is presented in table 1. The mechanical property of these hydrogels is determined using oscillatory rheology. The biocompatibility of 3D hydrogels has been assessed (against the ISO10993 and further demonstrated) by encapsulating different cell lines, for example human mesenchymal stem cells (hMSCs), bovine chondrocytes, human neuronal stem cells, cardiac progenitor cells, myocytes and many more. Our customers are particularly looking into cell morphology, proliferation, differentiation, and extra cellular matrix (ECM) production in vitro and in vivo.

RESULTS: The peptide-based hydrogels are well defined and biocompatible in nature with tunable mechanical properties ranging between 0.5 to 50 kPa, respectively. Cell culture studies reveal the hydrogels are reproducible and stable under physiological cell culture conditions up to five weeks in vitro (as shown in Figure 1).

Table 1. Product catalogue by PeptiGelDesign Technologies Ltd.

Product Name	*Pack Size (mL)*	*Catalogue #*
PGD-Alpha1	*1*	*X1012*
	5	*X1052*
	10	*X1102*
PGD-Alpha2	*1*	*X2012*
	5	*X2052*
	10	*X2102*
PGD-AlphaProA	*1*	*X3012*
	5	*X3052*
	10	*X3102*
PGD-AlphaProB	*1*	*X4013*
	5	*X4053*
	10	*X4103*
PGD-AlphaProC	*1*	*X5013*
	5	*X5053*
	10	*X5103*
PGD-StarterKit	*4X1*	*STK1234*

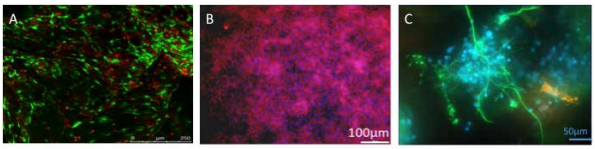

Figure 1: Cell culture. (A) Primary rat oesophageal stromal fibroblasts cultured within PGD-AlphaProB. Viable cells (in green) and nuclei of dead cells (in red). (B) Primary rat oesophageal epithelial cells cultured on PGD-AlphaProB. Cell nuclei (in blue) and ZO-1 (in red) (photos by courtesy of Polymers&Peptides Research Group at the University of Manchester, UK). (C) Differentiated neural stem cells encapsulated in PGD-AlphaProA. Cells stained for Tuj-1 (neurons, signal transducing cells) and MBP (oligodendrocytes insulating cells for nerve fibres) (photo by courtesy of Dr Chris Adams at Keele University, UK).

DISCUSSION & CONCLUSIONS: To summarise the material design platform developed by PeptiGelDesign Technologies Ltd. allows us to offer hydrogels with tailored properties to suit the needs of our customers.

ACKNOWLEDGEMENTS: We gratefully acknowledge the research information provided to us by Prof. AF Miller, Dr A Saiani, and Prof. JE Gough from University of Manchester (UK), Prof. D Chari from Keele University (UK) and Prof. F Quaini from University of Parma (Italy).

Engineering canine olfactory cell grafts using magnetic particle mediated delivery of therapeutic genes: Implications for canine spinal injury

C Adams[1], A Delaney[1], D Carwardine[2], N Granger[2], D Chari[1]

[1] Cellular and Neural Engineering Group, Institute of Science and Technology in Medicine, Keele University, UK. [2] School of Veterinary Sciences, University of Bristol, UK

INTRODUCTION: A recent clinical trial in companion dogs with spinal injury demonstrated that implantation of autologous olfactory mucosa cells (OMCs) recovered some motor function in the dogs (University of Cambridge). However, not all dogs responded to the treatment and there was no improvement in measures of long tract functionality. One strategy to enhance transplant mediated regeneration, is to genetically engineer OMCs to enable them to release therapeutic biomolecules, to promote additional repair mechanisms. Overwhelmingly, this is achieved using viral vectors which have significant translation drawbacks including safety and in large scale production. By contrast, magnetic particle (MP) based vectors are emerging as key non-viral alternatives for genetically engineering therapeutic cell populations. In particular, magnetofection (application of MP-DNA complexes in the presence of static and oscillating magnetic fields) has been shown to safely and efficiently transfect a range of neural cells. However, these platforms have never been tested in canine OMCs (cOMCs). Therefore our goals were to optimise MP mediated gene delivery to cOMCs and use these optimised protocols to deliver Brain Derived Neurotrophic Factor (BDNF; shown to promote repair in spinal injury) encoded by the advanced minicircle vector platform. Minicircles have significant advantages for translation compared to conventional plasmids, resulting from bacterial backbone removal. Therefore, they can incorporate larger genes, do not undergo transcription silencing and do not elicit immune responses, leading to higher safety.

METHODS: Reporter plasmids were complexed with MPs and delivered to OMCs under a range of magnetic field conditions. Subsequently, a static field was chosen to deliver minicircles encoding BDNF to cOMCs. Transfection efficiency and safety were determined at 24 h post transfection.

RESULTS: Cultures of cOMCs were successfully generated from the University of Cambridge clinical trial cell bank. Under the no-field condition a basal percentage of cells displaying MP uptake was estimated at 86 +/- 0.8% whilst the proportion of cells expressing the reporter gene was estimated to be 34.9 +/- 2.9%. These values were both significantly enhanced by application of all tested magnetic fields to ca. 95% (MP uptake) and 55% (transfection efficiency [Fig 1]), although there were no significant difference between field groups. Numbers of viable cells was high and unaffected by the developed protocols and similar numbers of proliferating cells were present across all conditions, suggesting there was no effect on cell health. Subsequently, minicircle encoded BDNF was successfully delivered to cOMCs with an estimated transfection efficiency of 8.1 +/- 0.3%. This resulted in a fourfold concentration increase of BDNF in the supporting media of transfected cells compared to non-transfected cells – suggesting BDNF is secreted by the engineered population.

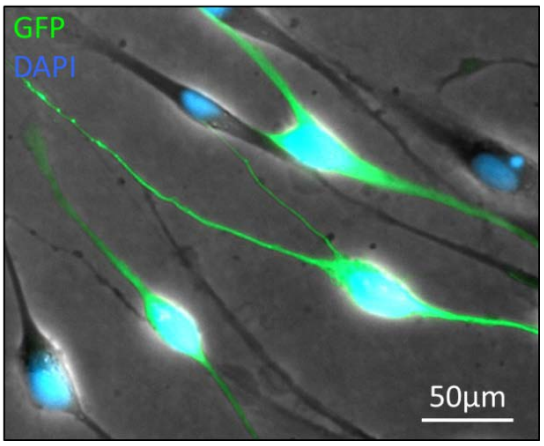

Fig. 1: Representative image of green fluorescent protein expressing cOMCs after MP mediated transfection performed under application of a static magnetic field.

DISCUSSION & CONCLUSIONS: Advanced MP-based vectors can successfully engineer cOMCs using reporter and therapeutic plasmids. Due to the high safety and efficiency of the procedures these protocols could be adopted/trialled in the veterinary clinic with future potential for translation into human cell transplantation strategies.

ACKNOWLEDGEMENTS: This template was modified with kind permission from eCM Journal.

Effect of collagen gel concentration gradients on neurite elongation

C.Kayal[1], R. Shipley[1], JB. Phillips[2]

[1]*Department of Mechanical Engineering, University College London* [2]*Biomaterials and Tissue Engineering, University College London*

INTRODUCTION: Collagen represents the main component of the extracellular matrix for peripheral nerves and is commonly used in tissue engineering to make conduits for nerve repair. However, little is known about the effect of the mechanical properties of collagen on the extension of neurites[1]. This study focuses on quantifying neurite extension in response to defined collagen gel gradients. Subsequently, experimental data will be integrated in a mathematical model to inform the design of tissue-engineered conduits combining both mechanical and chemical gradients in order to improve peripheral nerve repair approaches.

METHODS: PC12 cells were cultured *in vitro*, in the presence of nerve growth factor (NGF)[2] on the surface of collagen gel gradients. Stabilised collagen gel gradients were fabricated using rat tail collagen type I (First Link). A standard protocol[3] was used to generate neutralised collagen solutions (2 mg/mL) that were incubated at 37º for 10 min in 24-well plates at an angle[4] of 45 ˚ from the horizontal plane. The resulting wedge shaped gels were stabilised using RAFT™ absorbers (TAP Biosystems) to produce gradient gels. PC12 cells (5×10^4 cells/well) were seeded onto the upper gel surfaces, left to adhere for 1h at 37º, then culture medium added (supplemented with 0.663µg/mL NGF)[2]. Cultures were maintained at 37º, 5% CO_2 in a humidified incubator for 3 days. Different media formulations were compared, including conditioned media from C6 glioma cells and RPMI media supplemented with 10% serum.

To quantify the impact of the physical gradient on neurite growth, we used a collagen gradient with a predefined (left to right) density gradient from 55 mg/mL to 70 mg/mL. Each gel was separated into two parts, the lower density range section and the high density range section, for analysis. Gels were fixed and neurites were visualised using immunofluorescence labelling and confocal microscopy. Length and orientation of neurites were measured using ImageJ. For the orientation, the angle of each neurite in relation to the orientation of the gradient was determined (Fig 1).

RESULTS: On the lower density range gradient gel sections, 74.35% of neurites grew from the low density to the high-density regions of the gels. By comparison, neurites on the higher density range gradient gel sections showed no preferential direction (50% grew towards the lower density gel regions) (Fig 1). Further, neurites were longer on the high collagen density gel sections, with a cumulative neurite length of 2830 µm, which was reduced to 1720µm for the low collagen density gel sections.

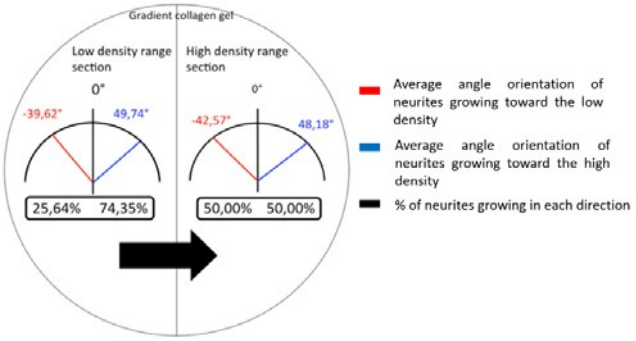

Fig.1: Mean orientation of the neurites depending on their position on the collagen gel gradient (high or low part of the gel), taking into account results for both media formulation conditions

DISCUSSION & CONCLUSIONS: This study shows that neurite orientation and length can potentially be influenced by physical gradients within collagen gels *in vitro*. In future, we will quantify the stiffness gradients within the gels[1] to correlate the stiffness gradient to the neurite extension. Mathematical modelling using these data will then be used to simulate how neurite extension might be improved and controlled[2]. These results, if extended to the *in vivo* situation, would assist significantly in the design and fabrication of constructs for neural tissue engineering in the future.

ACKNOWLEDGEMENTS: I would like to thank UCl for the award of a Dean's Prize and a PhD scholarship from the Department of Mechanical Engineering.

Viability and phenotype of differentiated *CTX* human neural stem cells in aligned RAFT-stabilised collagen hydrogels for nerve tissue engineering

L Thanabalasundaram[1], L Stevanato[1, 2], AGE Day[2], C Murray-Dunning[2], E Grace[3], G Cameron[3], J Sinden[1], JB Phillips[2]

[1] *ReNeuron Ltd, Pencoed, UK.* [2] *Biomaterials & Tissue Engineering, UCL Eastman Dental Institute, University College London, UK.* [3] *TAP Biosystems, Royston, UK*

INTRODUCTION: Collagen constructs containing Schwann cells or differentiated stem cells with Schwann cell-like phenotype have shown to aid peripheral nerve regeneration [1-3]. To advance the technology to a clinical grade product, a human neural stem cell line and an allogeneic source of therapeutic cells (*CTX*, ReNeuron, UK), was investigated. Previous work showed that *CTX* cells can differentiate and upregulate glial markers *in vitro* in stabilized collagen gel models [4]. The aim of this study was to test the viability and the phenotype of differentiated *CTX* cells in aligned and stabilised engineered neural tissue constructs suitable for therapeutic development.

METHODS: Differentiated *CTX* (d*CTX*) cells were seeded within 2 mg/ml bovine collagen hydrogels (Koken Co Ltd, Japan), self-aligned in tethered moulds for 24 hours and stabilized using the RAFT™ technology (TAP Biosystems, UK), then maintained in culture for a further 24 hours (n=4). Aligned d*CTX* cells in collagen were used as a control immediately after stabilizing (T0, n=4). Phenotype of the d*CTX* cells was then assessed by quantitative PCR.

RESULTS: A decrease in viable d*CTX* cells was observed after 24 hours in the aligned and stabilised collagen gels (Fig.1).

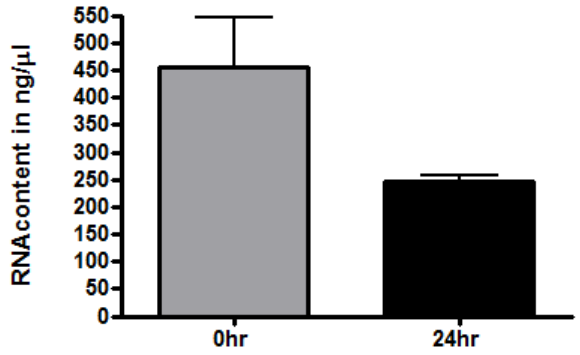

Fig. 1: Total RNA quantification was used to indirectly assess cell viability of dCTX in aligned collagen construct.

After 24 hours culture in aligned collagen gels, the d*CTX* cells exhibited an upregulation of glial markers glial fibrillary acidic protein (GFAP), S100B, as well as neuronal marker ßIII-tubulin (TUBB3) (Fig. 2) when compared with the control samples.

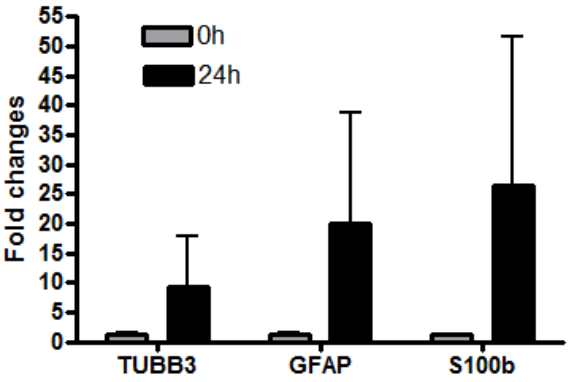

Fig. 2: Relative quantification of gene expression in dCTX cells cultured in tethered collagen constructs after 24hours.

DISCUSSION & CONCLUSIONS: These results suggest that *CTX* upregulate glial markers and have the potential to be Schwann cell-like which can be maintained within an aligned and stabilised collagen construct. This signifies their potential use as an allogeneic source of therapeutic cells in peripheral nerve tissue engineering.

ACKNOWLEDGEMENTS: This work was supported by funding from the UK Technology Strategy Board (101599).

A Design of Experiments (DoE) approach to identify the key fibre morphology influencing parameter interactions of electrospun scaffolds.

FAA Ruiter[1], C Alexander[1], FRAJ Rose[1], J Segal[2]

[1] *Division of Drug Delivery and Tissue Engineering, School of Pharmacy, University of Nottingham, UK* [2] *Advanced Manufacturing Research Group, University of Nottingham, UK*

INTRODUCTION: Electrospinning is a well-known process for 3D fibrous scaffold fabrication [1]. However, little research has focused on the impact of parameter interactions on scaffold morphology. This study uses a Design of Experiments (DoE) approach to identify the key parameter interactions which influence the three most common fibre morphologies (Fig.1). As the result of the DoE experiments, a linear regression equation was obtained and tested as predictive model. The scaffolds produced were then used for studies of 3T3 fibroblast proliferation.

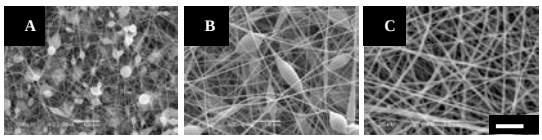

Fig. 1: Three common fibre morphologies. A) Big beads, B) beads-on-strings and C) uniform fibres. Scale bar: 10 µm.

METHODS: Poly lactic acid (PLA) Acetone/DMF (50/50) solutions were prepared. Scaffolds were electrospun in an EC-CLI machine (IME Technologies, Netherlands) with rotating target collector (EM-RTC) using an eight gauge needle. Average fibre diameter, standard deviations and number of beads per µm^2 were measured from SEM images using ImageJ software.

A DoE approach of 4 factors and 3 levels (Table 1) was performed, resulting in 81 scaffolds, including triplicates. Linear regression (Eq. 1) and data analysis was done with MODDE v10.1.1 software.

$$Y_i = \beta_0 + \sum_{j=i}^{m} \beta_i X_i + \sum_{i=1}^{m} \sum_{j=i}^{m} \beta_{ij} X_i X_j + \sum_{i=1}^{m} \sum_{j=i}^{m} \sum_{i=i}^{m} \beta_{ijk} XXX \quad (1)$$

RESULTS: Voltage, polymer concentration and flow rate and polymer concentration combined were identified as the main influencing parameters on the average fibre diameter. However, standard deviation was only significantly influenced by the concentration, whereas, the number of beads per µm^2 was influenced by both concentration and flow rate. The linear regression equations obtained were tested by comparison of measured data of scaffolds (produced using random combinations)

Table 1. Selected DoE parameters and levels.

Parameter	X_s	Unit	-1	0	1
Voltage	X_1	kV	15	20	25
Distance	X_2	cm	15	17.5	20
Flow rate	X_3	ml/hr	1	3	5
Polymer conc.	X_4	%*w/v*	15	20	25

intervals for estimates from calculated results. Significantly higher numbers of 3T3 fibroblasts (Fig. 2) were observed on the big beaded morphology scaffolds at day 6 compared with the other morphologies.

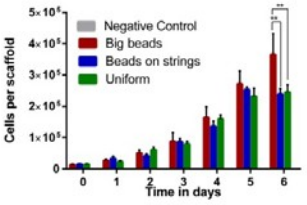

Fig. 2: 3T3 proliferation on the three different morphologies over a period of 6 days.

DISCUSSION & CONCLUSIONS: The DoE study has confirmed the main influencing parameters, additionally identifying flow rate and polymer concentration combined as having a significant effect on the resultant fibre morphology. Our results for average fibre diameter expand on a previous DoE study[2], in which only polymer concentration was observed to have a significant impact. However, only uniform fibre formation was considered in the prior study; our study has added to the previous work by the inclusion of other commonly observed fibre morphologies to further develop our understanding of the electrospinning process.

The obtained linear regression equations tested were found suitable as predictive models for electrospun scaffolds. The significant difference in cell growth observed on big beaded scaffolds is currently being investigated. No significant difference in cell growth was found between uniform and beads-on-string morphologies.

ACKNOWLEDGEMENTS: EPSRC Regenerative Medicine CDT for funding to FAA Ruiter. S.H.Y.Ruiter and G. Joseph for helping with the DoE model and mathematics.

Macroporous Microporous Scaffold for Adipose Tissue Reconstruction

J Appelt[1,2], AD Metcalfe[1,2], GJ Phillips[2],Y H Martin[1,2]

[1] Blond McIndoe Research Foundation, East Grinstead, UK [2] The Brighton Centre for Regenerative Medicine, University of Brighton, Brighton, UK

INTRODUCTION: The loss of subcutaneous adipose tissue due to the removal of tumours, congenital malformations, deep burns or trauma can have a severe disfiguring impact on the normal body contour. This can leave patients distressed both physically and emotionally. Current clinical treatment methods applied to replace lost adipose tissue often fail to restore the natural body contour. We present a bulk gelatin scaffold with a microporous and macroporous structure which supports the proliferation of adipose derived stem cells (ADSCs) and the expression of adipose extracellular matrix (ECM) components.

METHODS: Gelatin scaffold was created using particulate leaching of alginate beads as templates for the macroporous structure[1]. The microporous structure of the gelatin walls was controlled by freezing at -80 ºC and freeze drying (Fig. 1). Viability, distribution and ability to express adipose ECM components of human adipose-derived stem cells (ADSCs) within the scaffolds was assessed. The degradation of the scaffold structure was investigated visually and quantitativelyby measuring the scaffold volume over 56 days of culture with ADSCs.

RESULTS: The scaffold (Fig. 1) supported ADSC viability, cell distribution and the secretion of native adipose ECM components within the porous structure (Fig. 2).

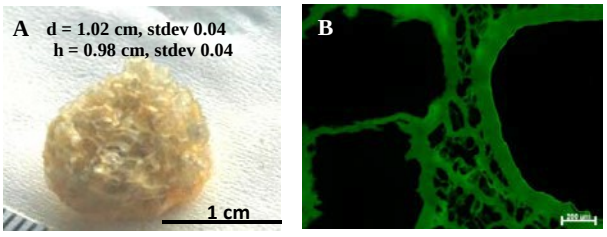

Fig. 1: Representative image and dimension (A) of a macro- microporous (MM) scaffold. Scale 1 cm. (B) The microporous structure was altered through the application of freezing and freeze drying. Scale is 200 µm.

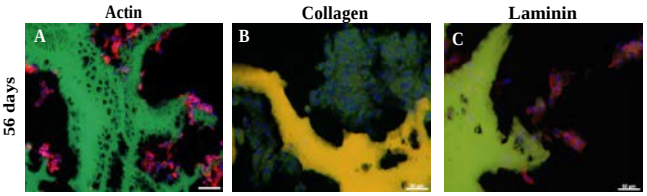

Fig. 2: ADSC cultured for 56 days within the MM scaffold fill (A) the porous structure and (B, C) express native adipose ECM components. Scale bars are 200 µm (A) and 100 µm (B, C). Green/yellow = scaffold, red = actin (A)/Laminin (C), green = collagen I.

The scaffold volume remained stable over 56 days, indicating that the cells do not degrade the scaffold in this time frame (Fig. 3).

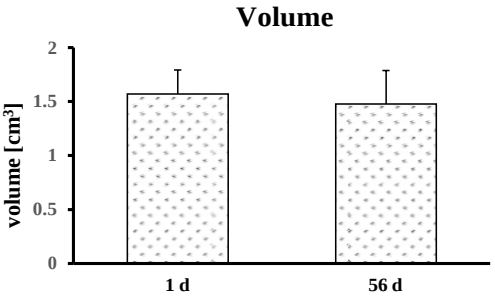

Fig. 3: The scaffold volume shows no significant changes over 56 days. n = 3. Error bars represent SD.

DISCUSSION & CONCLUSIONS: The porous gelatin sponge presented here has features essential for adipose tissue reconstruction. The scaffold supports both cell growth and the production of important components of native adipose ECM with minimal degradation at 56 days. This indicates the suitability of this scaffold for clinical application, with the potential to allow the long term remodeling of regenerated tissue.

ACKNOWLEDGEMENTS: This work was supported by charitable donations to the Blond McIndoe Research Foundation.

Development of a synthetic hydrogel system with tunable mechanical properties to support a 3D spinal cord injury model

JSL Kirk[1], RM Hall[1], JB Phillips[2], G Tronci[3], D Wood[4], RM Hall[1], JL Tipper[1]

[1]*Institute of Medical and Biological Engineering, University of Leeds,*

[2]*Biomaterials and Tissue-Engineering, UCL Eastman Dental Institute, University College London,*

[3]*Nonwovens Research Group, Centre for Technical Textiles, School of Design, University of Leeds,*

[4]*Biomaterials and Tissue-Engineering Research Group, School of Dentistry, University of Leeds,*

INTRODUCTION: Injury to the spinal cord can have devastating consequences. Advances in neuroregeneration have been made in the field of neurological medicine. where emphasis has been placed on biomaterials to deliver cellular therapies. However little is known about how the biomechanical properties of the matrix affect cellular behaviour. A 3D poly(ethylene glycol) hydrogel system has been designed which can be functionalised with biological molecules for cell attachment and the stiffness tuned 1000-fold to map cellular behaviour specific to matrix stiffness.

METHODS: Base molecules (Laminin, Fibronectin, Gelatin) were conjugated to Poly(ethylene glycol) diacrylate (PEGDA) using acrylate-PEG-N-hydroxysuccinimide (Ac-PEG-NHS)[1]. This allowed the introduction of acrylate groups for cross-linking and NHS moieties for linking lysine residues to PEG via an amide bond at the N-terminus. The gels underwent polymerisation under UV light (365nm) in the presence of 2-Hydroxy-4'-(2-hydroxyethoxy)-2-methylpropiophenone. The molecular weight of the base molecules and PEGDA were altered as well as PEGDA and Ac-PEG-NHS concentration to affect cross-linking density and functionalization yield. Rheology was used to determine the stiffness of hydrogels. TNBS assays were used to calculate the percentage of consumed free amino groups to determine the percentage functionalization of the biological molecules with PEG conjugate.

RESULTS: The higher the average molecular weight of the protein (laminin 400kDa, fibronectin 220kDa, gelatin 175g bloom 20kDa (supplier information)), the slower the functionalization reaction and therefore the lower the percent functionalization. The higher the molar ratio of Ac-PEG-NHS to gelatin (5:1, 1:1, 1:1(twice), 1:5) the higher the percent functionalization of gelatin (175g bloom) with Ac-PEG-NHS (48.48%, 16.51%, 40.00%, 11.26%). Repeat reactions with Ac-PEG-NHS increased the functionalization yield. The stiffness of PEGDA hydrogels can be tuned 1000-fold+ by changing the polymer concentration (Figure 1). The stiffness can also be modified (40Pa-42kPa) by changing the molecular weights of PEGDA (250-20,000kDa), Ac-PEG-NHS (1-10,000kDa), or gelatin (50-325g bloom) and by changing the degree of protein functionalization.

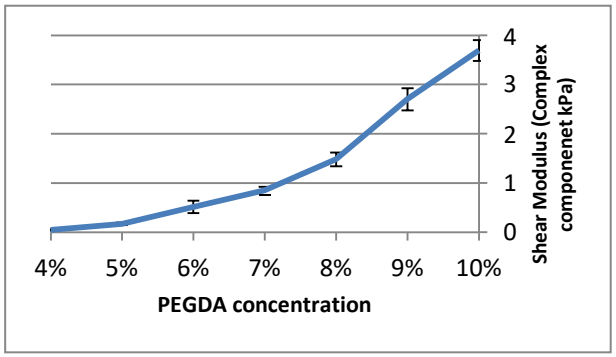

Fig.1. Stiffness of PEGDA hydrogels can be tuned 1000-fold+ from approximately 40Pa to 42kPa by changing PEGDA concentration from 4-20% (20%=42kPa data not shown). Error bars display standard deviation, n=5.

DISCUSSION & CONCLUSIONS: This unique PEG-gelatin functionalised hydrogel can be used to fine tune the biomechanical properties (such as stiffness) of the hydrogel by changing the molecular weight of PEGDA, PEG or bloom of gelatin, polymer concentration and protein density. This will allow investigation of how changes to the biomechanical properties of the matrix such as stiffness, cross-linking, polymer or protein density and porosity affect neural cellular behaviour. Investigations into cell viability are currently being performed with neural cell lines and primary mixed glial cell cultures.

ACKNOWLEDGEMENTS: This research was supported by the EPSRC as part of the DTC TERM Grant no EP/500513/1. This template was modified with kind permission from eCM Journal.

Functional expression of xenobiotic metabolising enzymes in human skin and tissue engineered skin equivalents

SA Smith[1], HE Colley[1], P Sharma[2], RJ Shipley[5], J Madden[4], M Cronin[4], SD Webb[3], C Murdoch[1]

[1]School of Clinical Dentistry, University of Sheffield, UK. [2]MRC Centre for Drug Safety Science, University of Liverpool, UK. [3]Applied Mathematics, Liverpool John Moores University, UK. [4]Pharmacy and Biomolecular Sciences, Liverpool John Moores University, UK. [5]Department of Mechanical Engineering, University College London, UK.

INTRODUCTION: The presence of xenobiotic metabolising enzymes in the skin is of considerable importance for the pharmaceutical/ cosmetic industries as these enzymes convert topically applied agents to either non-toxic or toxic metabolites that may lead to toxicity or hypersensitivity. The use of tissue engineered skin equivalents that replicate *in vivo* skin are extensively used in research and industry. However, whilst gene expression of xenobiotic metabolising enzymes in skin and skin equivalents has been detected by microarray analysis [1], data on protein expression and function of these enzymes in skin model systems is limited. Here we characterise gene expression and protein levels along with functionality of a sub-set of enzymes in whole skin and compare these to liver, commercially available and an in-house developed skin equivalent model to elucidate enzymatic profiles and activity.

METHODS: RNA and protein extracted from liver, whole skin, MatTek full thickness and our in-house skin models were used to determine gene expression by qPCR and protein levels using Western blotting. Enzyme activity and kinetics were assessed using commercially available assays.

RESULTS: From a selection of twelve enzymes examined qPCR revealed that liver expressed the most abundant levels of enzymes whilst, in general, whole skin expressed slightly more enzyme mRNA than skin models. However, ~90% of selected enzymes were increased in our in-house model compared to the commercial MatTek model. Similarly, Western blotting demonstrated protein expression for all except two of the twelve enzymes in whole skin. Decreased protein expression was observed in skin compared to liver, with the exception of FMO1, NAT1, COMT and GSTpi which showed increased expression (Fig. 1A). As an example, GST gene expression and protein levels from our in-house models is increased compared to MatTek models and equal to levels detected in skin (Fig. 1B). GST activity in our in house models (Fig. 1C) revealed similar levels of activity between the epidermal and dermal layers, indicating that this enzyme is uniformly distributed. GST specific activity peaked at 1 minute at a rate of 0.19 µmol/ml/min in the whole model.

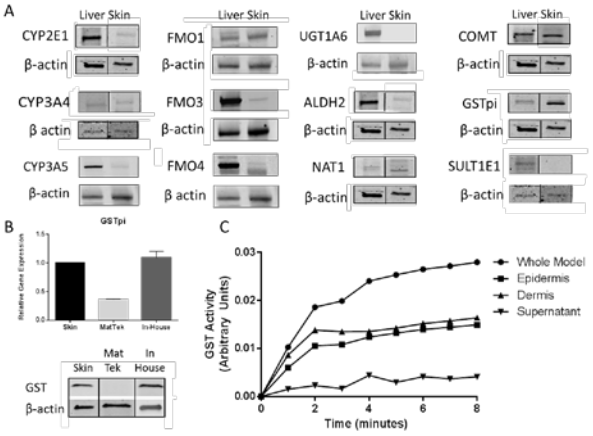

Fig. 1: Enzyme expression and activity levels. A. Protein expression in skin compared to liver. B. Gene expression, top, and protein levels, bottom, of GSTpi between skin and skin equivalents. C. GST activity in in-house skin models. GST specific activity in the whole model peaked at 1 min (0.19 µmol/ml/min).

DISCUSSION & CONCLUSIONS: Whilst at lower levels to liver, a high percentage of xenobiotic metabolising enzymes are expressed in the skin and skin equivalent models. We identified variations in enzyme expression between commercial and our in-house model. The main difference between these two models is the use of human dermis and not collagen as the scaffold in our in-house model. These data suggest that skin equivalents, in particular those based on dermis, will be a useful tool in investigating xenobiotic metabolism of topically delivered compounds.

ACKNOWLEDGEMENTS: This work was funded through a NC3Rs Phase 1 CRACK-IT award.

Engineered neural tissue model of the Schwann cell response to hypoxia *in vitro*

M Plotczyk[1], KS Bhangra[1], JB Phillips[1]

[1] *Biomaterials & Tissue Engineering, UCL Eastman Dental Institute, University College London*

INTRODUCTION: Engineered Neural Tissue (EngNT) technology combines cells with type 1 collagen matrix to build aligned constructs that support peripheral nerve regeneration[1]. Factors released by the cellular component in response to local environmental conditions have the potential to influence axon regeneration and vascularization, so understanding these responses is critical to therapeutic development. A number of Schwann cell-like cell types that can be used to generate EngNT and support neuronal growth have been identified and tested. These include rat Schwann cells[1], differentiated adipose-derived stem cells[2] and differentiated dental pulp stem cells[3]. However, *in vitro* and *in vivo* studies have revealed variations in their ability to support nerve regeneration and promote vascularization. One of the factors predicted to influence cell behaviour in EngNT is the hypoxic environment at the repair site caused by a lack of intrinsic vasculature. In the present study, we therefore aim to develop an *in vitro* platform for testing the effect of oxygen conditions on the survival and phenotype of cells in EngNT.

METHODS: A rat Schwann cell line SCL4.1/F7 was used in the initial experiments. Simplified EngNT constructs were assembled in 24-well plates, using 1ml cell-seeded type 1 collagen gels (2mg/ml) stabilised using plastic compression[1]. Gels were incubated in low ambient oxygen (1±0.2% or 3±0.2%) or standard ambient oxygen (16±0.2%) in a humidified 5% CO_2 environment for 24 hours prior to analysis. To assess cell death, gels were double-stained with propidium iodide (PI) and Hoechst and the percentage of PI-positive cells was counted. The expression of selected genes; brain-derived neurotrophic factor (BDNF) and nerve growth factor (NGF), was analysed using two-step RT-qPCR.

RESULTS: There was no significant difference in Schwann cell death between constructs exposed to different environmental oxygen conditions for 24 hours (Fig. 1). Initial gene expression analysis indicated reduced levels of NGF and BDNF in Schwann cell constructs cultured under low oxygen conditions (Fig. 2). Interestingly, the opposite pattern was observed for Schwann cells maintained in monolayer culture (data not shown).

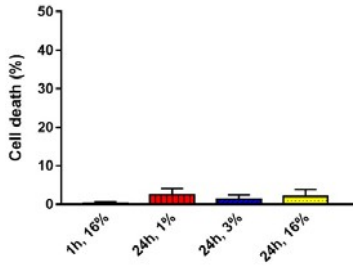

Fig. 1: Cell death of Schwann cells in stabilised collagen constructs under differential oxygen conditions. n=6, One-way ANOVA showed no significant difference between conditions (p≥0.05).

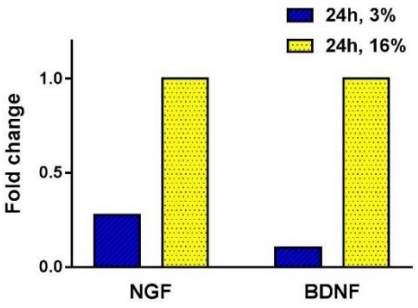

Fig. 2: Expression of neurotrophic factors by Schwann cells in stabilised collagen constructs in response to differential oxygen conditions. 3% values are normalised to 16% values (=1.0)

DISCUSSION & CONCLUSIONS: In the present study, a platform for testing the effect of oxygen conditions on cells in EngNT was developed. The model revealed minimal Schwann cell death when exposed to differential oxygen conditions. In addition, the study suggests that oxygen levels can elicit changes in gene expression of neurotrophic factors. However, further research is required to determine specific changes happening at both transcriptome and proteome level. In future experiments, a therapeutically relevant cell type, differentiated dental pulp stem cells, will be tested. The final goal of the study will be to tune EngNT to provide optimal cell responses to environmental conditions in order to improve its potential in regeneration of peripheral nerves.

Development of *in vitro* assays for functional testing of OECs for neural regeneration

Joana dos Reis[1], Melanie Georgiou[1], Ivan Wall[1]

[1]*Department of Biochemical Engineering, University College London, Gower Street, London WC1E 6BT, United Kingdom*

INTRODUCTION: Up to half a million people are affected by spinal cord injury every year worldwide. This has a major impact in the patient's lives, in the lives of their families and tremendous healthcare costs (http://www.who.int,19/02/2015). The central nervous system comprised by the brain and the spinal cord cannot regenerate itself due to the formation of a glial scar which forms a physical barrier that causes impaired growth of neurons (Silver & Miller 2004). Olfactory Ensheathing Cells (OECs) have shown to be a promising candidate for SCI treatment as they have the ability to regenerate neurons in the olfactory system guiding them from the mucosa to the brain. (Ramón-Cueto & Avila 1998). Nonetheless this cells are rare in the olfactory system and difficult to isolate and expand in culture. Moreover there is controversy to which extent the culture method will influence the cells regenerative properties. This project aims to develop *in vitro* functional assays to test this cells after expansion and set critical quality attributes.

METHODS: An injury in the spinal cord activates several secondary processes, such as hypoxia (Rossignol et al., 2007). For that reason we have examined variables including time and oxygen tension of co-culture of rat olfactory mucosal cells (OMCs) with NG108 neurons to determine whether these cells could support neurons in an environment mimicking the lesion site and the best time for them to do so.

RESULTS: Typically OMCs support neurons to a greater degree with Low O_2 (5 day co-culture: number of neurites: $p< 0.01$; neurite length $p< 0.05$, two-way ANOVA) compared with ambient O_2. OMCs perform similar or better than Schwann cell positive control at 5 day co-culture with Low O_2 compared to co-culture for 3 days.

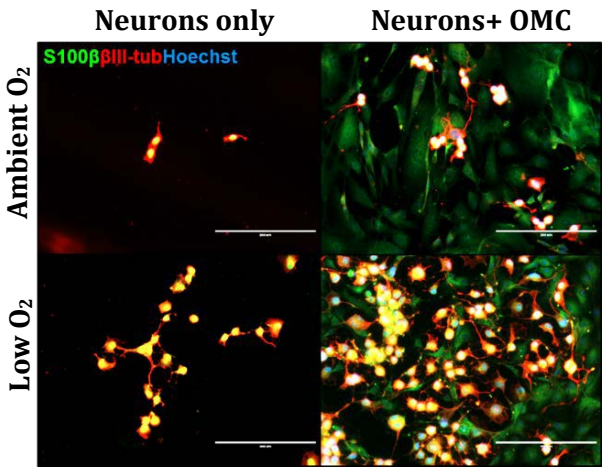

Fig. 1: Fluorescent micrographs of 5 day co-culture of NG108 neuronal cell line with rat olfactory mucosa-derived cell populations at Low and Ambient Oxygen. Scale bars are 200µm.

DISCUSSION & CONCLUSIONS: OMCs support neuronal proliferation and neurite growth in co-culture for 5 days having a similar or higher neurite support ability than the Schwann cell positive control. They also support neuronal growth to a bigger extent when co-cultured at Low O_2.

ACKNOWLEDGEMENTS: Funding bodies EPSRC, BBSRC and BRIC and Regenerative Medicine group, especially to Rachael Wood and Gerardo Santiago-Toledo.

Enhancing peripheral nerve repair through tissue engineering and gene transfer

Francesca Busuttil[1], Michael P. Hughes[1], Kulraj Singh Bhangra[2], Paul J. Kingham[3], James B. Phillips[2], Ahad A. Rahim[1]

[1] *Department of Pharmacology, School of Pharmacy, University College London, 29–39 Brunswick Square, London WC1N 1AX, UK.* [2] *Department of Biomaterials and Tissue Engineering, UCL Eastman Dental Institute, University College London, 256 Gray's Inn Road, London WC1X 8LD, UK.* [3] *Department of Integrative Medical Biology, Umeå University, Umeå, SE-901 87, Sweden.*

INTRODUCTION: Peripheral nerve injury (PNI) affects up to 5% of trauma patients and is associated with motor, sensory and autonomic impairment in the affected area[1]. Following PNI, axonal regeneration is dependent on Schwann cells, which express regeneration-assisting genes. However, this pro-regenerative phenotype is not always maintained long enough to ensure functional recovery[2]. Tissue engineered three dimensional (3D) constructs containing therapeutic cells that maintain the appropriate phenotype may help enhance nerve regeneration.

METHODS: An *in vitro* proof-of-concept study was carried out to deliver luciferase and green fluorescent protein (GFP) genes to rat Schwann cells (SCL4.1/F7) using a bicistronic lentivirus and to assess whether the transduced cells were still viable for the construction of 3D collagen constructs that can be used to enhance nerve repair. Fluorescence microscopy was used to visualise the GFP tag and the transduction efficiency was established using flow cytometry. Bioluminescence imaging was used to assess luciferase activity. The transduced Schwann cells were seeded into 3D collagen constructs and their distribution throughout the construct was shown using stereoscopic fluorescence microscopy and scanning confocal microscopy. Bioluminescence imaging was used to assess whether the transduced Schwann cells were still viable after incorporation into the constructs (figure 1).

RESULTS: Schwann cells were successfully transduced using the lentiviral vector produced. This was confirmed by fluorescence microscopy, bioluminescence imaging and flow cytometry. Following incorporation into the collagen constructs, stereoscopic fluorescence microscopy and confocal microscopy showed that the transduced cells had distributed evenly throughout the construct. Bioluminescence imaging confirmed that the F7 cells were still viable after seeding into the constructs. No fluorescence or bioluminescence was observed in the untransduced cells or in the control constructs seeded with the untransduced cells.

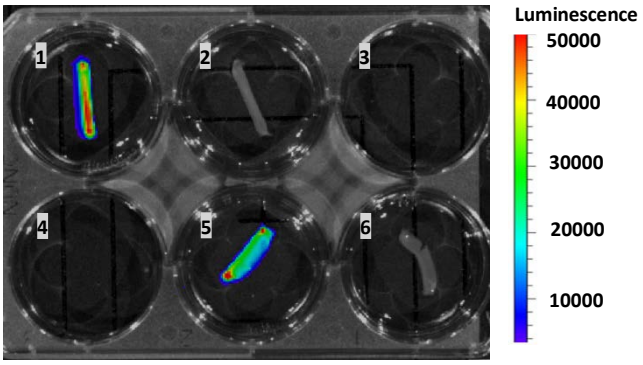

Figure 1: Bioluminescence image showing luciferase activity. Wells 1 and 5 contain the constructs seeded with transduced cells. Wells 2 and 6 contain the constructs seeded with control untransduced cells. Wells 3 and 4 are empty. Colour scale: min = 2695, max = 50280.

DISCUSSION & CONCLUSIONS: The results from this study suggest that Schwann cells can be transduced effectively using lentiviral vectors and used to engineer tissue engineered nerve repair constructs. The bioluminescent labelling achieved here provides a powerful means to track cell fate *in vivo* during preclinical testing. This approach is currently being applied to clinically relevant sources of therapeutic cells, such as adipose derived stem cells, bone marrow stem cells and *CTX* cells. Additionally, lentiviruses can be used to potentially deliver pro-regenerative genes that maintain the therapeutic cells in the appropriate phenotype or which increase vascularisation following implantation.

ACKNOWLEDGEMENTS: *CTX* cells were provided by ReNeuron, UK. Francesca Busuttil is partly funded by the ENDEAVOUR Scholarship Scheme, Malta.

The use of Poly(3-hydroxybutyrate-*co*-3-hydroxyvalerate) as a material for Peripheral Nerve repair and Nerve Guide Tissue Engineering

Caroline S. Taylor, Adam Glen, Frederik Claeyssens and John W. Haycock

Department of Materials Science & Engineering, Kroto Research Institute, Broad Lane, Sheffield S3 7HQ, UK.

INTRODUCTION: Peripheral nerve injuries affect 300,000 people in Europe every year. Autografting is the current 'gold standard' treatment to bridge larger gaps, although there is limited donor nerve and donor site morbidity. Nerve guide conduits (NGCs) are currently used instead but each has its limitations, such as acidic degradation products and limited success in large gaps. Providing internal guidance cues, such as electrospun fibres, have been used to improve current designs. Poly(3-hydroxybutyrate-*co*-3-hydroxyvalerate) (PHBV) is a thermoplastic polyhydroxyalkanoate (PHA) naturally produced by bacteria. PHAs already have FDA approval as a suture material, and are used widely in many tissue engineering applications. The mechanical properties of PHBV can be tailored to specific applications and it is highly biocompatible and biodegradable.

METHODS: Electrospinning was used to fabricate 5 different PHBV fibre diameter sizes. Average fibre diameter and alignment was quantified by scanning electron microscopy. 40,000 NG108-15 neuronal cells were seeded onto different fibre diameter sizes, for 6 days, with serum removed on day 2 to promote neuronal cell maturation and neurite outgrowth. Cell viability was determined by using live/dead analysis, and cells immunolabelled against β-III tubulin for neurite extension studies.

RESULTS: All fibre diameters supported the proliferation of NG108-15 neuronal cells, with 8µm fibres supporting the highest number of live cells (564.55 ± 215.69). The highest average number of neurites per neuron were detected by cells grown on the 8µm fibres (1.31 ± 0.21). 2, 4, 6 and 10µm fibres were 1.12 ± 0.21, 1.22 ± 0.18, and 1.24 ± 0.15 and 1.29± 0.11 respectfully. The longest neurites were recorded on the 8µm fibres (133.33 ±17.38µm) followed by the 6, 10, 4 and 2µm fibres. (115.58 ± 20.37µm, 86.58 ± 10.56µm, 60.85 ± 14.62µm and 44.89 ± 7.14µm respectfully)

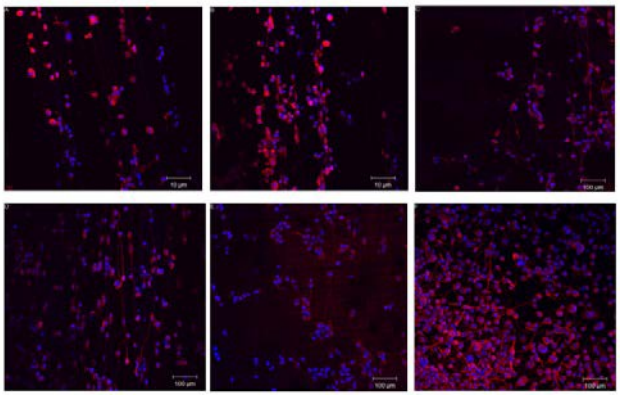

Figure 1. Confocal microscopy images of NG108-15 neuronal cells immunolabelled against β III tubulin (red) and cell nuclei (blue). Cells were stained after 6 days in culture on A) 2µm fibres, B) 4µm fibres, C) 6µm fibres, D) 8µm fibres, E) 10µm fibres, and F) PHBV spin coated flat films.

DISCUSSION & CONCLUSIONS: Overall, 8µm fibres were the most efficient fibre size for peripheral nerve regeneration, supporting the highest number of live cells, as well as promoting the highest average number of neurites expressing neurons, the highest average neurite length as well as the highest maximum neurite length. Future work includes in vitro testing of fibers with Rat primary Schwann cells and dorsal root ganglion as well as producing 3D printed hollow PHBV tubes, using microstereolithography for in vivo work.

ACKNOWLEDGEMENTS: We acknowledge the University of Sheffield for funding.

CXCR4 improves the migration of stem cells from osteopenic animals.

A Sanghani Kerai[1], M Coathup[1], S Samazideh[1], P Kalia[2], L Di Silvio[2], G Blunn[1]
[1]*Institute of Orthopaedics & Musculoskeletal system, UCL.* [2]*Department of Tissue Engineering & Biophotonics, King's College.*

INTRODUCTION: Mesenchymal stem cells **(**MSCs) from postmenopausal women have a slower growth rate and osteogenic differentiation ability compared to MSCs from premenopausal women. This causes lower bone density and reduced fracture healing capacity in osteoporotic women. Local MSCs from injured tissues and circulating MSCs are involved in fracture healing. Cytokines and chemokines such as SDF1 and its receptor CXCR4 play important roles in maintaining mobilization, trafficking and homing of stem cells from bone marrow to the site of injury(1-3). The aim of this study was to investigate the migration of MSCs transfected with CXCR4, towards SDF1 in a transwell assay.

METHODS: MSCs were harvested from femora of young, adult and OVX rats, genetically modified to over-express CXCR4 and put in a Boyden chamber to establish their migration towards SDF1. This was compared to the non-transfected and scrambled infected MSCs. Data was analysed using a Student t-test.

RESULTS: MSCs from OVX rats migrated less towards SDF1 (9±5%) compared to MSCs from adult (15±3%) and juvenile (25±4%) rats. Cells transfected with CXCR4 migrated more towards SDF1 compared to non-transfected cells irrespective of whether these cells were from OVX, young or adult rats.

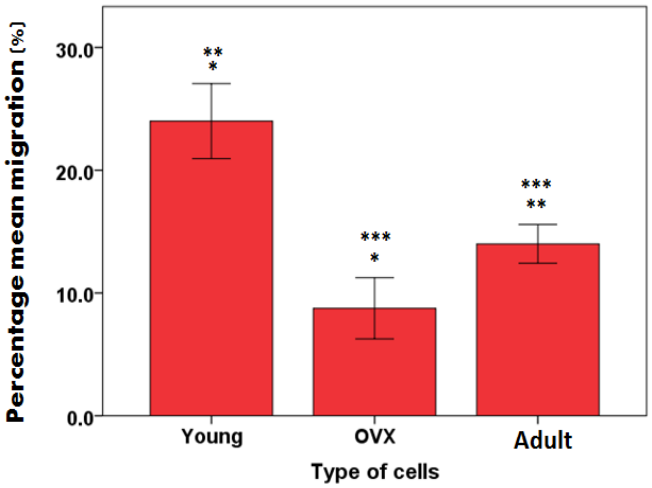

Figure 1: The mean percentage migration of uninfected MSCs from young, adult and OVX rats towards SDF1 in a Boyden chamber.*, ** and * represents significance p<0.05.**

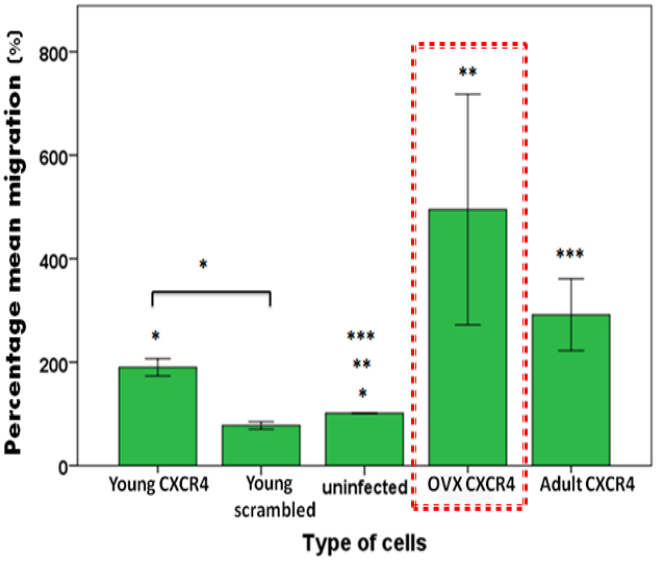

Figure 2: The percentage migration of infected cells normalised against uninfected cells. *, ** and * represents significance p<0.05.**

DISCUSSION & CONCLUSIONS: The impaired migration of MSCs from OVX and adult rats in comparison to MSCs from juvenile rats could be due to their diminished surface expression of CXCR4. The mobility of MSCs from OVX rats towards SDF-1 was increased when their CXCR4 expression was up-regulated. SDF1 causes cell migration by binding with CXCR4. Poor homing ability of the stem cells to bone could result in a significant reduction in bone formation which ultimately contributes to osteoporosis and delayed union in fractures (4). The migration of stem cells can be enhanced by up-regulating CXCR4 levels which could enhance fracture healing and bone formation in osteoporotic patients.

ACKNOWLEDGEMENTS: This study was funded by ORUK and The John Scales endowment fund.

Three-dimensional tumour models to study metastatic cancer invasion through aligned stroma

RN Pradhan[1], J Pape[1], M Pavlou[1], JB Phillips[2], U Cheema[1]

[1]Institute of Orthopaedics, University College London, England; [2]Eastman Dental Institute, University College London, England

INTRODUCTION: Cancers are one of the greatest healthcare challenges we face. Given the ethical issues and expense of *in vivo* modelling, *in vitro* models are being used to further our understanding of cancers and in particular the metastatic process; a potent feature of cancer[1]. These models are made more physiologically representative through the use of three-dimensional (3D) models and introduction of relevant cellular and biological factors into the stroma. However, the effect of stromal alignment on development of these non-aligned tumours *in vitro* is yet to be investigated, despite many cancers being found in aligned environments. This study aims to optimise a clinically relevant 3D cancer model with an aligned stroma and use this model to explore the effects of stromal alignment on invasion.

METHODS: Collagen hydrogels were seeded with varying concentrations of Human Dermal Fibroblasts (HDFs) and gel contraction was measured over 24 hours to ascertain the minimum concentration required to reliably produce 60% contraction. Gels in optimally shaped moulds were seeded with this concentration ($2x10^6$ cells/ml) for 24 hours, to confirm alignment would occur as in the literature[2]. Artificial cancer masses (ACMs) were created through compression of HT29 seeded hydrogels. These were implanted into the above tethered cellular gels to produce tumouroids. These tumouroids were left to align for 24 hours, then untethered and compressed. These compressed gels were maintained for 7 days, after which they were imaged and analysed to measure invasion.

Results: 60% hydrogel contraction was achieved at a HDF concentration of 2 million cells per ml ($p<0.05$). Alignment was achieved in tethered moulds at this concentration. Following implantation of ACMs, alignment was still achieved over 24 hours, although the pattern of alignment zones was altered. Following compression and maintenance for 7 days, invasive bodies were observed escaping the ACM into the stroma. The mean distance travelled from ACM and mean surface area of these invasive bodies were significantly higher in the gels set in tethered moulds ($p=0.010$ and $p<0.001$ respectively) relative to the non-aligned gels.

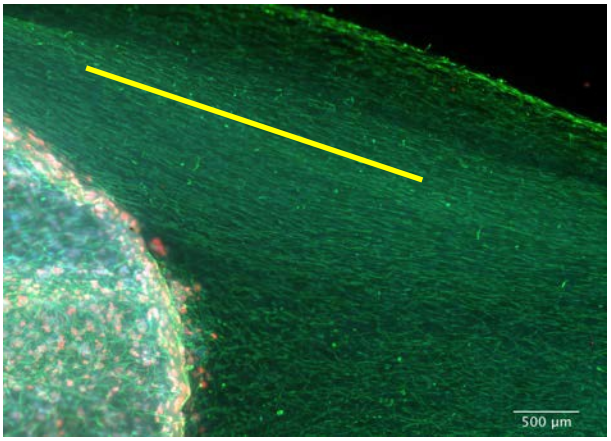

Fig. 1: A fluorescence microscopy image obtained using a 2.5x objective showing a non-compressed tumouroid. Stromal alignment to the axis of the principle line of tension can be observed (indicated by the yellow line)

DISCUSSION & CONCLUSIONS: A clinically relevant *in vitro* 3D aligned tumouroid model was successfully optimized. Results from this study show that alignment has a statistically significant effect on the mean distance travelled by and mean surface area of invasive bodies leaving ACMs in tumouroids. Whilst increases in number of invasive bodies and total surface area of invasion were also observed in the aligned gels, a larger sample size is required to ascertain statistical significance in these measurements. Future studies should investigate whether alignment affects the orientation of invasion relative to the principle axis of strain and aim to incorporate more biologically relevant factors in the stromal environment. This study is a step towards optimization of a truly clinically relevant *in vitro* cancer model with applications in both drug testing and the advent of personalised cancer medicine.

.

Osteoporosis and ageing affects stem cell function and migration.

A Sanghani Kerai, M Coathup, L Osagie, S Samazideh, G Blunn
Institute of Orthopaedics & Musculoskeletal system, UCL.

INTRODUCTION: There is interest in using anabolic factors such as stem cells to augment fracture repair. Another factor associated with fracture healing is the retention and migration of stem cells to the site of injury. Cytokines and chemokines such as SDF1 and its receptor CXCR4 play important roles in maintaining mobilization, trafficking and homing of stem cells from bone marrow to the site of injury (1-3). The aim of this study was to isolate stem cells from osteopenic rats and investigate and compare the CD marker expression, proliferation, migration, osteogenic and adipogenic differentiation. The hypothesis of this study is that the migration of MSCs from young, adult and ovariectomised (OVX) rats will have different proliferation, differentiation and migratory abilities.

METHODS: Ovariectomy was performed in 6-9 month old Wistar rats and osteopenia developed over a 4 month post-op period. MSCs were harvested from the femora of young, adult and osteopenic Wistar rats. Proliferation of the cells was measured using Alamar blue. Osteogenic differentiation was measured using ALP expression at day 0, 7, 14 and 21 and using Alizarin red. Adipogenic differentiation was measured at day 7, 14 and 21 using Oil red O. Cells were incubated in Boyden chambers to quantify their migration towards SDF1. For analysis the number of cells migrating across the membrane was expressed as a percentage of the cells remaining on the upper membrane surface. Data was analysed using a Student t-test where p values < 0.05 were considered significant.

RESULTS: The stem cells from all 3 groups of rats expressed on average the same amount of CD29 (>90%), CD90 (>96%), CD34 (<5%) and CD45 (approx 10%). The proliferation rate measured by Alamar blue normalised against DNA was also similar at day 3, 7, 10 and 14. However, interestingly the migration and differentiation ability was significantly different between the MSCs from the 3 groups of rats. The young MSCs were not only better at differentiating into bone (fig1) and fat as well, but they also migrated significantly more towards SDF1. The migration of SDF-1 doubled with young rats compared to the adult rats (p = 0.023) and it was four times higher when compared to cells isolated from OVX rats (p = 0.013).

DISCUSSION & CONCLUSIONS: MSCs from OVX rats are similar to MSCs from young rats. However when induced to turn into bone, fat and migrate towards SDF1, young MSCs are significantly more responsive than MSCs from OVX and adult control rats. The poor homing ability and differentiation of the stem cells and their retention may result in a reduction in bone formation leading to delayed union in fractures of osteoporotic patients(4).

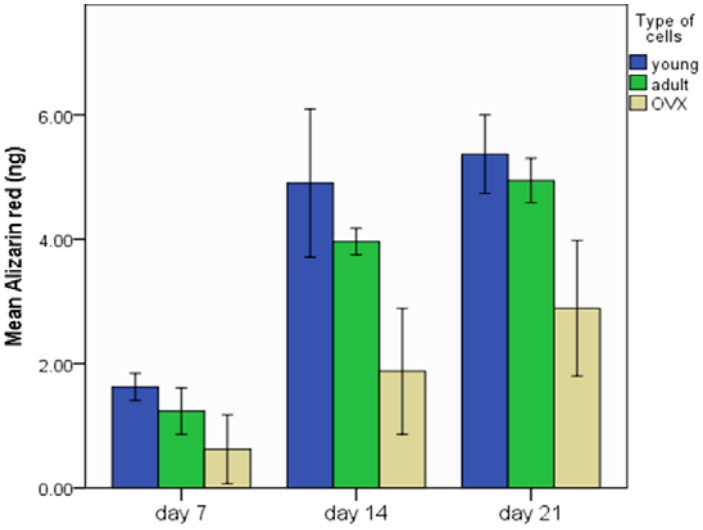

Fig 1: The average Alizarin red production in young, adult and OVX rats at day 7, 14 and 21.

ACKNOWLEDGEMENTS: This study was funded by ORUK and The John Scales endowment fund.

Mathematical Modelling Predicts the Spatial Distribution of Metabolism in Skin

RJ Shipley[1], SD Webb[2], J Madden[3], S Smith[4], P Sharma[5], M Cronin[3], HE Colley[4], C Murdoch[4]

[1] Department of Mechanical Engineering, University College London, UK. [2] Applied Mathematics, Liverpool John Moores University, UK. [3] Pharmacy and Biomolecular Sciences, Liverpool John Moores University, UK. [4] School of Clinical Dentistry, University of Sheffield, UK. [5] Department of Molecular and Clinical Pharmacology, MRC Centre for Drug Safety Science, Institute of Translational Medicine, University of Liverpool, UK

INTRODUCTION: The expression of RNA and protein for a multitude of different phase 1 & 2 xenobiotic metabolizing enzymes has been demonstrated both in *ex vivo* human skin and in *in vitro* tissue-engineered human skin equivalents by microarray and mass spectrometry techniques [1-2]. The presence of these enzymes in the skin is of considerable importance for the pharmaceutical/ cosmetic industry as xenobiotic compounds delivered topically or systemically to the skin may be metabolized to produce active metabolites that may either be beneficial (release of active drugs from pro-drugs) or may cause toxicity or hypersensitivity. Here we use mathematical models, parameterised against *in vitro* experimental data, to inform the spatial distribution of metabolism in tissue-engineered skin samples.

METHODS: A coupled system of partial differential equations was developed to describe the transport of parent compound and metabolites through a geometry representative of engineered skin equivalents (including corneum, granulosum, spinous, basal and dermal layers, with a fluid pool underneath, as used in the culture set-up). Diffusion and metabolism were defined based on literature values, and were specific to each layer [3-5]. The model was solved using COMSOL Multiphysics (a finite elements package), subject to boundary conditions that mimic the typical *in vitro* setup (for example, prescribed concentration of parent compound on the upper corneum surface, representative of topical delivery).

RESULTS: The model predicts spatial heterogeneity in the parent compound and metabolite concentrations within the skin (see Fig. 1). The parent compound concentration is highest at the upper corneum surface where it is delivered, and decays to a minimum within the basal cells at the bottom of the epithelium, as a consequence of cellular metabolism. The compound also diffuses through the extra-cellular spaces into the dermis, which consequently has a slightly higher concentration than the basal and lower spinous cell layers. This spatial distribution is mirrored by the metabolite, which is lowest in corneum/ granulosum/ dermal layers, and highest within the spinous cells. In both cases, intra- versus extra-cellular transport routes are easily identifiable, and the patterning of cells within the spinous layer is a strong determinant of the spatial distributions of parent compound and metabolite.

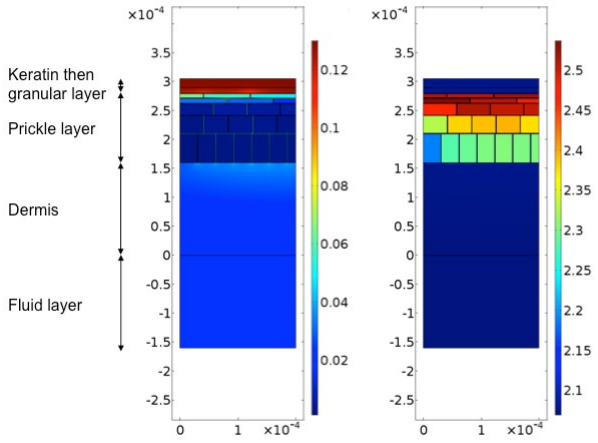

Fig. 1: Mathematical model predictions of the spatial distribution of parent compound (left) and metabolite (right) concentrations (both mol/m^3); parent compound delivered topically on the upper corneum surface with results shown after 10 hours. Physical dimensions measured in metres.

DISCUSSION & CONCLUSIONS: The mathematical model, parameterised by literature diffusion and metabolism parameters, was able to predict the spatial distribution of parent compound and metabolite within *in vitro* skin equivalents. This complete spatial information is particularly challenging to extract using a purely experimental approach. The model is generic, and next will be used to explore alternative delivery routes (e.g. systemic delivery of parent compound through the vasculature), and human skin geometries.

ACKNOWLEDGEMENTS: This work was funded through a NC3Rs Phase 1 CRACK-IT Award.

Modelling indentation testing of hydrogel discs for use in tissue engineering

JM Page[1], LS Kimpton[1], JP Whiteley[2], SE Dunphy[3], AJ El Haj[4], SL Waters[1]

[1] Mathematical Institute, University of Oxford, [2] Department of Computer Science, University of Oxford, [3] Department of Mechanical and Manufacturing Engineering, Trinity College Dublin, [4] Institute for Science & Technology in Medicine, Keele University

INTRODUCTION: Tissue engineering has developed as a response to the ever-increasing demand for tissue and organ transplants with the eventual aim to be able to replace donor transplants. Dunphy *et al*[1] aimed to engineer tissue *in vitro* that has the same mechanical properties as the lung alveolar wall *in vivo.* To do this they seeded lung fibroblasts into hydrogel discs comprised of varying amounts of collagen and elastin. We have modelled the indentation test used by Dunphy *et al*[1] to determine the material properties of the disc.

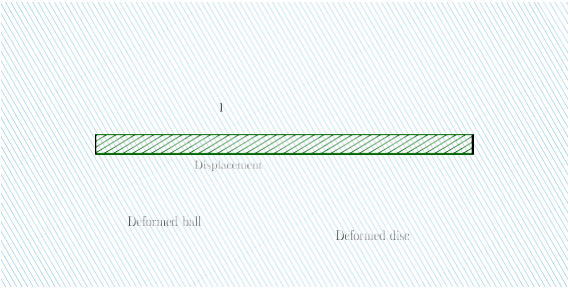

Fig. 1 Experimental setup used by Dunphy et al[1].

METHODS: Dunphy *et al*[1] used a non-destructive indentation test, designed by Ahearne *et al*[2] to measure the Young's modulus of the hydrogel discs, as they considered this to be the most important material property to replicate *in vivo* results. The indentation test used by Dunphy *et al*[1] involved clamping the outer radius of the disc, placing a sphere of known weight in the centre of the disc, and measuring the displacement at the centre of the disc, shown in Figure 1. By relating the applied force to the observed deformation it is possible to obtain the Young's modulus of the hydrogel disc, and this was done using a formula derived by Liu and Ju[3]. By balancing the forces acting within the disc and exploiting the geometry of the disc we have developed a system of ordinary differential equations to describe the profile of the deformed disc, which we solve numerically. This then allows us to find the force required to induce a given displacement. For small displacements we have used mathematical techniques to analytically obtain a relationship between the force and the displacement. Finally, we have investigated how heterogeneity in the disc, which we hypothesise can occur due to interactions between the different components of the disc, can affect these relationships. We include this in our model by allowing the shear modulus of the disc to vary spatially.

RESULTS: Our mathematical analysis shows that for small displacements gives an analytic relationship between the applied force and the induced displacement. The numerical relationship we obtain when fitting to simulated data points shows good agreement with the analytic results, indicating that it is suitable fit. However, when compared to the formula obtained by Liu and Ju[3] it shows significant deviation, both quantitatively and qualitatively. By applying our method to experimental data one obtains significantly different results than the current method, in some cases our method predicts the Young's modulus to be twice that of the current method. Further, we have found that if there is a small variation in the shear modulus, which we believe could occur due to small imperfections in the disc, then the relationship between the displacement and the force is unaffected. However, if there are larger variations in the shear modulus, which we believe can occur due to interactions between the components of the disc, then this relationship is significantly altered.

DISCUSSION & CONCLUSIONS: We have shown that our method, which is supported by analytical results, produces significantly different results to the method currently used. We have also shown that the composition of the disc may need to be considered when calculating it's Young's modulus, which is not currently the case.

A comparative study evaluating the ability of electro-bioreactors to deliver electric field for tissue engineering by finite element modelling

R Xue[1], S Mobini[1], S Cartmell[1]

[1] School of Materials, University of Manchester, UK.

INTRODUCTION: Tissue engineering provides promising alternative treatments to a variety of defects. Electric field (EF) was found ubiquitously in the biological system long ago, but its use in regulating tissue growth in vitro was popularized in past few years. A number of novel electro-bioreactors were developed recently [1, 2]. Among all, the electro-bioreactors with I-shape (design A) and L-shape (design B) electrodes are compatible with standard 6-well plate, providing an easy-to-use, inexpensive platform to study the effect of EF on cells in culture. However, their performance of delivering EF to cells remains unclear. Here, we attempted to answer the above question using finite element modelling (FEM). EF in design A and B were compared, leading to the proposal of an optimal bioreactor design (C) with rectangular shape electrodes. Design C is compatible with a standard rectangular 8-well Runc plate.

METHODS: Commercial COMSOL Multiphysics FEM software was used to simulate the A, B and C bioreactor design. The models were composed of two platinum (Pt) electrodes and one circular or rectangular main body with 3 ml cell culture media (figure 1). By using direct current, electric potential difference of 100 V/m was applied between the two electrodes. Electric insulation was applied on the outer boundary of the model. Free tetrahedral elements were used to mesh the geometry and a mesh sensitivity test was conducted to determine the optimal element size. The distributions of EF on bottom surface of culture media (cell culture area) were generated and their average values were calculated.

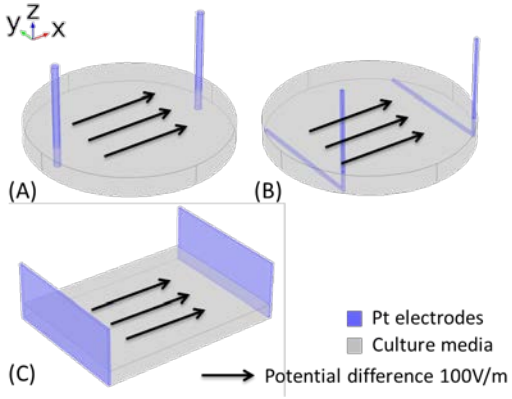

Fig. 1: FEA models of design A, B and C.

RESULTS: The average values of electric field on the cell culture area are shown in table 1. The EF distributions are visualized in figure 2. In terms of EF homogeneity, Electro-bioreactor with I-shape electrodes was the lowest, while the proposed design with rectangular electrodes was the highest. Although a 100 V/m electric potential difference was applied, design A only had an average EF of 63 V/m. In comparison, design B showed a higher value (85 V/m) and EF in the center region was close to 100 V/m. Design C resulted in a uniform electric field (100 V/m) throughout the model.

Table 1. Average EF values on cell culture area.

Design	A	B	C
Electric field (V/m)	63	85	100

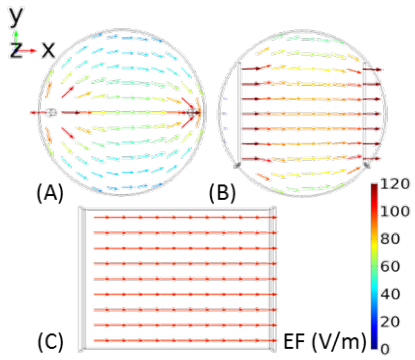

Fig. 2: EF distribution of design A, B and C.

DISCUSSION & CONCLUSIONS: It can be concluded from the FEM predictions that the geometry of both electrode and bioreactor chamber plays an important role in delivering electric field. In order to study the effect of EF on cells in culture, it is crucial to avoid EF gradient in the experiment. Compared with electro-bioreactors with I- and L-shape electrodes, the proposed design (C) has the best uniformity of applied EF.

ACKNOWLEDGEMENTS: This work is financially supported by Rose Trees Trust A921 grant and BBSRC BB/M013545/grant.

Poly(ethylene glycol) and chitosan hydrogels as scaffolds for soft tissue engineering applications

JA Morales-Valencia[1, 2], J Flores-Estrada[3], MV Flores-Merino [2, 4]

[1]*ITESM, Mexico,* [2]*Research Centre in Medical Science (CICMED), UAEM, Mexico,* [3]*Faculty of Chemistry, UAEM, Mexico,* [4]*Department of Chemistry, University College London, UK*

INTRODUCTION:

The design and evaluation of new polymer based biomaterials is a major goal in the area of tissue engineering. Moreover, the fabrication of combined materials with high performance and unusual properties is a strategy that have been explored to fullfill the requirements of a scaffold. Hydrogels are polymeric materials that have attracted the interest in the biomedical area due to their high water content and biocompatbility nature.[1,2] Therefore, in this work a hidrogel scaffold, made of two polymers: poly(ethylene glycol) (PEG) and chitosan (CH), was fabricated and its biocompatibility was studied.

METHODS:

Synthesis of the hydrogel of poly (ethylene glycol) and chitosan: samples were synthetized by free radical photo-polymerisation of a homogenous solution of poly (ethylene glycol) di-acrylate, chitosan (Sigma-Aldrich, USA) and a UV initiator (Sigma-Aldrich, USA) in a PTFE mold. Samples were washed with de-ionized water several times in order to remove any unreacted initiator. Before being used in cell culture experiments, the hydrogels were sterilized in 70 % ethanol (Sigma-Aldrich, USA) and then equilibrated in phosphate buffer saline (Sigma-Aldrich, USA).

Metabolic activity studies: MTT and XTT assays were employed to measure the number of viable or live cells. Two cell populations were used for this study: a) human mononuclear cells and b) human fibroblast (ATCC-CRL-2522). Briefly, hydrogel samples were put in direct contact with the cell population. Then, the metabolic activity was measured at established periods of time. Also, human fibroblast cells were seeded on the hydrogel surfaces and their capacity to support cell growth was evaluated.

RESULTS: Studies of hydrogels in direct contact with cells (human mononuclear cells and human fibroblast) showed cell metabolic activity higher than 80%. Mononuclear cells in contact with PEG-CH hydrogels (48 h) had a percentage of 95.7 ± 3.7 viable cells. Also, fibroblast in contact with the hydrogel samples that were evaluated for 24 h and 10 days showed a value above the 80% compared with the control (tissue well plate). Therefore, PEG-CH hydrogels are biocompatible in direct contact with both cell populations.

In the studies, where cells were seeded on the hydrogel surfaces (Fig. 1), it was observed an increase in metabolic activity compared with the tissue culture well plate. At the second day in culture the metabolic activity of fibroblast in PEG-CH hydrogels was 40% higher than the control (100%). The higher percentage of cells indicates that the hydrogel can support cell growth within the structure of the material.

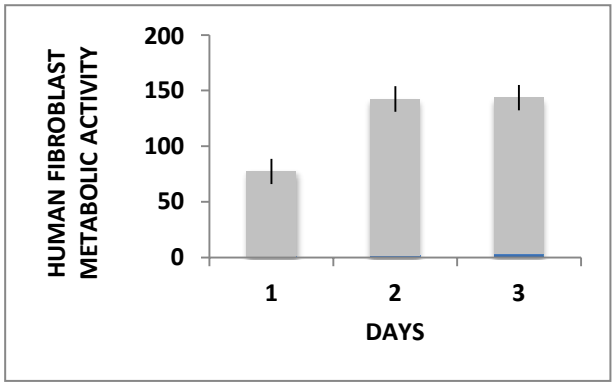

Fig. 1: Percentage of human fibroblast cells seeded on PEG-CH hydrogel (n=3) measured by MTT assay.

DISCUSSION & CONCLUSIONS: the studies of mono nuclear cells and fibroblast in contact with PEG-CH hydrogels did not show any decrease in metabolic activity compared with the control. Moreover, PEG-CH hydrogel was able to support cell growth. Therefore, the results suggest that the PEG-CH hydrogel have a potential as scaffold for soft tissue engineering applications.

ACKNOWLEDGEMENTS: The authors would like to thank UAEM (Grant no: 3890/FS2015) and COMECYT for providing financial support.

Effect of direct electrical stimulation on pH changes and viability of human mesenchymal stem cells

K Srirussamee[1], S Mobini[1], SH Cartmell[1]

[1] *School of Materials, The University of Manchester, Manchester, UK.*

INTRODUCTION: Direct electrical stimulation (D-ES) is one of the techniques which are used to deliver electrical signals to the cells. It has been reported to be effective in manipulating cell migration, orientation, and intracellular calcium level of mesenchymal stem cells (MSCs) [1]. However, it also has several considerations, e.g. change in pH, and faradic by-products [2]. Hence, this study aims to observe pH change caused by D-ES and whether it negatively affects cell viability.

METHODS: D-ES was delivered to the samples through platinum electrodes [3]. Electric field strength was set at 100 and 200 mV/mm. The stimulation has been carried out for 1 hour inside the incubator. Growth medium (GM) (DMEM high glucose with 10% FBS and 1% antibiotic antimycotic solution) and osteogenic medium (OM) (GM with 50 mg/ml ascorbic acid, 10 mM β-glycerophosphate, and 10 nM dexamethasone) were used in this experiment. Human bone marrow-derived MSCs were cultured in 6-well plates to investigate cell viability. D-ES has been applied to cells daily for 7 days. Media were changed every 3 days. Cell number was measured using alamarBlue® assay.

RESULTS: *Fig.* 1 shows that pH of fresh media after 1 hour of D-ES increased and was dependent on electric field strength. There was insignificant difference in pH between D-ES and control groups after 14-hour subsequent incubation. The media collected from cell culture showed higher pH than fresh media after 14-hour subsequent incubation, including control groups. *Fig. 2* shows that 7-day D-ES at 100 mV/mm exhibited higher cell number than control groups. However, D-ES at 200 mV/mm generated foamy texture to the media which were not suitable for cell culture studies (data not shown).

DISCUSSION & CONCLUSIONS: The results show that changes in pH were temporary due to the buffering capability of the media. Medium pH was raised during cell culture, possibly because of cell mitosis during proliferation cycle [4]. D-ES at 100 mV/mm seems to be not harmful to cells as the difference in average pH between fresh media after D-ES and those collected from cell culture were less than 1%. Therefore, we assessed that it did not negatively affect cell viability.

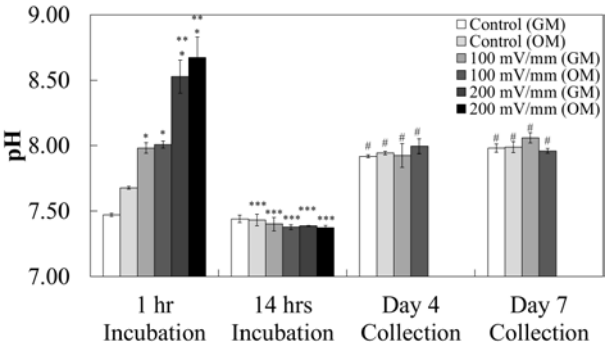

Fig. 1: pH of fresh media after 1-hour incubation with D-ES, after subsequent 14-hour incubation, and media collected from cell culture. (, **, ***, and # represents p<0.05 compared to control group, 100 mV/mm group, 1-hour incubation group, and 14-hour incubation group, respectively Error bars represent SD (n=3).)*

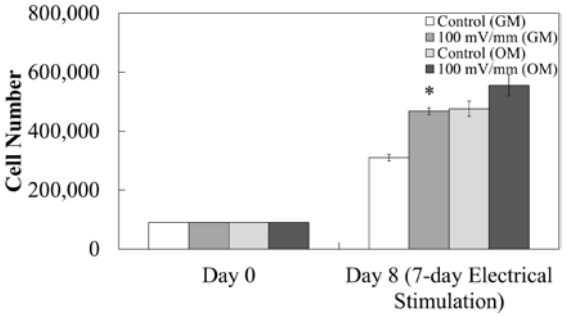

Fig. 2: Cell number measured by alamarBlue® assay after 7 days of D-ES (represents p<0.05 compared to control group. Error bars represent SD (n=3).)*

ACKNOWLEDGEMENTS: This work is financially supported by BBSRC BB/M013545/grant.

Development of a decellularised porcine dermis for cutaneous wound healing

J Helliwell[1], D Thomas[1], V Papathanasiou[2], S Homer-Vanniasinkam[2], E Ingham[1]

[1] *Institute of Medical and Biological Engineering, University of Leeds, Leeds, UK*

[2]*Leeds Vascular Institute, Leeds General Infirmary, Great George Street, Leeds, UK*

INTRODUCTION: In recent years, there have been a number of developments in the use of acellular dermal matrices for cutaneous wound repair. An acellular dermal matrix, produced by decellularisation of human cadaveric skin, using low concentration SDS and proteinase inhibitors, has been shown to be of utility in the treatment of chronic non-healing ulcers[1-2].

The aim of this study was to adapt the decellularisation method used for human skin to produce a decellularised dermis from porcine skin.

METHODS: Porcine skin was dissected from the backs of Large White pigs (circa 6 months old). Visible hairs were shaved before split-thickness sections (800-1500 μm) were obtained using a dermatome. Samples (6 x 4 cm) were dissected and then treated with NaCl for 18 hours, allowing the epidermis to be removed using forceps. Trypsin treatment paste (1.125 x 10^4 U.ml, 0.5% (w/v) agarose) was applied to the adjacent dermis for 2 hours, in order to remove hair follicles. Tissue was then disinfected using peracetic acid (0.1% v/v) for 3 hours. Next, hypotonic buffer plus proteinase inhibitors (10 mM tris, 2.7mM EDTA,10 $U.ml^{-1}$ aprotinin pH 8.0) was used to lyse the cells and detergent buffer (0.1% (w/v) SDS in hypotonic buffer) to remove cellular fragments[2]. Finally, the dermis was treated with nuclease (Benzonase 10 $U.ml^{-1}$) to remove nucleic acid fragments[2].

Native split-thickness and decellularised porcine skin were analysed using histology (H&E, DAPI and Sirius red Millers stain for elastin and collagen) and immunohistochemistry. The tissues were labelled with antibodies to collagen IV and laminin and the alpha -gal epitope was detected using GSL-1 lectin.

RESULTS: Histological analysis showed that the optimised decellularisation protocol removed all light microscopic evidence of cells, whilst maintaining the structure of the extracellular matrix, including the distribution of elastin fibres.

Subsequent analysis of specific ECM proteins in the decellularised porcine dermis, showed collagen IV was no longer present, but laminin was preserved. Labelling of the alpha-gal epitope indicated that there was residual alpha-gal within the matrix.

DISCUSSION & CONCLUSIONS: It was found that the decellularisation process used for human split-thickness skin was inadequate for decelluarisation of the porcine split-thickness skin[2]. Preliminary studies indicated that it was necessary to include additional steps of hair removal, including trypsin treatment, in order to produce the acellular porcine dermis.

Removal of collagen IV, one of the major components of the basement membrane, is likely to have been caused by peracetic acid disinfection. This has been shown to diminish immunohistochemical staining of collagen IV, following decellularisation of human femoral arteries[4]. Laminin, which is also a component of the basement membrane, did not appear to be affected by the process.

Whether the presence of residual alpha-gal in the matrix would lead to an adverse response to the acellular porcine dermis if used clinically is a matter of conjecture. Recent research has indicated that wound healing may be accelerated by the interaction of non-cellular alpha-gal with anti-alpha-gal antibodies [5].

Further research is required to provide a more detailed characterisation of the decellularised porcine dermis.

ACKNOWLEDGEMENTS: This work was supported by the Wolfson Foundation and Heart Research UK.

Cysts and low subchondral bone mineral density: are they relevant to cartilage damage?

Jing Niu[1], Johann Henckel [2], Alister Hart [2], Maryam Tamaddon[1], Chaozong Liu[1*]

[1] *Institute of Orthopaedic & Musculoskeletal Science, Division of Surgery & Interventional Science, University College London.* [2]*The Royal National Orthopaedic Hospital Stanmore, London*

INTRODUCTION: Osteoarthritis (OA) is a degenerative joint disease, typified by a loss of cartilage and subchondral bone at the interface of a joint. It affects bone cartilage and underlying bone. Mechanically, the underlying bone provides support to the healthy growth of the overlying cartilage. However, with the progress of OA, bone losses and cysts occur in the bone [1] and these would alter the biomechanical behaviour of the joint, and further leading to bone remodelling adversely affect the overlying cartilage. .

METHODS: Human femoral head and femoral condyle were collected during hip or knee replacement operation due to the end stage of osteoarthritis (age 50-70), and the cartilage patches were graded and marked [2]. The samples were preserved in 4% formaldehyde in phosphate buffered saline solution. A volunteer patient, with minor cartilage injury in his left knee while the right knee is intact, was used as control. Peripheral quantitative computed tomography (pQCT) was used to scan the bone. The sagittal and coronal slices were used for vBMD analysis. A 2 x 2 mm area of interest (AOI) was used to determine the volumetric bone mineral density (vBMD) distribution.

RESULTS: The examination of retrieved tissue explants from osteoarthritic patients revealed that patches of cartilage were worn away from the articular surface, and patches of intact cartilage were left (Figure 1(a)). The cysts, ranging from a millimetre to 10mm were existed in all osteoarthritic bones, and were located close to cartilage defects in the weight-bearing regions (Figure 1(b)), and closely associated with the grade of cartilage defect as measured by pQCT. The analysis of volumetric bone mineral density (vBMD) distribution demonstrated that the bones around cysts had much higher vBMD than the trabecular bone away from the cysts. The wall of cysts is formed of cancellous bone, whose trabeculae are reinforced by new bone formation. Compared to the subchondral bone under thicker cartilage, subchondral bone within cartilage defect has higher vBMD. This may result from the mechanical stimulation as a result of bone-bone direct contact with less protection of cartilage in cartilage defect regions.

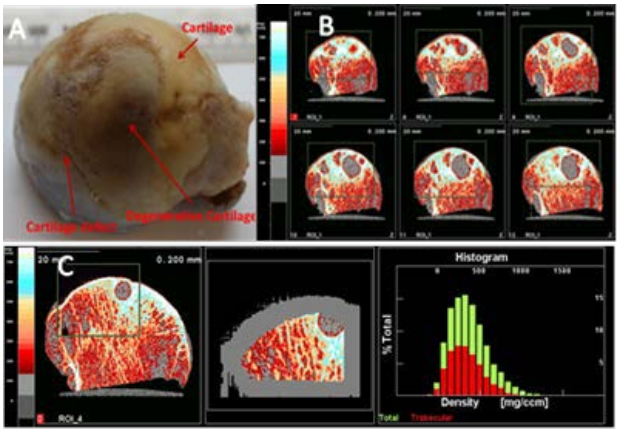

Figure 1: (a) Patches of undamaged cartilage, degenerative cartilage and large cartilage defects were observed (b) pQCT sequential scan revealed large cysts existed in the subchondral bone, and significant bone losses in the peripheral region of cartilage defects, and (c) vBMD distribution within subchondral bone

DISCUSSION & CONCLUSIONS: This study showed an association between cartilage defect and subchondral bone mineral density distribution. Cysts were observed in all osteoarthritic samples and they are located close to cartilage defects in the weight-bearing regions. Cartilage defect altered the loading pattern of the joints, this leading to the bone remodelling and resultant bone structural changes as compared to the normal bone tissues.

ACKNOWLEDGEMENTS: This work was financially supported by The ARUK Proof of Concept Award (grant no: 21160) and Rosetrees Trust (project no: A1184).

Growth by stretch: an interdisciplinary approach to improve current practice

RA Unadkat[1], M Riehle[1], R. Burchmore[2], A. Hart[3]

Centre of Cell Engineering, University of Glasgow, Glasgow, G128QQ

INTRODUCTION: Tissue expansion is a technique used by plastic and restorative surgeons to cause the body to grow additional skin, bone or other tissues. For example, distraction osteogenesis has been widely applied in lower limb surgery (trauma / congenital) and congenital upper limb reconstruction (e.g. radial dysplasia)[1]. This complex and tightly regulated expansion process can thus far only be optimised by long-term animal or human experimentation[1].

Here the intent is to develop an in vitro model of tissue expansion that will allow to optimise the extension regime (µm/h, continuous/ intermittent) and investigate which molecular pathways are involved in its regulation.

METHODS: Cells cultured onto sheets of pre-stretched polymer (PCL) were stretched by 1mm over 24 hours (after reaching confluency) using a stepper motor and various 3D printed and laser cut components. The system utilises plastic flow of the polymer, enabling the material to stay extended upon strain being released. Response of cells was analysed by quantifying nuclei orientation.

Tensile tests were used to determine the Young's Modulus and characterise the polymer's behaviour throughout its stretching range. Digital image correlation (DIC) was used to analyse homogeneity of the strain field.

RESULTS: Mechanical testing results determined that when PCL was spin coated at a weight:weight (wt/wt) ratio of 12% (PCL:chloroform), the material had the ideal stiffness to support fibroblast growth[2].

Nuclei orientation showed a morphological response to strain in comparison to controls which aligned to the direction of pre-stretch. However the stretching regime induced cells to disorientate.

DIC results showed that when the material is stretched in an identical manner to how it was in cell culture experiments, the strain field is inhomogenous

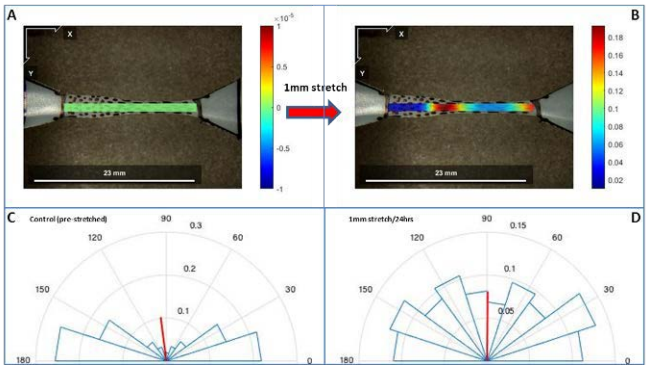

Fig. 1: Inhomogenous strain causes orientated cells to disorientate. A) Pre-stretched PCL. B) Inhomogeneous strain field after 1mm stretch. C) Rose plot indicating cells orientate in direction of pre-stretch (controls). D) Inhomogeneous cell orientation response to further 1mm stretch.

DISCUSSION & CONCLUSIONS: Fibroblasts orient in the direction of stretch when cultured onto pre-stretched PCL substrates; this is likely due to the change in structure of the material where the crystalline structure may develop ridges/microgrooves; this must be further investigated using AFM[3].

Furthermore, cells disorientate after undergoing further substrate stretch of 1mm after culture. This may be due to inhomogeneous strain fields and must also be further investigated using live imaging of focal adhesions.

ACKNOWLEDGEMENTS: Thank you to Dr M Riehle, Dr P Reynolds and R Caudoux for their practical help..

Mesenchymal stem cells differentiate in response to dynamic pressure

J R Henstock[1], JCFA Price[2], A J El Haj[2]

[1] *Institute for Ageing & Chronic Disease, University of Liverpool, UK*

[2] *Institute for Science and Technology in Medicine, University of Keele. UK*

INTRODUCTION: Hydrogel scaffolds provide an ideal culture environment for many cell types, being able to approximate some of the biochemical and structural elements of tissues. However, it can be challenging to provide an appropriate mechanical stimulus to cells in such a soft matrix – although physiological forces are known to be crucial in mediating critical aspects of tissue formation, function, growth and repair [1].

Dynamic hydrostatic pressure has been shown to be an important mechanical stimulus for cells in the body, transducing the compressive loading of bone and cartilage into a change in pressure in the interstitial fluid which can then be detected by cells. In this study, a range of hydrostatic pressure regimes were applied to human mesenchymal stem cells in tissue engineered hydrogels to study the effect of dynamic culture on osteogenesis.

METHODS: Human MSCs were seeded into 3D hydrogel scaffolds and cultured for 28 days in an osteogenic media. Hydrostatic pressure regimes of 0-280 kPa at 0.005 - 1Hz were applied to for 1 hour per day using a custom designed bioreactor (fig. 1) to simulate different types of physiological loading. Bone formation was assessed by weekly X-ray microtomography (μCT) and histology.

RESULTS: Stimulation of the cells with 280kPa cyclic hydrostatic pressure at 1Hz (matched to normal physiological exercise) resulted in up to 75% mineralisation in the hydrogel, whilst static culture, constant high pressure or either low-frequency or low-magnitude stimulation had no effect (<2% mineralisation), fig. 2.

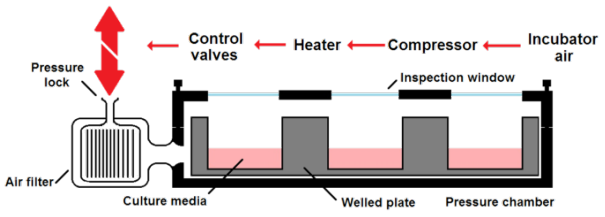

Fig. 1: Incubator air is compressed and directed into a chamber containing the cell-seeded hydrogels in a standard welled culture plate. Dynamic (cyclic) pressures are applied for one hour per day over 28 days.

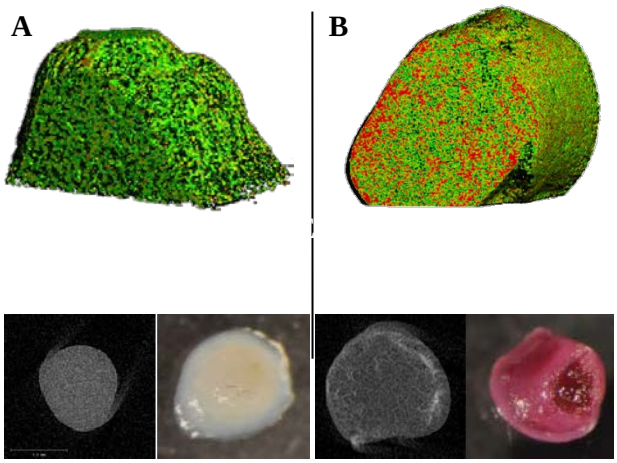

Fig. 2: Comparison of cell-seeded hydrogels after 28 days in either static culture (left) or stimulated (right). μCT reconstructions (A&B) show bone formation in red within the low-density green hydrogel. Mineralisation is also visible in 2D X-ray (C&E) and alizarin red staining (D&F).

DISCUSSION & CONCLUSIONS: These results suggest that dynamic hydrostatic pressure is a potent stimulus in MSC differentiation and cells may be primed to respond to loading forces within a specific physiological range [2].

As tissue engineering strategies are now entering clinical translation, understanding how physiological loading forces interact with, drive and direct tissue growth will be fundamental to optimising treatments. Appropriate mechanical signals are an essential component in recreating tissue environments and translating *in vitro* regenerative medicine into clinical treatments.

ACKNOWLEDGEMENTS: This work was supported by the BBSRC (sLoLa grant). We would like to thank our collaborators in groups led by Prof. R. Oreffo, Prof. K. Shakesheff and Prof. M. Stevens for their contributions to this project.

Nanofabricated cell culture surfaces to control self-renewal and differentiation of mesenchymal stem cells

J Zabala Mancebo[1], LS Wong[2], JA Hunt[3], JM Curran[4], SM Richardson[1]

[1] *Institute of Inflammation and Repair, Univ. of Manchester, UK.* [2] *School of Chemistry, Univ. of Manchester, UK.* [3] *Institute of Ageing and Chronic Disease, Univ. of Liverpool, UK.* [4] *School of Engineering, Univ. of Liverpool, UK*

INTRODUCTION: Mesenchymal stem cells (MSCs) have been proposed as a promising cell source for cartilage tissue engineering as they can differentiate towards the chondrogenic lineage. Up until now, MSC chondrogenesis has been achieved by using 3D cultures supplemented with bioactive substances (e.g. TGF-β), which can also act as limiting factors when larger cultures are needed. With these limitations in mind, material induced control of cell responses via control of initial cell adhesion is a promising tool [1]. For this to be effective the materials must provide a controlled stimuli at the sub-micron scale to effectively control integrin and focal adhesion formation.

The overall aim of this work is to generate surfaces with defined chemical features and associated nanotopographical profiles by varying the chain length of a silane used in the production of a self-assembled monolayer (SAM) and, assess their effect on MSC self-renewal and differentiation.

METHODS: High purity CH_3 alkylsilanes were purchased from Sigma-Aldrich. In particular, Dichloro-dimethyl-silane (DMDCS), Chloro-dimethyl-octylsilane (ODMCS), Chloro-trimethyl-silane (TMCS), Chloro-dimethyl-octadecylsilane (ODDMCS) and Chloro-methyldiphenylsilane (DPMCS) were coated onto 0.13mm Si coverslips. Coverslips were thoroughly cleaned with dH_2O and immersed in a 5% NaOH solution for 20 minutes. Once the reaction was complete, cover slips were immersed in 68% nitric acid for 15 minutes in the sonicator, after which cover slips were rinsed with dH_2O. A specific solution was prepared for each of the alkysilanes. In particular, a 95% 2-propanol, 0.5% dH_2O and 2% alkylsilane was used so that samples were exposed to the specific solutions for 2.5 hours. After that, cover slips were cleaned with 2-propanol and ethanol.

The hydrophilic nature of all surfaces was analysed using contact angle measurements and the alkylsilane coverage and roughness of the cover slips was assessed by atomic force microscopy in tapping mode.

Cartilage tissue was obtained from three different patients undergoing hip replacement surgery. Cell metabolic activity was assessed by Alamar Blue and PicoGreen on days 1 and 7 after seeding on SAM surfaces at 50000 cells/ml. The expression of Sox9, aggrecan, collagen type 1 and 2 was determined quantitatively by RT-qPCR at day 14 and qualitatively by immunofluorescence at day 21. In a similar way, cell morphology was assessed by DAPI and phalloidin staining.

RESULTS: SAM characterisation demonstrated subtle differences in dynamic contact angle and surface roughness. Although surfaces did not show any statistical significance in cell viability or morphology, PCR results demonstrated that ODDMCS induced the highest chondrogenic marker gene expression. Morphology wise, chondrocytes exhibited differences in cell shape depending on which SAM they were cultured on.

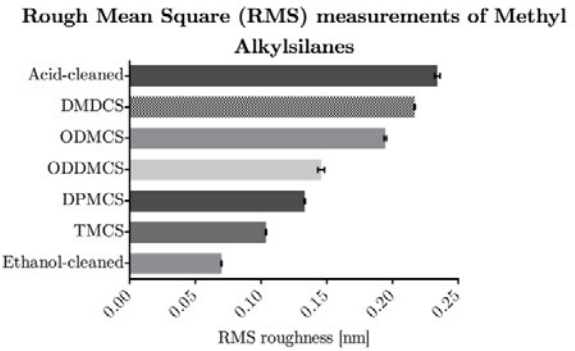

Fig. 1: AFM roughness measurements performed on different alkylsilane SAMs.

DISCUSSION & CONCLUSIONS: While a single optimal surface chemistry was not identified from this part of the study, the cell compatibility and influence on phenotype of the surfaces allows experiments to be initiated to assess how OH and NH_2 modified surfaces affect human MSC responses and whether alkylsilanes are able to induce MSC chondrogenesis.

Aerosol Jetting of Conductive Polymer Coatings for Neuronal Stimulation

A.J.Capel[1], M.Smith[3], M.Haghighi-Abyaneh[3], R.W.Kay[3], R.A.Harris[3], S.D.R Christie[2] and M.P. Lewis[2],

[1] *School of Sport, Health and Exercise Sciences,* [2]*Department of Chemistry Loughborough University, LE11 3TU,* [3]*Faculty of Engineering, University of Leeds, LS2 9JT.*

INTRODUCTION:

The physical topography and chemical properties of a material can promote a diverse range of cellular responses, with particular interest being shown by tissue and cell engineering research groups in the control of neuronal outgrowth. Precise control over neuronal outgrowth could allow the development of highly structured neurological bio-devices that are an accurate representation of the in vivo environment. Significant research has therefore been dedicated to the generation of bespoke materials that facilitate control over neuronal growth (Garcı et al. 2006). Of particular interest are a range of electrically conductive polymers including materials such as poly (3,4-ethylenedioxythiophene) polystyrene sulfonate (PEDOT) (Balint et al. 2014). Electrical stimulation can play an important role in the stimulation of both the proliferation and differentiation of neuronal cells (Langer et al. 1997). This research outlines the use of a novel aerosol jetting process that allowed the deposition of micron-sized tracks of this conductive polymer onto a glass substrate. These conductive tracks could be implemented to electrically and topographically control the growth of neuronal cells cultured onto the substrate.

METHODS:

PEDOT:PSS was patterned onto clean glass slides (piranha solution, DI water, acetone and methanol wash) via aerosol jetting. The patterns were oven baked onto the slides at 150 °C for 60 minutes. The cross-sectional area of the tracks was determined via non-contact scanning topography. SHSY-5Y cells, human derived neuroblastomas, were cultured onto the PEDOT formulation for 24 hours in growth media (GM), followed by 5 days in differentiation media (DM), with neurite extension being measured at 1, 3 and 5 days in DM.

RESULTS:

All PEDOT:PSS patterns produced via aerosol jetting were between 70-80 µm in diameter and approximately 2-4 µm in depth. These tracks also proved to be highly electrically conductive.

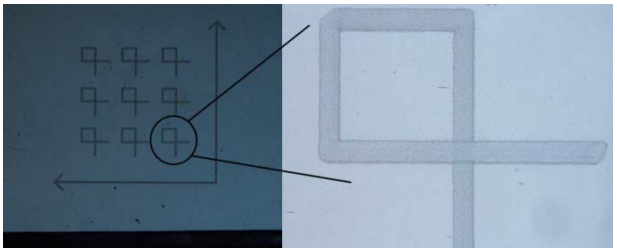

Fig. 1: Images of 75 µm PEDOT:PSS patterns.

The PEDOT:PSS material also proved to be a material which facilitated neuronal growth and promoted neurite extension, with an average neurite length in excess of 45 µm after 5 days of culture in DM.

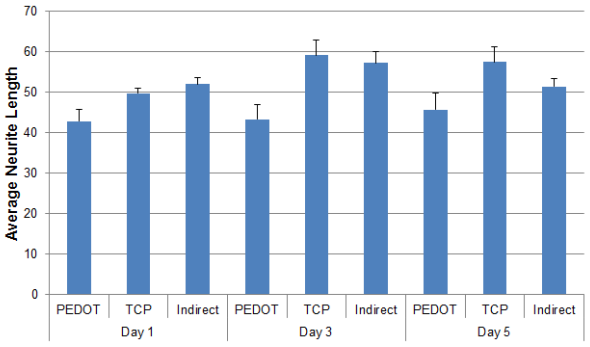

Fig. 2: Average neurite length of SHSY-5Y cells on PEDOT:PSS patterned onto glass.

DISCUSSION & CONCLUSIONS:

The topographical and electrically conductive patterns produced via aerosol jetting could be used to discretely manipulate neuronal behaviour. Future work will aim to determine if neuronal networks and interfaces can be created through electrical stimulation.

ACKNOWLEDGEMENTS: Thanks to EPSRC for supporting this project.

Characterising the enhanced intracellular delivery of Magnetic Nanoparticles by GET

Lia Andrea Blokpoel Ferreras, Kevin M. Shakesheff and James E. Dixon

Wolfson Centre for Stem Cells, Tissue Engineering, and Modelling (STEM), Centre of Biomolecular Sciences, School of Pharmacy, University of Nottingham, Nottingham, NG7 2RD, UK.

INTRODUCTION: Magnetic nanoparticles small size enables them to interact at cellular and molecular levels. Furthermore, their paramagnetic properties make them suitable for manipulation through a magnetic field opening a whole range of different applications in biomedicine including cell tracking, cell labelling, hyperthermia or drug delivery (1). GET (GAG-binding enhanced transduction) system is based on a novel fusion protein that couples a membrane docking peptide to heparan sulphate glycosaminoglycans (GAGs) with a Protein Transduction Domain (PTD) and has been previously reported to improve delivery of different cargoes into cells (2).

METHODS: Recombinant GET proteins were expressed and purified as previously described (2). The particles used were dextran coated Nanomag®-D MNPs (Fe3O4 core; 250nm; Micromod). MNP delivery to NIH 3t3s was evaluated by Prussian blue staining using a Nikon Eclipse TS1000 light microscope and by TEM analysis using a Tecnai G12 Biotwin run at 100Kv. Zeta potential and charge were measured on a Malvern Zeta Nano ZS.

RESULTS: GET significantly enhances delivery of MNPs to cells compared to passive uptake. TEM analysis shows localization of MNP in endosomes. When the complex MNP-GET is incubated in water the overall charge is positive, in the presence of foetal calf serum (FCS) the complex charge is negative.

DISCUSSION & CONCLUSIONS: We have demonstrated that GET enhances MNP uptake on NIH 3t3s in vitro. The localization of MNP in the endosomes suggests that particle uptake with GET occurs through endocytosis, as it has previously been reported for GET protein (2). Finally, zeta sizer analysis reports changes in the protein and the particles respectively when they are incubated together, suggesting strong interactions between GET and MNP. We have also demonstrated that biological fluids alter the physical properties of the GET-MNP system but these alterations don't affect the delivery capacity of our system.

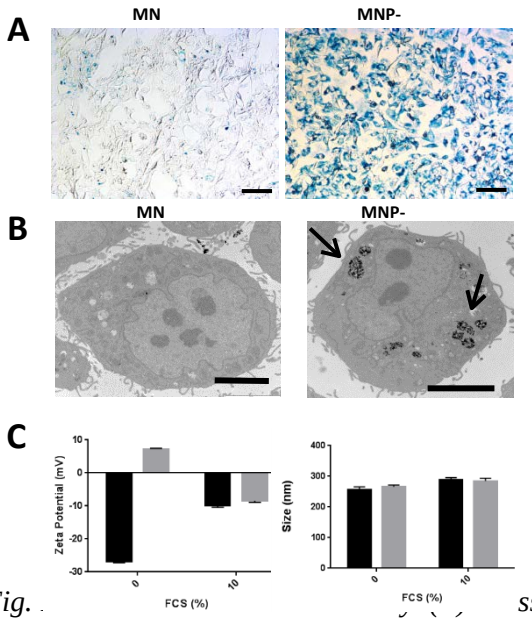

Fig. . ssian Blue staining of MNP delivered to NIH 3t3s with and without GET, scale bar20 µm; n=1.(B) TEM images of NIH 3t3s incubated with MNP with and without GET, scale bar5 µm; n=1. (C) Zeta potential and size changes in MNP (black) when incubated with GET (grey) in water and 10% FCS.

ACKNOWLEDGEMENTS: We would like to thank Denise McLean and the Advance Microscopy Unit in Queens Medical Centre for their invaluable help with the TEM imaging.

Study on suitable contrasting agents to resolve murine tendon internal structure with microCT

A Fotticchia[1], R Wong[2], LA Bosworth[1], J Wong[2], S Cartmell[1]

[1] *School of materials, The University of Manchester, UK.* [2] *Institute of Inflammation and Repair, The University of Manchester, UK*

INTRODUCTION: Microscopic computed tomography (µCT) is an imaging tool that can be useful for the analysis of the structure of materials of biological origin. µCT is based on the irradiation of the sample with an x-ray beam, which intensity, upon passing through the sample, is attenuated depending on the material atomic number. Mineralised biological tissues (e.g. bones) can be easily scanned due to the presence of relatively high atomic number elements. Different staining solutions have been developed to enhance soft tissue contrast based on Iodine, Tungsten and Osmium [1]. Here we present different staining protocols that allow us to considerably improve tendon 3D reconstruction.

METHODS: A device able to keep a humidified environment during scanning was designed, otherwise artefacts are formed due to tissue water evaporation that causes sample movement. Acquisition took place using a Xradia microXCT-400 system at 10x objective for approximately 9 hours, source distance at 40mm, detector distance at 6mm, source voltage of 40kV, 10W, exposure time of 25s, bin 1 with 901 radiographs taken over 182 degrees (pixel size of 1.2µm, giving an effective resolution of 3µm). Tendons treated with two different staining agents were compared. Fixation took place by 48h soaking in zinc fixative solution. 1% phosphotungstic acid (PTA) or 2% osmium tetroxide (OSO_4) were adopted as contrasting agents by tendon immersion for 30'. Using these two contrasting agents an in-vivo injury model was studied. A 3x1x1 mm^3 window was cut in mouse flexor digitorum longus tendon and a polycaprolactone (PCL) nanofibrous scaffold implanted [2]. Excised tendons were subsequently fixed, stained and scanned as described above.

RESULTS: Scanning of the non-fixed and non-stained tendon returned only sample shape and size but could not resolve the inner structure (Fig. 1). Instead, 1% PTA and 2% OSO_4 allowed resolution of the tissue; however it was found that cellular material could be more easily identified in 2% OSO_4 stained samples compared with those stained with 1% PTA (Fig. 2).

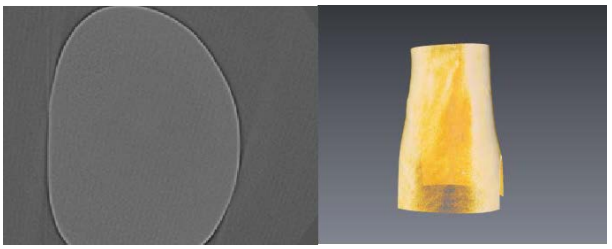

Fig. 1: Scanning of non-fixed and non-stained tendon. Left: orthogonal section; right: 3D reconstruction.

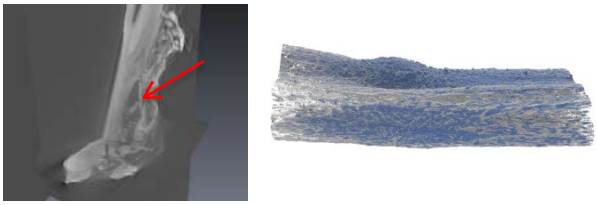

Fig. 2: Left: 1% PTA stained tendon with PCL scaffold (red arrow); right: PCL scaffold stained with 2% OSO_4 surrounded by cells (blue).

DISCUSSION & CONCLUSIONS: Despite the usage of a humidified microenvironment it is evident that architecture fixation and staining are necessary for resolution of the tendon. Both 1% PTA and 2% OSO_4 contrasting agents allowed clear reconstruction of the 3D tendon structure; however only with 2% OSO_4, which binds to cell membrane fatty acids, cell material could be detected. Further optimisation of the staining protocols presented here, in conjunction with a higher resolution apparatus [3], will provide a valuable tool to study tendon architecture, scaffold integration and cell infiltration.

ACKNOWLEDGEMENTS: This research could be carried out thanks to G1000788 and MR/M007642/1 MRC grants. The authors also want to acknowledge the Manchester X-ray Imaging Facility for their support.

Neuronal wiring *in vitro*: Chemical patterns for neuronal guidance

M.M. Pardo-Figuerez[1, 2], N.R.W. Martin[1], D.J. Player[1], A.J. Capel[1, 2], S.D.R. Christie[2] and M.P. Lewis[1]

[1] *School of Sport, Health and Exercise Sciences*
[2]*Department of Chemistry, School of Science*
Loughborough University, Loughborough, LE11 3TU

INTRODUCTION: There is an increasing need to develop accurate models that underpin functional neuronal wiring in *vitro*, in order to obtain novel bio-devices with a controlled neuronal organisation. Current methods in culture are limited by the lack of representation of the neuronal network, where the uncontrolled spreading of neurites prevents a non-accurate representation of the *in vivo* environment[1]. Improving the surface characteristics of the cultured material using e.g. surface chemistry, could solve this problem. Neurons are known to be influenced by their surroundings, indicating a strong crosstalk at the cell-material interface[2]. In addition, surface chemistry can be patterned, obtaining systems where cells could be placed in specific locations at specific sizes, guiding them into restricted pathways to reach particular targets[2]. We aimed to pattern neuronal cells by chemically modifying the surface in order to achieve a precise control over neurite directionality. In the long term, patterned neurons could be incorporated at the interface of biological devices, to significantly improve their functionality.

METHODS: PKSPMA brushes (poly (potassium 3-sulfopropyl methacrylate) were patterned on glass slides using photolithography. Photoresist SU1813 was spin coated onto glass slides, UV exposed, developed and finally hard baked. The areas with no photoresist were backfilled by attaching PKSPMA brushes by ATRP *grafting from* process. For cell biology experiments, SH-SY5Y human neuroblastoma cells were cultured at different cell densities (5,000, 10,000 and 15,000 cells/cm^2) for 3 days in growth media (GM), followed by 3 days in differentiation media (consisting of GM with 10 µM of *all trans* retinoic acid) to promote neurite outgrowth. To study the effect of cell confinement at different cell density we measured nuclei alignment, percentage of cells generating neurites and pattern efficiency.

RESULTS: SH-SY5Y neural cells were cultured on different channel sizes (20, 50, 75 and 100 µm) and at various cell densities. Results suggested that both factors (cell density and channel width) played an important role in alignment, confinement and in promoting neurite outgrowth. Channels with low and medium cell density showed good alignment along the channel sizes and a higher number of cells exhibiting neurites for the smallest channel width (20µm). Patterns at higher densities resulted in less nuclei alignment and a decrease in cell confinement due to the channel patterns becoming filled by multiple cells at the early stage of the culture. The reduction in channel width also resulted in a lack of cell spreading, obtaining a precise arrangement of SH-SY5Y along the axis of the smallest channels (*Figure 1*).

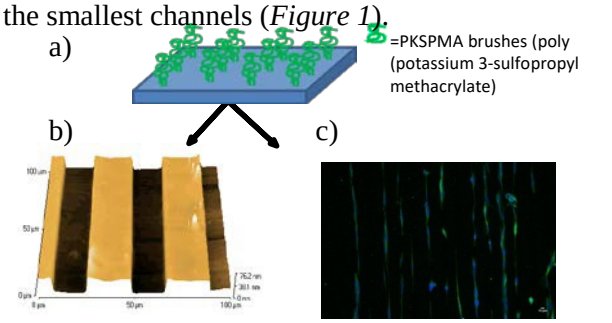

Fig. 1: a) Patterned polymer brush via photolithography. b) 3D AFM image of the pattern c) SH-SY5Y patterned at a density of 10,000 cells/cm^2 on 20 µm channel (Scale bar=10 µm).

DISCUSSION & CONCLUSIONS: Using patterning methods allows the control of chemical cues in a manner where cells can be manipulated and constrained to guide them in a specific direction and thus towards specific targets. The ability to obtain specific neurite orientation is an important factor in neuronal co-cultures when attempting to create organotypic culture systems such as the peripheral nervous system and muscle cells.

ACKNOWLEDGEMENTS: Thanks to Loughborough University and to the mini-CDT Smart Prosthetics group for their support.

Neutron diffraction to determine the short range order of strontium apatite-wollastonite bioactive glass

R. Hollings[1], Y. Hancock[2], D. J. Wood[3], A. C. Hannon[4], P. G. Genever[1], R. A. Martin[5]

[1] Department of Biology, University of York. [2] Department of Physics, University of York,[3] Department of Oral Biology, School of Dentistry, University of Leeds, [4]ISIS Facility, Rutherford Appleton Laboratory,[5] Aston Materials Centre, School of Engineering and Applied Science & Aston Research Centre for Healthy Ageing, University of Aston

INTRODUCTION: We have developed a series of novel Apatite-Wollastonite Glass Ceramics with increasing substitution of strontium (Sr) for calcium (SrAW-GC), intended for bone regeneration due to the material's strength and bioactivity[1]. Sr is osteoinductive, antimicrobial and preferentially locates to new bone forming sites, but controlled release is needed, as an excess of Sr is cytotoxic. Human mesenchymal stromal cells (MSCs) readily attach, proliferate and undergo osteogenic differentiation on SrAW-GC, with dissolution considered the primary mechanism of bioactivity, although it is not understood how the addition of Sr affects this. Neutron diffraction (ND) and a suite of complementary techniques were used to assess the effect of strontium content on the short range order of the SrAW glass, which cannot be determined *a priori*, and which may affect how the material responds to physiological environments, such as its dissolution rate.

METHODS: Six SrAW glass compositions with increasing strontium for calcium substitution were made using melt-quench (0, 6.2, 12.5, 18.7, 24.9 and 37.4 Mol% Sr), and were analysed using ND (GEM instrument, ISIS, Rutherford Appleton Laboratory), solid state MAS-NMR and Raman spectroscopy. Isomorphic substitution based analysis[2] alongside the MAS-NMR and Raman data and NXFit software[3] were used to deconvolute the ND signal. The release of Si, Ca, Sr, Mg and P from the glass after 24 hours of mixing in cell culture medium was measured using inductively coupled plasma optical emission spectroscopy (ICP-OES), with comparison to known standards.

RESULTS: The ND data indicated that the atomic separation (distance between atoms) and coordination number (amount of these atomic separations) did not change with strontium content, except for the proportional changes in the coordination numbers associated with the Sr and Ca contents (Fig. 1). The strontium ions released into the medium were found to be proportional to the Sr concentration in the glass, coinciding with a marked drop in Ca (and small drop in Mg), whilst the release of the other elements was comparatively unchanged with Sr (Fig. 2).

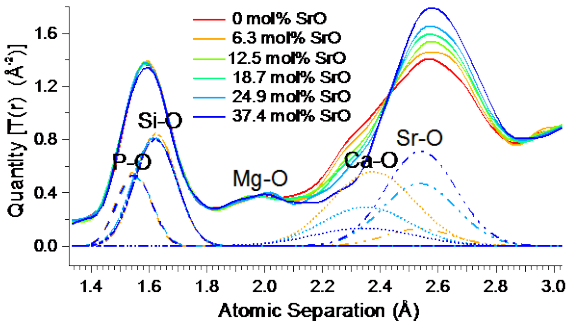

Fig. 1: Atomic separations measured by ND for different SrAW compositions. The deconvoluted peaks for key atomic separations and compositions are shown by the dotted curves.

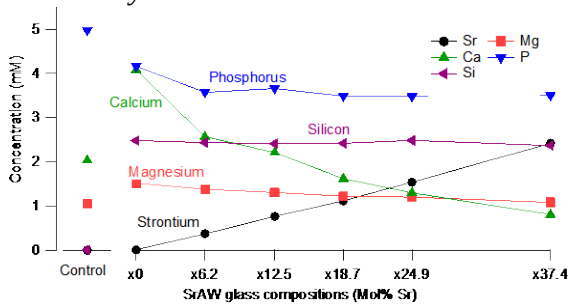

Fig. 2: Ion concentrations in the SrAW conditioned medium compared to the control medium.

DISCUSSION & CONCLUSIONS: The similarity of the atomic spacings determined for the different compositions indicate Sr substitutes directly for the modifier Ca in the glass, leaving the rest of the network unaffected. Consequently, the dissolution rates and products of the different glass compositions glasses are similar, with the differing Sr and Ca release with increasing Sr content proportionate to the amount of these elements in the glasses. Thus, potentially the addition of Sr does not compromise the dissolution, mechanical properties or bioactivity of the material, whilst offering bone regenerative effects, indicating SrAW-GC as a promising repair scaffold in orthopaedics.

Bioengineering a 3-D nerve conduit to enhance nerve regeneration

SE Thomson[1,2], C Charalambous[1], M Syntouka[1], R Wallace[3], B Nottelet[4], AM Hart[1,2], PJ Kingham[5], MO Riehle[1]. University of Glasgow [2]Canniesburn Plastic Surgery Unit, Glasgow Royal Infirmary, UK, [3]University of Edinburgh, [4]University of Montpellier, [5]Umeå University

INTRODUCTION: Peripheral nerve injury is common. Despite demonstrating regenerative potential healing is slow and often incomplete, conferring significant cost to the individual and society (1). There is a clear need to address the injury at the molecular level (1). Significant developments have been made *in vitro* and *in vivo* demonstrating the importance of topographical cues (2), provision of neurotrophic factors by supplementing support cells at the injury site (3) and pharmacological modulation (1). This study investigates the mechanism of action of these external cues and incorporates them into an optimised design specification of a bioengineered nerve construct to enhance nerve regeneration.

METHODS: *Topographically patterned polymer fabrication* Poly-caprolactone (PCL) scaffolds with refined topographical features were fabricated by adapted spin coating processes and rolled to form 3-D constructs.

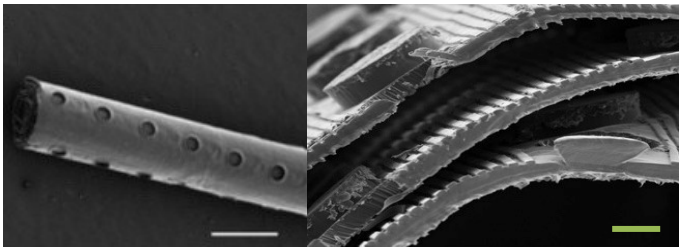

Fig. 1: SEM PCL nerve conduit SB 500µm/100µm

PCL was rendered radio-opaque through chemical modification with trioodobenzoate moieties (4).

Cell isolation and culture Dorsal root ganglion (DRG) organotypic explant model was used to assess the downstream effects of topography..DRGs were harvested from 2-day old Sprague Dawley (SD) neonates. Adipose derived stem cells (ADSC) were harvested from adult SD rats and differentiated towards a glial lineage as previously described (3).

Multimodal analysis The impact of topographical cues on neurite outgrowth and ADSC differentiation and function was measured. Target gene expression was quantified using qRT-PCR. Immunohistochemistry was used for protein localisation and In Cell Western for quantification. Phosphorylation assays and pharmacological inhibition were used to further interrogate pathways. ELISA quantified neurotrophic factors in ADSC supernatant. Neurite outgrowth, ADSC alignment and quantitative analysis of expression of glial markers was analysed using Fiji software. Non-destructive micro CT 3-D imaging of neural tissue within nerve conduits was performed (Skyscan 1072).

RESULTS: Topographical cues resulted in highly directed outgrowth and potentiated neurite extension from day 3 onwards (Fig 2).

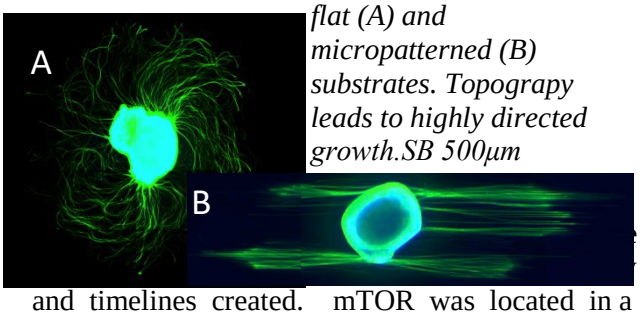

Fig. 2: Neurite outgrowth at 3 days on flat (A) and micropatterned (B) substrates. Topograpy leads to highly directed growth.SB 500µm

and timelines created. mTOR was located in a punctate manner along neurites and within support cells. Phosphorylation assays highlighted specific targets downstream of mTOR for future therapeutic manipulation. dADSCs adhered to, proliferated on and maintained expression of glial markers/neurotrophic factor secretion on topography. Topographical cues increased alignment of ADSC and promoted differentiation. microCT scans provided high resolution 3D reconstructions to assess neural tissue within the conduit.

DISCUSSION & CONCLUSIONS: Detail on the downstream molecular responses to topography are presented, highlighting potential therapeutic targets. Future work will assess the optimised conduit in an adult rat sciatic nerve model in order to progress towards clinical translation.

ACKNOWLEDGEMENTS: *We would like to thank the Medical Research Council (L017741/1).*

Directed differentiation of human mesenchymal stem cells by delivering transcription factors using GET system

L Thiagarajan[1], K M Shakesheff[1], J E Dixon[1]

[1] *Wolfson centre for Stem Cells Tissue Engineering, and Modelling (STEM), Centre of Biomolecular Sciences, School of Pharmacy, University of Nottingham, Nottingham, NG7 2RD, UK*

INTRODUCTION: Mesenchymal stem cells (MSCs) with their tri-lineage differentiation potential have tremendous scope in tissue engineering. Currently there are two challenges in directed differentiation of MSCs for therapeutic applications. Firstly, MSCs are difficult to transfect; both viral-mediated and lipid-mediated transfection systems have been proved inapplicable for therapy due to virus-based health risk and low efficiency in vivo respectively. Secondly, the predominant strategy to achieve directed osteogenic differentiation is the use of chemical induction or exogenous growth factors or hormones, all of which may elicit non-specific, pleiotropic effects on untargeted cells. Here, we overcame these challenges by the use of transcription factors (TFs) as they play very distinct, stage specific roles in differentiation pathways and these TFs are delivered using a peptide based intracellular delivery system developed in house called GAG-binding enhanced transduction (GET) system (1).

METHODS: We developed GET-fusion proteins using GET peptides (P21, 8R) and osteogenic transcription factors, (osteo-inductive RUNX2 and osteo-inhibitory RUNT) for better intracellular delivery. Primary MSCs from two different donors were used in this study. Transcriptional activity of P21-RUNX2-8R was assessed using a luciferase based OC promoter reporter gene (2). Osteogenic differentiation after protein delivery was assessed at different stages by the following assays – flow cytometric evaluation of stem cell markers; relative gene expression of early, intermediate and late markers; immunostaining for Osteocalcin and subsequent quantification; matrix mineralization quantification. The results were compared with conventional osteogenic differentiation methods such as use of Dexamethasone or BMP2.

RESULTS: After optimizing dosage, we observed significant upregulation and downregulation of osteogenesis related genes in hMSCs transduced with either P21-RUNX2-8R or P21-RUNT-8R. Expression of mesenchymal stem cell markers significantly reduced one week after the delivery of P21-RUNX2-8R, indicating commitment to differentiation.

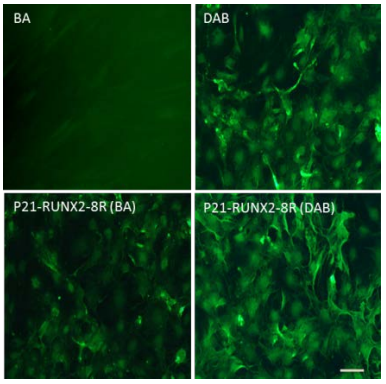

Fig. 1: hMSCs expressing osteocalcin after P21-RUNX2-8R (30µg/ml - twice) delivery. The cells were cultured with beta-glycerophosphate (10mM) and ascorbic acid (50µg/ml) for 3 weeks after protein delivery (BA). The cells were compared with dexamethasone (100nM) induced osteogenesis (DAB).

DISCUSSION & CONCLUSIONS: The GET peptides significantly increased the delivery. The delivered transcription factor, RUNX2 retained their transcriptional activity and significantly increased the expression of osteogenesis related genes during the early and intermediate stages of differentiation. Use of transcription factors and peptide based delivery system provide better control over directed differentiation and can be manipulated for controlled release in vivo.

ACKNOWLEDGEMENTS: The research leading to these results has received funding from the Medical Research Council, the Engineering and Physical Sciences Research Council, and the Biotechnology and Biological Sciences Research Council UK Regenerative Medicine Platform Hub "Acellular Approaches for Therapeutic Delivery".

3D printed PLA/collagen hybrid scaffolds for bone-cartilage interface tissue engineering

M Tamaddon[1], G Blunn[1], C Liu[1*]

[1] *Institute of Orthopaedic & Musculoskeletal Science, Division of Surgery & Interventional Science, University College London, Royal National Orthopaedic Hospital, Stanmore HA7 4LP*

INTRODUCTION: The bone–cartilage interface in an articulating joint is a biomechanically important region where calcified cartilage forms an intersection between the hyaline cartilage and subchondral bone. It is prone to fracture and may undergo abnormal thickening, which can lead to progression of osteoarthritis[1]. A biologically and mechanically stable bone-cartilage interface as part of an osteochondral scaffold can thus have considerable clinical relevance. In this study, we have reported on a porous 3D printed polylactic acid (PLA)/collagen hybrid scaffold as a junction between bone-cartilage and preliminary *in vitro* evaluation results such as biocompatibility and mechanical properties are presented.

METHODS: The PLA biopolymer scaffold was fabricated by a 3D printing technique that runs on fused deposition modelling (FDM) technology by heating and extruding thermoplastic filament. The scaffold has a unit cell size of 0.5 mm. The PLA scaffold was subjected to 10 minutes UV processing in a UV/ozone reactor to improve its surface wettability. Then, collagen was filtered into the porous structure to obtain PLA/collagen hybrid scaffold. Sheep bone marrow mesenchymal stem cells (BMMSCs) were used to assess the cell morphology, viability, proliferation and differentiation on these PLA/collagen scaffolds. Live/Dead and Alamar Blue assays were used to examine viability and proliferation. Scanning electron microscopy (SEM) and immunostaining were used to look at cell morphology. Osteogenic and chondrogenic differentiation of BMMSCs were also investigated. The mechanical stability of scaffolds was evaluated using compression testing.

RESULTS: It was shown that the 3D printed PLA scaffolds support cell viability (Fig.1) and proliferation throughout 28 days. The design of the scaffold affected cell attachment and proliferation. Well-developed actin cytoskeleton was shown by immunostaining, and cell spreading was confirmed by SEM (Fig.1). It was also confirmed that the scaffolds supported osteogenic and chondrogenic differentiation of BMMSCs. Compressive modulus and strengths of these scaffolds were 11MPa and 3.4MPa, respectively.

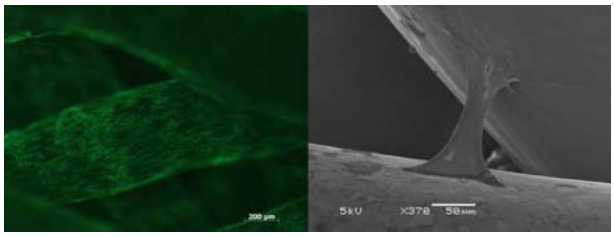

Fig. 1: Biocompatibility of the developed PLA hybrid scaffolds: Live/Dead assay - green shows viability of cells on day 14 (left); SEM micrograph shows cell bridging between two layers of the 3D printed scaffold (right)

DISCUSSION & CONCLUSIONS: It has been shown that the developed 3D printed PLA hybrid scaffolds have the potential to be used for bone-cartilage interface tissue engineering. They are biocompatible, with the potential to provide substrate for chondro- and osteogenic differentiation of stem cells. These scaffolds can be produced inexpensively and be tailored specifically to patients.

ACKNOWLEDGEMENTS: This work was supported by The ARUK Proof of Concept Award (grant no: 21160), and EPSRC MeDe Innovation (grant No: 103516).

Development of a novel notochordal cell culture system for long term in vitro population expansion and survival

MD Humphreys, SM Richardson, JA Hoyland

Centre For Tissue Injury and Repair, Institute of Inflammation and Repair, Faculty of Medical and Human Sciences, University of Manchester, Manchester

INTRODUCTION: Degeneration of the intervertebral disc has been implicated as a major contributor to chronic lower back pain. However, current therapies are ineffective and this has led to a focus on novel cell based therapies. The nucleus pulposus is the region most affected by degeneration and is derived from the notochord. Notochordal cells are lost with maturity; this is thought to be linked with the onset of degeneration. As such, notochordal cells may have potential in regenerative therapies [1]. Currently, notochordal cell phenotype and suitable culture conditions for research or therapeutic use are poorly described. This project aims to improve the characterisation of notochordal cell phenotype and to develop a suitable culture system to enable comprehensive study.

METHODS: Porcine notochordal cells were isolated from 6 week post-natal discs using enzymatic digestion and cultured *in vitro* on laminin-521, fibronectin, gelatin and untreated tissue culture plastic for 14 days in DMEM and αMEM media. Notochordal cells were also cultured in alginate beads, the current gold standard. Adherence, cell viability, morphology and expression of known notochordal markers (CD24, KRT8, KRT18, KRT19 and T) were assessed throughout the culture period.

RESULTS: Media choice and surface coating was shown to influence adherence, viability, morphology and phenotype of porcine notochordal cells. The greatest adherence, proliferation and viability of notochordal cells were observed in cultures using αMEM media, and those on laminin-521 and fibronectin coated surfaces. Notochordal cultures on laminin-521 coated surfaces in αMEM media retained notochordal morphology for the longest period of the 2D culture surfaces, while cultures in alginate beads retained morphology throughout. Alginate bead culture displayed no significant proliferation. Gene expression patterns were similar between alginate bead, laminin-521 and fibronectin cultures in both cell media.

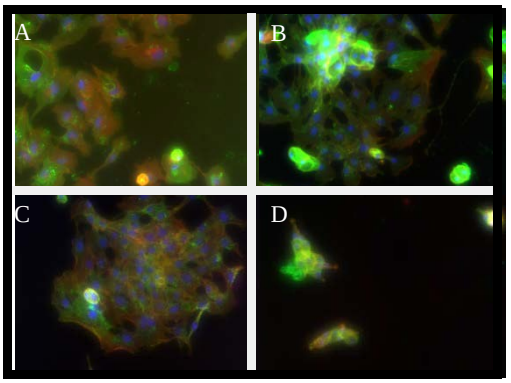

Figure 1: *Notochordal cell morphology following culture on laminin-521 (A), fibronectin (B), Gelatin (C) and untreated (D) surfaces in αMEM media.*

DISCUSSION & CONCLUSIONS: Notochordal cultures on laminin-521 coated surfaces and in αMEM media produce more favourable conditions for expansion and maintenance of phenotype in 2D *in vitro* culture. This population expansion and the comparative retention of gene expression of known notochordal markers suggests that, with further refinement, 2D culture may provide a more applicable culture system than alginate bead culture. Optimisation of this culture system will be followed by use of human notochordal cells in this system.

ACKNOWLEDGEMENTS: Funding Provided by the Henry Smith Charity. Porcine samples provided by Dr Norman Henry.

Tagging mechanoreceptors for promoting chondrogenesis

NC Foster[1], H Markides[1], E Hassan[1], AJ El Haj[1]

[1] *Institute of Science and Technology in Medicine, Guy Hilton Research Centre, Keele University*

INTRODUCTION: Owing to the high incidence of diseases such as osteoarthritis, combined with the poor regenerative capacity of native cartilage, there is a huge clinical demand for effective cell therapies which can improve cartilage repair. Our group has shown the importance of mechanical cues for the development of healthy tissues such as bone and cartilage in vivo. Tissue engineered constructs have been shown to respond positively to culture regimes that mimic some of these physiological stimuli [1]. Cell surface receptors such as integrins and ion channels, such as TREK type potassium channels act as mechano-transducers of mechanical stimuli and their activation initiates signalling cascades which may ultimately affect cell fate [2,3].

METHODS: Mesenchymal stem cells were isolated from bone marrow taken from 2 ovine donors. Magnetic nanoparticles (MNP) labelled with either TREK-1 or RGD binding motifs (Figure 1) were bound to the isolated and characterised MSCs. MNP-labelled cells were pelleted and cultured in either chondrogenic or basic media for 21 days and stimulated with a magnetic force bioreactor (MFB) for 1 hour/day, 5 days/week. Pellets were then digested with proteinase K and GAG content was determined using DMMB assay (normalised to DNA content via PicoGreen assay). In order to visualise levels of chondrogenesis, pellets were dehydrated, embedded in paraffin, sectioned and stained with Toluidine Blue, Alcian Blue and PicroSirius Red.

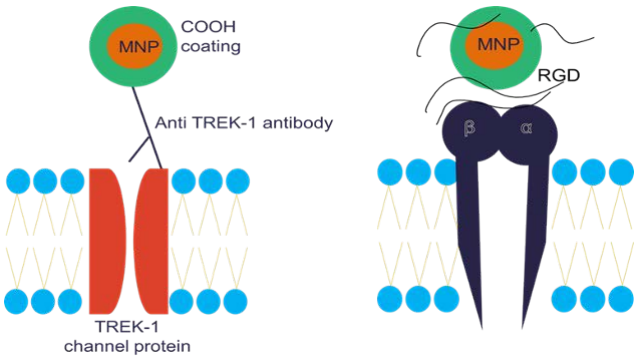

Fig. 1: Labelling cells with MNPs - MNP attached to either TREK-1 channel proteins via anti TREK-1 antibody (left) or integrins via RGD molecules (right)

RESULTS: As expected, markers of chondrogenesis are observed in all pellets cultured in chondrogenic media (Figure 2). However, enhanced staining patterns are evident in pellets with tagged and activated mechanoreceptors, suggesting higher levels of GAG production in these two groups. Quantitation of the GAG levels using the DMMB assay showed a similar trend.

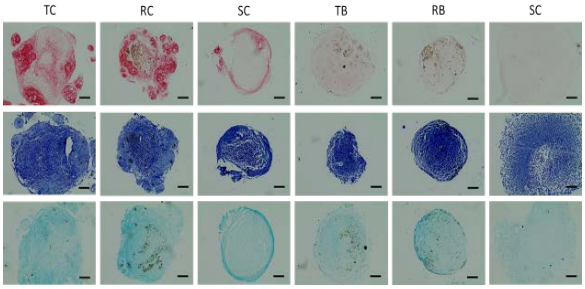

Fig. 2: Histology of MSc pellets stained with.: PicroSirius Red (top). Toluidine Blue (middle). And Alcian Blue (bottom). Abbreviations: TC, TREK-coupled MNPs, chondrogenic media; RC, RGD-coupled MNPs in chondrogenic media; SC, no MNPs, chondrogenic media; TREK-coupled MNPs, basic media; RGD-coupled MNPs, basic media; no MNPs, basic media. Scale = 100 µm.

DISCUSSION & CONCLUSIONS: Our results demonstrate that remote activation of mechanoreceptors can lead to enhanced formation of cartilaginous extracellular matrix in ovine MSC pellets. If translated to 3D models which incorporate human stem cells, this technique could be used for injectable cell therapies and ultimately improve the quality of tissue engineered constructs for OA therapies.

ACKNOWLEDGEMENTS: UKRMP Stem cell niche and UKRMP Cell delivery Hubs

Improving disease modelling for neurodegenerative drug development using engineered neural tissue with human iPSCs

C Lee-Reeves[1], JB Phillips[2] C O'Rourke[2]

[1] *Institute of Neurology, University College London, UK.* [2] *Biomaterials and Tissue Engineering, UCL Eastman Dental Institute, University College London, UK.*

INTRODUCTION: Neurodegenerative conditions remain untreatable due to the continual failure to see advancements in therapeutic research through to clinical trials. One of the obstacles that must be overcome is to develop enhanced models of disease. Tissue engineering techniques enable us to create organised artificial CNS tissue[1] that may improve the drug development process for preventative treatments. The difficulties in being able to quantify degenerative changes in cells can be overcome through the alignment of cellular processes, which allows for their accurate measurement. The aim of this research was to optimise a 3D model of neural tissue so that it may be used to study the degeneration of neurites, an early process that occurs prior to the death of nerve cells in neurodegenerative disease.

METHODS: Artificial neural tissue "EngNT" was constructed using neurons and glial cells in co-culture, within tethered collagen hydrogels. Tethering of the hydrogels allowed for glial cells to self-align, which provided structural cues for the neuronal processes to follow. The model was constructed using PC12, rat DRG or human iPSCs. Degeneration of neurites was induced through the addition of neurotoxic compounds Okadaic Acid or MPP^+ for 24hrs. PC12 gels were treated with a potentially neuroprotective compound, Salvianolic Acid B for 30mins and in the subsequent presence of MPP^+. Changes in neurite length for all conditions were measured and compared to a control.

RESULTS: Dose dependent degeneration of neurites was consistently observed with all neuronal sources. The use of an antioxidant compound, Salvianolic Acid B, protected PC12 neurites from degenerating within a toxic environment, induced through exposure to MPP^+. Pre-treatment prevented the degenerative changes in neurite length and these measurements remained comparable with the control [Fig 1]. The model was successfully scaled down in order to make it suitable for high throughput screening, generating smaller tissues that use fewer materials, where robust aligned neurite growth and degeneration was observed. Human iPS cells were found to be compatible with the scaled down model system and degenerated in response to MPP^+ [Fig 2].

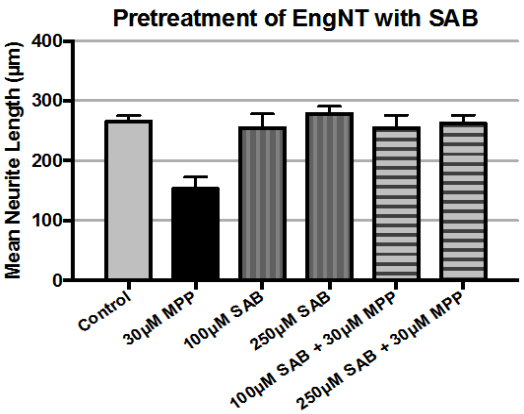

Fig. 1: Salvianolic Acid B prevents the degeneration of PC12 neurites in EngNT during exposure to 30µM MPP+. Mean neurite length ± SEM.

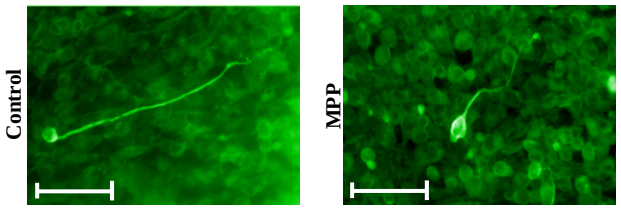

Fig. 2: The degeneration of hiPSC neurites in EngNT following 24hrs exposure to 30µM MPP^+. Scale bar = 100µm.

DISCUSSION & CONCLUSIONS: A replicable model of neurodegenerative pathology was created through exposing 3D artificial neural tissue constructs to neurotoxic compounds. Both the degeneration and protection of neurons could be observed and measured within this model, which may be adapted through the use of different neuronal sources and used to test further potential treatments. This model improves on traditional 2D monolayer cell culture by providing some of the 3D mechanical cues of the in vivo environment, whilst maintaining the high level of control possible in vitro. The successful integration of human iPS cells provides promise that this model could be used to study the response of patients' cells in future. Scaling down the model demonstrates how it may be used for neuroprotective drug development on an industrial scale.

Bone repair using collagen membranes and autologous cells: Comparison between bone marrow aspirate and platelet-rich plasma

KM Moisley [1], G Tronci [3], S Russel [3], E Jones [1], P Giannoudis [1&2]

[1] Leeds Institute of Rheumatic and musculoskeletal medicine, St James's University Hospital, Leeds. [2] Academic Department of Trauma and Orthopaedic Surgery, Leeds General Infirmary, Leeds. Textile Materials and Technology, School of Design, University of Leeds [3]

INTRODUCTION: The average cost for patients suffering from fractures following motor vehicle accidents has been estimated at £10,000 per case[1]. The fastest, most effective current treatment involves a two-stage reconstructive process, known as the masquelet technique[2], but there is a strong clinical need to streamline the procedure. One solution could be to use the induced membrane (IM) which forms around the Polymethyl methacrylate (PMMA) cement[3] spacer as a basis for a biomimetic scaffold. This scaffold will act as a guided bone regeneration device that can be loaded with bone marrow aspirate, as source of mesenchymal stem cells (BMSCs), and platelet-rich plasma (PRP), as a source of osteogenic growth factors. This study aims to compare the potential of loading a new custom-designed collagen membrane with these different biological products.

METHODS: 24 patients undergoing fracture repair surgery had bone marrow aspirate samples collected for BMSC quantification, of those, seven also had IM biopsies for histological analysis.
PRP was generated from healthy donors' whole blood using optimised centrifugation and separation steps. Scanning electron microscopy was also used to analyse the micro-structure of commercial collagen membranes.

RESULTS: Histological analysis uncovered the IM's bi-layer structure including a dense cellular layer and an open spongy fibrous layer, this was also seen in the commercial membranes shown in figure 1. Clinical analysis of bone marrow aspirate based on donor age, gender, aspirated volume and nucleated cell count were unable to predict MSC quantity which also proved to be a very rare and highly variable cell population. The PRP method was also optimised resulting in a 'pure' platelet plasma which has a 10-fold enrichment of platelets compared to a four-fold increase in commercial PRP products obtained using a Biomet BioCue. The optimised method also totally depleted the leukocytes unlike the commercial PRP which enriched the unwanted cell populations, most significantly, neutrophils.

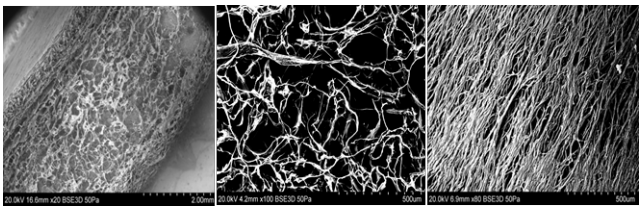

Fig. 1: Scanning Electron Microscopy images of commercially available Geistlich type I collagen membranes. There is a distinct bi-layer structure (left) composed of an open porous layer (middle) and a dense, organised layer (right).

DISCUSSION & CONCLUSIONS: Consistent with previous IM studies [3], the natural membrane had a definite bi-layer architecture which is also present in the commercial membranes. However a more targeted design of a biomimetic membrane would be needed to most closely reflect the IM bi-layered structure, collagen orientation and pore size. BMSCs are a rare and highly variable cell population requiring new in-theatre technologies to predict bone marrow aspirate quality. Commercial PRP produces a suboptimal blood product rich in red blood cells and neutrophils potentially detrimental to bone regeneration.
These limitations of the current treatment highlight the need to better understand and optimise biological products and in-theatre technologies as their potential is too great to miss.

ACKNOWLEDGEMENTS: This research is funded by the EPSRC and is a Leeds University CDT Tissue Engineering and Regenerative Medicine project.

EPAC: a pharmaceutical target for enhanced peripheral nerve regeneration?

K Bondarenko[1], M Riehle[2], S Thomson[2]

[1]*Faculté des sciences, Université de Montpellier II, France,* [2]*Centre for Cell Engineering, University of Glasgow, UK*

INTRODUCTION: It is known that cyclic adenosine monophosphate (cAMP), the ubiquitous second messenger, promotes axonal growth and myelination through various transcription-dependent pathways [1]. For a long time most cAMP effects have been attributed to the activation of protein kinase A (PKA) and cyclic nucleotide-gated ion channels. However, some of the cAMP mediated cellular events are insensitive to PKA inhibition, which led to the investigation of alternative targets for cAMP [2].

One of the targets discovered was the cAMP-regulated guanine exchange factor - exchange protein directly activated by cAMP (Epac). Its main function is to promote GDP/GTP exchange and thereby directly activate Ras family small GTPases Rap1 and 2 [3]. Numerous studies have proved that Epac in this way stimulates neuronal survival and neurite growth [2-4].

Epac-specific activators can be used to test their potential to enhance axonal regeneration *in vitro*. Epac activators maintain their activity under physiological conditions and thus have potential for clinical translation.

Current work aims to verify the effect of the Epac-specific agonist 8-pCPT-2'-O-Me-cAMP ("007") on neurite growth *in vitro*, attesting the results by using the Epac specific antagonist ESI-09.

METHODS:

Literature review: Epac activation mechanism, as well as its effect on neurons and Schwann cells has been studied as a part of literature review. Doses for Epac-selective activator and inhibitor were established according to their pharmacological properties and half maximal effective concentrations.

Preparation of the PCL: Constructs were prepared by spin coating 12% ε-polycaprolactone (PCL) dissolved in chloroform on a grooved silicone wafer to produce a non-porous membranes.

Preparation of the DRG culture: The dorsal root ganglia (DRG) are taken from neonatal (2-4-day old) Sprague-Dawley rats and placed on PCL. Cultures are maintained for 7 days in vitro in defined NGF containing media, supplemented with "007"/ESI-09/vehicle control.

Immunofluorescence and image analysis: Immunostaining will be performed using B3 tubulin, S100, DAPI. Samples will be imaged with the subsequent measurement of neurite and axon dimensions and support cell count using ImageJ.

RESULTS:

Dosing and delivery: DRG cultures will be treated with Epac activator and inhibitor that are dissolved in culture medium. Due to its high biological activity 8CPT-2Me-cAMP activates Epac with EC50 of only 2.2 µM. In order to track changes in the rate of axon growth it was decided to work with concentrations of "007" in between 5 and 50 µM.

Since ESI-09 is highly membrane permeable compound (as well due to its limited aqueous solubility), it will be tested within the 1–20 µM concentration range.

DISCUSSION & CONCLUSIONS:

Grooves directed neurite outgrowth in keeping with current literature and in house experience.

We hypothesis that treatment with "007" will promote nerve regeneration and *in vitro* testing is ongoing using ε-polycaprolactone (PCL) scaffolds and dorsal root ganglion explant model.

The impact of surface topography on adipose derived stem cell proliferation and differentiation towards a Schwann cell like phenotype

[1]Nina Jetter, [1]Suzanne Thomson, [1]Marianna Syntouka, [1]Andrew Hart, [1]Mathis Riehle, [2]Paul Kingham

[1]*Centre for Cell Engineering, University of Glasgow;*
[2]*Department of Integrative Medical Biology, Umeå University*

INTRODUCTION: Providing neurotrophic support at the nerve injury site is a critical strategy to improve nerve healing following injury (1). Adipose derived stem cells (ADSC) can be differentiated towards a glial lineage and delivered within bioengineered constructs (2). Current protocols employ *in vitro* expansion and differentiation over a two-week period and supplemental cells remain within the construct for a limited period of time. The ability of topography to direct cell fate, survival and proliferation has been demonstrated. Here we study the impact of topography on ADSC proliferation and differentiation with a view to optimise peripheral nerve regeneration.

METHODS: Flat and microgrooved Polycaprolactone (PCL) crown surfaces were fabricated in house. Surfaces were plasma treated and coated with Poly-L-Lysine. ADSC were harvested from adult Sprague Dawley rats. Alamar blue assays were performed to evaluate cell proliferation and therefore undifferentiated and differentiated ADSCs were seeded at a density of 0.5×10^4 cells/well. Tissue culture plastic was used as a control. The measurement was performed at day 1, 3, 5, and 6 after cell seeding. To determine whether grooved topography can be used to achieve more rapid in vitro differentiation a new protocol was established. First PCL were fabricated as explained above and then undifferentiated ADSC were seeded on three different conditions flat PCL, grooved PCL and tissue culture plastic as a control. Further treatment followed differentiation protocol from Kingham et al., 2007. Immunohistochemistry was used to study morphology and ELISA were used to evaluate differentiation.

RESULTS: Both differentiated and undifferentiated cells adhered to and proliferated on PCL surfaces. ADSC aligned to topography (Fig 1) with a significant difference seen in Ferret angle.
A difference in cell proliferation can be noticed on ADSCs between flat and grooved topography. Significant higher NGF concentration was detected on grooved surfaces after day 6 and day 15 of differentiation (Fig 2).

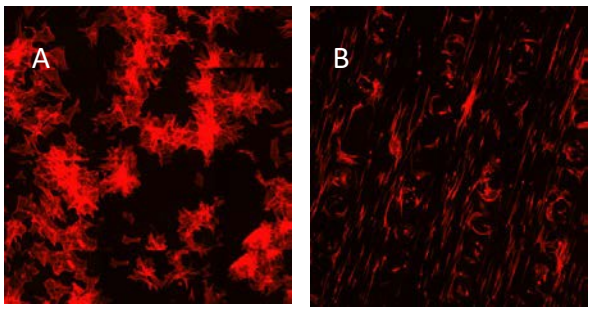

Figure 1: ADSC aligned to PCL topography, scale bar is 500µm

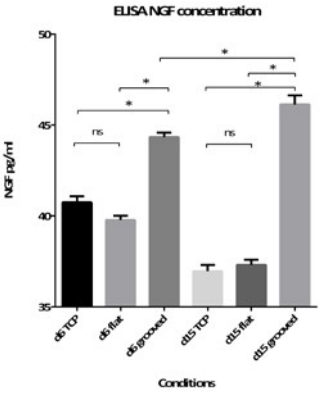

Figure *2: NGF concentration for uADSC differentiated to a Schwann cell-like lineage on flat and grooved surfaces, on grooves the NGF concentration is higher than on flat topography.*

DISCUSSION & CONCLUSIONS

ADSC proliferated better on flat than on grooved PCL. However ADSC alligned on grooves, adopting a more extended “glial like’ morphology. Differentiated ADSC show a hiågher NGF concentration on grooved PCL topography as well as maintained differentiation markers and topography may provide a means of enhancing the neurotrophic activity of ADSC.

ACKNOWLEDGEMENTS: I would like to thank whoever enabled me to come to Glasgow to do the work especially Mathis Riehle, and Ralf Kemkemer as well as the Baden-Württemberg Stiftung, Germany for supporting me.

Mesenchymal Stem Cell and MSC Conditioned Medium influence T cell differentiation to moderate immune responses in Antigen Induced Arthritis

AG Kay[1], G Long[2], J Middleton[3,1], O Kehoe[1]

[1]Keele University, ISTM at RJAH Orthopaedic Hospital, Oswestry, Shropshire, UK [2]Keele University, School of Medicine, David Weatherall Building, Staffordshire, UK [3]University of Bristol, Faculty of Medicine and Dentistry, Bristol, UK

INTRODUCTION: Rheumatoid arthritis (RA) is a debilitating and painful autoimmune disorder affecting more than 400,000 people in the UK with 12,000 new cases reported annually[1]. Mechanisms underlying the development of RA are not fully understood, however it is hypothesized that the presentation of auto-antigens to T helper cells promotes pro-inflammatory cytokine expression increasing the formation of Th1 and Th17 auto-reactive T helper cells. This in turn controls the inflammatory processes that characterise RA[2].

Mesenchymal stem cells (MSCs) possess anti-inflammatory and immunosuppressive properties which could function to modulate the immune response as therapy in refractory RA[3]. This study compares the activity of MSCs and MSC serum-free conditioned medium (CM-MSC) in moderating T cell proliferation and differentiation of naïve T helper cells in antigen-induced arthritis (AIA).

METHODS: To investigate proliferation of T cells, splenocytes retrieved from healthy C57Bl/6 mice were purified for CD4+ naïve T helper cells and stimulated with MACSibead particles with CD3ε/CD28 (T cell Activation/Expansion Kit, Miltenyi). T cells were seeded at a density of $5.0x10^5$ per well with 250µl culture medium (RPMI medium with 10% FBS) into a 96 well plate and co-cultured with $5.0x10^4$ adhered MSC or with CM-MSC in culture medium for 7 days. Purified T cells were seeded alone as control. Proliferation was assessed through reduction in signal intensity using VPD450 Violet proliferation dye (BD Biosciences).

T cell activation was investigated using spleens of C57Bl/6 mice with AIA following treatment with $5.0x10^5$ MSC or 15µl of concentrated CM-MSC injected intra-articularly 1 day following induction of arthritis. Serum-free medium (SFM) was applied as a control. The effects on the immune system were examined, through isolation of T cells and examination of their responses to AIA. Regulatory T cells (Treg) were isolated from spleen and CD4, CD25 and FOXP3 expression assessed. The numbers of cells isolated and comparative levels of marker expression were evaluated. Freshly isolated splenocytes were re-stimulated with PMA and Ionomycin (eBioscience) for 4 hours. T cells were assessed for intracellular cytokines indicative of Th1 (IFN-γ), Th2 (IL-4) and Th17 (IL17a).

RESULTS: Isolation of CD4+CD25+FOXP3+ Treg showed a trend for increased cell induction in MSC and CM-MSC treatments, and significant increases in FOXP3 expression ($p<0.05$). Preliminary data shows reduction in percentage of proliferating CD4+ T cells when co-cultured with MSCs. Intracellular cytokine expression showed significant increase in Th2 cells from mice treated with MSCs ($p<0.05$) with no change in Th1 or Th17.

DISCUSSION & CONCLUSIONS: We demonstrate immunomodulatory properties of stem cell therapy with MSC or CM-MSC in isolated T cells and delivered intra-articularly in a pre-clinical RA model. Restoring the T helper cell balance in RA could be a key therapeutic option in treating refractory RA. Further work will investigate the mechanism by which MSC influence T cell activation and proliferation to inform clinical translation.

ACKNOWLEDGEMENTS: Research was funded by the Dowager Countess Eleanor Peel Trust, the Institute of Orthopaedics Ltd and Oswestry Rheumatology Association. We thank the LSSU of Liverpool John Moores University for housing the mice.

Mimicking the annulus fibrosus with electrospun nanofibre scaffolds

A.H. Shamsah[1], S.M. Richardson[2], S.H. Cartmell[1], L.A. Bosworth[1]

[1]*School of Material, The University of Manchester, Manchester, UK*

[2]*Institute of inflammation and repair, The University of Manchester, Manchester, UK*

INTRODUCTION: Degenerative disc disease is a leading cause of low back pain and considered as a major international health problem. The current treatment options, such as surgeries, are effective to eliminate the pain; however, they treat only the symptoms and cause instability and biomechanical disturbance. Intervertebral disc (IVD) tissue regeneration aims to replace the damaged tissue with biomaterial scaffolds, such as polymers, that mimic the architecture of the native extracellular matrix (ECM). The disc has heterogeneous biphasic structure that consists of fibrous concentric lamellar sheets - annulus fibrosus (AF), which surrounds a gel-like material - nucleus pulposus (NP). In the AF region, each lamellar sheet is orientated at 30^{o} and alternatively to each other; and fibres within each lamella layer are aligned parallel to each other [1]. To provide a biological analogue, scaffold formulation should imitate the structural aspects of ECM in order to promote an appropriate biological response. Strategies involving electrospinning to produce electrospun fibres could offer the ideal fibre structures that can best imitate the tissue structure and hence provide the right environment for cell response [1]. The primary research objective was to examine the structure and morphology of native AF fibres; and evaluate its resemblance with electrospun fibre scaffold using Scanning Electron Microscopy (SEM).

METHODS: A lumbar IVD was dissected from 6-week postnatal female pig (10-12kg) and fixed with 3%v/v glutaraldehyde in phosphate buffered saline at $4^{o}C$ overnight. The sample was dehydrated by placing in hexamethyldisilazane solution and once dry mounted onto SEM stubs and coated with platinum. For comparison, polycaprolactone electrospun fibre mat was fabricated using electrospinning technique. Fibre samples were mounted on SEM stubs and coated with platinum. All samples were imaged using a Philips XL30 SEM. Both AF and electrospun fibres diameter were measured using SEM measurement software.

RESULTS: Images of PCL electrospun fibres and AF tissue fibres topography, shape and diameter were acquired at different magnifications using SEM (Figure 1). The calculated mean value of native AF fibre diameters was 170 nm and 153 nm for the electrospun polymeric fibres.

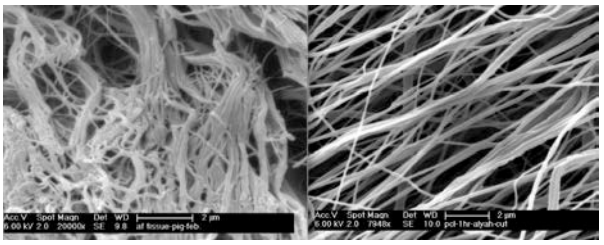

Figure 1: SEM images of native AF tissue fibres (left) compared with electrospun nanofibres (right). Scale bar = 2μm

DISCUSSION & CONCLUSION: SEM is an ideal tool for morphological research as it has high resolution and an intensity of focus that gives the SEM images a pseudo-three-dimensionality [2]. Comparison of the AF tissue and electrospun fibres demonstrated a similarity in fibre structure. The average fibre diameter of the electrospun fibres was comparable to the native measurements. Thus, electrospun nanofibre structures fabricated via electrospinning could be used to mimic natural AF fibres. This research demonstrates the importance of understanding the morphology and structural properties of native ECM in order to select the best fabrication method for scaffold mimicry. Fabricating aligned fibres in an angle ply manner to mimic the orientation of the natural AF is required in future work.

ACKNOWLEDGEMENTS: We acknowledge the scholarship institution in Kuwait for their funds

Development of resorbable nanocomposite polymers for paediatric airway tissue engineering.

G.Z. Teoh [1,3], M. Kasimatis[1], A. Darbyshire[1], W. Song[1], B.G. Cousins[1], M.A. Birchall[2].

University College London ([1]Centre for Nanotechnology and Regenerative Medicine, [2]UCL Ear Institute, Royal National Throat, Nose & Ear Hospital), London [3]TWI Ltd, Great Abington, Cambridge, UK.

INTRODUCTION: Advances in regenerative medicine have inspired the development of resorbable, nanocomposite polymers for airway tissue engineering. At present, tracheal resection with primary repair is the Gold Standard for those with airway disorders; however, the maximum resectable length of the trachea is 30% of the total length in children and therefore requires the development of a safe, functional tracheal prosthesis.

METHODS: An ethylene-diethylene glycol based nanocomposite polymer (POSS-EDS) was synthesized and scaffolds manufactured by solvent casting, phase separation and 3D printing, or a combination of the aforementioned techniques. The polymeric solution and manufactured scaffolds were characterized for viscosity, tensile strength, suture retention, thromboelastography and degradation. Laminated bilayer polymeric scaffolds, mimicking native tracheal tissue, were seeded with human tracheobronchial epithelial cells and bone marrow derived mesenchymal stem cells for an *in vitro* assessment of cytocompatibility before examining scaffold integration and vascularization and whole construct behavior *in vivo.*

RESULTS: Data indicate a suitable *in vivo* degradation profile as well as good epithelial cell attachment and proliferation *in vitro*. Bone marrow derived mesenchymal stem cells were found to maintain their stem cell phenotype[1] and exhibited some penetration throughout the network of interconnected pores of the scaffolds, a key step to achieving successful tissue regeneration within a bio absorbable scaffold.

Subcutaneous implantation of the scaffolds in a mouse model illustrates formation of vasculature and good material integration.

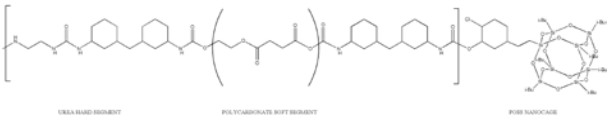

Fig. 1: Structure of the newly synthesised POSS enhanced ethylene-diethylene glycol succinate (POSS-EDS) polymer.

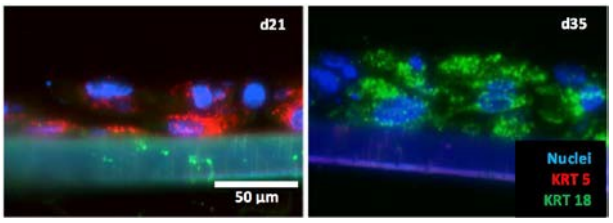

Fig. 2: Immunofluorescent staining (keratin 5 (KRT5) and keratin 18(KRT18)) indicating the organisation of cells and the differences in the epithelium following 21 and 35 days in culture on POSS-EDS scaffolds.

DISCUSSION & CONCLUSIONS: The three dimensional nanocomposite scaffolds fabricated from the newly synthesized POSS-EDS polymer are non-toxic and provide a suitable environment for tracheal specific cell adhesion and proliferation, comparable to tissue culture plastic. Overall, a promising material candidate for use in airway tissue engineering has been developed.

Cell microfactories: Manufacturing cell-based therapeutics

RP Harrison[1,3], J Thurman-Newell[2], N Medcalf[1], J, Petzing[2], QA Rafiq[3]

[1] *Centre for Biological Engineering (CBE), Loughborough University, UK.* [2] *Healthcare Technologies Group, Loughborough University, UK.* [3] *Aston Medical Research Institute, School of Life and Health Sciences, Aston University, UK*

INTRODUCTION: Cell-based therapies may offer solutions for many of the worlds health problems. Early Biotech-led approaches are supporting novel cell and tissue based therapeutics (CATBTs) through biomedical trials. However, their potential benefits are currently curtailed by challenges associated with high cost of goods (COGs) linked to high cell dose requirements which pose availability and manufacturing challenges. Previously we have investigated reducing dose requirements through more effective delivery strategies. Although efficiency can be improved on the delivery side, successful commercialisation of autologous products has remained challenging. To this end, we have developed a cost model examining business strategies for CATBTs with a particular focus on redistributed manufacturing (RDM) to identify those which present the highest probability of success for future business.

METHODS: Human Mesenchymal Stem Cell (hMSC) Culture: Three human bone marrow derived mesenchymal stem cell (hMSCs) lines were cultured for 18 days passaging every 6 days. Culture was performed both manually and in an automated manner with the Compact SELECT platform (TAP Biosystems). Cell counts and viability were obtained using the Nucleocounter NC-3000 automated cell counting system (manual culture) and the Roche Cedex system (automated culture).

Development of the cost model: A detailed cost model was developed using guidance of several key stakeholders in the regenerative medicine field. Input variation caused by biological variability were provided through culture of multiple cell lines known to display a spectrum of growth kinetics. Variation between manual and automated culture conditions were examined using the Compact SELECT automated culture platform. Accurate values for all direct and indirect costs as well as business strategies were supplied through research, quotes or personal communications.

RESULTS: The model created here is based on real cell culture data from both manual operators and automated culture platforms across a range of donor cell lines known to have variable growth kinetics. This provides a robust base on which to extrapolate theoretical cell expansion potentials in various manufacturing scenarios (Fig 1B). this has been further augmented by a range of data on current business practices for not only manufacturing, but delivery, and adoption of therapeutic products. Furthermore, detailed costs and usage patterns for GMP-grade equipment and consumables have been obtained. This has allowed the theoretical costs for various manufacturing scenarios to be calculated over whole production runs

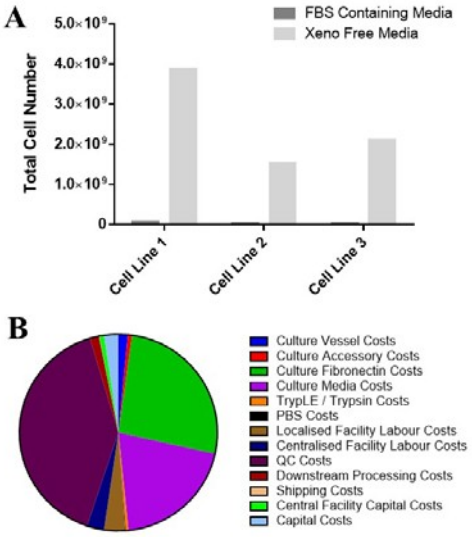

Fig. 1: Predictive data of example CATBT manufacturing obtained through the model. Cells able to be manufactured from various donor patient lines demonstrate considerable difference between lies as well as culture substrates (A). Percentage costs attributable to manufacturing process stages are outlined (B).

DISCUSSION & CONCLUSIONS: A range of different business models were examined for their potential to provide cost-effective and efficacious manufacturing of CATBTs we present a sample of potential data outputs from the model. The overall goal of this model is to provide a tool with which stakeholders in the industry can identify winning business strategies at an early stage, reducing the risk of building large facilities with high sunk capital costs for poor business ventures.

Scalable production of tissue engineered microunits for bone regeneration using bioactive glass microspheres and dynamic culture conditions

D R. De Silva-Thompson[1], J Knowles[2], M. Micheletti[1], I. Wall[1]

[1] Department of Biochemical Engineering, UCL, London, UK [2] UCL Eastman Dental Institute, London, UK

INTRODUCTION: Mesenchymal stem cells (MSC) are showing great potential in their ability to fill the gap within the tissue-engineering sector. However, a major limitation for MSCs is their limited replicative capacity and diminished multipotency during expansion. Current MSC expansion methods predominantly rely on cell culture plates, yet the substrate properties of cell culture plastic are not comparable to those of human bone. Using bioactive phosphate glass processed into microspheres can serve as a dual-purpose substrate to 1) support osteogenic differentiation and 2) facilitate dynamic, scalable tissue engineering. Incorporation of oxidizing metals, such as titanium dioxide can control stability. Our work to date has focused determining the optimal titanium concentration to provide a stable substrate and support cell viability. In the absence of titanium dioxide, rapid degradation of the microspheres was seen within 3 days of cell culture. Phosphate glass microspheres doped with titanium dioxide were found to provide a suitable platform for effective culture of an osteoblastic cell line and was not cytotoxic.

METHODS: Evaluation of the effect of dynamic conditions on cells cultured on microspheres was performed using microwell studies under orbital agitation. Using dimensionless parameters such as the Froude number, suitable agitation speeds were used to understand how different dynamic conditions effect cell proliferation and microunit formation.

RESULTS: Results showed that at small scale there isn't a significant increase in cell proliferation between the titanium concentrations studied, however dynamic conditions provide favoured culture conditions. It was also concluded, that size of desired microunit could be manipulated by the agitation speeds used correlating to the Froude number. These small-scale experiments were then used to gain an understanding of the impact of fluid flow forces that would become more significant when scaling up to process technologies that can deliver clinical quantities of cell-microsphere units. Using 125ml Erlenmeyer flask, successful scale up was achieved, with a shift from microunit sizes of 2-3mm in diameter, to a range of cluster up to and including 11mm.

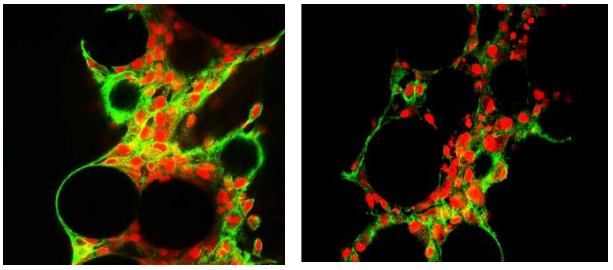

Fig. 1: Confocal Image of Ti5mol% (Right) and Ti7mol% (Left) on day 13 of 150rpm study

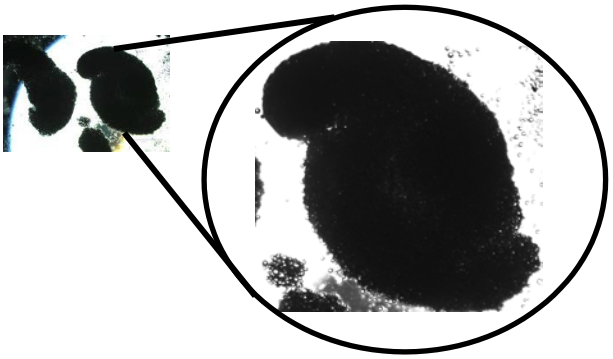

Fig 2: Transmitted light microscopy image of cell microcarrier clusters formed in 125ml Erlenmeyer flask after 14 days of culture under 50rpm conditions

DISCUSSION & CONCLUSIONS: The effective scaling up of microwell plate to clinical size quantities of tissue engineering constructs, helps elucidate that biomaterials and their scale up play a key role in the bone tissue engineering field.

ACKNOWLEDGEMENTS: Regenerative Medicine Bioprocess Consultants Ltd

Development of Potency Assays to Assess MSCs Functionality for the Treatment of Ischemic Injury

Giulia Detela[1], Ana Valinhas[1], Ivan Wall[1]

[1]Department of biochemical Engineering, University College London, Gower Street London WC1H 0AH, UK

INTRODUCTION: Mesenchymal Stem Cells (hMSCs) are a promising alternative for the treatment of ischemic injury. hMSCs have been used to restore in vivo therapeutic vascularization in combination with endothelial cells[1] and they have the ability to migrate to the infarcted myocardium, a phenomenon attributed to their oxygen sensing capacities[2]. This study describe the development of potency assays to investigate hMSCs vascular support capacity.

METHODS: human umbilical cord vein endothelial cells **(**hUVECs) and hMSCs were labelled green and red respectively. hMSCs were pre-stimulated with two soluble ligands (L1 and L2) at 37^{o}C for 45 min. Suspensions of hUVECs and primed hMSCs were prepared and seeded on top of matrigel coated wells. Co-cultures were maintained for 18 hours either at normal (20% O2) or reduced (2% O2) oxygen. After 18 hours incubation at normoxia or reduced oxygen conditions, pictures were taken to the intirety of each well.

RESULTS: Reduced oxygen levels generate wider networks (Fig 1-B) that contain more branch points (Fig 1-A). hUVECs only form larger networks with significantly smaller tubule length (Fig 1-B). Co-cultures that used L1 primed hMSCs significantly formed wider and more branched networks in lower oxygen conditions (Fig 1).

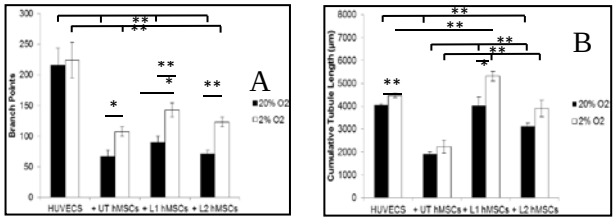

*Fig 1: Number of branch points (A) and cumulative tubule length (B). Error bars represented as standard error of the mean (SEM). Non-parametric Mann-Whitney U test, * p<0.05m«, ** p<0.01, n=5.*

A Principal Component Analysis (PCA) was used to compare experiments performed with hMSCs primed with L1 at normal and reduced oxygen. The number of branch points (bp) and cumulative tubule length (CTL) were the chosen variables for this comparison. The results (Fig 5) show that there are two main groups: experiments performed at low oxygen which score higher number of branch points and cumulative tubule length and experiments performed at normal oxygen with lower scores for both variables.

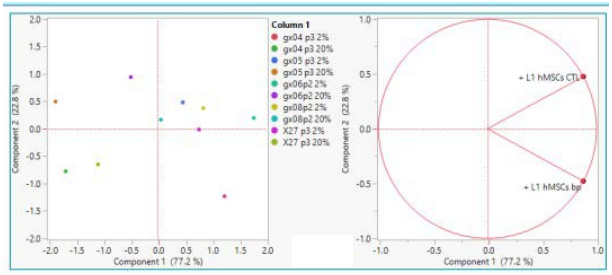

Fig 2: Mean vectors for experiments performed at 20% and 2% oxygen are different (p<0.05 HotllingdT2 for 2 dependent samples). Bp – number of branh points; CTL – cumulative tubule length.

DISCUSSION & CONCLUSIONS: Hypoxic co-cultures where hMSCs were pre-stimulated with L1 formed wider and more branched networks suggesting that this ligand enhances hMSCs cascular support role. PCA can be used as a control tool to assess if a batch of cells presents the product attributes which make the cells adequate for transplantation into a patient.

Mathematical modelling as a tool to inform the design of spray systems for cell-based therapies

M Nweze[1, 3], T Baker[1], GA Limb[2], RJ Shipley[1]

[1] *Department of Mechanical Engineering, University College London, London, UK* [2] *Institute of Ophthalmology, University College London, London, UK and* [3]*Institute of Medical Physics and Biomedical Engineering, University College London, London, UK*

INTRODUCTION: Chronic degenerative disease such as cancer, Parkinson's disease and cardiovascular diseases are the leading cause of mortality worldwide[1]. According to the World Health Organisation, chronic diseases constitute 85%[2] of deaths in the United Kingdom; they also cause permanent loss of cells and organ dysfunction. Cell-based therapies provide a diverse range of treatment options, and spraying of cells directly to the affected area is one delivery mechanism that has been shown to promote cell proliferation and cell viability, as cells are delivered on a layer-by-layer basis in a fast and controlled manner, thus accelerating the healing process[3,4]. The requirements of cell spraying are specific to the tissue being treated, especially due to geometric variability between tissues. It is essential to understand the link between cell spraying output (e.g. volume of cells delivered, surface area and the spatial distribution of delivery), and input (air pressure, nozzle dimensions, volume flow rate of cell suspension); we aim to use computational modelling as a tool to inform these relationships, enabling organ-specific application of spray systems for cell delivery. Here we present a case study based on spraying cells to the back a human eye, a therapeutic option for treating blindness.

METHODS: We use the CFD solver, STAR-CCM+®, to enable spatial simulations of spraying in realistic clinical geometries. The human eye is represented by a three dimensional hemisphere with a diameter of 25 mm, where an injector with a nozzle diameter of 0.6 mm, positioned using cylindrical coordinate system at (3,7,0) from the centre of the geometry provides the location at which cells are sprayed into the eye. Typically a cell suspension (cells plus supporting matrix components) is injected at a rate of 2ml/s at a spraying angle of 120° for 2s, with an air pressure of 2 bars applied at the injector (these are realistic parameters used for commercially available cell-delivery spraying systems[3]). A continuum mechanics approach was used with the cellular suspension drops described using a multiphase model, and the spatial distribution of drops tracked in time. Boundary conditions on the hemisphere and nozzle input were chosen to represent the input parameters described above

RESULTS: For given output parameters, we are able to predict the thickness of the cellular suspension (see Fig 1), which varied over 1.3-2mm over the time course of one spraying event. The thickness and variability of this layer thickness is determined by the flow rate of delivery and spraying pressure. The section of the eye that is covered is determined by the spraying direction and nozzle geometry, and the model enables these parameters to be varied to inform spray operation.

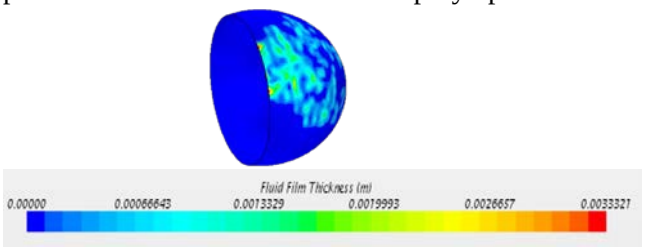

Fig. 1: Image of the hemisphere showing fluid film thickness distribution over the surface area.

DISCUSSION & CONCLUSIONS: The computational models developed provide insight into the link between spraying pressure and flow rate, and the spatial distribution of delivered cells. These simulations provide a starting point for building standardised computational models relevant to more complex geometries and spraying scenarios, with a view to informing cell delivery parameters in a way that minimises costly and time consuming experimentation.

ACKNOWLEDGEMENTS: This work is supported by the EPSRC and the NIHR.

Myoblast compatibility with a two-dimensional zein scaffold

TJ Callue[1], MJ Ellis[2], PA De Bank[1]

[1] Department of Pharmacy and Pharmacology, University of Bath, BA2 7AY, U.K. [2] Department of Chemical Engineering, University of Bath, BA2 7AY, U.K.

INTRODUCTION: The current environmental implications of conventional meat production, coupled with the projection of a 70% increase in global human population by the year 2050, shows the practice to be unsustainable.[1] In-vitro meat offers a more viable alternative, and indeed research is being conducted into developing this biotechnology; the first lab-grown hamburger was cooked and eaten in 2013.[2] A crucial element in the development of this biotechnology is a suitable and, ideally, edible scaffold on which to expand myogenic cells. This work investigates the compatibility between C2C12 myoblasts and zein, an edible storage protein found in corn, compared to tissue culture plastic (TCP) as the positive control.

METHODS: Two-dimensional zein films were formed by dissolving zein (from two different sources) in trifluoroethanol, plating into multiwell plates and allowing the solvent to evaporate. All films were sterilised under UV light before use. Adhesion of C2C12 myoblasts to the films was assessed by quantification of cell number 3 hours post-seeding following staining with CellTracker Green. To assess C2C12 proliferation, cell metabolism was analysed over time by measuring the reduction of resazurin. To confirm cell viability, manual cell counts were performed following staining with LIVE/DEAD. Differentiation was analysed *via* immunostaining for myosin heavy chain after confluent cultures had been incubated in differentiation medium for 1 week.

RESULTS:

Zein films, from both Sigma-Aldrich and Acros, were comparable with TCP in supporting C2C12 myoblast adhesion when assessed three hours after seeding, with no significant differences observed. The interaction of myoblasts with the surfaces was assessed by examining their spreading over time and, again, the reduction in circularity was comparable between TCP and zein (*Fig. 1*). This was also the case for proliferation, with all surfaces supporting a similar rate of growth (*Fig. 2*). Cell viability was also high on all surfaces, with no significant differences observed between the different materials or suppliers. Preliminary results suggest that all surfaces also support myoblast fusion into myotubes, although further quantification of differentiation is required.

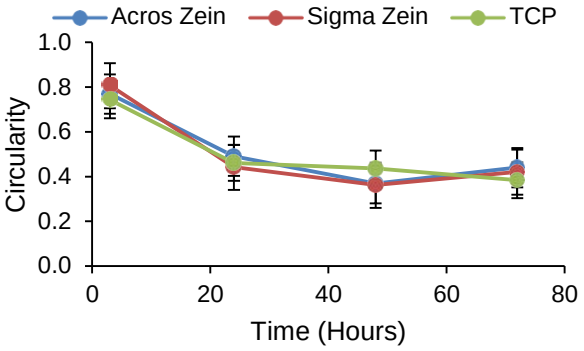

Fig. 1: C2C12 morphology on zein films vs vs TCP over a period of three days. Data represent mean ± standard error (n=3).

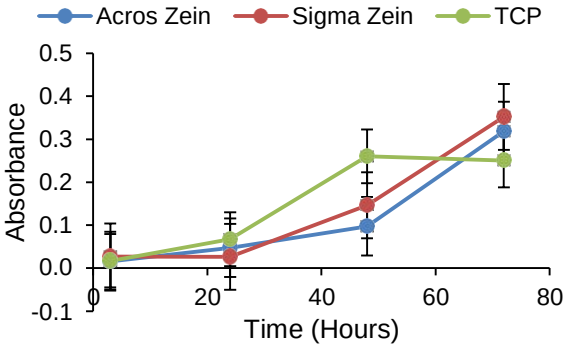

Fig. 2: C2C12 proliferation on zein films vs TCP over a period of three days. Data represent mean ± standard error (n=3).

DISCUSSION & CONCLUSIONS:

This work demonstrates that zein can support the adhesion, growth and differentiation of C2C12 myoblasts, suggesting it is a suitable biomaterial for development into edible 3D scaffold for applications in the production of *in vitro* meat, and the wider field of tissue engineering.

The investigation of mechanisms about bacteria-hydrogels interactions

Nehir Kandemir[1], Nicholas Jakubovics[2], Waldemar Vollmer[3], Jinju Chen[1*]

[1] *School of Mechanical & System Engineering, Newcastle University, Newcastle Upon Tyne*
[2] *School of Dental Sciences, Newcastle University, Newcastle Upon Tyne* , [3]*The Centre for Bacterial Cell Biology, Newcastle University, Newcastle Upon Tyne*
*corresponding author: Jinju.chen@ncl.ac.uk

INTRODUCTION: The structure and function of eukaryotic cells can be regulated by altering their micromechanical environment [1-3]. However, little work has been done for bacteria which might be affected by similar interactions. Therefore, we combined experimental and modelling approaches to study the cellular behaviour of bacteria subjected to various micromechanical environments.

METHODS: We established compression tests to obtain the mechanical properties of *Escherichia coli* BW25113 (Gram negative) and *Staphylococcus epidermidis* SB1CHA1 (Gram positive) encapsulated in 1% agarose hydrogels made with different buffers and media such as Phosphate Buffered Saline (PBS), Luria Bertani (LB) and Nutrient Broth (NB). We used finite element method (FEM) to characterize the mechanical responses of bacterial cells in hydrogels and compared the results to different theoretical models (e.g. Voigt model, Reuss model, HS lower and upper bound models).

RESULTS: Figure 1 displays how bacterial cells (1% volume fraction) would affect the overall stiffness of the cell-hydrogel composites. Statistical analysis showed that there was no significant difference between the gels with or without encapsulated cells when the PBS and NB media were used. However, when LB media was used, there was a significant increase of the stiffness of the hydrogels caused by the cells possibly due to different interactions between cells and hydrogels made with different media.

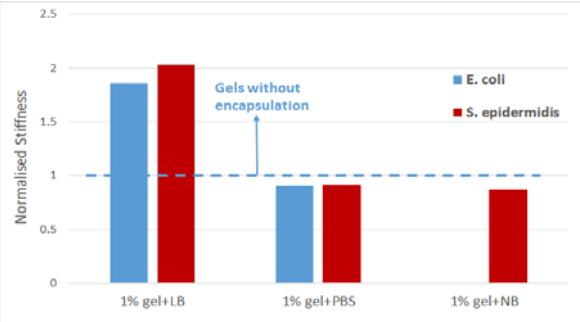

Fig. 1: The bacterial cells (1% volume fraction) affect the overall stiffness of the cell-hydrogel composites. The tests on 1% gel+NB were not done for E. coli.

Figure 2 compares the elastic moduli of cell-hydrogel composites determined by experimental measurement, finite element modelling and theoretical models.

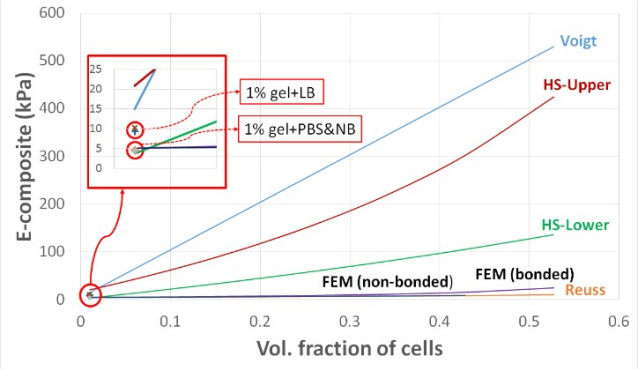

Fig. 2: The comparisons of the elastic moduli of cell-hydrogel composites determined experimentally (data points) or by FEM (solid line) and theoretical models (solid line).

DISCUSSION & CONCLUSIONS: This study has revealed that bacterial cells may decrease or enhance the mechanical integrity of hydrogels depending on the nutrients supplied. In addition, the micromechanical environment may also affect the mechanical behaviour of bacterial cells. Our findings are important as they will enhance the understanding of cell-materials interactions which have great potential impact for various healthcare industries.

ACKNOWLEDGEMENTS: NK acknowledges PhD studentship provided by Newcastle University. JC acknowledges funding from the Engineering and Physical Sciences Research Council (EP/K039083/1).

Growth differentiating factor 6 receptor expression in intervertebral disc cells and mesenchymal stem cell populations – implications for stem cell therapy

T Hodgkinson[1], J.A. Hoyland[1], S.M. Richardson[1]

[1] *Centre for Tissue Injury and Repair, Institute of Inflammation and Repair, Faculty of Medical and Human Sciences, University of Manchester, UK.*

INTRODUCTION: In the intervertebral disc (IVD) one sub-group of the BMP family - the growth differentiating factor family (GDF) - is required for correct development and homeostasis. This family contains GDF5, 6 and 7, which perform specialised but complementary roles in directing IVD cells. Recently, we showed that stimulation of bone marrow- and adipose-derived MSCs (BM-MSCs; Ad-MSCs) with GDF6 promotes differentiation to a phenotype similar to that of nucleus pulposus (NP) cells from the IVD[1] and that GDF6 promotes this differentiation better than other commonly used growth factors, namely GDF5 and TGFβ. However, patient-matched MSCs from these two sources showed different responses to GDF6, with Ad-MSCs forming a phenotype more closely resembling NP cells. We aimed to investigate if altered GDF6 signalling in NP and annulus fibrosus (AF) cells changes during IVD degeneration (IVDD). Furthermore, we investigated if GDF6 signalling differed in BM-MSCs and Ad-MSCs with a view to optimising differentiation and enhancing the efficacy of future therapies.

METHODS: Protein was extracted from NP and AF cells from patients with mild (n=3), moderate (n=3) and severe (n=3) IVDD and BMP receptors profiled through western blot analysis. NP and AF cellular response to GDF6 and TGFβ3 stimulation *in vitro* was assessed through a time resolved SMAD activation assay. Similarly BMPR expression was profiled in patient-matched BM-MSCs and Ad-MSCs (n=3) and differences in SMAD activation following GDF6 or TGFβ3 stimulation quantified.

RESULTS: BMPR profiles on disc cells were observed to differ during IVDD and between patient-matched Ad-MSC and BM-MSC populations. In NP and AF cells from severely degenerative discs we observed a significant increase in activin receptor IIA expression, an alternative receptor for GDF6, in comparison to cells from mildly degenerative IVDs. Similarly, we observed an increased BMPR-1B and a decreased BMPR-1A expression, the type I receptors for GDF6 signalling, in degenerate cells. In Ad-MSCs, levels of a GDF6 type II receptor, BMPR2 ($p<0.05$) were significantly higher compared to BM-MSCs. Correspondingly SMAD1/5/8 phosphorylation following GDF6 stimulation was also significantly higher in Ad-MSCs compared to BM-MSCs ($p<0.05$). GDF6 was observed to act through the SMAD1/5/8 pathway and did not stimulate the SMAD2/3 pathway. TFGβ3 was able to stimulate both SMAD2/3 and to a lesser extent SMAD1/5/8 in this system. Taken together, these results indicate altered GDF signalling in these populations.

DISCUSSION & CONCLUSIONS:

GDF6 signalling in NP and AF cells-TGF/BMP signalling is critical in directing multiple cellular processes in the IVD. Altered expression of BMPRs on cell surfaces during IVDD could contribute to ECM production changes and drive fibrotic cell phenotypes. The upregulation of the alternative GDF6 type II receptor ACVRIIA and type I receptor BMPR-1B in cells during IVDD may indicate a change in signal transduction away from signalling through BMPR-1A/ BMPR2 receptor complexes in non-degenerate disc cells. Given, the inherent complexity of TGFβ/BMP signalling, further work is required to elucidate important changes in signal transduction in disc cells during IVDD.

GDF6 signalling in BM- and Ad-MSCs-Receptor profile differences suggest a link to enhanced discogenic response in Ad-MSCs in comparison to BM-MSCs[1], when stimulated with GDF6. In particular, the upregulation of BMPR2 in Ad-MSCs vs. BM-MSCs and corresponding enhanced SMAD1/5/8 phosphorylation in response to GDF6 stimulation suggests signalling through receptor complexes containing this type II receptor is of importance for directing NP-like differentiation. The isolation of $BMPR2^{HI}$ Ad-MSC sub-populations may enhance stem cell-mediated disc regeneration.

ACKNOWLEDGEMENTS: This project was funded by UoM awarded MRC CiC.

Effect of controlled growth differentiating factor 6 release from PLGA microparticles on adipose-derived mesenchymal stem cell differentiation towards a nucleus pulposus-like phenotype

T Hodgkinson[1], L White[2], K Shakesheff[2], J.A Hoyland[1], S M. Richardson[1]

[1] *Centre for Tissue Injury and Repair, Institute of Inflammation and Repair, Faculty of Medical and Human Sciences, University of Manchester, UK.* [2]*Centre for Biomolecular Sciences, School of Pharmacy, Nottingham University, UK.*

INTRODUCTION: Nucleus pulposus (NP) cells in degenerative intervertebral discs (dIVD) display changes in phenotype and extracellular matrix (ECM) secretion, leading to progressive tissue dehydration and fibrosis. Stem cell therapy has been suggested as a potential strategy to repair the degenerate IVD. GDF6, a member of the BMP family, differentiates adipose-derived MSCs (Ad-MSCs) into a NP-like phenotype[1]. This study investigated the efficacy of microparticle (MP) controlled release of GDF6 on NP-like differentiation of Ad-MSCs in 3D culture.

METHODS: Initially, the release kinetics of GDF6 from MPs in PBS solutions and embedded in collagen gels under culture conditions were calculated through BCA protein assays and GDF6 ELISA's. Ad-MSCs (n=3) were seeded into collagen type I hydrogels and separated into four culture groups: 1) GDF6-MP loaded gels, 2) Control HSA-MP loaded gels, 3) Collagen gels cultured with 100 ng/ml exogenous GDF6 and 4) GDF6-free gels. All groups were cultured in NP differentiation media. After 14 days, qRT-PCR analysis of discogenic markers and sGAG content analysis (DMMB) was performed. Effect of MP loading density was assessed by scanning electron microscopy (SEM) and histology.

RESULTS: Recombinant human GDF6 was successfully encapsulated into MPs and released over 14 days in 3D culture. MPs were distributed throughout collagen hydrogels and did not interfere with gel formation. The GDF6 released from MPs induced upregulation of NP marker genes in Ad-MSCs in a comparable manner to exogenously delivered GDF6 added to media. Sox9 ($p<0.001$), collagen II ($p<0.05$) and aggrecan ($p<0.05$) expression were significantly increased compared to GDF-free and HSA-MP controls. Importantly, there was a significant upregulation in aggrecan in gels treated with GDF6 compared to TGFβ3, mimicking differences between the NP matrix and articular cartilage. NP-specific markers FOXF1 ($p<0.05$), KRT18 ($p<0.001$) and KRT19 ($p<0.001$) were significantly upregulated and sGAG production by cells increased in constructs in comparison to GDF-free and HSA-MP controls.

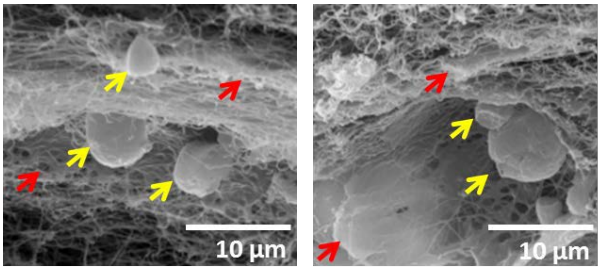

Fig. 1: SEM images of GDF6-loaded PLGA microparticles in collagen gels. Yellow arrows indicate microparticles, red arrows indicate Ad-MSCs.

DISCUSSION & CONCLUSIONS: In 3D collagen gel cultures, Ad-MSCs responded equally to GDF6 stimulation from both the media-supplemented and MP-delivered sources, indicating maintained activity of GDF6 in MPs. Of note, GDF6 stimulation significantly increased aggrecan expression versus GDF-free gels, a crucial requirement for the development of NP-like tissue and highlighting the accurate differentiation of Ad-MSCs into an NP-like phenotype through GDF6 signaling. GDF6 delivery and controlled release within an Ad-MSC seeded hydrogel may be an effective regenerative therapy for IVD degeneration.

ACKNOWLEDGEMENTS: This project was funded by UKRMP and UoM awarded MRC CiC.

Innovative design of an electrochemical anodisation setup for *in-vitro* medical applications

JS Khaw[1], A Němcová[1], M Curioni[1], P Skeldon[1], C Bowen[2], SH Cartmell[1]

[1] *School of Materials, The University of Manchester, UK.* [2] *Department of Mechanical Engineering, University of Bath, UK.*

INTRODUCTION: Nanostructured materials are believed to increase cellular activities and trigger excellent interaction between the targeted cells and biomaterials. Protein adsorption to material surfaces is key to effective cell adhesion, proliferation and differentiation[1]. Biomaterial surfaces are therefore modified to enhance protein adsorption. Electrochemical anodisation is a reliable technique in generating nanotubes on metallic materials due to its simplicity, controllability and reproducibility[2]. However, conventional anodising rigs commonly used in many labs have a few limitations like anodising only on a specific area over a large piece of sample, thereby imposing material wastage and difficulty in trimming the anodised area for *in-vitro* studies owing to the hard ceramic layer. The experiment aims to design an anodising rig for fabricating titania nanotube (TiNT). The TiNT discs will then be used to investigate cellular behaviour and osseointegrative properties of TiNT via *in-vitro* cell culture and biological assays.

METHODS: Titanium foils (0.25 mm thick, 99.5% purity, Alfa Aesar) were cut into a disc shape using a fiber laser cutting machine. Before the anodisation process the discs were deburred and successively sonicated in degreasing solution (ethanol, propanol and deionized water) followed by air-dried. In the customised anodisation setup, titanium discs served as an anode, while an inert platinum foil (0.1 mm thick, 99.99% purity, Alfa Aesar) was used as a cathode. Saturated colomel electrode served as a reference electrode. 1M H_3PO_4 with 0.3wt% HF was used as an electrolyte for the anodisation. Applied voltage as 20V, the anodisation was set to run for 1 hour at room temperature. The current density of the samples was obtained and plotted. Surface morphology of the specimens were characterised using Scanning Electron Microscope. The anodised specimens were then sonicated and finally sterilised before conducting the cell experiments.

RESULTS: Human mesenchymal cells seeded onto pure titanium specimen showed an increase in cell number at day 7 as compared to tissue culture plate as experimental control.

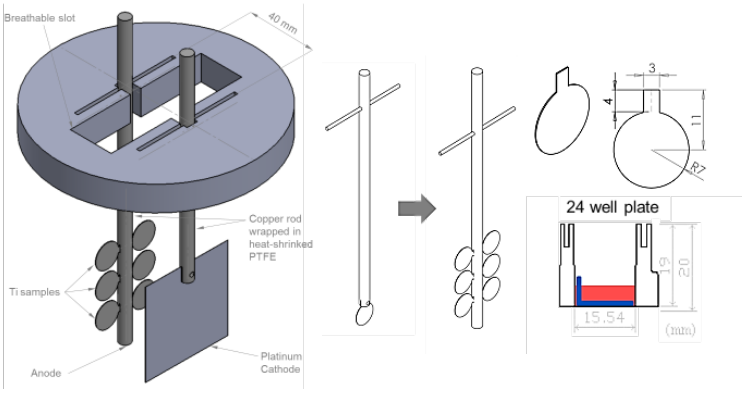

Fig. 1: Anodisation setup design. The number of specimens scaled up from one specimen to six specimens per process. Anodisation took place over the entirety of the specimens. Specimens were designed specifically to fit into 24-well plate for in-vitro cell culture experiments

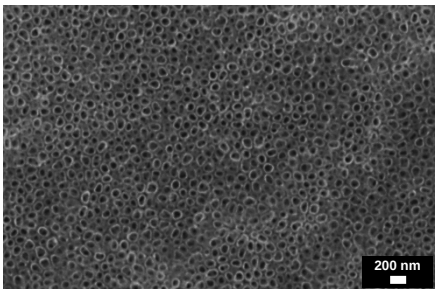

Fig. 2: Top view SEM image of the nanotube. Self-organised nanotube structures with pore diameters of 100 nm can be observed.

DISCUSSION & CONCLUSIONS: The current passing through the electrodes was consistent. This anodisation setup design allows maximised productivity and consistent production of anodised TiNT. This cost effective and highly reproducible design also offers customisation of specimen shape which facilitates different tests and assays. The effectiveness of *in-vitro* biocompatibility test processes was preserved.

Cultured meat bioprocessing – bioreactor selection and design based on cell culture conditions and energy requirements

Javier Vega and MJ Ellis

Department of Chemical Engineering, University of Bath, Bath, UK

INTRODUCTION: The first cultured burger was launched in 2013 by Prof Mark Post. There are now more than five companies and tens of research groups globally aiming to introduce various cellular agriculture products to the market, including milk (Muufri) and egg whites (Clara Foods). Cultured meat is a cellular agriculture product – an animal product made from cell cultures. There is a long way to go to produce a tissue engineered piece of bovine muscle for eating, but growing large numbers of skeletal muscle cells and adipocytes is the starting place. Cell culture is expensive and energy intensive, currently prohibitively so on the scale required to grow cells for cultured meat which will ultimately be a commodity (a low value, high volume product). Here we begin to optimise the bioreactor design – the process unit where the design is critical to muscle cell culture and where the highest costs are incurred.

METHODS: Mass, energy and momentum balances were performed across three types of bioreactor: stirred tank, fluidised bed, and hollow fibre membrane. Based on media and energy requirements, a hollow fibre membrane was selected and detailed mass transport calculations performed to optimise the design. In the absence of stoichiometric data for mesenchymal stem cell or myosatalite cell culture, hybridoma cell data was used [1]. A number of initial assumptions were made including 100% cell viability; 15^{o}C ambient temperature; glucose and oxygen as the key feed components; lactate and ammonia as the key waste components; Krogh cylinder sub-unit geometry, hexagonal packing, and fibre properties of poly(lactide-co-glycolide). Sensitivity analysis around cell viability, bioreactor dimensions and media consumption was performed, based on models for HFBs in literature [2,3] and modifying these as required.

RESULTS: A hollow fibre bioreactor was shown to be most appropriate based on media and energy requirements. This was due to the high surface area to volume ratio compared to the other two bioreactor types. For the target 1800 kg of protein per batch from a starting number of 1.8 x 10^{8} cells, the culture process took 60 days. Whether the energy balance was exothermic or endothermic depended on cell number and bioreactor dimensions, as such the bioreactor can be optimised for energy efficiency. Heat/cooling is then part of the control system (Fig 1).

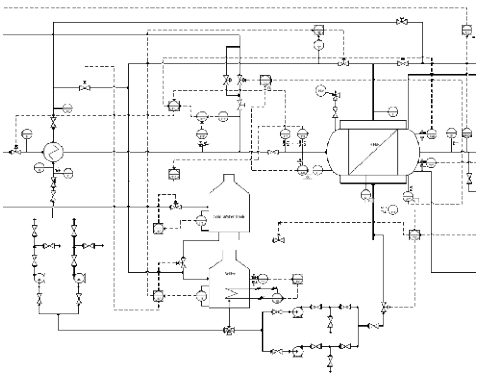

Fig. 1: P&ID of HFB for cultured meat.

DISCUSSION & CONCLUSIONS: A hollow fibre bioreactor was found to be the most appropriate device for cultured meat expansion due to the lower media and energy requirements compared to stirred tanks and fluidised bed bioreactors. The calculations used data from literature as this is a relatively new process, however this introduces a number of errors, especially the stoichiometry of hybridoma cells. It is clear that for cultured meat to be available, a more cost effective media needs to be created, alongside careful bioprocess design.

ACKNOWLEDGEMENTS: University of Bath for supporting the work.

Laser based additive and subtractive manufacturing techniques of emulsion based biomaterials

C Sherborne, IU Rehman, F Claeyssens

Department of Materials Science & Engineering, University of Sheffield, United Kingdom

INTRODUCTION: Laser based 3D printing has the ability to fabricate bespoke multiscale porous structures using an emulsion based material to have control over the micro (30µm) and larger millimeter features. This is an additive manufacturing technique, and the object is built layer by layer. This has been reported on in our group previously on the PolyHIPE material (Polymerised High Internal Phase Emulsion) [1]. As versatile as this technique is, the minimum achievable feature size is limited by the scattering of light around a water droplet suspension, which can result in connecting bridges of over cured polymer between separate structures and a closed outer surface which potentially limits cell ingrowth and the minimum feature size that is attainable. This abstract reports on the use of a light absorber to reduce the scattering of light caused by this effect and the reduction in the surface skin effect. Furthermore we present the use of a laser cutter to create detailed topographical structures that currently cannot be produced by the stereolithographic structuring approach of this material. This post processing technique is limited to surface 2.5D structures only, however this limitation is circumvented by its superior minimum feature size achievable, as well as a wider range of usable materials for tissue specific material processing.

METHODS: Porous polymeric structures were fabricated using the monomers 2-ethylhexy acrylate, isobornyl acrylate and a trimethylolpropane triacrylate mixed with the photoinitiator diphenyl (2, 4, 6 - trimethylbenzoyl) phosphine oxide / 2 – hydroxyl – 2 –methyl propiophenone) (Sigma). The surfactant hypermer B246 was added to facilitate a stable emulsion. This was mixed at 350 rpm with the gradual addition of water to create a water-in-oil emulsion.

Fabrication of porous structures: The polymerisation of the continuous phase of the emulsion preserves its morphology. This is achieved by irradiation with ultraviolet light (355nm).

The interconnectivity, pore size and bulk mechanical properties can be controlled by the emulsion conditions and water volume ratio. Connecting bridges are formed by selective polymerisation of the HIPE within close proximity.

Laser etching of porous material: Bulk cross-linked porous sheets were laser etched with varying speeds and powers to create complex topographical features using an Epilog laser mini laser cutter.

RESULTS: The addition of a light absorber decreased the minimum feature size of the stereolithography approach. SEM images confirmed the surface skin effect was not seen within the laser etched samples, which retained an open pored outer surface. Laser etched kerf was seen within the polyHIPE material and selectively polymerised bulbs, with a connecting polymer bridge and surface skin shown in *Figure 1*.

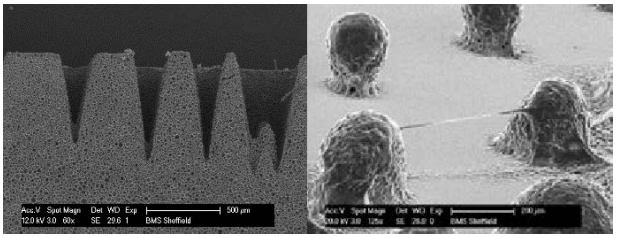

Fig. 1: Left, Laser cut kerf into the polyHIPE material. Right, Connecting polymer bridge between two separate structures caused by light scattering during its fabrication.

DISCUSSION & CONCLUSIONS: The incorporation of a light absorber improved the achievable minimum feature size with the light induced 3D fabrication. This increased control over light scattering and also removed the excess crosslinking which caused connecting polymer bridges to form between adjacent structures. The laser cutter was used to create an open pored outer surface and has been demonstrated with emulsion formulations that cannot be used with the additive manufacturing approach. This highlights the benefit of both additive and subtractive manufacturing techniques for biomaterials scaffold fabrication.

ACKNOWLEDGEMENTS: This research was supported by the EPSRC

Human platelet lysate as a bioactive scaffold coating for endothelial progenitor cell culture

TM Fortunato, G Pula, PA De Bank

Department of Pharmacy & Pharmacology and Centre for Regenerative Medicine, University of Bath, BA2 7AY, U.K.

INTRODUCTION: Vascularization of engineered tissues, and their integration with the patient's existing vasculature is a key factor in the long-term survival of the tissue. We have recently shown that a hydrogel derived from human platelet lysate (hPL) can support the formation of microvascular networks by encapsulated endothelial colony forming cells (ECFCs), and induce sprouting of existing vessels [1]. Here, we extend this work to examine the effect of adsorbed hPL on the behaviour of ECFCs on electrospun polyester scaffolds, a potential support for the generation of vascular grafts.

METHODS: Human platelet lysate (hPL) was isolated by ultrasonication of platelet-rich plasma. Scaffolds were fabricated by electrospinning blends of poly(lactic-co-glycolic acid) (PLGA) and polycaprolactone (PCL) at a total polymer concentration of 20% w/v in 9:1 trifluoroethanol/hexamethylisopropanol. Fibres were collected in an ethanol bath and wound around a Teflon cylinder to form, after drying, a tubular scaffold. Sections of scaffold were incubated in hPL solution, either as-spun or following treatment with N_2 plasma for between 30 seconds and 2 minutes. Adsorption of hPL was examined by the BCA protein assay and FTIR analysis. ECFCs, isolated from human blood [1], were seeded on the scaffolds and their proliferation and number assessed by PrestoBlue and PicoGreen assays, respectively.

RESULTS: Plasma treatment for 1 minute was sufficient to render the electrospun scaffolds hydrophilic as determined by water contact angle analysis. Incubation of scaffolds in hPL, or foetal bovine serum (FBS) as a positive control, demonstrated significantly increased protein adsorption following plasma-treatment on all but 75:25 PLGA/PCL scaffolds, and this was reflected by FTIR analysis. Determination of ECFC proliferation (*Fig. 1*) and cell number (*Fig. 2*) following incubation with FBS or hPL demonstrated that both protein sources supported ECFC culture, but cell growth and number was higher on plasma-treated scaffolds, which supported the formation of a monolayer of ECFCs.

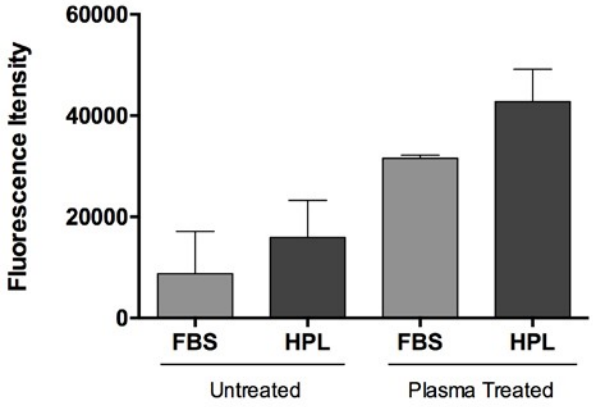

Fig. 1: Relative ECFC metabolic activity on 50:50 PLGA/PCL electrospun scaffolds, treated with FCS or hPL, 5 days post-seeding as determined by the PrestoBlue assay.

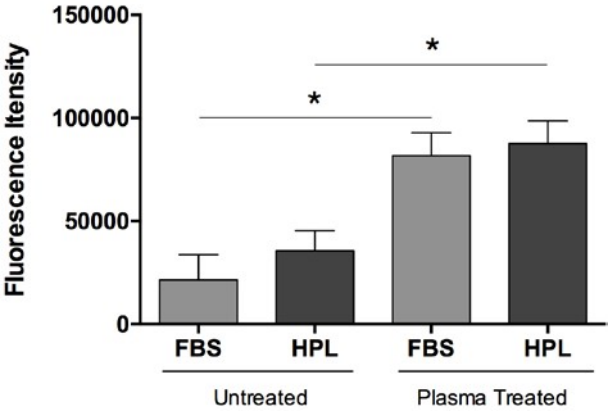

Fig. 2: Relative ECFC number on 50:50 PLGA/PCL electrospun scaffolds, treated with FCS or hPL, 5 days post-seeding as determined by the PicoGreen assay.

DISCUSSION & CONCLUSIONS: These results suggest that hPL treatment is suitable for use as a patient-derived, bioactive scaffold coating for vascular tissue engineering, with a potential for application to other tissue targets.

ACKNOWLEDGEMENTS: TMF was supported by a University of Bath studentship.

Mesenchymal stem cells osteogenic differentiation on 3D printed titanium scaffolds

S Samizadeh[1], C Liu[1]

[1] *John Scales centre for biomedical engineering, Institute of Orthopaedics and Musculoskeletal science, University College London, Royal National Orthopaedics Hospital, Stanmore, London*

INTRODUCTION: 3D scaffolds are increasingly used in orthopaedics and maxillofacial surgery to augment bone repair. The aim of this study was to test a 3D scaffold designed for use as bone anchor in rotator cuff repair. So far strategies for rotator cuff repair have not been effective enough in achieving long-term fixation and avoiding failure. The aim of this study is to evaluate the bioactivity of 3D printed titanium scaffolds *in vitro*. Hydroxyapatite is known to enhance bone formation on titanium scaffold[1]. Therefore, we hypothesize that 3D titanium scaffolds would allow more bone deposition within the scaffold hence encouraging better osteointegration of the scaffold. In addition nano sized HA coating of the titanium would further enhance bone deposition by bone marrow derived stem cells.

METHODS. 3D titanium scaffolds (n=3) with and without Hydroxyaptite (HA) coating with porous structures of 2x2 mm were seeded with 10,000 ovine bone marrow derive stem cells (BMSCs). Samples were incubated for 21 days in normal DMEM and osteogenic culture media. Alamar Blue, DNA quantification and ALP assay were used to confirm cell proliferation and osteogenic differentiation of the cells. Scanning Electron Microscopy (SEM) and immunohistochemistry using DAPI and phalloidin staining assessed cell attachment and morphology on the scaffolds.

RESULTS: The results of this study indicated cell attachment and proliferation on the surface of both coated and non-coated scaffolds (Fig 1.). HA coated scaffolds showed enhanced cell proliferation in comparison to non-coated scaffold. ALP assay confirmed the osteogenic differentiation of the seeded cells. Fluorescent imaging confirmed the attachment of the seeded cells on the surface of the scaffold.

DISCUSSION & CONCLUSIONS: 3D scaffolds have the potential to encourage bone formation as a function of their architectural design and material composition. In this study we showed that both HA coated and non-coated titanium scaffolds support bone marrow derived stem cells attachment, proliferation and osteoblastic differentiation *in vitro*. Study of bone formation within the scaffold core and on the periphery of scaffold when implanted *in vivo* would further prove the success of these designs in promotion of bone formation and augmentation of osteointegration and ultimately better fixation of rotator cuff anchors.

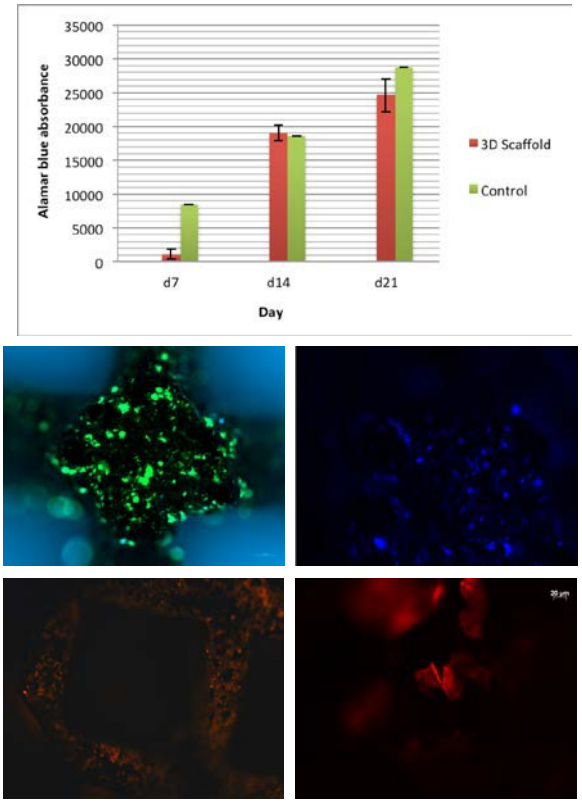

Fig. 1: Graph indicating alamar blue absorbance of bone marrow derived stem cells on the 3D scaffold within 21 days. Images indicating fluorescent-labelled cells on the surface of the scaffold. Blue: DAPI staining, Red and green phalloidin staining

ACKNOWLEDGEMENTS: MeDe innovation, the EPSRC centre for Innovative Manufacturing in Medical Devices kindly supported this study.

Augmentation of bone repair via delivery of pro-angiogenic, pro-osteogenic genes to human skeletal and endothelial populations.

RMH Rumney[1], S Lanham[1], L Thiagarajan[2], J Dixon[2], KM Shakesheff[2], ROC Oreffo[1].

[1] Faculty of Medicine, University of Southampton, Institute of Developmental Sciences Building, Mailpoint 887, Southampton General Hospital, Tremona Road, Southampton, SO16 6YD, United Kingdom. [2] Centre for Biomolecular Sciences, University Park, Nottingham, NG7 2RD, United Kingdom.

INTRODUCTION: Non-union of bone fractures arises following a failure of blood vessels to regenerate, thereby blocking bone self-repair mechanisms. Current surgical treatments are invasive, utilising bone grafts and metal plate fixation, while doing little to directly modulate angiogenesis. An attractive approach entails the use of cell scaffolds augmented with vectors capable of delivering genes associated with increased angiogenesis and osteogenesis. The aims of this study were to increase the expression of pro-angiogenic and osteogenic genes in skeletal and endothelial cells to increase proliferation and function.

METHODS: MG63 osteoblastic and EAhy926 human endothelial cell lines, primary human umbilical vein endothelial cells (HUVECs), and STRO+ skeletal stem cells (SSCs) were transfected with transgenes for pro-osteogenic BMP2, or pro-angiogenic HIF1a or VEGF using either plasmid or lentiviral vectors or lipofectamine delivery of RNA. Changes in gene expression were quantified by SYBR green real time PCR. DNA was quantified with the PicoGreen assay as a measure of cell proliferation.

RESULTS: Transfection of MG63 cells with plasmids for BMP2 and BMP2-P21 increased BMP2 gene expression at 48 hours by ~300-fold ($P<0.01$) and ~400-fold ($P<0.0001$), respectively, with no effect on proliferation. Transfection of MG63 cells with lentivirus had no effect on gene expression at 72 hours, however proliferation was significantly increased by BMP2 ($P<0.05$), VEGF ($P<0.05$), VEGF-P21 ($P<0.0001$), and αVEGF ($P<0.05$). Similarly, lentiviral transfection had negligible effect on gene expression in EAhy926 cells after 72 hours, however VEGF-P21 significantly increased proliferation ($P<0.05$). HUVECs did not respond to lentiviral transfection, although recombinant VEGF increased proliferation ($P<0.01$). Transfection of enriched STRO+ SSC populations with VEGF-P21 lentivirus significantly increased VEGF expression ($P<0.05$), while the BMP2-P21 lentivirus significantly increased proliferation ($P<0.01$).

Transfection of MG63 cells with RNA for BMP2 and BMP2-P21 increased BMP2 gene expression at 24 hours by 36 and 33-fold respectively ($P<0.0001$) while BMP2-P21 RNA increased proliferation ($P<0.05$). Similarly, transfection of STRO+ SSC populations with BMP2 and BMP2-P21 RNA increased BMP2 expression by 11 and 13-fold respectively ($P<0.0001$) and BMP2-P21 RNA increased proliferation ($P<0.01$).

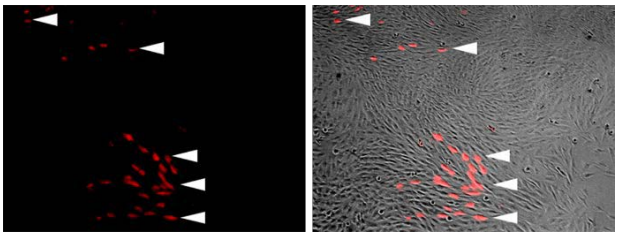

Fig.1. MG63 cells 72 hours after transfection with RFP lentivirus particles. Fluorescence only (left) and overlay with light image (right).

DISCUSSION & CONCLUSIONS: These studies demonstrate the up-regulation of genes associated with angiogenesis and osteogenesis following transfection with plasmid, lentiviral and RNA vectors into skeletal and endothelial cells leading to increases in proliferation. Transfected cells are being tested in current studies focused on evaluation and validation within *in vitro* and *ex vivo* models prior to use in *in vivo* systems.

ACKNOWLEDGEMENTS: The authors acknowledge support from the Medical Research Council, the Engineering and Physical Sciences Research Council and the Biotechnology and Biological Sciences Research Council UK Regenerative Medicine Platform Hub "Acellular Approaches for Therapeutic Delivery" (MR/K026682/1).

Mathematical modelling of oxygen, glucose and lactic acid reaction kinetics for osteoblasts and mesenchymal stem cells

ID Burova[1], IB Wall[2, 3], RJ Shipley[1]

[1] Department of Mechanical Engineering, University College London, UK. [2] Department of Biochemical Engineering, University College London, UK. [3] Department of Nanobiomedical Science & BK21 PLUS NBM Global Research Center for Regenerative Medicine, Dankook University, South Korea.

INTRODUCTION: Osteoporosis causes 8.9 million fragile fractures a year worldwide[1], which often result in non-unions and require either autologous or allogeneic grafting. Complications associated with these procedures, such as morbidity of the donor site and rejection of the implant[2], drive bone tissue engineering. Protocols for dynamic, 3D cell cultures, able to produce viable and sufficiently large tissue constructs, are investigated. Mathematical modelling is a useful tool in this process, highlighting the balance of chemical (nutrients) and mechanical (shear force) factors in the cell culture environment.

METHODS: One potential strategy for producing human-like bone tissue is using bioglass microspheres as scaffolds for MG63 osteoblasts and mesenchymal stem cells (MSCs), which are then allowed to self-assemble. Modelling is used to propose a suitable scaling-up approach. The work here focuses on cellular metabolism in the initial stages of the set-up, under diffusive only transport.

The reaction equations for oxygen and glucose uptake are based on Michaelis-Menten kinetics[3]:

$$R_i = \phi\, c_i\, V_{max} / (P_{50} + c_i) \qquad (1)$$

where R_i *[mol/s.m^2]* is the consumption rate of the chosen nutrient, c_i *[mol/m^3]* is its concentration, ϕ *[cells/m^2]* is the cell density, V_{max} *[mol/s.cell]* is the maximum rate of consumption and P_{50} *[mol/m^3]* is the concentration at which the consumption rate is 50% of V_{max}.

The level of aerobic oxidation of glucose also determines the amount of lactic acid produced by anaerobic fermentation of glucose due to oxygen deficiency[4]. This relationship can be described by:

$$R_l = -2(R_g - R_c/6) \qquad (2)$$

The model was solved in COMSOL Multiphysics. The geometry of a well from a 96-well plate (Corning) was used. Initial conditions reflecting oxygen saturation of the media, glucose concentration of 1 g/l and no lactic acid, were chosen. A constant concentration was assumed at the top boundary of the well due to oxygen diffusion from air. The cells were modelled as an infinitely thin layer on the bottom of the well, with consumption or production of the relevant species represented as flux loss/gain boundary conditions.

RESULTS: Cell-type specific coefficients need to be generated for a predictive model. A sensitivity analysis was used to characterise their behaviour. Values for V_{max} and P_{50} were obtained from literature, and the smallest and largest values used to create a range for testing. Changes in V_{max} result in greater variation in the concentration than those in P_{50} (Fig.1). In the case of oxygen, for a range encompassing one order of magnitude for both coefficients, the parameter sweep of V_{max} caused a 57 times bigger difference between the minimum and maximum oxygen concentration compared to P_{50}.

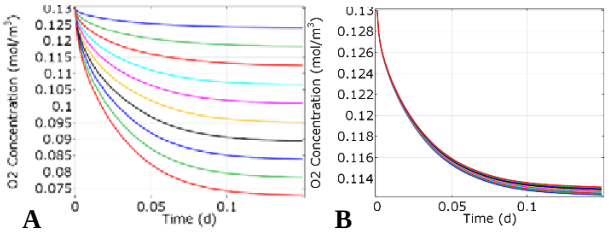

Fig. 1: Different oxygen concentrations for A) V_{max} from 9×10^{-18} to 9×10^{-17} mol/s.cell and B) P_{50} from 7×10^{-4} to 9×10^{-3} mol/m^3.

DISCUSSION & CONCLUSIONS: This analysis suggests that the next step in improving the model is to data fit V_{max} with the experimental results. This would pave the way to establishing a relationship between cell number, metabolic activity and ultimately, flow sheer stress.

ACKNOWLEDGEMENTS: IDB thanks the Rosetrees Trust for kindly funding this work.

Photochemical internalisation in 3D compressed collagen models of breast and ovarian cancer

L Mohammad Hadi, E Yaghini, M Loizidou, A.J MacRobert

Division of Surgery and Interventional Sciences, University College London

INTRODUCTION: Photochemical internalisation (PCI) is a light activated drug delivery method, which uses sub-lethal photodynamic therapy (PDT) to enhance the delivery of therapeutic agents that are prone to endolysosomal degradation to their intracellular target sites of action. The technique relies on the localization of photosensitisers within the endocytic membranes, which upon light activation leads to formation of reactive oxygen species and the rupture of the vesicles releasing the endocytosed compounds into the cytosol where they can have their effects on their targets.[1]

Since compressed 3D collagen models mimic the dense extracellular matrix of a human tissue more closely and also take into account the interactions between the cancer cells and the extracellular matrix, they are considered as ideal alternatives to 2D and animal models.[2]

Aim: To investigate the efficacy of PCI on compressed 3D collagen models of breast and ovarian cancer.

METHODS: Compressed 3D collagen models of Breast and Ovarian cancer were created using RAFT kit as well as MCF-7 (breast cancer) and SKOV3 (ovarian cancer cells). The models were treated with either the photosensitiser (PS) ($TPPS_{2a}$) alone or macromolecular toxin (saporin) alone or a combination of both drugs and were incubated for 24 hours then exposed light. Cell viability was measured at 48 hours after illumination using Alamar blue assay and images were obtained using Live-dead assay and a fluorescence microscope to observe level of cell kill with PCI.

RESULTS: PCI lead to a synergistic effect when using 20nM and 40nM saporin compared to using PDT or saporin alone with the PCI effect being slightly higher using 40nM saporin compared to 20nM. For cells that were illuminated for 5 minutes PCI produced 4.9 fold higher efficacy in cell kill vs. PDT ($p< 0.001$) using 20nM saporin and 5.1 fold higher efficacy vs. PDT ($p<0.001$) using 40nM saporin in MCF-7 cells. In SKOV3 cells also there was 2.8 fold higher efficacy vs. PDT ($p<0.001$) when using 20nM saporin and 3.6 fold higher efficacy vs. PDT ($p<0.001$) when using 40nM saporin**.**

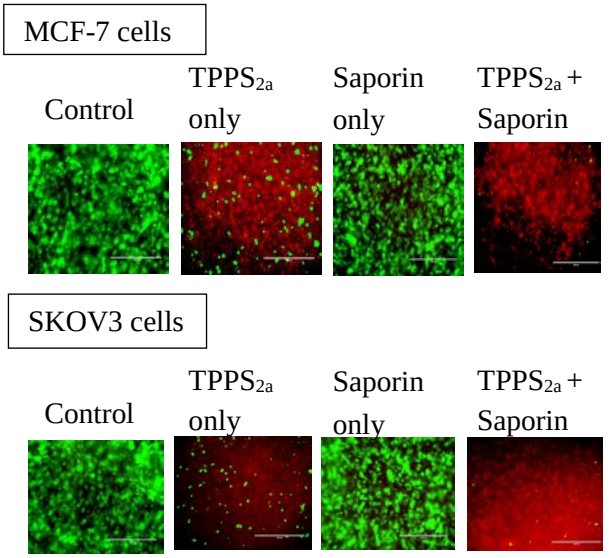

Fig1: images showing the amount of live (green) cells and dead (red cells) in 3D models of MCF-7 and SKOV3 cells after treatment with TPPS2a (0.3µg/ml) (PDT), Saporin 40nM or a combination of both drugs (PCI).

DISCUSSION & CONCLUSIONS: These results have indicated that the compressed 3D cancer model is promising way to study PCI as well as demonstrating the potential of PCI as a minimally invasive method for treating breast and ovarian cancer in the future. The significant difference between PCI and PDT results shows the synergistic effect produced with the combination of both $TPPS_{2a}$ and Saporin.

ACKNOWLEDGEMENTS: I would like to thank Prof. MacRobert, Prof. Loizidou and Dr Yaghini for their support during this study.

Chemical modification of urethane pre-polymer to enhance endothelial cell fate

Jun Hon Pang[1], Arnold Darbyshire[1], Janice Tsui[1,2], Brian G Cousins[1]

[1]Division of Surgery & Interventional Science, University College London, London, UK. [2]Vascular Unit, Royal Free London NHS Foundation Trust, London, UK

INTRODUCTION: Current cardiovascular devices are associated with impaired endothelialisation leading to complications such as thrombosis and inflammation. New biomaterial platforms that encourage endothelialisation are highly desirable in the field of regenerative medicine.[1] Urethane based pre-polymers are commercially used as moisture cure coatings and adhesives.[2] However, their application to promote cell behaviour has yet to be explored. The pre-polymer chains are typically terminated by reactive isocyanate (-NCO) groups, hence we hypothesise that -NCO groups of pre-polymers could be utilised for further reactions to yield a range of surface chemistries to enhanced cell behaviour.

METHODS: A polycarbonate-urethane pre-polymer was synthesized and spin coated on to 316L grade stainless steel discs followed by chemical treatment using ethylenediamine (EDA) and 3-mercaptopropionic acid (MPA) at a concentration range of 25mM to 500mM. It is envisaged that -NCO groups react with EDA or MPA giving rise to amine (-NH_2) and carboxylic acid (-COOH) functionality, respectively. Surface morphology and chemistry of samples were characterised using scanning electron microscopy (SEM), colorimetric assays, water contact angle (θ) and x-ray photoelectron microscopy (XPS). Human umbilical vein endothelial cells (HUVECs) were seeded on to the coated samples followed by cell based assays including AlamarBlue® and total DNA, as well as, immunofluorescent staining.

RESULTS: Varying EDA and MPA treatment concentration resulted in varied micro- and nano-scale surface morphology. SEM images revealed formation of micro-ridges and nano-features at 25mM EDA treated samples, which diminished to exhibit a flat morphology at 500mM EDA (Fig. 1). For MPA-treated samples, nano-ridges was observed on higher MPA concentration (250-500mM), but became less observable and increasingly similar to untreated controls with decreasing concentration (Fig. 2). Surface –NH_2 and –COOH were detected on all EDA and MPA treated sample respectively, and was further supported by θ and XPS data. Both EDA and MPA modified coating systems were shown to enhance HUVEC activity, growth and proliferation with changes in morphology when compared with controls.

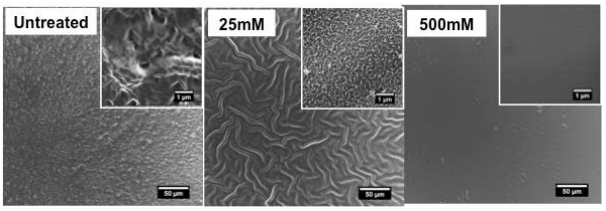

Fig. 1: SEM images of EDA-treated samples at 25mM and 500mM with respect to untreated controls.

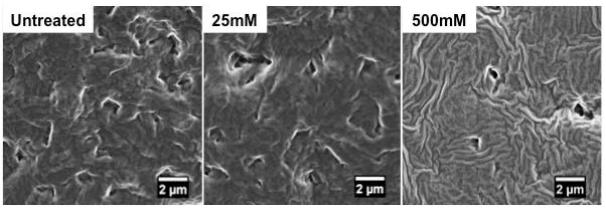

Fig. 2: SEM images of MPA-treated samples at 25mM and 500mM with respect to untreated controls.

DISCUSSION & CONCLUSIONS: We have developed a novel and simple chemical-curing approach using urethane based pre-polymers, incorporating surface functionality and micro- and nano-scale features to enhance endothelial cell fate. Such coatings can be used for further bio-conjugation of pro-endothelialising biomolecules to promote in situ endothelialisation, creating a new generation of pro-healing composite, which are now in demand.

ACKNOWLEDGEMENTS: We would like to thank EPSRC for funding of this research.

A novel collagen cross linker for various tissue engineering applications.

Miriam Zegeye[1], Prasad Sawadkar[2], Zahra Merchant[3] Laurent Bozec[4] and Vivek Mudera[2]

[1] Imperial College School of Medicine, London, [2] Tissue Repair and Engineering Centre, Division of Surgery and Interventional Science, UCL Stanmore campus, London, [3]UCL school of Pharmacy, [4] Division of Biomaterials and Tissue Engineering, UCL Eastman Dental Institute London

INTRODUCTION: Plastic compressed collagen gels have been used to produce tissue constructs for various tissue engineering applications (1). However, these collagen constructs are mechanically weak. To increase mechanical properties cross-linking agents are added but biocompatibility of the constructs is compromised. To overcome this issue we have used a novel crosslinking agent Biobond TG-EB32 (meat-glue) used in the food industry. Results were compared to published collagen crosslinking agents in the literature including maltodextrin, transglutaminase and riboflavin.

METHODS: Each collagen hydrogel was cast by the standard method previously described by Brown et al (1). Addition of crosslinking agent was added to the 10% DMEM at 1% and 0.5% concentrations of Biobond TG-EB32, transglutaminase and maltodextrin. Riboflavin (0.25mM and 0.125mM) was added to the 10% DMEM. The mechanical properties and cell viability tests were performed and thermal assays by FT-IR and DSC.

RESULTS: The calculated mean break strength of Biobond TG-EB32 at 1% was 725.53 mN and was statistically significant compared to control (270nM, $p<0.05$), maltodextrin (252.19mN, $p<0.05$) and riboflavin (484.91 mN, $p<0.05$).

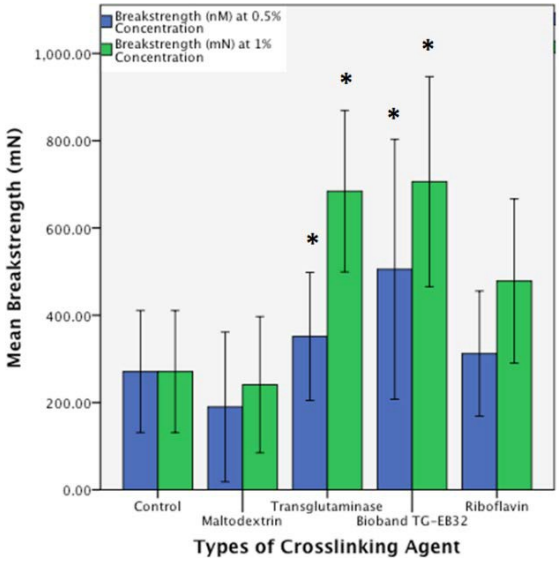

Fig. 1: Break strength of compressed collagen constructs with various cross-linking agents .

At 0.5% concentration, Biobond TG EB32 break strength was 561.71 mN, which was statistically significant compared to the control (270.96 mN $p<0.05$), maltodextrin (189.89mN $p<0.05$), transglutaminase (344.15 mN, $p<0.05$) and riboflavin (312.1545nM, $p<0.05$) (Figure 1).

At x25 000 magnification in SEM; riboflavin and Biobond TG-EB32 constructs had a greater density and a less porous structure in comparison to the control, maltodextrin and transglutaminase constructs (Figure 2).

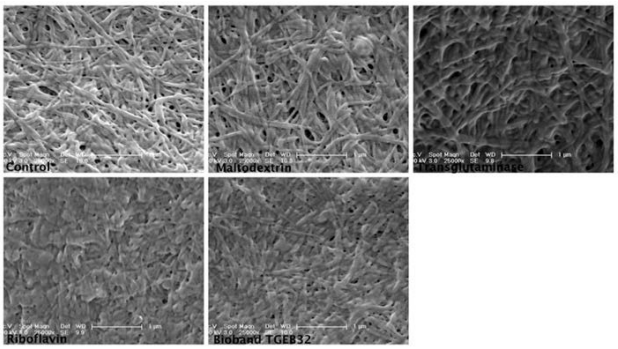

Fig 2. SEM mages (at 25000X) with various cross linkers.

The thermal assay DSC showed that Biobond TG-EB32 had increased thermal stability in comparison to the other cross-linking agents. The mean percentage live/dead for Biobond TG-EB32 was 99% at 24 hours and 98% for 48 hours. The average live/dead% after 24 hours for maltodextrin , transglutaminase and riboflavin was 42%.

DISCUSSION & CONCLUSIONS: This study has shown that the novel crosslinking agent Biobond TG-EB32 significantly increased mechanical strength of collagen constructs. Furthermore, Biobond TG-EB32 does not negatively affect cell viability and thermal stability compared to other agents.

ACKNOWLEDGEMENTS: Project funded by BAPRAS/Healing Foundation

The fabrication of novel phase separated PCL/collagen scaffolds for cartilage tissue engineering

N Munir[1], A Callanan[1]

[1] *Institute of Bioengineering, School of Engineering, University of Edinburgh, Scotland*

INTRODUCTION: Cartilage damage has become increasingly common and is a challenging clinical problem, thus emphasizing the need for effective treatment options [1-2]. Polymer scaffolds provide one tissue-engineering avenue in restoring cartilage damage. The use of phase-separated scaffolds has gained widespread attention due to the highly porous structure with aligned unidirectional pores and interconnected networks [1]. These scaffolds have been enhanced through coating with collagen type 1, which has improved cell attachment and proliferation [2]. However, equal distribution of collagen and collagen penetration throughout the scaffold have been poor. Alternate to coating, evenly mixing water soluble factors such as collagen with hydrophobic synthetic materials still remains a challenge. Thus, this study aims to investigate the effects of phase separating a blended solution of polycaprolactone (PCL) and collagen type 1 on collagen distribution throughout the scaffold, scaffolds mechanical properties and its ability to promote cell attachment and proliferation.

METHODS: PCL (5% wt/vol) and blends of PCL/collagen varying in collagen concentration were used (08%, 04%, and 0.2 %) where acetic acid (0.25M acetic acid and glacial acetic acid) was used as the solvent. These scaffolds were prepared via thermally induced phase separation using a cold plate (-40^{o}C). Scaffold morphology was evaluated using Scanning Electron Microscopy (SEM). To localise and evaluate distribution of collagen, collagen type 1 antibody staining was performed on sectioned scaffolds (10 µm). Additionally mechanical properties analysis and biochemical quantification on cell-seeded scaffolds were performed.

RESULTS: The SEM images show that the phase separated scaffolds possess a common feature of a very porous structure, however, 0.8% collagen type 1 scaffolds presented to be the most porous (Figure 1). Collagen type 1 antibody staining revealed the presence of collagen within the PCL fibres as a darker stain was observed in the collagen scaffold compared to the control (Figure 2). PCL/collagen scaffolds presented improved mechanical properties. Additionally, good cell attachment and proliferation was evident in PCL/collagen scaffolds.

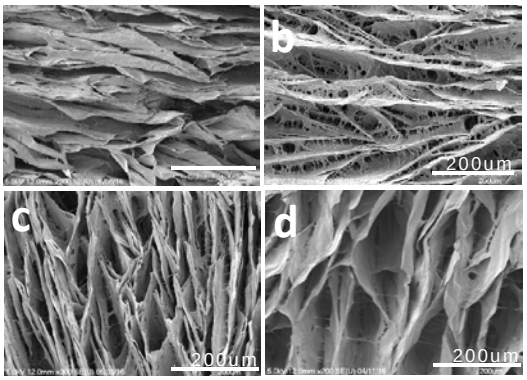

Figure 1: SEM images of (a) PCL control scaffold, (b) 0.8% collagen/PCL scaffold, (c) 0.4% collagen/PCL scaffold and (d) 0.2% collagen/PCL scaffold

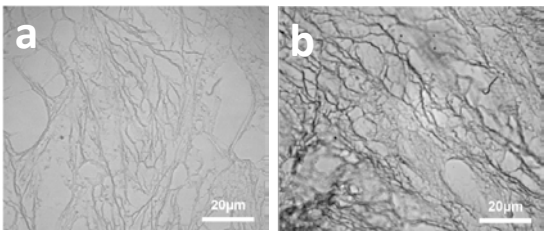

Figure 2: Collagen type 1 antibody staining (Brightfeild Images). (a) PCL control scaffold and (b) 0.8% collagen/PCL scaffold.

DISCUSSION & CONCLUSIONS: This study clearly demonstrates that phase separated PCL/collagen scaffolds allows the integration of collagen type 1 throughout the scaffold. These preliminary results warrant further investigation on the long-term capabilities of these scaffolds to support cell attachment, proliferation and cartilage extracellular matrix production.

ACKNOWLEDGEMENTS: This work is funded by an Engineering & Physical Sciences Research Council Doctoral Training Partnership studentship.

Injectable peptide based hydrogels for cardiac regeneration

Kyle Burgess[1]; Victoria Workman[1]; Delvac Oceandy[2]; Alberto Saiani[1]

[1] School of Materials & Manchester Institute for Biotechnology , University of Manchester, Manchester, UK; [2] Institute of Cardiovascular Sciences, University of Manchester, Manchester, UK.

INTRODUCTION: Self-assembling peptide based hydrogels are of interest in regenerative medicine as they can be used as injectable scaffolds for the targeted delivery of drugs/ cells into damaged or diseased tissue. In this paper we discuss the potential use of a family of peptide hydrogels based on the alternation of hydrophobic / hydrophilic residues for cardiac regeneration. We have shown that these hydrogels can support the growth of both iPS cells as well as iPSC-derived cardiomyocytes.

METHODS: The hydrogels were prepared using FEFKFEFKK (F9) peptide sequence. The same sequence was also funcionalised with fluorescein isothiocyanate (F9-FITC) to create fluorescent gels. F9 was dissolved in distilled water to form a hydrogel with a final concentration of 2% (w/v). Following this, the F9-FITC peptide (FITC, Ex: 490/Em: 520) was dissolved in DMSO (1% v/v) and titrated into the F9 peptide solution (95.5:4.5 (w/w) mix). The solution containing both peptide sequences was then titrated with 0.5M NaOH to a pH of ~ 5.5. Mice were anaesthetized with a combination of ketamine and xylazine. Anaesthesia was induced in an induction box with isofluorane and oxygen, and maintained by passive inhalation of isofluorane and a mixture of oxygen and nitrous oxide. The heart was exposed via a left thoracotomy and 15µl of gel was intramyocardially injected into the left ventricular wall between the midline and apex using a 29-gauge insulin needle. The mice were then euthanized either 5 hours (A, C) or 1 day (B, D) following surgery. Cryostat sections of 10µm thickness were then taken ~1mm from the apex of the heart and stained with either DAPI (A, B) or hematoxylin and eosin (H/E) (C, D).

RESULTS: To demonstrate the injectability of these peptide hydrogels, a peptide gel tagged with the fluorescent fluorophore 'FITC' was injected into the myocardium of a healthy mouse heart. Figure 1 shows that the gel is clearly visible after 24 hours and spreads between the myofibrils within the interstitial space. On further analyses of the H/E sections (C, D) there does not appear to be any obvious signs of inflammation around the gel.

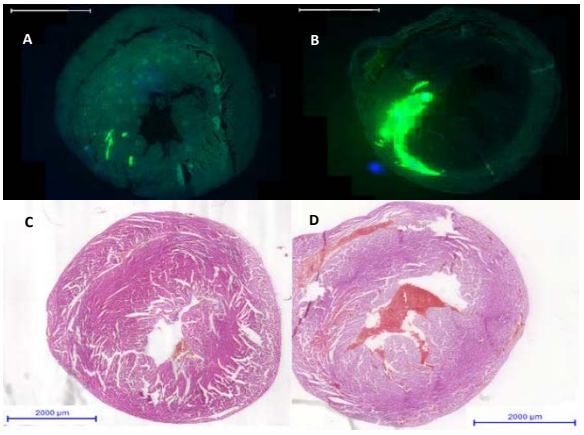

Fig. 1: Images of a healthy mouse myocardium which has been injected with FITC-labelled peptide hydrogel. Serial sections were stained with either DAPI (A, B) or hematoxylin eosin (C, D). Scale bar=2000µm.

DISCUSSION & CONCLUSIONS: A more diffusive distribution of gel is beneficial in that the amount of interstitial spreading correlates with a lower risk of biomaterials inducing arrhythmia. A better spread of gel throughout the tissue will also help reinforce the scar area and reduce the mechanical stress on the area of infarct, when using a mouse model of MI. Also the lack of inflammation around the gel indicates a reduced foreign body response and thus a reduced risk of graft rejection. Future work will assess whether the gel can reduce detrimental remodelling post-MI in a mouse model of MI when used to inject stem cell-derived cardiomyocytes.

ACKNOWLEDGEMENTS: The authors acknowledge an EPSRC Fellowship (EP/K016210/1) and the joint grant from the MRC and EPSRC (CDT in Regenerative Medicine) for providing financial support to this project.

Hypothermic storage of engineered neural tissue

KS Bhangra[1], AGE Day[1], JB Phillips[1]

[1]*Biomaterials & Tissue Engineering, UCL Eastman Dental Institute, University College London, UK*

INTRODUCTION: Advances in biomaterials and tissue engineering have led to the development of an innovative tissue-engineered technology for peripheral nerve repair; Engineered Neural Tissue (EngNT)[1]. However, there remain considerable challenges involved in the clinical translation and commercialisation of this novel technology[2]. In particular, it is critical to consider the logistical feasibility of the storage and distribution of EngNT as part of a repair device without compromising functionality[3]. Cold storage has commonly been used for preserving tissues for a short time prior to clinical use[4]. The aim of this study was to investigate the effect of hypothermic preservation for storing EngNT.

METHODS: Bovine collagen gels (2 mg/ml) containing $4x10^6$ SCL4.1/F7 cells per ml were made in purpose-built PEEK moulds and stabilised using RAFT™ absorbers (TAP Biosystems). Following stabilisation, the cell-seeded constructs were cut into four parts, where one part was used as a control sample and analysed for viability immediately whereas the remaining samples were placed in 1 ml Hibernate®-A (Gibco, UK) preservation media and stored at 4°C for either 2,3,4,7 or 14 days. Cell viability was assessed via membrane integrity assay and metabolic assay. The membrane integrity test involved quantifying cell death using Syto-9 (5µM) and propidium iodide (200 µg/ml) staining followed by fluorescence microscopy (% cell death in the relevant control sample was subtracted).

Metabolic activity of EngNT was assessed using CellTiter-Glo® 3D cell viability assay (Promega, UK) following 72 h storage in (a) culture media at 37°C, 5% CO_2 or (b) Hibernate®-A at 4°C. Following storage, samples were placed in culture conditions for 24 h at 37°C, 5% CO_2; where culture media was renewed in (a), and Hibernate®-A was removed and replaced with culture media in (b). Control samples were unpreserved samples that were analysed immediately. Samples were placed in a 96-well plate reader (BioTek FLx800) and luminescence readings quantified the amount of ATP in the preserved and unpreserved EngNT.

RESULTS: Cell death steadily increased from day 2 (1.7±1.6%) through to day 14 (38.1±1.4%), where cell death values at days 3,4 and 7 were 7.1±2.3%, 15.2±0.6% and 21.4±1.8%, respectively (*Fig 1).*

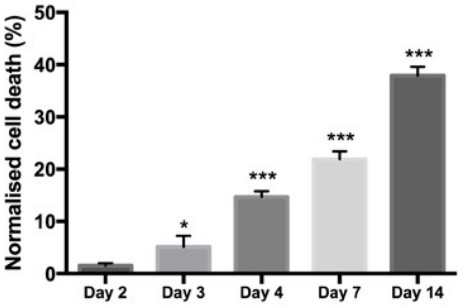

*Fig. 1: Normalised percentage of SCL4.1/F7 cell death in EngNT following storage in Hibernate®-A at 4℃ (n=6, data are means ± SEM after subtraction of % cell death in corresponding controls). One-way ANOVA with Dunnett's to compare Hibernate®-A data with control samples. (*p<0.05, ***p<0.001).*

Table 1. Average metabolic activity in relative light units (RLU) from preserved and unpreserved EngNT, n=4.

ATP present following construct stabilisation (RLU)	ATP present 24 h post-storage (RLU)	
Control	*Storage in culture media*	*Storage in Hibernate®-A*
186061	82851	118535

DISCUSSION & CONCLUSIONS: This study demonstrates that EngNT can be successfully stored under hypothermic conditions with Hibernate®-A media, although cell death gradually increases with time. *Table* 1 shows that constructs preserved in Hibernate®-A for 72 h then placed into culture for 24 h were more metabolically active than those stored in culture media. However, both samples were less metabolically active than a fresh sample analysed immediately after stabilisation. Future work involves understanding the effect of hypothermic storage on the structure of EngNT..

Materials 3D Printed via fused deposition modelling elicit myofibrillar alignment and enhanced differentiation of skeletal muscle cells *in-vitro*

R P Rimington[1,3], A J Capel[1], S D R Christie[2,3], M P Lewis[1,3].
[1]*School of Sport, Exercise and Health Sciences,* [2]*School of Science, Loughborough University, UK.*
[3]*Micro-CDT in Bespoke Flow Reactors, Loughborough University, UK*

INTRODUCTION: 3D printing allows the generation of physical devices within short time-periods from bespoke CAD designs. 3D printing technologies such as selective laser sintering (LS) and stereolithography (SL) are now being utilised within biomedical engineering for the fabrication of microfluidic devices[1] and scaffolds for living cells[2], using what is hoped are biodegradable and biocompatible 3D printed materials. If these technologies are going to form the platforms within which complex cellular physiological process are to be re-created then understanding and defining the compatibility between various mammalian cell types and the printed materials is of paramount importance. This investigation sought to examine the biocompatibility of C_2C_{12} muscle cells on commercially available polymers; poly-lactic acid (PLA), acrylonitrile butadiene styrene (ABS), polyethylene terephthalate (PET) and polycarbonate (PC) when 3D printed via FDM.

METHODS: Biocompatibility experiments were designed to simultaneously assess both the direct (cells cultured directly on the material) and in-direct (cells cultured in chemically leached medium) effects of each polymer on cellular viability, morphology and differentiation after 3 days in GM (GM72hrs) and 5 days in DM (DM120hrs). C_2C_{12} muscle precursor cells (MPCs) were seeded into eight six-well plates at a density of $6x10^5$ cells for each repeat (n=3). Each well/six-well plate was considered n=1 per condition (Control & Material), per analysis at each time-point totaling n=18 per analyses. This protocol was completed separately for each polymer (PLA, ABS, PET and PC). After alamarBlue® cellular viability analysis was conducted, cells were stained for the actin cytoskeleton and nucleic DNA in addition to being harvested for PCR assays.

RESULTS: Polymer dependent reductions in cell viability were observed when cultured directly on 3D printed materials (GM72hrs: PLA; P≤0.05, PC; P≥0.05, DM120hrs: PLA; P≤0.05, PC; P≤0.05). Cells cultured on PET also showed reduced viability (P≤0.05); however this was not evident in cells cultured on ABS (P≥0.05). In-direct observations outlined increases in cell viability when cultured in leached constituents of PLA after DM120 (P≤0.05) and ABS after GM72

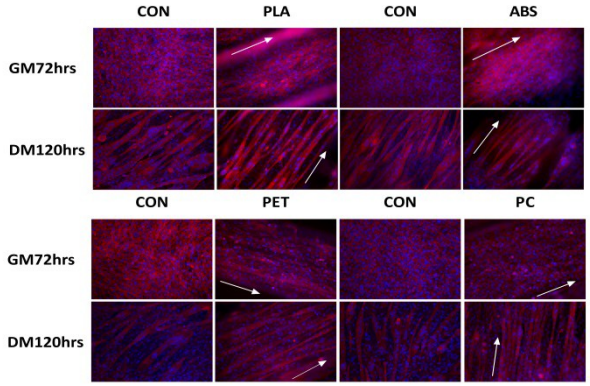

Fig.1: Morphological staining of the actin cytoskeleton (red) & nucleic DNA (blue) for PLA, ABS, PET, PC and respective controls at GM72 & DM120 time-points.

(P≤0.05), however this was not evident in PET (P≥0.05) or PC (P≥0.05).

Morphological observations (*Fig.1*) outlined reduced myotube widths in cells cultured on PLA (P≤0.0001), PC (P≤0.05) and PET (P≤0.0001) however this was not apparent in ABS (P≥0.05). Thinner myotubes were observed in cells cultured in chemical leachable of ABS (P≤0.05), however no difference was observed between other in-direct conditions. C_2C_{12} cultured on 3D printed materials also exhibited significant nucleic (PLA; P≤0.0001, ABS; P=≤0.05, PET; P=≤0.05, PC; P≤0.0001) and myofibrillar alignment (PLA; P≤0.0001, ABS; P≤0.05, PET; P≤0.05, PC; P≤0.0001).

Augmented myogenin $\Delta\Delta C_T$ expression was documented at early time-points; GM72 in PLA (P≤0.0001), ABS (P≤0.05) and PC (P≤0.0001), however this was not observed in PET (P≥0.05). Myogenin remained potentiated after DM120 in PLA (P=≤0.05), however this response was reduced in ABS (P≥0.05), PET (P≥0.05) and PC (P≥0.05). No difference was observed in cells cultured in the leached medium of materials.

DISCUSSION & CONCLUSIONS: This investigation observed biocompatible polymers 3D printed via FDM which exhibit morphological alignment and enhanced differentiation of C_2C_{12} cells, providing rationale for use when re-creating platforms for cellular physiological processes.

Using advanced 3D engineered cell cultures to analyse the effect of drugs on peripheral nerve regeneration *in vitro*.

MLD Rayner[1,2], J Healy[2] and JB Phillips[1].

[1] *Biomaterials & Tissue Engineering, Eastman Dental Institute, UCL, London, UK.* [2] *School of Pharmacy, UCL, London, UK.*

INTRODUCTION: Injuries associated with peripheral nerve damage affect ~1 million patients per year. Damage to the peripheral nervous system can be extremely debilitating and result in loss of end organ function, coupled with poor neuron regeneration capacity [1]. Currently the treatment options for injuries are microsurgical and there are no drug therapies available to improve recovery. Pharmacological treatments could potentially be used to maintain neuronal viability, encourage axonal growth, improve axonal specificity to end-organ targets and reduce neuropathic pain. Some drugs and targets have been identified but there are challenges associated with understanding mechanisms of action and moving therapies towards clinical translation. For successful regeneration following injury Schwann cells need to support regeneration and myelination of neurons [2]. This 3D cell-cell interaction is a key feature that needs to be recreated in order to build effective in vitro models. Engineered neural tissue (EngNT) supports the regeneration of neurons within an aligned 3D Schwann cell-seeded collagen gel environment. Initial results demonstrated the use of EngNT as an effective co-culture model to analyse the effect of drugs on neurite growth. The aim of this study was to use the model to explore the effects of ibuprofen treatment, a drug that has shown some positive outcomes in animal models of nerve regeneration [3].

METHODS: Anisotropic 3D co-culture gels were prepared by tethering 1ml of solution containing; 80% Type I rat tail collagen, 10% 10x MEM, 5.8% neutralising solution and 4.2% Schwann cell suspension, within rectangular moulds to facilitate cellular self-alignment. After 24h incubation at 37°C, the aligned cellular gels were stabilised using plastic compression and PC12 neurons were added to the surface. Co-cultures were subjected to drug treatments for 72h before fixing. Neurites were visualised using βIII-Tubulin immunoreactivity and fluorescence microscopy. Neurite growth was quantified by measuring neurite length using ImageJ software.

RESULTS: Treatment with 10µM and 100µM ibuprofen elicited an increase in neurite length in 3D co-culture gels, whereas neurite length was reduced following treatment with 200µM ibuprofen (Fig 1). Minimal neurite growth was seen in the prese

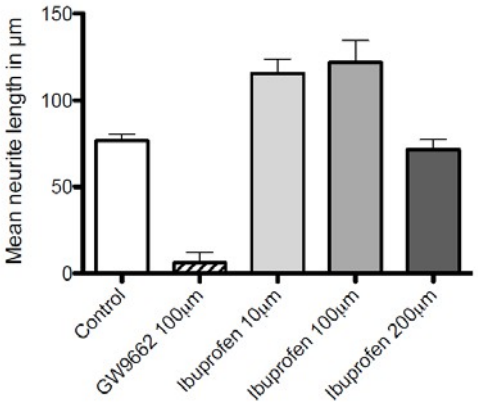

Fig. 1: Neurite length after 72 h in the presence or absence of 10µM, 100µM, and 200µM, ibuprofen or 100µM GW9662.

DISCUSSION & CONCLUSIONS: The results demonstrate that this engineered tissue model containing neurons and Schwann cells aligned within a collagen hydrogel mimics the pro-regenerative effects of ibuprofen seen previously *in vivo*. This indicates that the 3D engineered co-culture gels can be used as an effective assay for screening drugs and allows us to generate dose response profiles.

ACKNOWLEDGEMENTS: This research was made possible through the support and funding of the EPSRC (Grant EP/L01646X).

Micro-computed tomography as a correlative imaging tool for the assessment of bone morphology

A Syed[1], T Burnett[2], P Withers[2], A Hidalgo-Bastida[1]
1.School of Healthcare Science, Manchester Metropolitan University, Manchester M1 5GD
2.The Manchester X-Ray Imaging Facility, University of Manchester, Manchester M13 9PL

INTRODUCTION: MicroComputed Tomography (micro-CT) is an ever growing field of imaging which utilizes the power of X-rays to three-dimensionally reconstruct an object for in depth analysis of extreme detail, non-invasively and rapidly[1]. Structures can be visualized at extremely high resolution, and extremely large volumes of interest can be analyzed using powerful processing software.

The aim of this research was to determine if micro-CT could significantly establish quantitative and qualitative differences between a whole region of bone that had been progressively treated with histological methods. The research hypothesized that micro-CT could effectively identify differences between each step of treated bone.

METHODS: Fresh bovine bone was fixed in 4% formaldehyde overnight prior to a micro-CT scan, following this, the sample was demineralised at 4°C in 10% Ethylenediaminetetraacetic acid (EDTA), pH 8, for two weeks and imaged. Finally, the sample was stained in 10% Lugol solution as a contrast staining overnight and washed before scanning.

An XRadia VersaXRM-500 scanner was used at 40 keV, 3-4 W and pixel size 14-16 µm, resulting in scanning times of 2.5-3.5 hours. Avizo 9.0 was used to process all micro-CT data. Scanning Electron Microscopy (SEM) was performed after each sequential scan and conventional histology was performed after the final scan in order to cross-examine the findings of each technique.

The sample was embedded in Paraplast Plus and sectioned into 5 micron thick sections before being stained with H&E, von Kossa and Safranin O, and imaged by light microscopy.

RESULTS: Micro-CT was effective in visualizing qualitative changes in bone microarchitecture and displayed how changes in micro-CT parameters caused different levels of image resolution and contrast. Segmentation also allowed volumetric changes to be accurately recorded. SEM found that there was a loss of extracellular matrix and that the surface of the bone gradually degraded after each treatment, while histological staining confirmed the absence of calcium.

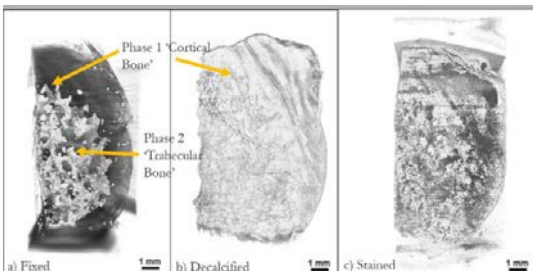

Figure 1. Micro-tomography reconstructions of a) Fixed bone, showing clearly the cortical and trabecular sections, b) Decalcified bone, with no trabecular matrix, and c) Stained bone in 10% lugol showing a white edge to the bone, indicating incomplete penetration of the contrast agent.

DISCUSSION & CONCLUSIONS:

This method presents challenges when correlating in between steps, as the sample is changing, as is the contrast. The decalcified dataset had the highest resolution and displayed the most accurate shape of the bone sample with features being most easily distinguished (Fig. 1). As expected, the trabecular region originally highlighted in the fixed sample was not observed in the subsequent decalcified sample. This supported previous studies which stated that micro-CT had the capacity to investigate a ride range of parameters such as qualitatively assessing whole bone geometry and tracking changes in trabecular arrangement[2]. Micro-CT is a rapid and novel technique, the non-destructive nature of micro-CT could allow a wide range of testing to be performed at progressive stages of *ex vivo* studies of osteoporosis. The coupling of SEM and micro-CT provide powerful features as a 'virtual histological tool' although their diagnostic value still needs to be established.

ACKNOWLEDGEMENTS We would like to thank the fellow users and staff of HXMIF for their assistance.

Novel growth factor delivery using clay gels for the treatment of diabetic foot ulcers

DJ Page[1, 3], JI Dawson[1], R Mani[4], ROC Oreffo[1], CE Clarkin[2], ND Evans[1, 3]

[1]Centre for Biological Sciences, Faculty of Natural and Environmental Sciences, University of Southampton, UK; Department of Bioengineering, Faculty of Engineering and the Environment, University of Southampton, UK; [2]Centre for Human Development and Health, Stem Cells & Regeneration, Faculty of Medicine, University of Southampton, U.K; [3]Department of Bioengineering, Faculty of Engineering and the Environment, University of Southampton, UK; [4]Medical Physics & Bioengineering, University Hospital Southampton NHS Foundation Trust, UK

INTRODUCTION: Biological agents, including vascular endothelial growth factor (VEGF), have been investigated as agents that improve wound healing, yet delivery in an active, economical form remains a significant clinical challenge[1,2]. To address this problem, we propose using a synthetic clay biomaterial called Laponite; its unique layered silica/metal cation structure allows formation of a hydrated gel network which retain and deliver biological agents[3]. Here we tested whether, i) Laponite can localise bioactive VEGF to stimulate in vitro angiogenesis ii) whether Laponite incorporated within VEGF can localise bioactive VEGF at skin injury sites to improve the rate and quality of wound healing in healthy and diabetic mice..

METHODS: To investigate in vitro bioactivity, aqueous rhVEGF165 was added to 3% Laponite hydrogel surfaces and incubated for 2 hours at 37°C. RhVEGF165 was then removed and Laponite surfaces washed with PBS (adsorbed VEGF gels). Separately, rhVEGF165 was pre-mixed within Laponite hydrogels prior to well coating (incorporated VEGF gels). Human umbilical vein endothelial cells (HUVECs) were seeded on all Laponite surfaces and incubated at 37°C for 18 hours. Microscope images were taken and tubule networks quantified by image analysis. To investigate in vivo bioactivity, two left and right side surgical wounds were created on the dorsum of male C57BL/6 (healthy) and db/db mice (diabetic) and a Tegaderm dressing applied. One-day post-surgery, left wounds were treated with 3% Laponite hydrogel pre-mixed with 1 μg/ml VEGF and right wounds with a vehicle control. Photos of wounds were taken to measure the rate of wound closure. Wound tissue was harvested ≥11 days, fixed with 4% PFA, paraffin embedded, sectioned and stained.

RESULTS: VEGF-mediated stimulation of HUVEC tubules was successful on Laponite hydrogel surfaces; it was shown that adsorbed VEGF gels significantly increased the formation of tubules ($p = <0.001$). Tubule formation by HUVECs was also significantly increased when cultured on incorporated VEGF gels containing >1 μg/ml VEGF. Laponite biomaterial applied to skin injury sites was retained ≥11 days, as revealed by acridine orange staining. No significant differences in the rate of wound closure was measured between VEGF-Laponite and vehicle controls in healthy and diabetic mice. Preliminary histological data suggested that there was increased cellular infiltration within wound granulation tissue in VEGF-Laponite treated wounds in healthy mice.

DISCUSSION & CONCLUSIONS: These results suggest that Laponite biomaterial could have significant clinical potential to localise proangiogenic VEGF to chronic wounds.

ACKNOWLEDGEMENTS: Many thanks to Tizard, Grundy Educational Trust, and Novo Nordisk for providing funding for this project.

Investigation of hydrogen sulphide effect on the reducing reperfusion injury in an acute myocardial infarction model

Shuting Huang[1,2], Kun Chen[2], Ying Yang[1]

[1] *Institute of Science and Technology in Medicine, Keele University Stoker-on-Trent ST4 7QB, UK*

[2] *School of Life Science. Guangzhou University, Guangzhou, China*

INTRODUCTION: The healing property of reperfusion therapy is limited by the subsequent damage called ischemia-reperfusion injury (IRI). Hydrogen sulfide (H_2S) has great protection potential to cardiac tissues of IRI. In this research, two types of H_2S medication have been introduced. Compared with one-off treatment, continuous H_2S medication was investigated in order to improve the healing efficiency. Using 3D nanofiber as the carrier for H_2S delivery has been studied as well.

METHODS: Rat neonatal cardiocytes were injured by culturing in Ischemic Preconditioning Solution (IPS) for 25min in order to build post-ischemic model. IPS was removed and then topped up with fresh media with 50μM of NaHS (a progenitor of H_2S), this medication was repeated for 3 time each 24h. Polylactic acid (PLA) nanofiber meshes were electrospun and soaked in NaHS solution for 24 h, then drying. The meshes were added in the culture media after IPS stimulation instead of adding NaHS solution as above. MTT assay was conducted for cell viability and proliferation rate assessment. The cells without IPS were used as control.

RESULTS: The table 1 shows that cell viability was 80% of original value at 24h, and the 48h and 72h groups had higher value over the control, 131.2% and 138.6% respectively. After IPS stimulation, cells were too weak to be tested by MTT assay, they died without H_2S treatment.

	CON	24 h	48 h	72 h
OD（420nm）	0.77	0.65	1.01	1.06
Repair rate	100%	84.9 %	131.2%	138.6%

Table 1. The repair rate vs medication duration.

IPS stimulation damaged almost all cells if no H_2S addition. The recovery of the damaged cells by H_2S was time dependent (Figure 1). With continuous addition of H_2S in culture media, it is found that H_2S can also stimulate the proliferation of cardiocytes. The IPS damaged and H_2S medicated cell samples had higher MTT value.

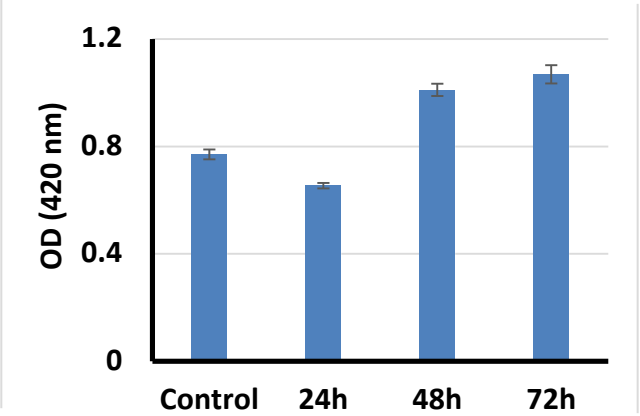

Fig. 1: The cell viability after IPS stimulation and H_2S treatment in comparison to control.

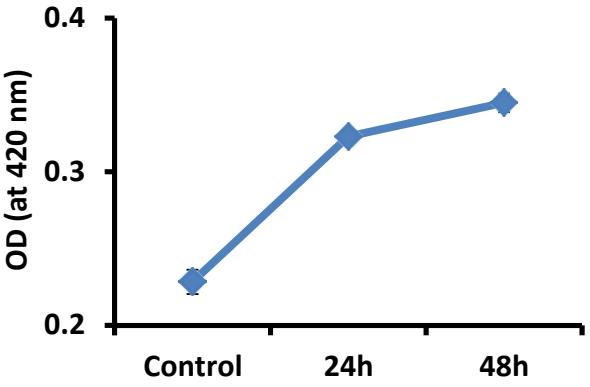

Fig. 2: The cell viability after IPS stimulation and H_2S treatment by3D nanofiber meshes in comparison to the control.

The figure 2 shows that nanofiber meshes as the H_2S carrier for the treatment of IRI was not as significant as direct H_2S solution medication. However, it has demonstrated the protection effect against IPS stimulation.

DISCUSSION & CONCLUSIONS: IRI damages heart tissue, and it causes subsequent damage because of the further inflammation. Longer medication is necessary. This study has been proved that H_2S can protect heart cells against IRI and longer H_2S medication was more effective as H_2S has the ability of decreasing the inflammation. Further study is required to optimize the 3D nanofiber as the carrier for H_2S delivery.

The potential of novel silk-based biomaterial in combination with growth promoting cues to promote central nervous system axonal regeneration

A Varone[1], S. Lesage[2], D. Knight[2], F. Vollrath[2], AM Rajnicek[1], W Huang[1]

[1]School of Medicine, Medical Sciences and Nutrition, Institute of Medical Sciences, University of Aberdeen, Foresterhill, Aberdeen, Scotland, United Kingdom [2]Oxford Biomaterials Ltd., Magdalen Centre, Oxford Science Park, Oxford, United Kingdom

INTRODUCTION: The mammalian central nervous system (CNS) is poor at spontaneous repair following traumatic injuries such as spinal cord injury, which has no cure available. One attractive treatment strategy would be to use a biomaterial scaffold to support axonal regeneration in combination with drugs that have growth promoting properties and guidance cues to direct regenerating axons across the lesion. Previously, we have shown that a silk-based biomaterial called Spidrex® supports excellent axonal regeneration in a rat model of peripheral nerve injury[1]. In addition, the omega-3 polyunsaturated docosahexaenoic acid (DHA) has been shown to promote neurite outgrowth of rat dorsal root ganglion neurons in vitro[2]. Here, we investigated the potential of Spidrex®, DHA or a combination of both for CNS axonal regeneration in vitro.

METHODS: Tensile tests of the silk biomaterial were conducted using a Zwick testing machine. For in vitro degradation tests silk fibres were kept up to 60 days and the tensile properties tested in the same way. Primary CNS neurons were cultured from *Xenopus Laevis* embryos and from postnatal rat cerebral cortex. Neurons were seeded on to Spidrex® silk fibres that were secured and aligned in parallel on PDL coated glass coverslips. DHA at various concentrations was added to cortical neuronal cultures for 48h. Then the optimal concentration of DHA was then applied to cortical neurons seeded on silk fibres for 48h. The interaction of neurites with silk fibres was observed using a time-lapse microscopy followed by immunocytochemistry. HCA-vision and Image J software was used to quantify neurite outgrowth. The inflammatory response was tested by exposing primary microglial cells, isolated from postnatal rat cortex, to Spidrex® for 48h. Expression of iNOS inflammatory marker and levels of nitrite release were assessed using immunocytochemical staining and Griess assays respectively.

RESULTS: Tensile tests results showed that a Spidrex® fibres had a tensile elasticity that was very close to that of fresh rat spinal cord tissue. Moreover, Spidrex® silk degraded *in vitro* as shown by a gradual decrease in mechanical strength over time. We showed that Spidrex® silk fibres supported outgrowth of CNS neurons. Thus, there was a significant proportion of Xenopus and rat cortical neurons engaging with the silk fibres. We also showed that the omega-3 DHA promoted neurite outgrowth of rat cortical neurons in a concentration-dependent manner. Furthermore, rat cortical neurons that grew on Spidrex® silk fibres and received DHA treatment in culture medium simultaneously had significantly better neurite outgrowth when compared to those of either silk biomaterial or DHA alone. Finally, we found minimal microglial activation with similar levels of iNOS and nitrite release as compared to those of the controls.

CONCLUSIONS: We have demonstrated that Spidrex® silk has excellent mechanical properties, biodegradation, and biocompatibility for CNS tissue engineered scaffold. Our in vitro data show that Spidrex® silk supports neurite outgrowth of CNS neurons, and this is further enhanced with the combination of the omega-3 DHA, suggesting the potential of a novel combinational strategy for CNS injury repair. Future work will explore the potential of combining with other strategies that have guidance cue properties such as the use of electrical stimulation, and to test our novel combinational strategies in the presence of growth inhibitory molecules in vitro and in animal models of CNS injuries.

ACKNOWLEDGEMENTS: This work was supported by the Sottish Rugby Union, Institute of Medical Sciences at the University of Aberdeen, Medical Research Scotland and the R S MacDonald Charitable Trust. We thank Oxford Biomaterials Ltd. for the kind support in supplying Spidrex® silk.

Synergistic or antagonistic? The interaction between topography induced signalling and growth factor signalling in regenerating dorsal root ganglia

R Docherty[1], M Riehle [2]

Centre for Cell Engineering, College of Medical, Veterinary and Life Sciences

University of Glasgow, Scotland

INTRODUCTION: Peripheral nerve injury often results in a devastating impact on a patient's ability to function in everyday life despite its intrinsic ability to regenerate following an injury. Most treatment strategies involve the use of a nerve guidance conduit which employs various topographies to promote directional axonal growth and growth factors that enhance the extent of axon growth[1]. There is a lack of research however, on the results of combining these two factors, their signalling interactions and the optimal conduit setup when considering their combined effect[2].

METHODS: To answer these questions, we analysed the axonal growth of neo-natal dorsal root ganglia (DRG) explants cultured for 10 days on polydimethylsiloxane (PDMS) devices with a flat and grooved (12.5µm wide ridges spaced 12.5µm, 5µm deep) pattern at differing nerve growth factor (NGF) concentrations (0, 10, 50, 100 and 150ngml^{-1}).

Resultant axon networks were imaged through immunostaining β3-tubulin followed by fluorescence microscopy. Surface area (SA) and length of DRG networks were measured using the Fiji Particle Analysis Plugin and the orientation of axon growth on flat substrates was analysed using the Directionality Plugin[3]. To standardise results, all networks were rotated to align along the axis of the roots protruding from the DRG.

RESULTS: Grooved topographies promoted an elongated rectangular axon network whilst flat control networks were of a circular, radial shape. On flat, the SA steadily increased with increasing NGF concentration from 5.7mm^2 (0) to a maximum of 21.9mm^2 (150). On grooves, average axon length increased to a maximum of 9.7mm (10). Further increases in concentration above 10NGF lead to stinted growth with a sharp decrease in axon length to a minimum of 5.8mm (150). Directionality analysis revealed no promoted orientation at each NGF conc. Orientation of axon growth was random however, the overall network shape was found to be conserved across all conc. as the same general profile was observed in all orientation histograms.

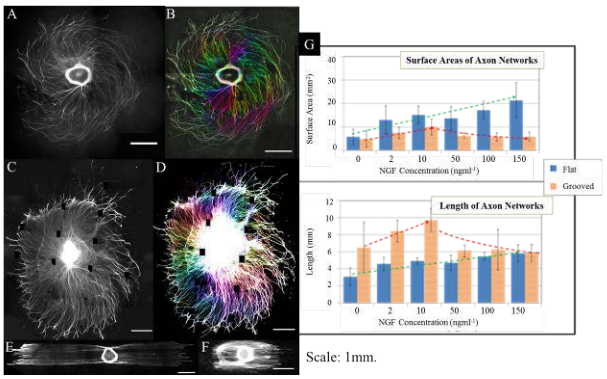

Fig. 1: Fluorescent images of DRG axon growth on flat (A: 10, C: 150NGF) and grooves at (E: 10, F: 150NGF). Directionality analysis of each network (B, D) and trends in network size (flat: blue, grooves: orange) at different NGF conc.

DISCUSSION & CONCLUSIONS: These results are consistent with previous findings[4] impressing that grooved topographies have a detrimental effect on DRG axon regrowth at high NGF conc. Our hypothesis is that axons stretch out further on a grooved substrate increasing tension within the cell and leading to a change in the usual topographical signalling which interacts with the NGF pathway via crosstalk causing a decrease in axonal outgrowth. Also, this study gives further reasoning to the use of DRG as a valid model for measuring axon growth as the DRG structure was not found to promote any direction of growth or resultant morphology.

Textured microparticles to study the influence of particulate topography on mammalian cell adhesion

M. Alvarez-Paino[1], M.R. Alexander[1], C. Alexander[1], K. Shakesheff[1], D. Needham[2] and F.R.A.J Rose[1]

[1]School of Pharmacy, University of Nottingham, Nottingham, UK [2]Department of Mechanical Engineering and Material Science, Duke University, Durham, North Carolina, USA.

INTRODUCTION: Understanding biomaterial-cell interactions is important in order to establish the basis for successful tissue engineering. Material properties including topography,[1] chemistry[2] and stiffness[3] have been demonstrated to have a high impact on mammalian cell fate. Our aim is to study this concept in 3D. In this work, biodegradable microparticles with different sizes and topographies have been fabricated using solvent evaporation oil-in-water emulsion. As a first step, fibroblast cell attachment was studied on this range of particle types.

METHODS: Microparticles of poly(lactic acid–co-glycolic acid) (PLGA) 50:50 (50 KDa) were prepared by a solvent evaporation oil-in-water emulsion technique. PLGA dissolved in dichloromethane (2% or 10% w/v) was homogenized in a 1% w/v polyvinylalcohol (98% hydrolysed, 13-23kDa) aqueous solution (600 rpm, 4h). To produce textured microparticles, fusidic acid (FA) was introduced in the organic phase at 20% or 30% w/w to polymer.[4] Emulsification was performed as described above and dimpled particles were obtained after FA release in water over 7 days. Red fluorescence protein expressing 3T3 mouse fibroblast cells were seeded at 50,000 cells/well on a layer of particles at the bottom of non-tissue culture treated plates. Cell adhesion was studied by fluorescence microscopy and scanning electron microscopy (SEM).

RESULTS: Non-porous microparticles with smooth surfaces were obtained when only polymer was employed (fig. 1a). When FA was incorporated into the sample, dimpled particles were formed (fig. 1b, c). The average particle diameter was 50 µm and 20 µm when polymer concentration employed was 10% or 2%, respectively. Also, dimple diameter varied with the largest dimples observed on the smallest particles (fig. 1c ~12 µm dimples against fig 1b ~4 µm dimples).

Cell adhesion to the particles was imaged over 6 days. As can be seen in fig 2., cells were attached to the particles after 1 day of culture (2a). After 6 days (2b), cells had proliferated, spreading on the zones where the particles are located.

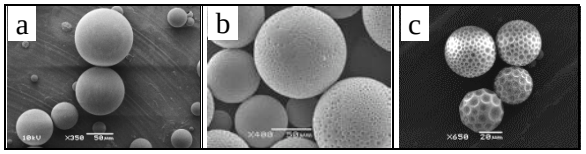

Fig. 1: SEM images of PLGA particles prepared from 10 w% solutions: a) 0% and b) 20% FA; c) PLGA particles from 2 w% solutions with 30% FA.

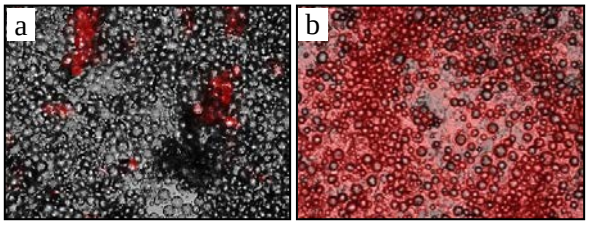

Fig. 2: Overlaid bright field and fluorescence microscope images of cells (red) cultured on smooth PLGA particles (grey) at a) day 1 and b) day 6. Magnification: 20x.

DISCUSSION & CONCLUSIONS: Our aim in this study was to fabricate a range of smooth and textured particles and to assess mammalian cell adhesion. PLGA microparticles were fabricated by emulsion and the size modified by changing the emulsification conditions. Dimpled microparticles were obtained when PLGA was emulsified in the presence of FA. This immiscible polymer-drug system phase separates during solvent evaporation and after subsequent drug release, FA-free particles with a porous inside and a characteristic 'golf ball'-like pattern on the surface (fig 1b and 1c) are obtained. In addition, dimple size can also be tuned by the drug content in the initial mixture and smaller dimpled particles that previously described[4] for this methodology were obtained.

Preliminary studies on cell adhesion and proliferation indicate that these biomaterials are good candidates to assess the influence of topography on mammalian cell adhesion and differentiation in 3D.

ACKNOWLEDGEMENTS: Authors acknowledge EPSRC for grant funding (EP/N006615/1).